CHALMERS

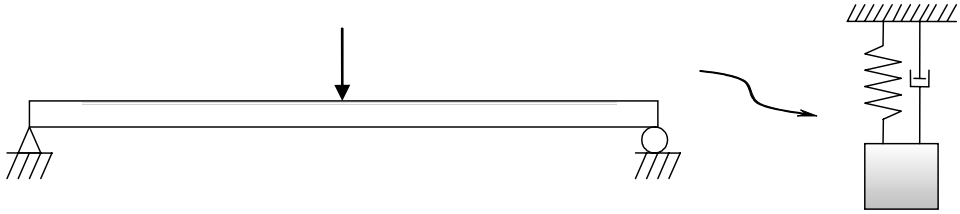

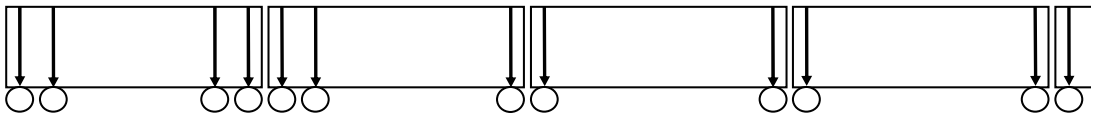

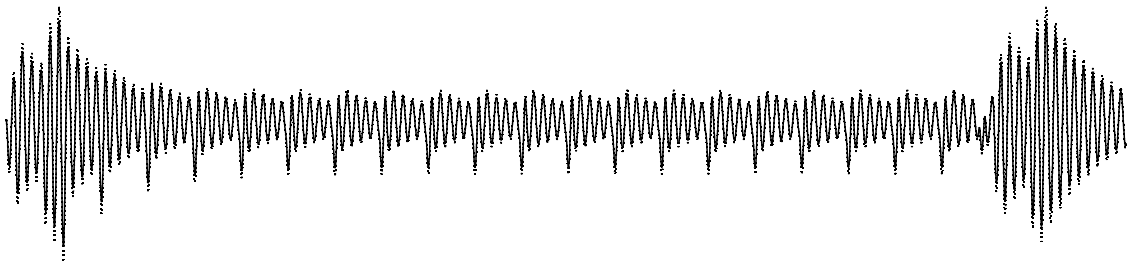

Dynamic analysis of railway bridges

Simplified modelling using SDOF technique

Master's Thesis in the International Master´s Programme Structural Engineering

DANIEL EKSTRÖM

LARS-LEVI KIERI

Department of Civil and Environmental Engineering
Division of Structural Engineering
Concrete Structures
CHALMERS UNIVERSITY OF TECHNOLOGY
Göteborg, Sweden 2007

Master's Thesis 2007:8

MASTER'S THESIS 2007:8

Dynamic analysis of railway bridges

Simplified modelling using SDOF technique

Master's Thesis in the International Master´s programme Structural Engineering

DANIEL EKSTRÖM, LARS-LEVI KIERI

Department of Civil and Environmental Engineering
Division of Structural Engineering
Concrete Structures
CHALMERS UNIVERSITY OF TECHNOLOGY
Göteborg, Sweden 2007

Dynamic analysis of railway bridges
Simplified modelling using SDOF technique
Master's Thesis in the International Master`s programme Structural Engineering
DANIEL EKSTRÖM
LARS-LEVI KIERI

Master's Thesis 2007:8
Department of Civil and Environmental Engineering
Division of Structural Engineering
Concrete Structures
Chalmers University of Technology
SE-412 96 Göteborg
Sweden
Telephone: + 46 (0)31-772 1000

Chalmers Reproservice / Department of Civil and Environmental Engineering
Göteborg, Sweden 2007

Dynamic analysis of railway bridges
Simplified modelling using SDOF technique
Master's Thesis in the International Master`s Programme Structural Engineering
DANIEL EKSTRÖM
LARS-LEVI KIERI
Department of Civil and Environmental Engineering
Division of Structural Engineering
Concrete Structures
Chalmers University of Technology

ABSTRACT

Today, the design of railway bridges to withstand dynamic loads caused by high speed trains is both complicated and time consuming. Therefore simplifications are desirable in order to facilitate the calculations. Based on literature studies some simplified methods used to analyse beams subjected to dynamic loads are compiled and also compared with finite element analysis in order to verify the results.

The method of transforming and reducing deformable structures into a single degree of freedom system, giving calculations that are easy to handle, is discussed and investigated in this thesis. When a beam is simplified into a single degree of freedom system the beam is assumed to have a specific shape of deformation and therefore tabled beam equations can be used in order to estimate the capacity of the beam. These simplifications of the beam equations can also be applicable for dynamic loads, and used to describe the system response.

In this thesis a single degree of freedom system is examined for various simple types of loading, where the main focus has been to compare the response of displacement and acceleration between different load types. This comparison gives a basic understanding of the dynamic phenomena that causes oscillations and also their effects.

Further the loading in the single degree of freedom system is modified to resemble a train load model, HSLM-A. The results between the system and a finite element model of a simply supported beam are compared, where the results show that the system can be used to give an approximation of the response on the beam.

The simplified methods discussed above are only investigated for mutual parameters. Since railway bridges often are made of reinforced concrete, which have a complex structure and behaviour, the responses from the simplified methods due to dynamic loads needs to be studied more in detail.

Key words: Beam vibrations, damping, differential equation, dynamics, SDOF system, train load model HSLM

Dynamiska analyser av järnvägsbroar
Förenklad modellering med genom användande av enfrihetsgradsystem
Examensarbete inom Civilingenjörsprogrammet Väg och vattenbyggnad

DANIEL EKSTRÖM

LARS-LEVI KIERI
Institutionen för bygg- och miljöteknik
Avdelningen för Betongbyggnad

Chalmers tekniska högskola

SAMMANFATTNING

Analyser och beräkningar av järnvägsbroar utsatta för dynamiska laster från höghastighetståg är idag komplicerade och tidskrävande, därför är förenklade beräkningsmetoder önskvärda för att underlätta analyserna. Genom litteraturstudier har en förenklad beräkningsmetod studerats och sedan undersökts i denna rapport. Resultat beräknade med hjälp av den förenklade beräkningsmetoden är jämförda med resultat från finita element analyser av balkar för att kunna verifiera metoden.

Balkar, och andra deformerbara kroppar, kan omvandlas till ett enfrihetsgradsystem som tillskrivs ekvivalenta egenskaper för att ge samma deformation som den deformerbara kroppen. När balken har omvandlats till ett enfrihetsgradsystem kan tabellerade, så kallade, balkekvationer användas för att direkt uppskatta balkens respons.

Den här rapporten behandlar och undersöker responsen av ett enfrihetsgradsystem som belastas av olika typer av laster. Responsen för systemet är i huvudsak undersökt i form av förskjutningar och accelerationer och dessa skall ge grundläggande förståelse för dynamiska svängningar och dess effekter.

Ytterligare så modifieras lasten i enfrihetsgradsystemet för att beskriva tåglast-modellen HSLM- A. Resultat mellan enfrihetsgradsystemet och en fritt upplagd balk visar att ett enfrihetsgradsystem ger en god approximation av balkens respons.

De förenklade beräkningsmetoderna är endast undersökta för inbördes jämförelse. Eftersom järnvägsbroar som dimensioneras för dynamiska laster oftast är gjorda av armerad betong med komplexa material egenskaper, bör denna förenkling analyseras och verifieras mer i detalj.

Nyckelord: Balk vibrationer, differential ekvation, dynamik, dämpning, SDOF system, tåglastmodell HSLM

Contents

Preface

In this Master's Thesis methods to simplify analyses of railway bridges subjected to dynamic loads, caused by high speed trains, are compiled and investigated. The project has been performed within a co-operation between Reinertsen Sverige AB and the Division of Structural Engineering at the Department of Civil and Environmental Engineering of Chalmers University of Technology, Göteborg. The work has been carried out at Reinertsen's office in Göteborg from September 2006 to February 2007 and the examiner has been Professor Kent Gylltoft.

Morgan Johansson, PhD, from Reinertsen Sverige AB, has supervised us with engagement, and we specially thank him for his support and good ideas. Thanks also to the rest of Reinertsen's staff for answering various questions that appeared during the work.

Our opponents, Simon Skoglund and Johan Nesset, have continually assisted with the development of this thesis and we thank them for grateful help and good ideas of improvements.

Göteborg February 2007

Daniel Ekström and Lars-Levi Kieri

Notations

Roman upper case letters

A	Amplitude [m], Area [m^2]
C	Damping matrix [Ns/m]
$C_{Rayleigh}$	Rayleigh damping matrix [Ns/m]
DAF	Dynamic Amplification Factor
DE	Differential Equation
E	Modulus of elasticity [N/m^2]
F_D	Damping force [N]
F_E	Elastic force [N]
F_I	Inertia force [N]
$F_{I,e}$	Equivalent internal force [N]
G	Shear modulus [N/m^2]
$HSLM$	High Speed Load Models
I	Moment of inertia [m^4]
K	Stiffness matrix [N/m]
L	Length of beam [m]
M	Mass matrix [kg], Moment [Nm]
$\hat{M}$	Lumped mass matrix [kg]
N	Axial force [N], Number of coaches [-]
$\overline{N}$	Sectional force vector
P	External load vector [N]
P_e	Equivalent external load [N]
$\hat{P}$	Lumped load vector [N]
$SDOF$	Single Degree Of Freedom
T	Period [s]
T_d	Damped period [s]
U	Displacement/deflection vector [m]
$\dot{U}$	First derivative of U with respect to time t, velocity vector [m/s]
$\ddot{U}$	Second derivative of U with respect to time t, acceleration vector [m/s^2]
V	Shear force [N]
W_k	Kinetic energy [J]
W_p	Potential energy [J]
$W_{p,ext}$	External potential energy [J]
$W_{p,\text{int}}$	Internal energy [J]

Roman lower case letters

a	Acceleration [m/s^2]
$\overline{a}$	Mean acceleration [m/s^2]
b	Width of beam/cross section [m]
c	Damping [Ns/m]
c_e	Equivalent damping [Ns/m]

d	Bogie axle spacing [m]
f	Frequency [Hz]
f_n	Natural Frequency [Hz]
g	Gravity [m/s^2]
h	Height of beam/cross section [m]
k	Stiffness [N/m]
k_e	Equivalent stiffness [N/m]
l	Length of beam [m]
m	Mass [kg]
m_e	Equivalent mass [kg]
p	Load [N]
p_0	Initial load [N]
p_e	Equivalent load [N]
s	Distance [m]
$\dot{s}$	Velocity [m/s]
$\ddot{s}$	Acceleration [m/s^2]
t	Time [s]
u	Displacement/deflection [m]
u	Translation freedom in x-direction [m]
$\dot{u}$	First derivative of u with respect to time t, velocity [m/s]
$\ddot{u}$	Second derivative of u with respect to time t, acceleration [m/s^2]
u_h	Homogenous solution
u_p	Particular solution
u_s	Displacement of system point [m]
u_{static}	Static displacement, deflection [m]
$u''(x)$	Curvature [rad]
v	Velocity [m/s], translation freedom in y-direction [m]
v_s	Velocity of system point [m/s]
$\bar{v}$	Mean velocity [m/s]
v	Translation freedom in y-direction [m]
v'	First derivative of v with respect to space
v''	Second derivative of v with respect to space
$\dot{v}$	First derivative of v with respect to time t, velocity [m/s]
$\dot{v}'$	First derivative of v with respect to space, and associated velocity
w	Translation freedom in z-direction [m]
$\dot{w}$	First derivative of w with respect to time t, velocity [m/s]
$\ddot{w}$	Second derivative of w with respect to time t, acceleration [m/s^2]
x	Space coordinate
y	Space coordinate
z	Space coordinate

Greek upper case letters

Π	Work [Nm]
Π_{int}	Internal work [Nm]
Π_{ext}	External work [Nm]

Greek lower case letters

β	Ratio between load circular frequency and natural circular frequency [-]
ε	Strain [-]
ε_0	Initial strain [-]
ε_r	Remaining strain [-]
$\dot{\varepsilon}$	Strain velocity [1/s]
$\dot{\varepsilon}_H$	Strain velocity for a Hooke material [1/s]
$\dot{\varepsilon}_N$	Strain velocity for a Newton material [1/s]
η	Viscous coefficient [Ns/m^2]
θ	Phase coefficient [rad]
θ_x	Rotation [rad]
κ_C	Transformation factor for the damping [-]
κ_{CP}	Combined transformation factor for the damping and external load [-]
κ_K	Transformation factor for the internal force [-]
κ_{KP}	Combined transformation factor for the internal force and external load [-]
κ_M	Transformation factor for the mass [-]
κ_{MP}	Combined transformation factor for the mass and external load [-]
κ_P	Transformation factor for the external load [-]
λ	Roots to the characteristic equatin
ξ	Damping coefficient [%]
ρ	Density [kg/m^3]
σ	Stress [N/m^2]
σ_0	Initial stress [N/m^2]
σ_H	Stress for a Hook material [N/m^2]
σ_N	Stress for a Newton material [N/m^2]
$\dot{\sigma}$	Stress velocity [N/m^{2}s]
τ	Shear stress [N/m^2]
υ	Poisson's ratio [-]
ϕ_i	Mode shape [rad]
ω	Circular frequency [rad/s]
ω_d	Damped circular frequency [rad/s]
ω_n	Natural circular frequency [rad/s]
ω_p	Load circular frequency [rad/s]

1 Introduction

1.1 Background

Recently the Swedish railway bridge codes were upgraded by the Swedish Railway Administration, Banverket, due to the structural requirements of bridges trafficked by high speed trains. Therefore all bridges subjected to high speed trains that have a speed of more than 200 km/h needs to be checked regarding their dynamic behaviour.

Dynamic analyses of railway bridges are today very complicated and time consuming, because of the large, complex 2D- and 3D computer models and the different load cases from high speed train models. Therefore the company Reinertsen has interest in examining the dynamic phenomena's and find out if there is a more simple way to analyse bridge structures than the 2D modelling.

1.2 Aim

The aim of this thesis is analysing and increasing the knowledge of the dynamic behaviour of railway bridges. This thesis should give a basic understanding of dynamic phenomena that causes bridges to oscillate and give a guidance of simplifications that can be made during modelling of bridges. The simplifications are mainly aimed to be used in the early stages in the design process and lead to simpler models than those used today. Further, the study aims to make it possible to decide if any of the high speed train models can be neglected.

1.3 Method

Literature studies have been done in order to find, understand and compile different simple methods used when analysing the behaviour of structures exposed for dynamic loads. Literature studies have also been made in order to get a deeper understanding of dynamics, their appearance and effects. The agreement between such simple methods is investigated by comparing results from simple models with the real behaviour, assumed to be found by using a multi degree finite element model. The finite element analyses are made by means of the commercial finite element software ADINA (2004).

1.4 Limitations

The methods described in this thesis, used in order to simplify analyses of structures subjected to dynamic loads, can be used on different types of deformable structures. However, only the application on single degree of freedom systems (SDOF systems) and simply supported beams are treated in this thesis.

The geometry on the investigated beams is chosen to be simple to make the dynamic analysis easier to understand.

When investigating the train load, only the model HSLM-A1 is used and the investigated responses are displacement, velocity and acceleration. The reason for using only one train model is due to the limited time for this thesis.

Complex material behaviour leads to complex calculations and expressions and therefore only idealized material behaviours; linear elastic and viscous elastic, are used here. When analysing the beam, only the traffic load generated by the train is taken into account.

Dynamic loads and their effects on railway bridges is a huge subject which requires long time to fully understand. Due to the limited time and in order to keep this scope within reasonable limits only SDOF systems and simply supported beams that are subjected to a dynamic load are discussed in this thesis.

1.5 General layout

The outline of the report can be divided into three major parts; basic theory (Chapters 2 to 5), design methods (Chapter 6) and finally problem descriptions and results (Chapters 7 to 10).

In chapters 2 to 5 the basic theories of material responses, dynamics and solution methods for differential equations are shown in order to facilitate the understanding for the rest of the report. Since analyses of the response of beams subjected to dynamic loads requires a good knowledge of dynamics and heavy calculations, not manageable to perform by hand, it is of interest to simplify these calculations. In Chapter 4 it is discussed how the response of beams subjected to dynamic loads can be calculated by transforming the beam to an equivalent single degree of freedom system (SDOF system) which will achieve the same displacement as a prescribed point in the beam, the so called system point. When beams are transformed to equivalent single degree of freedom systems, the transformation factors for the load, mass and the internal force are used, which are derived for linear elastic material.

Chapter 6 describes some of the rules that the Swedish railway administration has for designing bridges for train speeds above 200 km/h.

Chapters 7 and 8 describe the SDOF system and how it is examined for various types of loading. The responses of the SDOF system are calculated and the behaviour of the system is examined for both undamped and damped systems with various loading. Chapters 9 and 10 describe the finite element model of a simply supported beam that is investigated for various loading. The response of the beam is calculated by use of this finite element model and its behaviour is examined for both undamped and damped beams with various loading. The results from the finite element model are compared with the results from the SDOF system.

Chapter 11 presents conclusions and ideas on further investigations are presented.

2 Material

The response of a loaded structure is highly dependent of the choice of material and its behaviour. In this report only linear elastic material and viscous elastic material are discussed, where the behaviour of both linear elastic material and viscous elastic material is time dependent. This chapter will only describe the material responses and behaviour for a 1D model, but the principle is same for 2D and 3D models.

2.1 Linear elastic material

In a linear elastic material the stress is linear proportional to the strain and it is described with Hooke's law as:

$$\sigma = E\varepsilon \tag{2.1}$$

The proportional constant E is called the modulus of elasticity. The principle relation between stress and strain of a linear elastic material is shown in Figure 2.1(a). The linear elastic material can be described by a spring, see Figure 2.1(b). A loading of the structure with the stress $\sigma=\sigma_0$ gives the response of a strain ε_0. If the load is removed at time t_1 the strain will also disappear, see Figure 2.1(c-d).

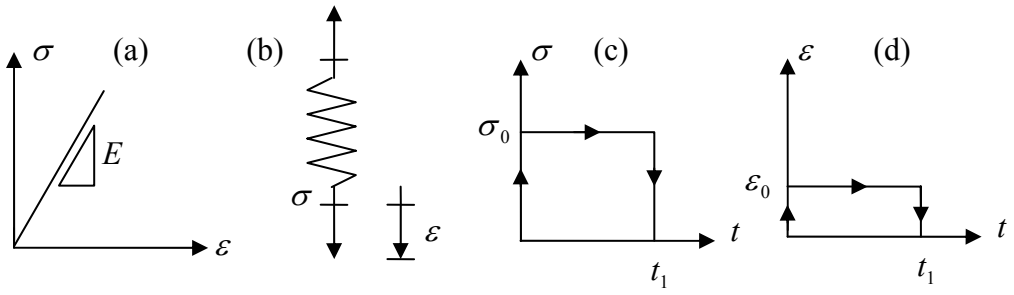

Figure 2.1: The behaviour of a linear elastic material.

The elastic force F_E in a 1D structure subjected to a load will thus be linear proportional to the displacement u, i.e.:

$$F_E = \sigma A = EA\varepsilon = \frac{EA}{L}u = ku \tag{2.2}$$

where k is the stiffness of the 1D spring. A principle relation between the elastic force and the displacement for a 1D linear elastic material is shown in Figure 2.2.

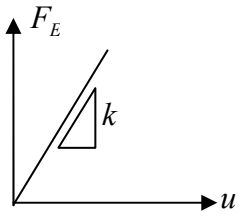

Figure 2.2: The principal relation between the elastic force and the displacement for a 1D linear elastic material.

2.2 Viscous elastic material

The deformations that arise from a linear elastic material are modelled to be time independent, but in reality all deformations in materials are time dependent. Time dependent elastic materials are called viscous elastic materials and the deformation can be divided into two different types of phenomena's; creep and relaxation. In a creep situation the strain increases with a constant stress, see Figure 2.3(a-b), and in a relaxation situation the stress decreases with a constant strain, see Figure 2.3(c-d). In this report the creep and relaxation are not further discussed. Viscous elastic materials can be described by different types of models, but in this thesis only models for a Newton material and a Kelvin material are discussed.

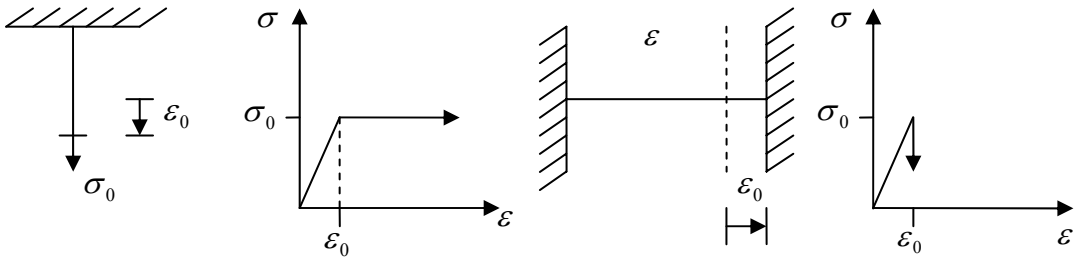

Figure 2.3: The creep and relaxation phenomena for a viscous elastic material.

2.2.1 Newton material

For a Newton material the constitutive relation is stated as:

$$\frac{d\varepsilon}{dt} = \dot{\varepsilon} = \dot{\varepsilon}_N = \frac{\sigma}{\eta} \tag{2.3}$$

The stress is linearly proportional to the time dependent strain and η is the constant of viscosity, see Figure 2.4(a). An instantaneous loading of the structure with the stress $\sigma=\sigma_0$ gives the response of a time dependent strain. If the load is removed at time t_1

the structure receives a remaining strain, see Figure 2.4(b-c), and the remaining strain is derived as:

$$\varepsilon_r = \int_0^{t_1} \left(\frac{\sigma_0}{\eta} \right) dt = \frac{\sigma_0 t_1}{\eta} \tag{2.4}$$

The Newton material can be described by a model of a damper, see Figure 2.4(d).

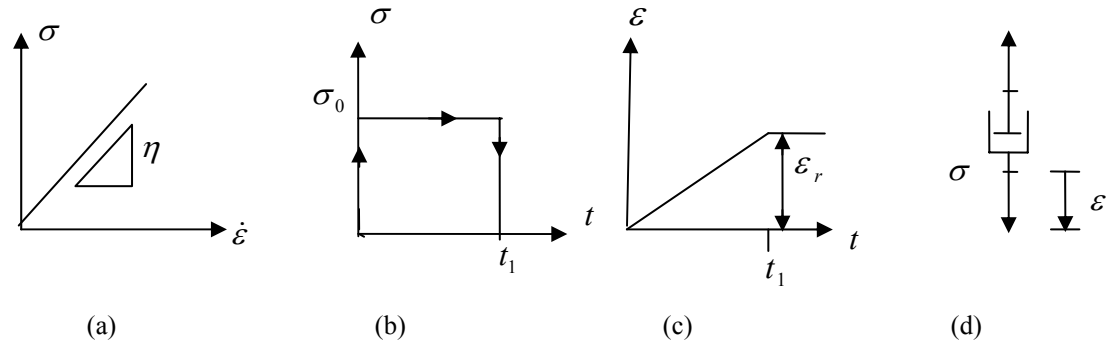

Figure 2.4: The behaviour for a Newton material.

The damping force F_D in a 1D structure with area A subjected to a load will thus be linearly proportional to the velocity $\dot{u}$, i.e.:

$$F_D = A\eta\dot{\varepsilon} = c\dot{u} \tag{2.5}$$

where c is the damping of the 1D structure. A schematic relation between the damping force and the velocity for a viscous elastic material is shown in Figure 2.5.

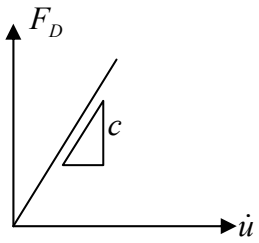

Figure 2.5: The principle relation between damping force and the velocity for a viscous elastic material.

2.2.2 Kelvin material

The Kelvin material consists of a parallel coupling between an elastic material and a viscous elastic material, i.e. Hooke and Newton material respectively, see Figure 2.6.

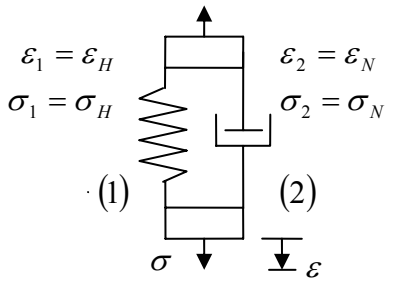

Figure 2.6: The model for a Kelvin material.

The constitutive relation and the differential equation for the Kelvin material can be derived as:

$$\sigma = \sigma_H + \sigma_N = E\varepsilon_H + \eta\varepsilon_N = E\varepsilon + \eta\dot{\varepsilon} \quad \text{where } \dot{\varepsilon} + \frac{E}{\eta}\varepsilon = \frac{\sigma}{\eta} \tag{2.6}$$

To be able to describe instantaneous loading of the structure with a stress $\sigma=\sigma_0$, the derivative of the strain has to be rewritten by use of the chain rule as:

$$\dot{\varepsilon} = \frac{d\varepsilon}{dt} = \frac{d\varepsilon}{d\sigma}\frac{d\sigma}{dt} = \frac{d\varepsilon}{d\sigma}\dot{\sigma} \tag{2.7}$$

By combining Equation (2.6) and Equation (2.7) gives:

$$\frac{d\varepsilon}{d\sigma} + \frac{1}{\dot{\sigma}}\frac{E}{\eta}\varepsilon = \frac{1}{\dot{\sigma}}\frac{\sigma}{\eta} \tag{2.8}$$

For instantaneous loading at time $t=0$ it holds that if $\dot{\sigma} \to \infty$ Equation (2.8) gives:

$$\frac{d\varepsilon}{d\sigma} = 0 \Rightarrow \varepsilon(\sigma) = \text{Constant}$$

$$\text{but since } \varepsilon = 0, \text{ when } \sigma = 0 \text{ this means that } \frac{d\varepsilon}{d\sigma} = 0 \tag{2.9}$$

The solution of Equation (2.6) with $t>0$ and $\sigma=\sigma_0$ is:

$$\varepsilon = Ce^{\frac{-E}{\eta}t} + \frac{\sigma_0}{E} \tag{2.10}$$

The initial condition of $\varepsilon(0)=0$ gives $C=-\sigma_0/E$ and the strain is then:

$$\varepsilon = \frac{\sigma_0}{E} - \frac{\sigma_0}{E} e^{\frac{-E}{\eta} t} \tag{2.11}$$

The instantaneous loading at t=0 affects at first the viscous part only which carries the whole stress $\sigma=\sigma_0$. When $t\rightarrow\infty$ the strain limit is obtained:

$$\varepsilon_\infty = \frac{\sigma_0}{E} \tag{2.12}$$

The strain at time t_1 is:

$$\varepsilon_1 = \frac{\sigma_0}{E} - \frac{\sigma_0}{E} e^{\frac{-E}{\eta} t_1} = \frac{\sigma_0}{E}\left(1 - e^{\frac{-E}{\eta} t_1}\right) \tag{2.13}$$

If the loading is released at time $t=t_1$, such that $\sigma(t<t_1)\neq 0$ and $\sigma(t_1)=0$, see Figure 2.4(b), this will give no jump in the strain ε according to Equation (2.9). The differential equation in Equation (2.6) can now be solved with the condition $\sigma(t_1)=0$.

$$t \geq t_1: \quad \dot{\varepsilon} + \frac{E}{\eta}\varepsilon = 0 \tag{2.14}$$

The differential equation has the solution:

$$\varepsilon = Ce^{\frac{-E}{\eta} t} \tag{2.15}$$

The initial condition is $\varepsilon(t_1)=\varepsilon_1$ according to Equation (2.14) which gives the solution of Equation (2.16):

$$\varepsilon = \varepsilon_1 e^{\frac{-E}{\eta}(t-t_1)} \quad \text{for } t > t_1 \tag{2.16}$$

When $t \rightarrow \infty$ means that $\varepsilon \rightarrow 0$ and there is no remaining deformation, see Figure 2.7.

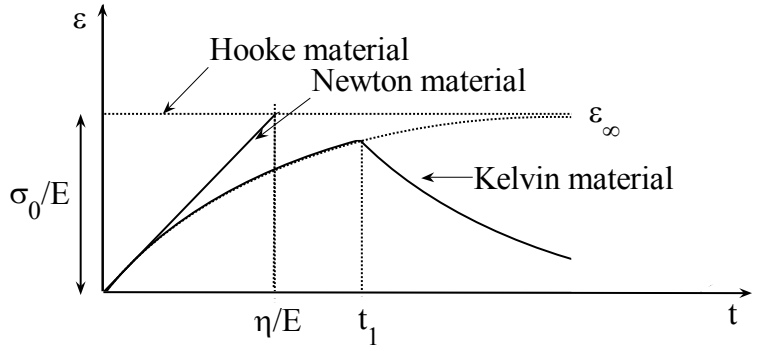

Figure 2.7: The behaviour of a Kelvin material.

3 Basic dynamics

The basic theory of dynamics includes both the terms of kinematics and kinetics. Kinematics describes the geometrical movement of a particle or a body in terms of displacement, velocity and acceleration, while kinetics is the science of a body movement caused by a force. This chapter treats free and forced vibrations, both damped and undamped. In the case of forced vibrations, only the case with systems excited by harmonic loads are treated and derived analytically. Later in this thesis, non harmonic loading is used and these cases are solved with numerical methods and then verified through comparison with results based on this chapter.

3.1 Kinematics

The linear motion of a particle is the simplest way to describe a movement of the particle. A particle P, see Figure 3.1, is restricted to move along the s-axis and the position is described by a function $f(t)$, where t is the time. At time t the particle has the position s and with a provided time step of Δt the particle moves a distance Δs.

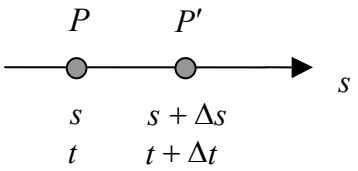

Figure 3.1: Linear motion of a particle.

3.1.1 Velocity

The velocity for the same particle as described in Figure 3.1 is derived by studying how fast the position of the particle is changing. When the time changes from t to $t+\Delta t$ the particle moves a distance Δs and by that the mean velocity during the movement can be stated as:

$$\bar{v} = \frac{\Delta s}{\Delta t} \tag{3.1}$$

The velocity of the particle is stated by letting the time step Δt go towards zero. That will lead to P' moves closer to P and the mean velocity will approach a boundary value. Therefore the velocity of the particle at time t is defined by the boundary value as:

$$v(t) = v = \lim_{\Delta t \to 0} \frac{\Delta s}{\Delta t} = \frac{ds}{dt} \equiv \dot{s} \tag{3.2}$$

When $v>0$, the particle movement is defined to be positive along the s-axis and negative when $v<0$.

3.1.2 Acceleration

It is often interesting to know how fast the velocity varies as the particle is moving, therefore the velocity of the particle is studied in the points P and P', see Figure 3.1. The particle in these points has a velocity of v and $v+\Delta v$ respectively. The mean value of the acceleration is defined as the mean velocity change per time unit with a particle movement from point P to P'. The mean value of the acceleration can be stated as:

$$\overline{a} = \frac{\Delta v}{\Delta t} \tag{3.3}$$

In the same way as when deriving the velocity of the particle the acceleration can be written as:

$$a(t) = a = \lim_{\Delta t \to 0} \frac{\Delta v}{\Delta t} = \frac{dv}{dt} \equiv \dot{v} = \frac{d^2 s}{dt^2} \equiv \ddot{s} \tag{3.4}$$

An important aspect of describing the particle movement is that there can occur several combinations of sign changes of the values v and a. In the case when the particle moves in a positive direction along the s-axis, the velocity has a positive value and an increasing acceleration will lead to an increasing velocity. If the acceleration would decrease, this instead corresponds to a decreasing velocity. The same phenomena occur if the particle moves in the negative direction along the s-axis, but instead with a negative velocity.

3.2 Kinetics

The response of bodies subjected to dynamic forces can be described by means of differential equations abbreviated as DE. This chapter will only describe linear vibrations with a single degree of freedom abbreviated as SDOF. In a SDOF system the position for the body is defined by one coordinate. Before deriving these equations of motion for dynamic loads the Newton's second law is defined.

3.2.1 Newton's second law

Newton's formulation of the second law is: "The change in the quantity of motion is proportional to the pressing force and occurs along the straight line, where the force is acting". This can be defined as an inertia force:

$$F_I = k \frac{d}{dt}(mv) \tag{3.5}$$

The quantity of motion corresponds to mv, the "change" corresponds to the derivative d/dt and k is a constant of proportionality. By using SI units, which will give k=1, and assuming that the mass is constant, Equation (3.5) can be written as:

$$F_I = \frac{d}{dt}(mv) = ma = m\ddot{s} \tag{3.6}$$

3.2.2 Single degree of freedom (SDOF) system

A simple SDOF system consists of a vertical spring and damper attached to a rigid body with a mass m, see Figure 3.2. The mass can move only in the vertical direction and therefore has only one degree of freedom. The spring is assumed to be light and linear elastic, with the stiffness k and damping c.

In a stable equilibrium position the force in the spring is equal to the gravity force of the mass. The force changes with the deformation of the spring, while the gravity force is independent of the position.

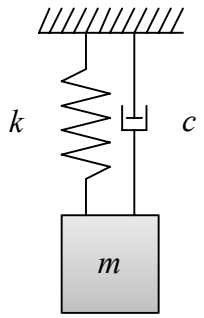

Figure 3.2: Mass-Spring system with single degree of freedom.

Dynamic vibrations occur when the system is disturbed from its stable equilibrium position. The disturbance creates internal forces that try to bring back the system to its equilibrium position and this phenomena causes oscillations. The system will oscillate around its equilibrium position until the damping has reduced the oscillation to zero and finally a new stable equilibrium has occurred.

3.2.3 Free vibration – Undamped

Consider a mass attached to a spring as illustrated in Figure 3.3. The unloaded equilibrium position for the system is noted as u_e and is the static equilibrium position when the dead weight is the only presented load. u is the coordinate describing the distance from the unloaded equilibrium position to the current position. The elastic force F_E for the system, described in Section 2.1, can be expressed as:

$$F_E = ku \tag{3.7}$$

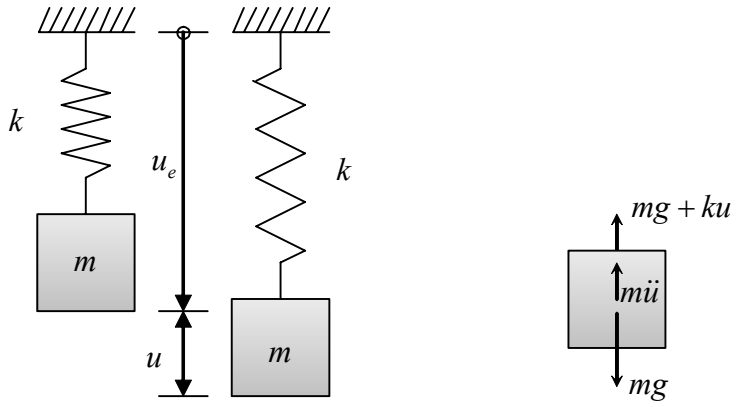

Figure 3.3: System with undamped free vibration.

When the body is moved a distance u from the unloaded equilibrium position and then released the system will undergo an undamped free vibration about the unloaded equilibrium position. The forces acting on the isolated body is shown in Figure 3.3 where mg is the dead weight of the system.

Due to dynamic equilibrium conditions the sum of the forces shall be zero.

$$mg - (mg + ku) - m\ddot{u} = 0 \tag{3.8}$$

where the displacement u varies in time i.e. $u=u(t)$.

The DE of motion is linear, homogenous and it has constant coefficients. The DE is defined as:

$$m\ddot{u} + ku = 0 \tag{3.9}$$

By introducing the circular frequency ω, Equation (3.9) can be written as:

$$\ddot{u} + \omega^2 u = 0 \text{ where } \omega = \sqrt{\frac{k}{m}} \text{ (Circular frequency)} \tag{3.10}$$

The general solutions of the differential Equation (3.10) are:

$$u(t) = A\sin(\omega t + \theta) \text{ or } u(t) = C_1 \sin\omega t + C_2 \cos\omega t \tag{3.11}$$

where the A and θ respectively C_1 and C_2 are constants of integration and they are determined from the boundary conditions.

When the system has started to oscillate, it will oscillate endlessly with the same amplitude A since the system is not affected by any kind of damping, see Figure 3.4.

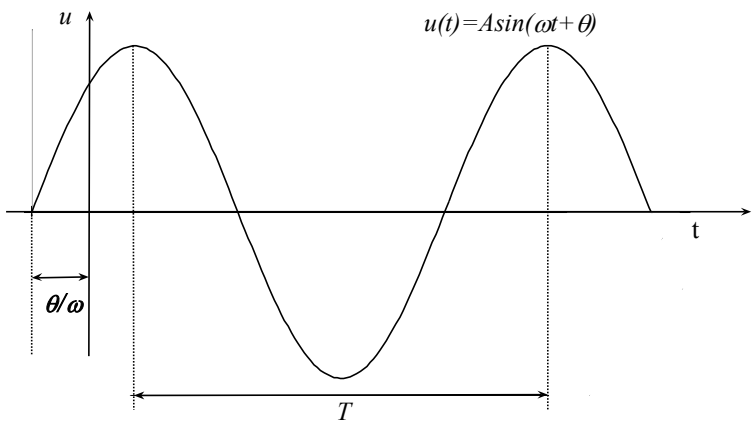

$|A|$ - Amplitude

$f = \frac{\omega}{2\pi}$ -Frequency

$T = \frac{1}{f} = \frac{2\pi}{\omega}$ - Period

$\omega t + \theta$ - Phase angular

(If A>0)

θ - Phase constant

Figure 3.4: Oscillation of an undamped system.

The oscillation can be described by terms of frequency f, amplitude A, phase constant θ and period T. The frequency for the system describes how often an occurrence appears during a time period. The phase constant determines the amount that $u(t)$ lags the function $sin\ \omega t$ and the period describes the time for an oscillation to move from one position and return to the same position. It should be remembered that this undamped case is a solely theoretical state. All structures in reality have some kind of damping.

3.2.4 Free vibration - Damped

Using the same notations as in the case of undamped free vibrations, see Section 3.2.3, and also taking the damping into consideration the differential equation of motion of a damped free system can be derived.

The system in Figure 3.5, reminds a lot about the Kelvin material described in Section 2.2.2. So, here the properties for the spring and damper are combined together. The damping of the system is noted as c and the damping force F_D for the system, described in Section 2.2.1, can be expressed as:

$$F_D = c\dot{u} \tag{3.12}$$

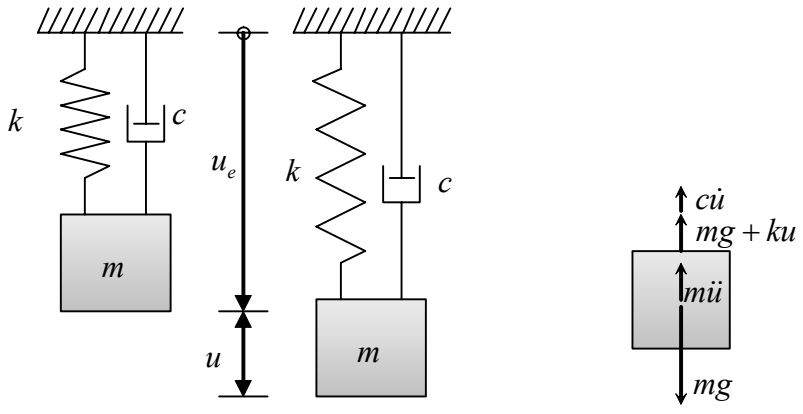

Figure 3.5: System with damped free vibration.

When the body is moved a distance u from the unloaded equilibrium position and then released the system will undergo a damped free vibration about the unloaded equilibrium position. The forces acting on the isolated body is shown above.

Due to dynamic equilibrium conditions the sum of the forces shall be zero.

$$mg - (mg + ku) - m\ddot{u} - c\dot{u} = 0 \tag{3.13}$$

where the displacement u varies in time i.e. $u=u(t)$.

The DE of motion is linear, homogenous and it has constant coefficients. The DE is defined as:

$$m\ddot{u} + c\dot{u} + ku = 0 \tag{3.14}$$

By introducing the damping coefficient ξ and the circular frequency ω, Equation (3.14) can be written as:

$$\ddot{u} + 2\xi\omega\dot{u} + \omega^2 u = 0 \text{ where } \xi = \frac{c}{c_{cr}} = \frac{c}{2\sqrt{km}} \text{ and } \omega = \sqrt{\frac{k}{m}} \tag{3.15}$$

As can be seen in Equation (3.15), ξ is a percentage of the critical damping c_{cr}, see Section 3.2.4.1. Setting $u=e^{\lambda t}$ gives the characteristic equation as:

$$\lambda^2 + 2\xi\omega u\lambda + \omega^2 = 0 \text{ with roots } \lambda_{1,2} = \left(-\xi \pm \sqrt{\xi^2 - 1}\right)\omega \tag{3.16}$$

Hence the general solution of the differential Equation (3.16) is:

$$u(t) = C_1 e^{\lambda_1 t} + C_2 e^{\lambda_2 t} \tag{3.17}$$

Depending on whether $\sqrt{\xi^2 - 1}$ is imaginary, real or zero, the value of $u(t)$ has different mathematical form:

Critical damping: $\xi = 1$ Strong damping: $\xi > 1$ Weak damping: $\xi < 1$

3.2.4.1 Critical damping $\xi = 1$

The two roots of Equation (3.16) have the same value and that leads to a solution that contains a polynomial. In this case of a first order equation as:

$$u(t) = (At + B)e^{-\omega t} \tag{3.18}$$

where A and B is constants of integration and they are determined from the boundary conditions. This function is also a non-periodic and has the same principal shape as in Figure 3.6.

3.2.4.2 Strong damping ξ >1

If the roots for Equation (3.16) are both real this result in a general solution as:

$$u(t) = C_1 e^{\lambda_1 t} + C_2 e^{\lambda_2 t} \tag{3.19}$$

where C_1 and C_2 are constants of integration that are real and determined from the boundary conditions.

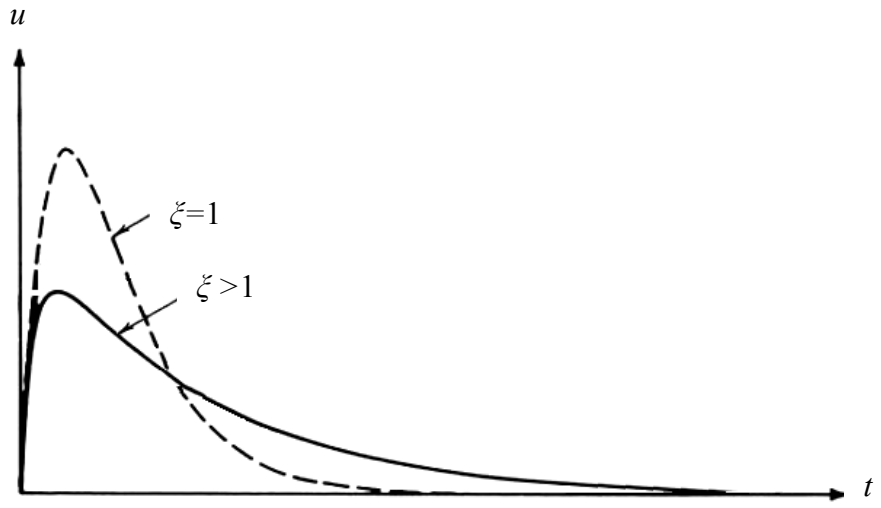

Figure 3.6: Example of typical oscillation of a damped system with critical and strong damping.

The boundary conditions for the system decide the curvature of the oscillation and a period can not be found. The amplitude approaches exponentially towards zero with time due to the roots of Equation (3.16) are negative, see Figure 3.6.

3.2.4.3 Weak damping ξ <1

If the roots for Equation (3.16) are imaginary, then the general solutions of the differential equation (3.14) are:

$$u(t) = e^{-\xi\omega t}\left(B_1 \sin \omega_d t + B_2 \cos \omega_d t\right) \text{ or } u(t) = Ae^{-\xi\omega t} \sin\left(\omega_d t + \theta\right) \tag{3.20}$$

where $\omega_d = \omega\sqrt{1-\xi^2}$ - Damped circular frequency

B_1 and B_2 are constants of integration that are real and determined from the boundary conditions.

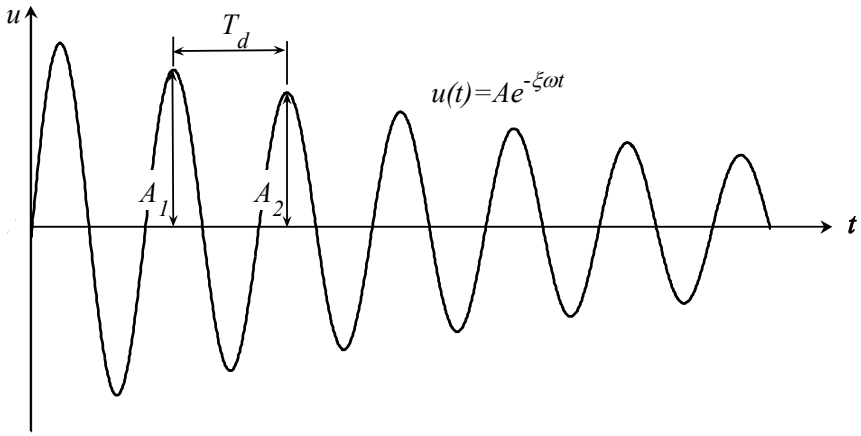

Figure 3.7: Oscillation of a damped system with weak damping.

The difference between the undamped and the weak damped case is that the amplitude is decreasing exponentially with time and the oscillation has a lower circular frequency ω_d, which leads to a longer period T_d, see Figure 3.7. According to Bergan and Larsen (1986), the case of critical and strong damping rarely or never occurs in real structures and therefore only weak damping will be treated further in this thesis. Whenever damping is discussed or mentioned it is the case of weak damping.

3.2.5 Forced vibration – Undamped with a harmonic load

Consider again the system shown in Section 3.2.3. Now the system is subjected to an external dynamic load $p(t)$ and in this case the damping is neglected as shown in Figure 3.8.

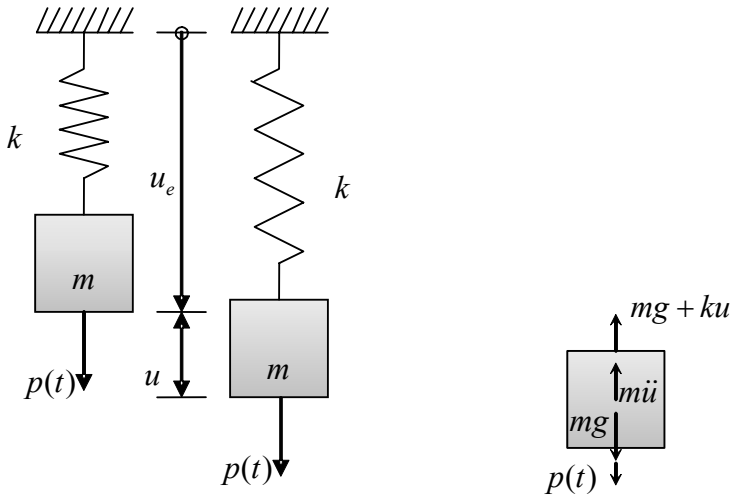

Figure 3.8: System with undamped forced vibration.

Due to dynamic equilibrium conditions the sum of the forces shall be zero.

$$mg + p(t) - (mg + ku) - m\ddot{u} = 0 \tag{3.21}$$

where the displacement u varies in time i.e. $u=u(t)$.

The DE of motion is linear, inhomogeneous and it has constant coefficients. The DE is defined as:

$$m\ddot{u} + ku = p(t) \tag{3.22}$$

Assume that the load in this case is harmonic and therefore periodic and has a shape of sinus function. The load is defined as:

$$p(t) = p_0 \sin \omega_p t \text{ where } \omega_p \text{ is the load circular frequency} \tag{3.23}$$

The DE with a harmonic load can thus be written as:

$$m\ddot{u} + ku = p_0 \sin \omega_p t \tag{3.24}$$

The general solution to the DE consists of a homogenous solution $u_h(t)$ and a particular solution $u_p(t)$. The system is undamped and therefore the homogenous solution is the same as in Equation (3.11). The general solution is defined as:

$$u(t) = u_h(t) + u_p(t) \text{ where } u_h(t) = C_1 \sin \omega t + C_2 \cos \omega t \tag{3.25}$$

Assume the particular solution as:

$$u_p(t) = C_3 \sin \omega_p t \tag{3.26}$$

The constant C_3 is solved by combing Equation (3.24) and Equation (3.26).

$$\left(-m\omega_p{}^2 + k\right) C_3 \sin \omega_p t = p_0 \sin \omega_p t \quad \text{where}$$

$$C_3 = \frac{p_0}{k - \omega_p{}^2 m} = \frac{p_0}{k} \frac{1}{1 - \left(\frac{\omega_p}{\omega}\right)^2} = \frac{p_0}{k} \frac{1}{1 - \beta^2} \quad \text{and} \quad \beta = \frac{\omega_p}{\omega} \tag{3.27}$$

The general solution for the DE is then:

$$u(t) = (C_1 \sin \omega t + C_2 \cos \omega t) + \frac{p_0}{k} \frac{1}{1 - \beta^2} \sin \omega_p t \tag{3.28}$$

where C_1 and C_2 are constants of integration that are determined from the boundary conditions.

3.2.6 Forced vibration – Damped with a harmonic load

Again consider the damped mass-spring system in Section 3.2.4 but now subjected to an external dynamic load $p(t)$ as shown in Figure 3.9.

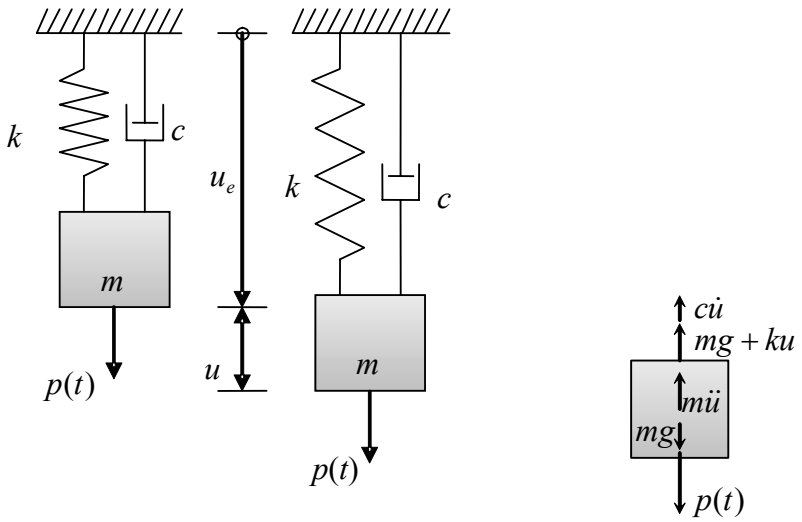

Figure 3.9: System with damped forced vibration.

Due to dynamic equilibrium conditions the sum of the forces shall be zero.

$$mg + p(t) - (mg + ku) - m\ddot{u} - c\dot{u} = 0 \tag{3.29}$$

where the displacement u varies in time i.e. $u=u(t)$.

The DE of motion is linear, inhomogeneous and it has constant coefficients. The DE is defined as:

$$m\ddot{u} + c\dot{u} + ku = p(t) \tag{3.30}$$

Assume that the load in this case is harmonic and therefore periodic and has a shape of a sinus function. The load is defined as:

$$p(t) = p_0 \sin \omega_p t \tag{3.31}$$

The DE with a harmonic load can be written as:

$$m\ddot{u} + c\dot{u} + ku = p_0 \sin \omega_p t \tag{3.32}$$

The general solution to the DE consists of a homogenous solution and a particular solution. The damping is assumed to be weak and therefore the homogenous solution is same as in Equation (3.20). The general solution is defined as:

$$u(t) = u_h(t) + u_p(t) \quad \text{where} \quad u_h(t) = e^{-\xi\omega t}\left(B_1 \sin \omega_d t + B_2 \cos \omega_d t\right) \tag{3.33}$$

Assume the particular solution as:

$$u_p(t) = C_1 \sin \omega_p t + C_2 \cos \omega_p t \tag{3.34}$$

The constant C_1 and C_2 are solved by combing Equation (3.32) and Equation (3.34).

$$\begin{aligned} C_1 &= \frac{p_0}{k} \frac{1-\beta^2}{\left(1-\beta^2\right)^2 + (2\xi\beta)^2} \quad \text{where } \beta = \frac{\omega_p}{\omega} \\ C_2 &= -\frac{p_0}{k} \frac{2\xi\beta}{\left(1-\beta^2\right)^2 + (2\xi\beta)^2} \end{aligned} \tag{3.35}$$

The particular solution for the DE is then:

$$u_p(t) = \frac{p_0}{k} \frac{1}{\left(1-\beta^2\right)^2 + (2\xi\beta)^2} \left[\left(1-\beta^2\right) \sin \omega_p t - 2\xi\beta \cos \omega_p t \right] \tag{3.36}$$

The general solution for the DE is then:

$$\begin{aligned} u(t) &= e^{-\xi\omega t} \left(B_1 \sin \omega_d t + B_2 \cos \omega_d t \right) + \\ &+ \frac{p_0}{k} \frac{1}{\left(1-\beta^2\right)^2 + (2\xi\beta)^2} \left[\left(1-\beta^2\right) \sin \omega_p t - 2\xi\beta \cos \omega_p t \right] \end{aligned} \tag{3.37}$$

where B_1 and B_2 are constants of integration that are determined from the boundary conditions.

The particular solution can be rewritten as one harmonic function.

$$\begin{aligned} u(t) &= u_p = R \sin\left(\omega_p t - \theta\right) \text{ where} \\ R &= \left(C_1^2 + C_2^2\right)^{\frac{1}{2}} = \frac{p_0}{k} \frac{1}{\sqrt{\left(1-\beta^2\right)^2 + (2\xi\beta)^2}} \text{ and} \\ \theta &= \arctan\left(-\frac{C_2}{C_1}\right) = \arctan\left(\frac{2\xi\beta}{1-\beta^2}\right) \end{aligned} \tag{3.38}$$

3.3 Resonance and dynamic amplification factor

Resonance occurs when the load circular frequency ω_p coincide with the natural circular frequency ω of the system. This results in a noticeable magnifying of the amplitude for the oscillation in the system. The effects of resonance for the system are described by a dynamic amplification factor abbreviated as *DAF*, which is dependent of the damping coefficient ξ, see Figure 3.10.

3.3.1 Undamped system

A real system is always affected by damping. This leads to that the homogenous solution in Equation (3.28) will die out and the particular solution will dominate. Assume that the boundary conditions for the undamped system are:

$$u(0) = u_0 = 0 \text{ and } \dot{u}(0) = \dot{u}_0 = 0 \tag{3.39}$$

Then the constant of integration C_1 and C_2 are solved from Equation (3.28) and the total solution is derived as:

$$u(t) = \left(\frac{\dot{u}_0}{\omega} - \frac{p_0}{k} \frac{\beta}{1-\beta^2} \right) \sin \omega t + u_0 \cos \omega t + \frac{p_0}{k} \frac{1}{1-\beta^2} \sin \omega_p t \tag{3.40}$$

Since the boundary conditions in Equation (3.28) describe that the system initially was in a stable equilibrium position, i.e. $u(0) = u_0 = 0$ and $\dot{u}(0) = \dot{u}_0 = 0$, the response can be stated as:

$$u(t) = u_{static} \frac{1}{1-\beta^2} \left(\sin \omega_p t - \beta \sin \omega t \right) \tag{3.41}$$

where $u_{static}=p_0/k$ describes the static displacement of the system. The dynamic amplification factor is derived by:

$$DAF = \left| \frac{u_p(t)_{\max}}{u_{static}} \right| = \left| \frac{1}{1-\beta^2} \right| \text{ where } \beta = \frac{\omega_p}{\omega} \tag{3.42}$$

The dynamic amplification factor increases rapidly when the load frequency closes the natural frequency of the system and decreases when it has larger frequencies.

3.3.2 Damped system

In a similar way as for the undamped system the dynamic amplification factor is derived from Equation (3.38) and the static response of the loaded system.

$$DAF = \left| \frac{u_{\max}}{u_{static}} \right| = \left| \frac{1}{\sqrt{\left(1-\beta^2\right)^2 + \left(2\xi\beta\right)^2}} \right| \tag{3.43}$$

The dynamic amplification factor has the same effects as in the undamped case, but it will be smaller when the system is damped, see Figure 3.10.

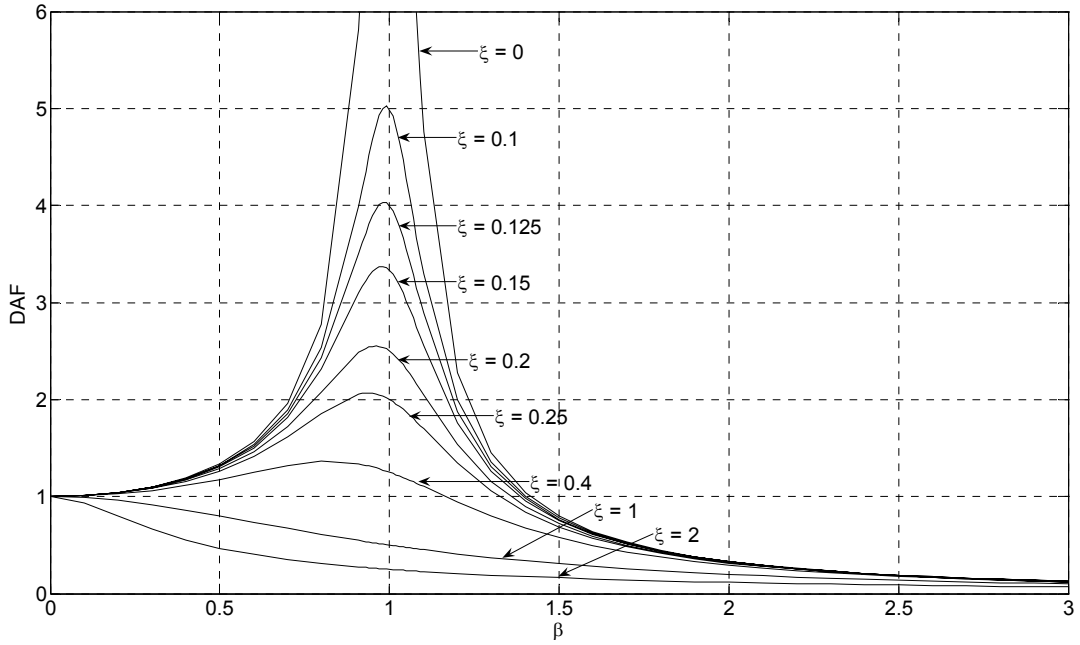

Figure 3.10 Illustrate the effects of DAF, damping coefficient and relationship between the load frequency and the natural frequency of the system.

4 Beam dynamics

4.1 Eigenmodes and frequencies for a uniform beam

For a structure, in this case a beam, the eigenfrequencies are the frequencies for which the structure will vibrate of its own accord when exposed to a perturbation. The different shapes of the structure for the different eigenfrequencies are called eigenmodes, and each eigenmode is related to one specific eigenfrequency.

To determine the beam response versus time the eigenmodes for a simply supported beam can be computed, by verifying the eigenvalue equation with the homogeneous boundary conditions.

$$EI\frac{d^4u}{dx^4} - \omega^2 mu = 0 \text{ for } 0 < x < l$$
$$u = \frac{d^2u}{dx^2} = 0 \text{ at } x = 0, l \tag{4.1}$$

After normalization they can be expressed as:

$$u_{(n)}(x) = \sqrt{\frac{2}{ml}}\sin\frac{n\pi x}{l} \text{ where } n = 1, 2, 3,\ldots.. \tag{4.2}$$

with the associated eigenvalues:

$$\omega_{(n)}{}^2 = (n\pi)^4\frac{EI}{ml^4} \tag{4.3}$$

The above stated expressions are based and derived from energy expressions for a continuous beam. An attempt to give a background and derive the expressions above, in a simplified way, can be seen in Appendix A.

In Figure 4.1, the three first eigenmodes for a simply supported beam are shown. The first eigenmode corresponds to the lowest eigenfrequency.

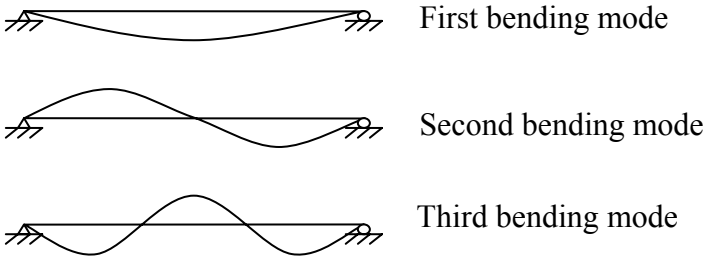

Figure 4.1: The three first eigenmodes for a simply supported beam.

Normally, when a beam is subjected to a dynamic load, the load frequency will not coincide with the eigenfrequencies and therefore the resulting shape of deformation

will not be the same as any of the eigenmodes. However, the dominating shape of deformation is usually the first eigenmode but it is influenced by higher modes. SDOF systems have only one eigenmode and hence there are no influences from higher modes.

4.2 Transformation from deformable body to SDOF system

To be able to simplify analyses of continuous systems, which have an infinite number of degrees of freedom, the system needs to be discretized to a finite number of elements and degrees of freedom. In practice, beams and plates have a limited possibility to move and this makes it possible to transform the structures into a single degree of freedom system, see Figure 4.2.

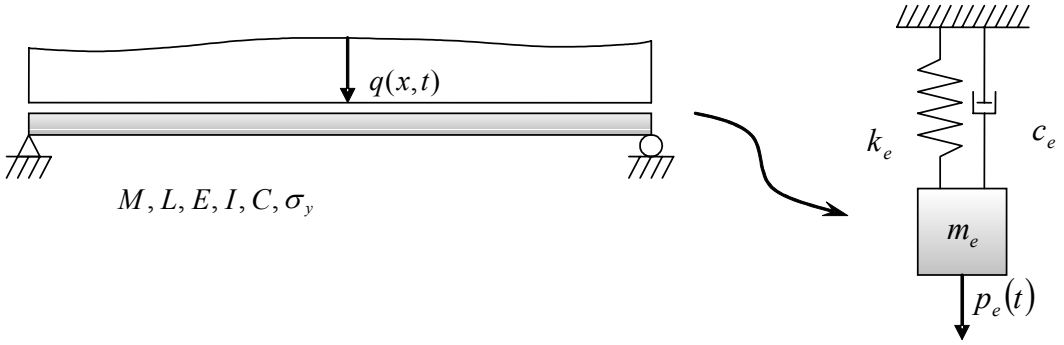

Figure 4.2: Transformation from continuous system to a SDOF system

The simplification to a SDOF system implies that the properties of the continuous system has to be assigned with equivalent quantities for the mass m, the internal force F_I, the damping force F_D and the load $p(t)$ applied to a certain system point. The deflection in the system point is assumed to be described by the same function as for the SDOF system. The system point is chosen to coincide with the point that normally will achieve the largest displacement, i.e. the midspan in the case of a simply supported beam, see Figure 4.3. One condition, for the transformation of the properties to be possible, is that a uniform change of the deformation is assumed. This means that if the displacement increases in one point the displacements in all other points will increase proportional to this displacement.

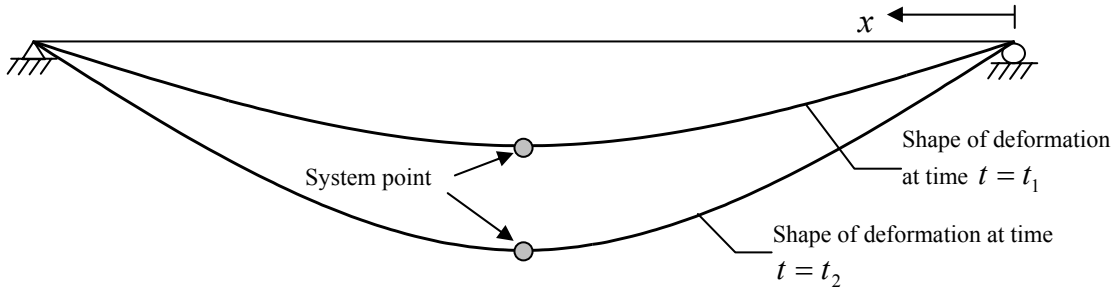

Figure 4.3: Illustration of the system point chosen to appear in midspan.

The transformation of the properties for the real structure to equivalent properties used in the SDOF system is made by use of transformation factors. The equivalent quantities and the transformation factors are derived from the condition that the energy exerted by the equivalent SDOF system must be equal to the energy exerted by the beam, when exposed to a certain load. Hence, the transformation factors will depend on the applied load and the deflection shape of the beam.

As discussed earlier in Section 3.2.6, the differential equation for the SDOF system in Figure 4.2 can be stated as Equation (3.30). Using the notations from Figure 4.2 the differential equation can be stated as:

$$m_e \ddot{u}_s + c_e \dot{u}_s + k_e u_s = p_e(t) \tag{4.4}$$

The equivalent quantities for the mass, internal force and the load can be expressed by means of transformation factors.

$$\kappa_M m \ddot{u}_s + c_e \dot{u}_s + \kappa_K k u_s = \kappa_P p(t) \tag{4.5}$$

Combining Equation (4.4) and (4.5), we obtain the definition of the transformation factors.

$$\kappa_M = \frac{m_e}{m} \tag{4.6}$$

$$\kappa_K = \frac{k_e u_s}{ku} \tag{4.7}$$

$$\kappa_P = \frac{p_e(t)}{p(t)} \tag{4.8}$$

If the expression in Equation (4.5) is divided with Equation (4.8), we can state three new transformation factors.

$$\kappa_{MP} = \frac{\kappa_M}{\kappa_P} \tag{4.9}$$

$$\kappa_{KP} = \frac{\kappa_K}{\kappa_P} \tag{4.10}$$

Now the expression in Equation (4.5) can be stated as:

$$\kappa_{MP} m \ddot{u}_s + c_e \dot{u}_s + \kappa_{KP} k u = p(t) \tag{4.11}$$

4.3 Transformation factors for beams

4.3.1 Transformation factor for the mass

In order to derive the transformation factor for the mass, the condition that the equivalent mass m_e shall generate the same amount of kinetic energy as the real system, when following the oscillation of the system point u_s, can be used.

The kinetic energy generated by the equivalent mass in the SDOF system is:

$$W_k^{SDOF} = \frac{m_e v_s^2}{2} \tag{4.12}$$

where $v_s = \frac{\Delta u_s}{\Delta t}$ is the velocity of the system point in the vertical direction.

The kinetic energy for the beam is:

$$W_k^{beam} = \int_{x=0}^{x=L} \frac{v^2}{2} \rho A dx \tag{4.13}$$

where x coordinate with origin in one end of the beam [m]

A cross-section area [m^2]

ρ density [kg/m^3]

$v = v(x) = \frac{\Delta u}{\Delta t}$ velocity of arbitrary point in the vertical direction [m/s]

Setting Equation (4.12) to be equal to Equation (4.13) this gives:

$$\frac{m_e v_s^2}{2} = \int_{x=0}^{x=L} \frac{v^2}{2} \rho A dx \quad \Leftrightarrow \quad m_e = \int_{x=0}^{x=L} \frac{v^2}{v_s^2} \rho A dx \tag{4.14}$$

The change of the displacement in an arbitrary point in the beam can be expressed as:

$$\Delta u = u(x,t_2) - u(x,t_1) = \alpha u(x,t_1) - u(x,t_1) = (\alpha - 1) u(x,t_1) \tag{4.15}$$

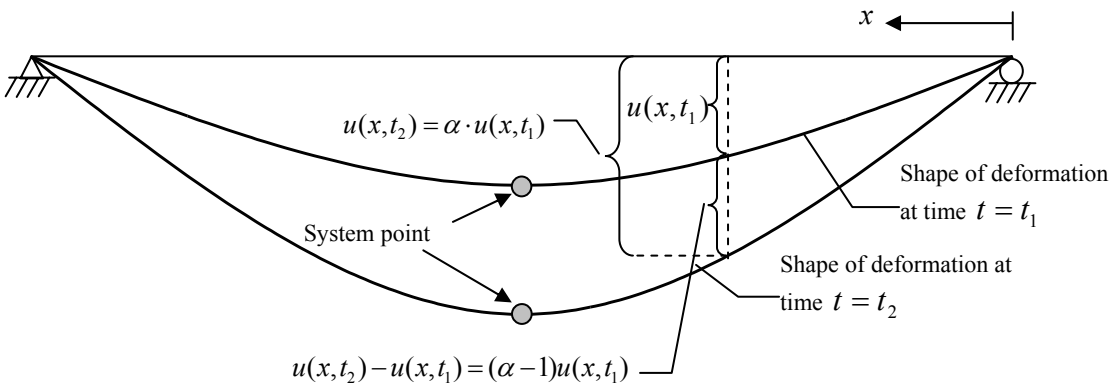

Figure 4.4: Illustration of the uniform change of displacement.

Where $u(x,t_1)$ is the displacement at time $t=t_1$ at the distance x from the end of the beam and $u(x,t_2)$ is the displacement at the same point in the longitudinal direction of the beam at time $t=t_2$. Due to that the change in displacement is uniform, it can according to Figure 4.4 be said that:

$$u(x,t_2)=\alpha(x,t_1) \tag{4.16}$$

The change of displacement in the system point, when time goes from $t=t_1$ to $t=t_2$, can be expressed as, see Figure 4.4:

$$\Delta u_s = u_s(t_2)-u_s(t_1)=\alpha u_s(t_1)-u_s(t_1)=(\alpha-1)u_s(t_1) \tag{4.17}$$

and since the assumption of uniform displacement in valid for all times t, the general form of Equation (4.15) and (4.17) can be written as:

$$\Delta u=(\alpha-1)u(x,t) \tag{4.18}$$

$$\Delta u_s=(\alpha-1)u_s(t) \tag{4.19}$$

Using Equation (4.18) and (4.19) together with that the velocity in any arbitrary point x in vertical direction can be expressed as $v=\Delta u/\Delta t$, Equation (4.14) can be rewritten as:

$$m_e=\int_{x=0}^{x=L}\frac{\left((\alpha-1)u(x,t)\right)^2}{\left((\alpha-1)u_s(t)\right)^2}\rho A dx=\int_{x=0}^{x=L}\frac{u(x,t)^2}{u_s(t)^2}\rho A dx \tag{4.20}$$

Now using Equation (4.6) together with the assumption of uniformly distributed mass along the beam length, the transformation factor for the mass can be written as:

$$\kappa_M=\frac{1}{m}\int_{x=0}^{x=L}\left(\frac{u(x,t)}{u_s(t)}\right)^2\rho A dx=\frac{1}{L}\int_{x=0}^{x=L}\left(\frac{u(x,t)}{u_s(t)}\right)^2 dx \tag{4.21}$$

i.e. the transformation factor for the mass is depending on the assumed shape of the deformation.

4.3.2 Transformation factor for the internal force

In order to derive the transformation factor for the internal load, the condition that the equivalent internal force shall perform a work that is equivalent to the work of the deformation of the beam, when following the oscillation of the system point u_s, can be used.

The internal force and the work it performs are depending on the behaviour of the material. For the SDOF system this is shown in Figure 4.5, where the shaded areas represent the total internal work for the material. $F_{I,\mathrm{e,max}}$ is the maximum value of the equivalent internal force. In the case of linear elastic material the maximum internal force is corresponding to $F_{I,e,\mathrm{max}}=K_e \cdot u_{s,\mathrm{max}}$.

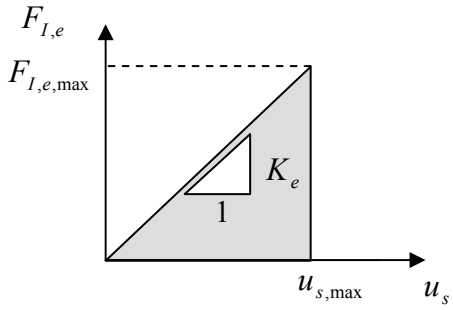

Figure 4.5: Work for a SDOF system for a linear elastic material.

The internal force for the SDOF system can be expressed by the the spring relation shown in Figure 4.5.

Linear elastic behaviour:

$$F_{I,e} = k_e u_s \tag{4.22}$$

where k_e is the stiffness of the linear spring in the SDOF system.

Following Samuelsson and Wiberg (1999) the work of deformation for the beam made of linear elastic material can be derived by studying a lamella of length Δx and the sectional forces, $\overline{N}$, and deformations, $\Delta\overline{n}$, belonging to it, see Figure 4.6.

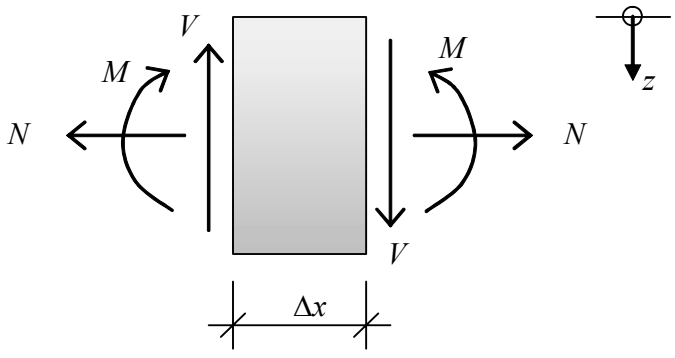

Figure 4.6: Segment, with length Δx, of the beam.

The constitutive relationship between the sectional forces $\overline{N}$ and the deformations $\Delta\overline{n}$ are:

$$\overline{N} = \frac{1}{\Delta x}\begin{bmatrix} EA & 0 & 0 \\ 0 & GA/\beta & 0 \\ 0 & 0 & EI \end{bmatrix}\Delta\overline{n} \quad , \quad \overline{N} = \begin{bmatrix} N \\ V \\ M \end{bmatrix} \; \Delta\overline{n} = \begin{bmatrix} \Delta n \\ \Delta t \\ \Delta m \end{bmatrix} \tag{4.23}$$

where	E	modulus of elasticity	[Pa]
	A	cross-section area	[m^2]
	$G = \frac{E}{2(1+\upsilon)}$	shear modulus	[Pa]
	υ	Poisson's ratio	[-]
	β	constant, shape factor	[-]
	I	moment of inertia	[m^4]

The meanings of the deformations Δn, Δt and Δm are shown in Figure 4.7 .

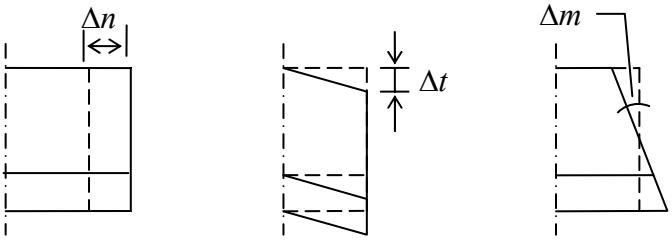

Figure 4.7: Deformation of beam lamella.

The constant β can be derived from the statement that the work of deformation due to shear force shall be equal to the work of deformation due to shear stress.

$$V\overline{\gamma} = V\frac{V\beta}{GA} = \int_{z=0}^{z=h} \tau(z)\gamma(z)b(z)dz \tag{4.24}$$

where	$\overline{\gamma} = \frac{V\beta}{GA}$	average value of shear angle	[-]
	τ	shear stress	[Pa]
	b	width of the cross-section	[m]
	h	height of the cross-section	[m]
	$\gamma = \frac{\tau}{G}$	shear angle	[-]

For a certain time in the loading the sectional forces will increase from $\overline{N}$ to $\overline{N}+d\overline{N}$ and the deformations will increase from $\Delta\overline{n}$ to $\Delta\overline{n}+d\Delta\overline{n}$. The change of the work of deformation is defined as the change of the work during the change of deformation $d\Delta\overline{n}$.

$$d\Pi_i^s = Nd\Delta n + Vd\Delta t + Md\Delta m \tag{4.25}$$

where index *s* and *i* stands for segment and internal respectively.

When using Hooke's law Equation (4.25) can be rewritten

$$d\Pi_i^s = \frac{EA}{\Delta x}\Delta n\ d\Delta n + \frac{GA}{\beta\Delta x}\Delta t d\Delta t + \frac{EI}{\Delta x}\Delta m\ d\Delta m = \overline{N}^t d\Delta\overline{n} \tag{4.26}$$

In order to get the total work of deformation of the segment, Equation (4.26) will be integrated over the deformation $\Delta\overline{n}$.

$$\begin{aligned}\Pi_i^s &= \int_{\Delta n=0}^{\Delta n}\frac{EA}{\Delta x}\Delta n\ d\Delta n + \int_{\Delta t=0}^{\Delta t}\frac{GA}{\beta\Delta x}\Delta t\ d\Delta t + \int_{\Delta m=0}^{\Delta m}\frac{EI}{\Delta x}\Delta m\ d\Delta m = \\ &= \left(EA(\Delta n)^2 + \frac{GA}{\beta}(\Delta t)^2 + EI(\Delta m)^2\right)\frac{1}{2\Delta x}\end{aligned} \tag{4.27}$$

Once again using Hooke's law and integrating the work of deformation for the segment over the length, *L*, of the beam will give the total work of deformation for the beam.

$$\Pi_i^{beam} = \int_{x=0}^{x=L}\frac{\Pi_i^s}{\Delta x}dx = \int_{x=0}^{x=L}\left(\frac{N^2}{EA} + \frac{\beta V^2}{GA} + M(x)u''(x)\right)\frac{1}{2}dx \tag{4.28}$$

If the influences from the normal- and shear forces are neglected the total work of deformation for the beam can be written as:

$$\Pi_i^{beam} = \frac{1}{2}\int_{x=0}^{x=L}M(x)u''(x)dx \tag{4.29}$$

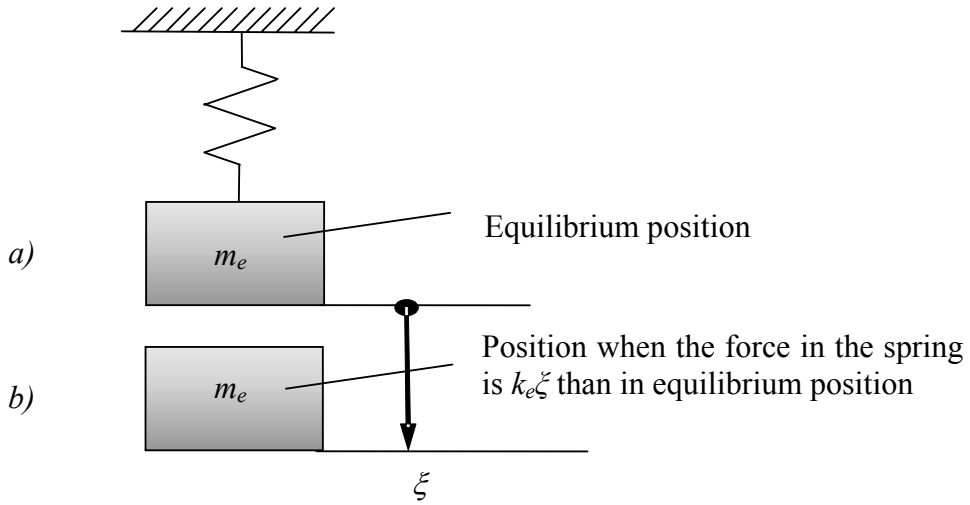

Figure 4.8: Mass in a) equilibrium and b) moved ξ from equilibrium position.

Study the undamped SDOF system in Figure 4.8. The displacement ξ causes an internal work for the SDOF system which by use of Equation (4.22) can be written as:

$$\Pi_i^{SDOF} = \int_{\xi=0}^{\xi=u_s} k_e \xi d\xi = \frac{k_e u_s^{\,2}}{2} = \kappa_K \frac{k u_s^{\,2}}{2} \tag{4.30}$$

As stated earlier the total internal work of the SDOF system shall be equal to the total work of deformation of the beam, meaning that Equation (4.29) shall be equal to Equation (4.30).

$$\kappa_K \frac{k u_s^{\,2}}{2} = \frac{1}{2} \int_{x=0}^{x=L} M(x) u''(x) dx \tag{4.31}$$

The stiffness k of the beam is depending on shape of the load and is determined by:

$$\int_{x=0}^{x=L} q(x,t) dx = k u_s \tag{4.32}$$

The definition of stiffness k of the beam according to Equation (4.32) together with Equation (4.31) gives the final expression of the transformation factor for the internal force when having a linear elastic material.

$$\kappa_K = \frac{1}{k u_s^{\,2}} \int_{x=0}^{x=L} M(x) u''(x) dx = \frac{1}{u_s} \frac{\int_{x=0}^{x=L} M(x) u''(x) dx}{\int_{x=0}^{x=L} q(x,t) dx} \tag{4.33}$$

For high beams it might be necessary to include the influences from the shear forces to get adequate results, see Section 4.3.5 for further discussion.

4.3.3 Transformation factor for the damping force

In the calculations no transformation factor for the damping force κ_c has been introduced, see Equation (4.11). Instead an equivalent damping c_e is used. In an attempt to guarantee that this assumption is correct, the two previous derived transformation factors are used. As mentioned earlier in Section 3.2.4, the damping c is a percentage of the critical damping c_{cr}:

$$c = \xi c_{cr} = \xi 2m\omega = \xi 2m\sqrt{\frac{k}{m}} = \xi 2\sqrt{km} \tag{4.34}$$

As can be seen in Equation (4.34), the damping is determined by the mass m and the stiffness k. By inserting the equivalent values derived earlier, and thereby adjusted, the expression for the equivalent critical damping can be stated as:

$$c_e = \xi c_{cr,e} = \xi 2m_e\omega = \xi 2m_e\sqrt{\frac{k_e}{m_e}} = \xi 2\sqrt{k_e m_e} \tag{4.35}$$

Later in the thesis this assumption is verified by comparing the results between different solution methods, see Section 10.2.2. Here the results between a SDOF solution using the regular c, and a solution based on the transformed equivalent c_e, are compared and shows coinciding results.

4.3.4 Transformation factor for the load

In order to derive the transformation factor for the load, the condition that the equivalent load shall generate the same amount of work as the total load does in the real system, when following the oscillation of the system point u_s, can be used.

The work generated by the equivalent load in the SDOF system during a time increment Δt is:

$$\Pi^{SDOF} = p_e(t)u_s(t) \tag{4.36}$$

The corresponding work for the beam is:

$$\Pi^{beam} = \int_{x=0}^{x=L} q(x,t)u(x,t)dx \tag{4.37}$$

where: x is the coordinate with origin at one end of the beam [m]

$\int_{x=0}^{x=L} q(x,t)dx = p(t)$ is the total load on the beam [N]

Due to the statement above, Equation (4.36) shall be equal to Equation (4.37).

$$p_e(t)u_s(t) = \int_{x=0}^{x=L} q(x,t)u(x,t)dx \quad \Leftrightarrow \quad p_e(t) = \int_{x=0}^{x=L} q(x,t)\frac{u(x,t)}{u_s(t)}dx \tag{4.38}$$

The transformation factor for the load, see Equation (4.8), can now be written as:

$$\kappa_P = \frac{\int_{x=0}^{x=L} \frac{u(x,t)}{u_s(t)} q(x,t)dx}{\int_{x=0}^{x=L} q(x,t)dx} \tag{4.39}$$

Also the transformation factor for the external load is depending on the assumed shape of deformation. It is further depending on the shape of the load.

4.3.5 Derived transformation factors for a simply supported beam

The values of the transformation factors for mass, load and internal force for the beam in Figure 4.9 are shown in Table 4.1. The system point is placed in the middle of the beam, as mentioned earlier in Section 4.2 and when having linear elastic material the natural shape of deformation, meaning the shape of deformation according to theory of elasticity for a beam subjected to a static load, is assumed.

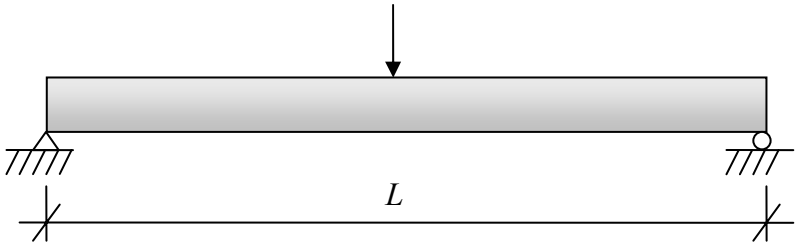

Figure 4.9: Simply supported beam loaded with a concentrated load in midspan.

Table 4.1: Transformation factors for a simply supported beam shown in Figure 4.9

Material	κ_P	κ_M	κ_K	κ_{MP}	κ_{KP}
Elastic	1.0	0.486	1.0	0.486	1.0

5 Numerical solution methods

Due to the dynamic equilibrium conditions for a damped system, from Equation (3.29) the force equilibrium can be stated as:

$$F_I(t) + F_D(t) + F_E(t) = p(t) \tag{5.1}$$

where $F_I(t)$ are the inertia forces, $F_D(t)$ are the damping forces and $F_E(t)$ are the internal forces and $p(t)$ are the external forces. The forces in Equation (5.1) are all time-dependent. From the equation of equilibrium governing the linear dynamic response this can be stated as:

$$M\ddot{U} + C\dot{U} + KU = P \tag{5.2}$$

where M, C and K are the mass, damping and stiffness matrices respectively and P is the vector of externally applied loads. U ,$\dot{U}$ and$\ddot{U}$ are the displacement, velocity and acceleration vectors. The Equation (5.2) is a linear DE of the second order with constant coefficients.

5.1 Direct integration methods

The direct integration method solves the Equation (5.2) through integration by using a numerical step-by-step procedure. The numerical integration is based upon two ideas. The first idea is trying to satisfy the Equation (5.2) in a discrete time interval Δt instead of satisfying it at any time t. The second idea is that the form of the assumption on the variation of the displacement, velocity and acceleration within each time interval Δt and the variation within this interval that determines the accuracy, stability and cost of the solution procedure.

In the direct integration method in Equation (5.2) it is assumed that at time t=0 the displacement, velocity and acceleration vectors are known and they are donated as ${}^0U$, ${}^0\dot{U}$ and ${}^0\ddot{U}$. The solution is made for the time span $0 \leq t \leq T$, where the time is divided into n time steps $\Delta t = T/n$. The step-by-step procedure calculates the solution to the next required time from the solutions at the previous times. Assume that the solutions at times $t_{t-\Delta t}$ and $t_{\Delta t}$ are known, then the next solution is calculated at time $t_{t+\Delta t}$. Finally the integration procedure will give an approximate solution to the DE within the time interval at times Δt, $2\Delta t$,…, t, $t+\Delta t$,..T. In this report only linear analysis will be used with a constant time step Δt.

5.1.1 The Newmark method

The Newmark method can be both explicit and implicit time integration, depending on the parameter values α and δ. The method solves the Equation (5.2) at time $t+\Delta t$ by using the equilibrium conditions at time $t+\Delta t$. According to Bathe (1996), the Newmark method is an extension of the linear acceleration method and it is based on the following assumptions of the velocity and the displacement:

$$
\begin{aligned}
{}^{t+\Delta t}\dot{U} &= {}^{t}\dot{U} + \left[(1-\delta)\,{}^{t}\ddot{U} + \delta\,{}^{t+\Delta t}\ddot{U}\right]\Delta t \\
{}^{t+\Delta t}U &= {}^{t}U + {}^{t}\dot{U}\Delta t + \left[\left(\frac{1}{2}-\alpha\right){}^{t}\ddot{U} + \alpha\,{}^{t+\Delta t}\ddot{U}\right]\Delta t^{2}
\end{aligned}
\tag{5.3}
$$

The parameters α and δ determines the accuracy and stability of the integration. When δ=1/2 and α=1/6, the relations between Equation (5.3) corresponds to the linear acceleration method, while δ=1/2 and α=1/4, the relations corresponds to the constant-average-acceleration method (also called trapezoidal rule). The trapezoidal rule is an unconditionally stable scheme, meaning that there is no demand on the incremental time step to reach a stable solution, see Figure 5.1.

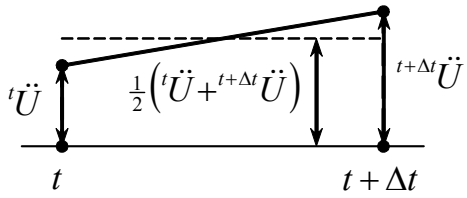

Figure 5.1: Newmark's constant-average-acceleration scheme.

The solution of the displacements, velocities and accelerations at time $t+\Delta t$ are achieved by combining Equation (5.3) and Equation (5.2). The implicit time integration is one of the available methods to solve dynamic problems in the finite element program ADINA. The complete solution procedure according to Bathe (1996) is shown in Table B.1 in Appendix B.

5.1.2 The central difference method

The central difference method is an explicit method that solves the DE by using the equilibrium conditions at time t instead of at $t+\Delta t$ as in the Newmark method. In this report the solution is valid for elastic and a viscous elastic material. The explicit method is a conditionally stable scheme, where the time step for the solution must be less than a certain critical time step, which depends on the smallest element size and the material properties.

5.1.2.1 Derivation of equation

The central difference method is derived from the Newmark method by using the values of δ=1/2 and α=0 in Equation (5.3). When combining the two equations with each other this leads to:

$$
{}^{t+\Delta t}U = {}^{t}U + {}^{t+\Delta t}\dot{U}\Delta t - \frac{1}{2}{}^{t+\Delta t}\ddot{U}\Delta t^{2} \tag{5.4}
$$

Thereafter using the definition of the velocity at time $t+\Delta t$, see Figure 5.2.

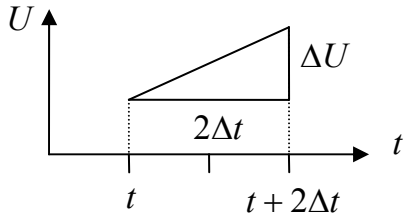

Figure 5.2: The definition of velocity.

The velocity can be derived as:

$$v(t) = v = \lim_{\Delta t \to 0} \frac{\Delta U}{\Delta t} = \frac{dU}{dt} \equiv \dot{U}$$

$$^{t+\Delta t}\dot{U} = \frac{1}{2\Delta t}\left(^{t+2\Delta t}U - {}^{t}U\right) \tag{5.5}$$

The acceleration and the velocity are approximated in terms of displacements, and by combining Equation (5.5) into Equation (5.4) and changing the variable $t+2\Delta t$ to $t+\Delta t$. The acceleration is derived as:

$$^{t}\ddot{U} = \frac{1}{\Delta t^2}\left(^{t-\Delta t}U - 2\,{}^{t}U + {}^{t+\Delta t}U\right) \tag{5.6}$$

The velocity is derived as:

$$^{t}\dot{U} = \frac{1}{2\Delta t}\left(-{}^{t-\Delta t}U + {}^{t+\Delta t}U\right) \tag{5.7}$$

The displacement is solved for time $t+\Delta t$ by considering equilibrium conditions in Equation (5.2) at time t:

$$M\,{}^{t}\ddot{U} + C\,{}^{t}\dot{U} + K\,{}^{t}U = {}^{t}P \tag{5.8}$$

By inserting Equation (5.6) and Equation (5.7) into Equation (5.8) gives:

$$\left(\frac{1}{\Delta t^2}M + \frac{1}{2\Delta t}C\right)^{t+\Delta t}U = {}^{t}P - \left(K - \frac{2}{\Delta t^2}M\right)^{t}U - \left(\frac{1}{\Delta t^2}M - \frac{1}{2\Delta t}C\right)^{t-\Delta t}U \tag{5.9}$$

From Equation (5.9) it can be seen that calculations of $^{t+\Delta t}U$ is dependent of ^{t}U and $^{t-\Delta t}U$. By solving the DE by the central difference method at time Δt, the step-by-step procedure needs a starting value of $^{t-\Delta t}U$. The values of ^{0}U, $^{0}\dot{U}$ and $^{0}\ddot{U}$ are known boundary conditions, therefore the value of $^{-\Delta t}\ddot{U}$ can be calculated by combing Equation (5.6) with Equation (5.7).

That gives:

$$^{-\Delta t}U = {}^{0}U - \Delta t \cdot {}^{0}\dot{U} + \frac{\Delta t^2}{2}{}^{0}\ddot{U} \tag{5.10}$$

To have a more effective procedure of solving the DE, the mass matrix and damping matrix are chosen to be diagonal. This results in that the mass matrix and the load vector can be lumped and introduced into Equation (5.9). The lumped mass matrix is calculated as:

$$\hat{M} = \frac{1}{\Delta t^2} M + \frac{1}{2\Delta t} C$$

$$\hat{M} = \begin{bmatrix} M_1 & 0 & . & 0 \\ 0 & M_2 & . & 0 \\ . & . & . & . \\ 0 & 0 & . & M_n \end{bmatrix} \tag{5.11}$$

The lumped load vector is calculated as:

$$^{t}\hat{P} = {}^{t}P - \left(K - \frac{2}{\Delta t^2} M \right) {}^{t}U - \left(\frac{1}{\Delta t^2} M - \frac{1}{2\Delta t} C \right) {}^{t-\Delta t}U \tag{5.12}$$

Using this, Equation (5.10) can be written as:

$$\hat{M}\, {}^{t+\Delta t}U = {}^{t}\hat{P} \tag{5.13}$$

The displacement at time $t + \Delta t$ is solved by using Equation (5.13):

$$^{t+\Delta t}U = \hat{M}^{-1}\, {}^{t}\hat{P} \tag{5.14}$$

5.1.2.2 Critical time step

To have accuracy of the solution based on the central difference method, the time step needs to be small enough. The time step should be smaller than the value of a critical time step, which can be calculated as:

$$\Delta t \le \Delta t_{cr} = \frac{T_n}{\pi} = \frac{2}{\omega_{\max}} \tag{5.15}$$

A time step that is too large is easily noticed from the solution, by that the responses of the displacements, velocities and accelerations grows very fast and finally becomes unrealistic. The complete solution procedure according to Bathe (1996) is shown in Table B.2 in Appendix B.

5.1.3 Rayleigh damping

The implicit time integration can be used both when the damping matrix is lumped or consistent, while the explicit time integration can be used only with lumped damping matrix and where the damping is mass proportional according to ADINA (2004).

If the damping is specified as Rayleigh damping, the contributions of the following damping matrix $C_{Rayleigh}$ are added to the total damping matrix C, which is described in Equation (5.2). The Rayleigh damping is defined as:

$$C_{Rayleigh} = \alpha M + \beta K \tag{5.16}$$

where M is the mass matrix in Equation (5.2), which can be lumped or consistent, and K is the stiffness matrix that corresponds to zero initial displacements. The Rayleigh damping constants α and β can be determined from a minimum of one given damping ratios ξ_i that correspond to two unequal circular frequencies of vibration ω_i and ω_j, see Figure 5.3.

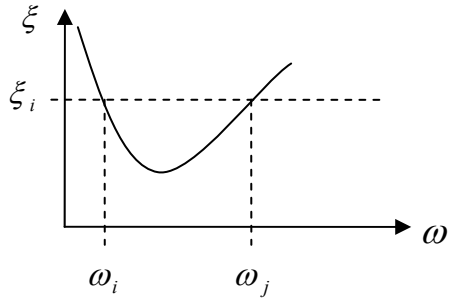

Figure 5.3: Damping as a function of frequency.

By using the two unequal circular frequencies the damping ratio can be stated in two different expressions as can be seen in Equation (5.17). The Rayleigh constants α and β are then determined by combining the two expressions with each other:

$$\xi_i = \frac{\alpha}{2\omega_i} + \frac{\beta\omega_i}{2} \text{ and } \xi_i = \frac{\alpha}{2\omega_j} + \frac{\beta\omega_j}{2} \tag{5.17}$$

A disadvantage with Rayleigh damping is that the higher modes are considerably more damped than the lower modes, for which the Rayleigh constants have been selected. Also the damping is incorrect for all other modes except for the two mode shapes related to the given circular frequencies.

The mass proportional damping in the explicit time integration is defined as:

$$C_{Rayleigh} = \alpha \hat{M} \tag{5.18}$$

Where $\hat{M}$ is the lumped mass matrix and the damping matrix $C_{Rayleigh}$ is replacing the damping matrix C in Equation (5.2).

5.2 Mode superposition

In mode superposition analysis, the governing DE equations are solved by substituting the following transformation into Equation (5.2):

$$U = \sum_{i=r}^{s} \phi_i u_i \tag{5.19}$$

where ϕ_i, $i=r,\ldots, s$ are the mode shapes calculated in a frequency analysis, and the u_i are the corresponding unknown generalized displacements. The displacements u_i are calculated by solving the decoupled modal equations:

$$\ddot{u}_i + 2\xi_i \omega_i \dot{u}_i + \omega_i^2 u_i = p_i \tag{5.20}$$

where ξ_i is the critical damping ratio corresponding to the circular frequency ω_i, and $p_i=\phi_i P$. This equation can be recognised from Chapter 3. The mode superposition method can be solved with many different time integration methods, but the Newmark method, following trapezoidal rule, is used in ADINA, see Equation (5.3). Mode superposition is effective when the time integration has to be carried out over many time steps. The cost of calculating the required frequencies and mode shapes is reasonable.

In the mode superposition method the damping is specified for each mode and the values of the modal damping ξ_i, $i=r,\ldots., s$ can all be different. The modal damping for each mode can be determined by using Rayleigh damping or it is also possible to define it directly for each mode in ADINA.

6 Swedish railway bridge code

6.1 BV BRO

The Swedish railway bridge code BV BRO, Banverket (2006), has rules for designing bridges for train speeds above 200 km/h, where dynamic calculations and controls shall be done for train speeds in the interval of 100 km/h until v_{max} +20%, where v_{max} is the theoretical design speed for the railway. The code also has limitation for vertical deformation and acceleration and they should be controlled for characteristic values of loading. The loading is presented in different train load models.

6.1.1 Vertical acceleration

The rules in the Swedish code say that calculations for vertical accelerations for a bridge deck shall be controlled for characteristic load values. Bridges that has a layer of ballast on the deck allows a maximum vertical acceleration of 3.5 m/s² within the ballast area. For bridges which are laid on sleepers the vertical accelerations are allowed for amount of 5.0 m/s². The vertical accelerations shall be controlled for frequencies up to 30 Hz.

6.1.2 High speed load models (HSLM)

There are two different types of train load models in the Swedish codes, HSLM-A and HSLM-B, where only the first one is used in this report. The train model HSLM-A consist of 10 different loading types, which all are theoretical idealisations of real trains, see Figure 6.1 and Table 6.1. This train model should always be used except for simple bridges, where HSLM-B should be used.

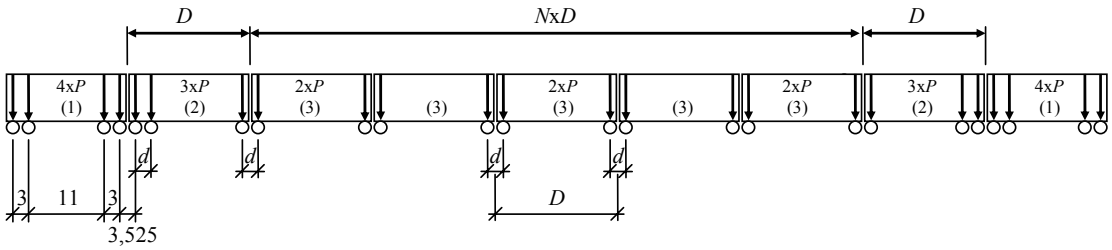

(1) Power car (leading and trailing cars identical)
(2) End coach (leading and trailing and coaches identical)
(3) Intermediate coach

Figure 6.1: The load distribution for train model HSLM-A.

Table 6.1: The load distribution for train model HSLM-A.

Train model	Number of intermediate coaches *N*	Coach length *D* [m]	Bogie axle spacing *d* [m]	Point force *P* [kN]
A1	18	18	2.0	170
A2	17	19	3.5	200
A3	16	20	2.0	180
A4	15	21	3.0	190
A5	14	22	2.0	170
A6	13	23	2.0	180
A7	13	24	2.0	190
A8	12	25	2.5	190
A9	11	26	2.0	210
A10	11	27	2.0	210

The model HSLM-B shall be used for simple bridges, for bridges with one span and a span length less than 7.0 m. By simple bridges means simply supported beam bridges and simply supported slab bridges. The model HSLM-B consists of *N* number of point loads with a value of 170 kN and a spacing of *d*, see Figure 6.2 - Figure 6.3.

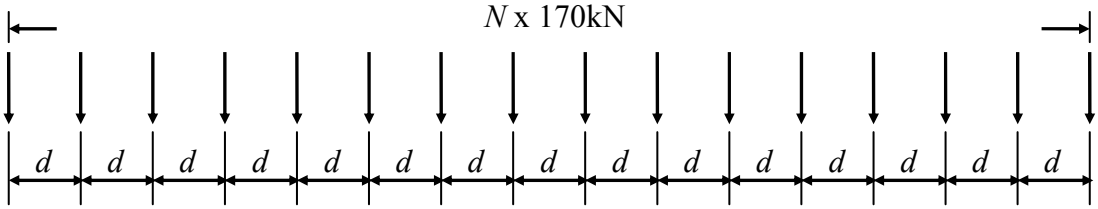

Figure 6.2: The load distribution for train model HSLM-B.

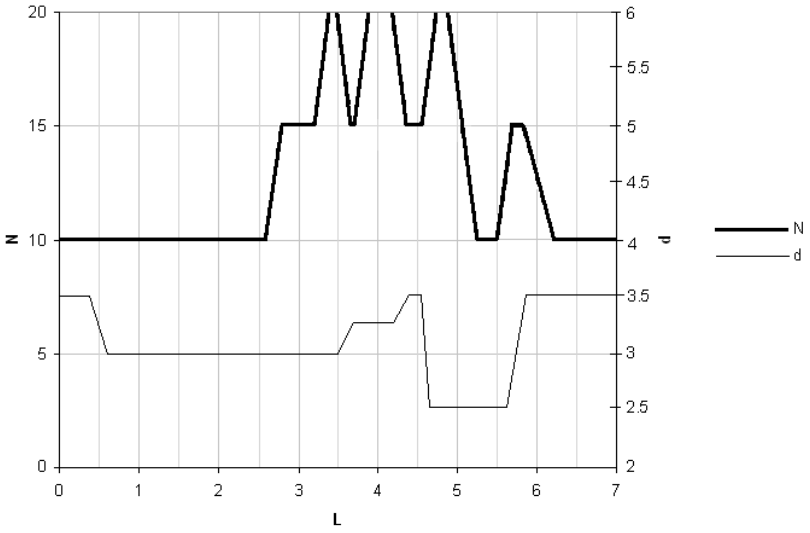

Figure 6.3: The spacing d between loads and number of loads N dependent on the span width.

6.1.3 Damping

During dynamic analysis of a bridge structure a damping factor is used. The damping factor is calculated according to Table 6.2, except if there is another value that describes the structure in a more accurate way.

Table 6.2: Damping factor for different spans and type of bridges.

Bridge type	ξ Lower limit of damping [%]	
	Span L < 20m	Span L ≥20m
Steel and composite	$\xi = 0{,}5+0{,}125(20\text{-}L)$	$\xi = 0{,}5$
Prestressed concrete	$\xi = 1{,}0+0{,}07(20\text{-}L)$	$\xi = 1{,}0$
Reinforced concrete	$\xi = 1{,}5+0{,}07(20\text{-}L)$	$\xi = 1{,}5$

6.1.4 Speed step

The speed step within the examined interval is allowed to be increased with a step of 5 km/h between every controlled speed. If resonance effect occurs, the steps at these velocities should be limited to 2.5 km/h, to find the most dangerous response of the structure.

7 SDOF analysis

7.1 General

During the first part of modelling, the aim is to get a basic knowledge of the dynamic behaviour of a SDOF system which is loaded by a harmonic load. This is done by using the analytical solution of the DE, derived in Chapter 3. Later on, the load is changed stepwise in an attempt to get more realistic and approach the actual load case from a real train. This change in load characteristic makes it complicated to use the analytical solution of the DE and therefore, also a numerical solution is used. The numerical solution used is in this case the central difference method previously described in Section 5.1.2. The result from the analytical solution is used to increase the knowledge of the dynamic behaviour of SDOF system and also to verify the numerical solution method.

When using the numerical solution different types of loading are used but the total impulse of each load pulse is kept constant in order to determine if some type of load is more dangerous than others. Finally a train load based on the train model HSLM-A is used as excitation of the SDOF system. The results from the analysis of a SDOF system will later be compared with the results from a finite element model. This in order to examine to what degree a simplified analysis, such as the SDOF system, can be used.

Based on the assumptions, material properties, load magnitude etc. used in the calculations and that will be presented later, none of the calculated values in the thesis are intended as real values, but are only intended as mutual comparison with each other. The inputs used have been chosen in order to simplify the comparison between different load cases.

All the solutions described in this chapter is programmed and solved with the commercial computer software MATLAB 7.0.1.

7.2 Analytical solution

7.2.1 Undamped system

To achieve a basic understanding, one of the first steps is to examine the effects of the displacements, velocity and acceleration for a SDOF system loaded by a harmonic load. The system, see Figure 7.1, is first assumed to be undamped and the analytical solution is derived from the Equations (3.22) and (3.23).

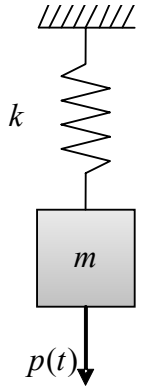

Figure 7.1: System with undamped forced vibrations.

If assuming that the system initially is at rest, the displacement can be stated as:

$$u(t) = \frac{p_0}{k}\frac{1}{\left(1-\beta^2\right)}\left(\sin\omega_p t - \beta\sin\omega t\right) \tag{7.1}$$

The velocity is stated as:

$$v(t) = \frac{p_0}{k}\frac{1}{\left(1-\beta^2\right)}\left(\omega_p\cos\omega_p t - \beta\omega\cos\omega t\right) \tag{7.2}$$

and the acceleration as:

$$a(t) = \frac{p_0}{k}\frac{1}{\left(1-\beta^2\right)}\left(-\omega_p{}^2\sin\omega_p t + \beta\omega^2\sin\omega t\right) \tag{7.3}$$

7.2.2 Damped system

By introducing a damper into the system in Figure 7.1, the system can be displayed as in Figure 7.2.

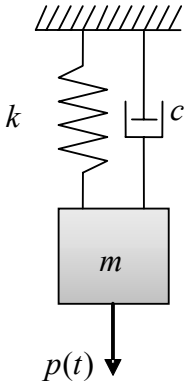

Figure 7.2: System with damped forced vibrations.

In the damped case the analytical solution is also derived from the equations presented in Chapter 3, but now with Equations (3.31) and (3.32). If assuming that the system initially is at rest the displacement can be stated as:

$$u(t) = G\left[e^{-\xi\cdot\omega\cdot t}\left[A\cdot\sin\omega_d t + \sin\theta\cos\omega_d t\right] + \sin(\omega_P t - \theta)\right] \tag{7.4}$$

where the constants A and G are:

$$\begin{aligned} A &= \left(\frac{\xi\omega}{\omega_d}\sin\theta - \frac{\omega_P}{\omega_d}\cos\theta\right) \\ G &= \frac{p_0}{k}\frac{1}{\sqrt{\left(1-\beta^2\right)^2 + \left(2\xi\beta\right)^2}} \end{aligned} \tag{7.5}$$

The velocity is stated as:

$$\begin{aligned} \dot{u}(t) = G\Big[e^{-\xi\omega t}\big[&\left(\omega_d A - \xi\omega\sin\theta\right)\cos\omega_d t - \left(\omega_d\sin\theta + \xi\omega A\right)\sin\omega_d t\big] \\ &+\omega_p\cos\left(\omega_p t - \theta\right)\Big] \end{aligned} \tag{7.6}$$

The acceleration is stated as:

$$\begin{aligned} \ddot{u}(t) = G\Big[e^{-\xi\omega t}\big[&\left(-\omega_d{}^2 A + \xi\omega\sin\theta\right)\sin\omega_d t - \left(\omega_d{}^2\sin\theta + \omega_d\xi\omega A\right)\cos\omega_d t - \\ &-\left(\xi\omega\omega_d A - \xi^2\omega^2\sin\theta\right)\cos\omega_d t + \left(\xi\omega\omega_d\sin\theta + \xi^2\omega^2 A\right)\sin\omega_d t\big] - \\ &-\omega_p\sin\left(\omega_p t - \theta\right)\Big] \end{aligned} \tag{7.7}$$

The complete derivation and solution, for both the undamped and damped case, can be seen in Appendix C.

7.2.3 Assumptions and analysed parameters

To simplify the analyses the calculations are made by assuming a natural frequency of the system to 1 Hz. By setting the load as p_0 and the stiffness as k and thereby considering the static deflection, $u_{static}=p_0/k$, in Equation (7.1) as a constant, the formulation can be calculated without any regard to applied load and stiffness of the spring. This leads to that the formulation in Equation (7.1) is only depending upon two parameters, which are the natural circular frequency ω and the circular frequency for the applied load ω_p.

Obviously, the influence of the ratio between the frequency of the applied load and the natural frequency of the system is of interest. The ratio is described by the circular frequency and stated as $\beta=\omega_p/\omega$. The influence on the system is examined for both the undamped and damped system, and the value of β is varied between 0.1-10. The main focus in this thesis is consistently on values of $\beta<1$, since it in reality is not

accepted that the ratio $\beta > 1$ for a load acting on a bridge. This in an attempt to guarantee that resonance is avoided, and therefore the train load should be considered as a slow load. $\beta > 1$ are therefore only examined by the analytical solution in order to capture the dynamic behaviour of the system and determine if there are any specific frequency ratios, except when ω_p is close or equal to ω, that are more dangerous than others.

Mainly during the analyses the damping factor is set to 2.5 %, but to determine the influence of the damping, the system is provided with different values of the damping factor ξ during excitation by the harmonic load. The reason for the damping factor to be chosen to be 2.5 % is based on damping factors normally used for bridges and the formulations in Table 6.2.

7.2.4 Excitation

Two different load cases were examined by using the analytical solution.

$$p(t) = p_0 \sin \omega_P t \qquad \text{Load case 1} \tag{7.8}$$

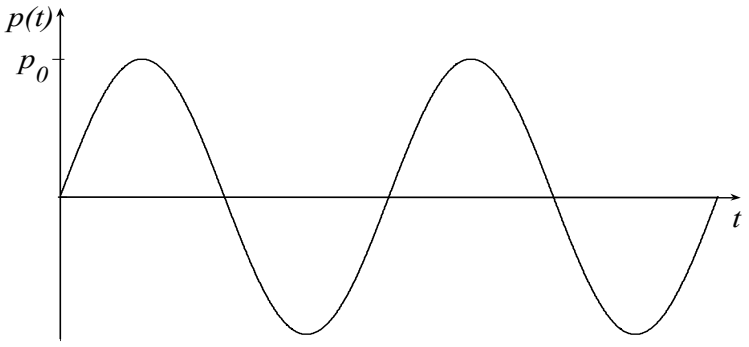

Figure 7.3: Load case 1, the original harmonic loading.

Load case 1 is the normal sinus function that oscillates around 0, see Figure 7.3.

$$p(t) = p_0 + p_0 \sin \omega_P t \tag{7.9}$$

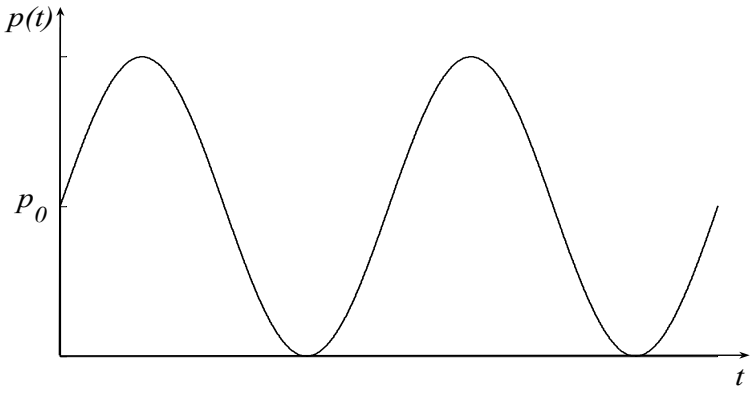

Figure 7.4: The uplifted harmonic loading.

Load case 2 is the same harmonic load as in load case 1 but with a change of equilibrium point and also a phase shift. The load is lifted so that the load oscillates around p_0 instead of around 0, see Figure 7.4 and Equation (7.9). This change is done to prevent that there are any negative values of the load, and to represent a more realistic load case.

$$p(t) = p_0 - p_0 \cos \omega_P t \qquad \text{Load case 2} \tag{7.10}$$

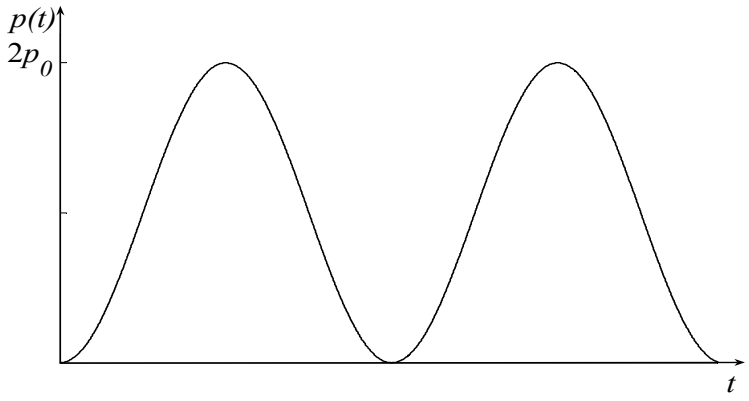

Figure 7.5: Load case 2, the uplifted harmonic loading with an angular shift.

In order to prevent the instantaneous loading p_0 that occur in Figure 7.4, an angular shift is introduced to retrieve the load in load case 2, see Figure 7.5 and Equation (7.10). Now the load do not starts so suddenly and therefore corresponds more to a real train load.

7.3 Numerical solution

7.3.1 Numerical formulation

The calculations made with the numerical solution are, as mentioned earlier, based upon the central difference method. From Section 5.1.2 it can be seen that the formulations for the displacement ${}^{t+\Delta t}U$ can be stated as:

$${}^{t+\Delta t}U = \left[{}^{t}P - \left(K - \frac{2}{\Delta t^2} M \right) {}^{t}U - \left(\frac{1}{\Delta t^2} M - \frac{1}{2\Delta t} C \right) {}^{t-\Delta t}U \right] \left[\frac{1}{\Delta t^2} M + \frac{1}{2\Delta t} C \right]^{-1} \tag{7.11}$$

with the damping matrix C as:

$$C = 2M\omega\xi \tag{7.12}$$

and the velocity ${}^{t}\dot{U}$ and the acceleration ${}^{t}\ddot{U}$ as:

$${}^{t}\dot{U} = \frac{1}{2\Delta t} \left(-{}^{t-\Delta t}U + {}^{t+\Delta t}U \right) \tag{7.13}$$

$$ {}^{t}\ddot{U} = \frac{1}{\Delta t^{2}}\left({}^{t-\Delta t}U - 2{}^{t}U + {}^{t+\Delta t}U\right) \tag{7.14} $$

The calculations have been made mainly for the damped case, but for calculations for the undamped case the damping matrix C in Equation (7.12) is set to zero.

7.3.2 Assumptions and analysed parameters

As mentioned in Section 7.2.4, two load cases are analysed by analytical calculations. By using a numerical method several more load cases for the SDOF system are to be examined. There are three different types of loads used: sinusoidal-, rectangular- and triangular-shaped, and after applying different combinations there are a total of five different load cases. The sinusoidal load is the same as the harmonic load in the analytical solution. The response of the system is calculated in terms of displacement, velocity and acceleration. The different types of excitations are tested and compared with each other in an attempt to determine if some types are more dangerous than others, and then the triangular loads are used to model the train load.

To be able to keep the calculations as simple as possible also in the numerical analyses, the natural frequency is set to be equal to 1 Hz. In this case it is not possible to consider the static deflection as an independent constant, and therefore it has to be kept in the formulation. As can be seen in Equation (7.11), the numerical expression is dependent of the mass M, stiffness K, damping C and applied load P. To keep the natural frequency equal to 1 Hz, the mass and stiffness have to be adjusted. By assuming that the mass is equal to 1 kg, the stiffness can be set to $(2\pi)^2$ to receive f_n=1 Hz.

As for the analytical solution described in Section 7.2, the same parameters are of interest and studied here. When damping is introduced to the system the damping factor is set to 2.5 % in all cases.

Further it is studied what influence a change in the natural frequency f_n has on the system, when the value of the load frequencies f_{p1} and f_{p2} are kept constant.

7.3.3 Excitation

Load case 1 and 2, i.e. the two harmonic load cases that also are used in the analytical analysis, are mainly used as a verification of the numerical solution. By comparing the results from the numerical analysis with the analytical result, the numerical analysis can be verified.

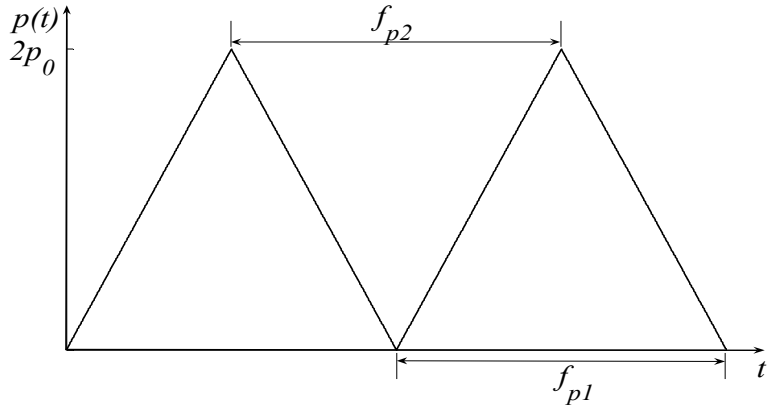

Figure 7.6: Load case 3, the continuous triangular loading.

The third load consists of a continuous triangular load, see Figure 7.6. The triangle is basically a simplification of the sinusoidal load in load case 2, see Figure 7.5, and has the same total area. The triangular load is dependent of the two frequencies f_{p1} and f_{p2}, where the width of the load is described by the frequency f_{p2} and the distance between the peaks by frequency f_{p1}, see Figure 7.6. In this case where it is continuity in the load, f_{p1} and f_{p2} will be equal, and here the continuity is based on a system that is not unloaded at any time. The result from this load case is compared with load case 2, because they have similar shape, and to elucidate if there are any differences even though they have similar load shape and area.

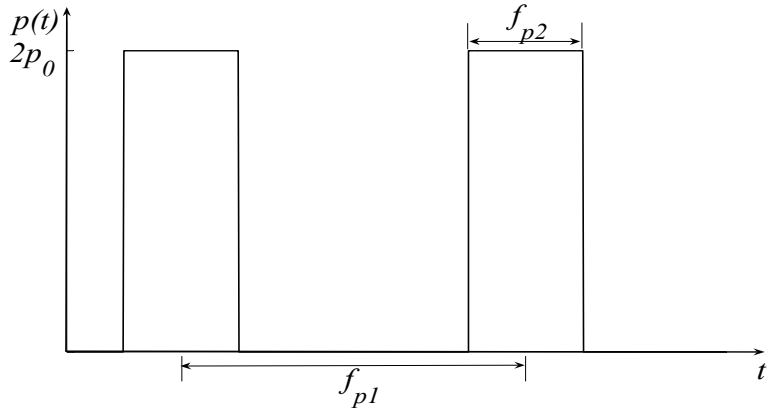

Figure 7.7: Load case 4, the rectangular loading.

The fourth load case consists of a rectangular load, and this load is an attempt to describe the bogie axle load generated by the train, described in Section 6.1.2, with only one impulse. The width of the load is dependent of the frequency f_{p2} and the distance between the peaks by frequency f_{p1}, see Figure 7.7. The area under the continuous triangular load and the rectangular load is chosen to be equal.

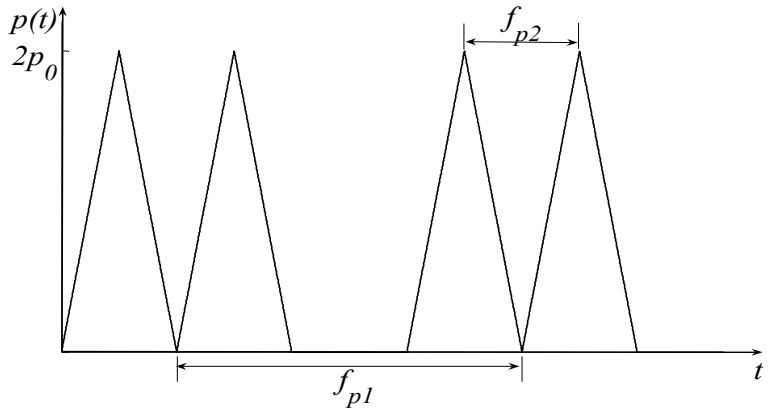

Figure 7.8: Load case 5, the double triangular loading.

The fifth load case consists of a double triangular load, which is intended to describe the bogie axle load from a train. The width of the double load is dependent of the frequency f_{p2} and the distance between the pairs by the frequency f_{p1}, see Figure 7.8. The area under the rectangular load and the double triangular load is chosen to be equal in order to achieve values fairly related to each other. To compare the double triangular and rectangular load directly in the same way as between the previous load cases are impossible. When transforming the continuous triangular load into the rectangular load, the frequency $f_{p1}=2f_{p2}$ in order to keep the same area of the load pulse. When transforming the rectangular load into the double triangular load, the area is divided into two impulses and will therefore generate a continuous triangular load with a frequency increased by a factor 2. To avoid this problem the frequency ratio f_{p1}/f_{p2} needs to be larger than 2.

7.3.4 Train load

The final train load is based on the same principle as load case 5, seen in Figure 7.8, consisting of double triangular loads that represent the bogie axle loads from the train. Each load represents one wheel of the train and is simulated as a triangular. The size of f_{p1} and f_{p2} is determined by the HSLM-A load cases stated by the Swedish railway bridge code, see Table 6.1. To simplify the analysis, the natural frequency, as mentioned earlier, is set to 1 Hz. In order to adjust the train loads from HSLM-A to the simplified system, the load frequencies f_{p1} and f_{p2} are built up by assuming that the train resonance velocity is D m/s. As can be seen in Section 6.1.2, the HSLM-A model is built up in terms of coach length D and bogie axle spacing d. Taking the train load A1 as example, see Table 6.1, with D=18 m and d=2 m it means that the train loads resonance velocity is 18 m/s. Hence β=0.1 gives a train velocity v=1.8 m/s, see Figure 7.9.

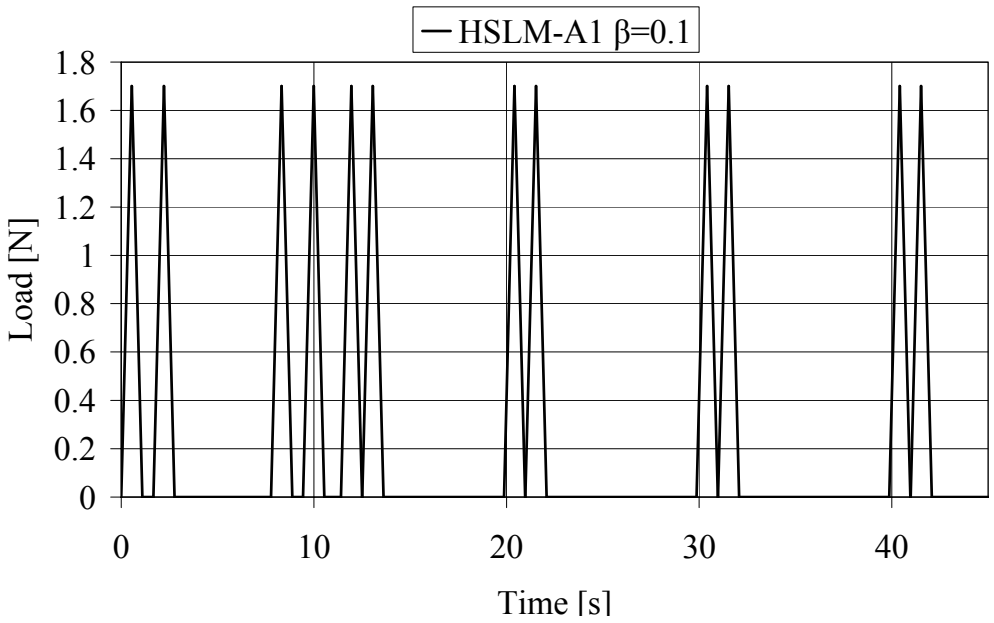

Figure 7.9: Train load HSLM-A1 with β=0.1, i.e. loading generated by a train velocity v=1.8 m/s. The figure displays the power car, end coach and the two first intermediate coaches.

As can be seen in Table 6.1 there are different values on the load for the different models. Earlier, to keep the system as simple as possible, the unit load 1 N is used. To keep the simplicity and to be able to make comparison between different trainloads, the loading needs to keep its mutual relationship. Therefore the tabled load values are divided by 10^5, i.e. the load for A1 is P_{A1}=1.7 N.

8 Results of SDOF analysis

The results presented in this chapter are valid for an undamped and damped system based on the solution methods in the previous chapter. As mentioned, none of these received values of velocities and accelerations are relevant in real calculations, but intended as mutual comparisons. The focus of interest is on the results for β <1 and therefore only results from these values are presented in this section. Apart from analysis concerning the influence of damping in the system where a varying value of the damping factor has been applied, the damping factor is set to 2.5 % as described earlier in Section 7.2.3.

8.1 Analytical solution

In this section the results from the analytical analysis is presented. The system is here only loaded by a harmonic load, i.e. load case 1 and 2, see Figure 8.1 and Appendix D.

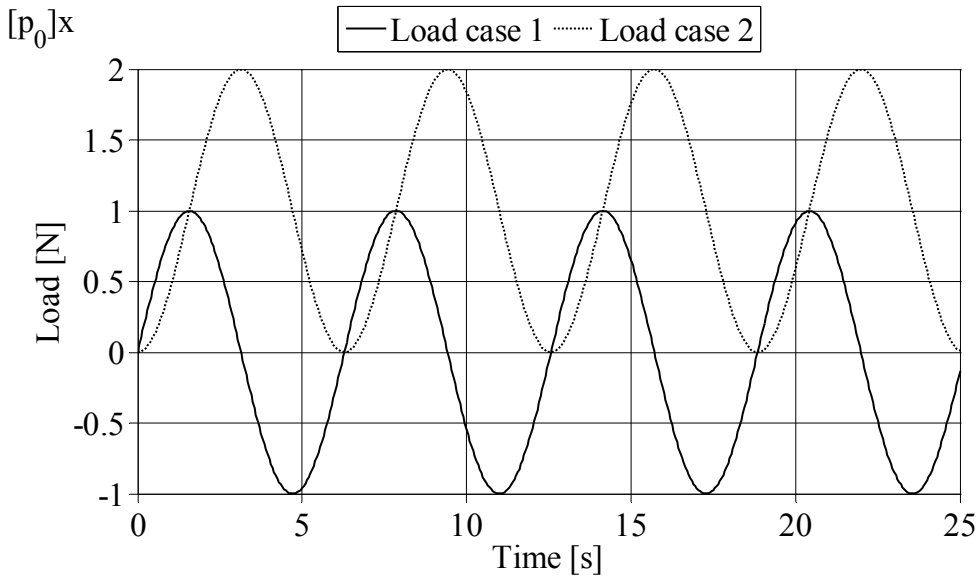

Figure 8.1: Different harmonic loads acting on the system in the analytical solution.

8.1.1 Undamped system

Remembering the undamped system displayed in Figure 7.1, excited by a harmonic load as seen in Figure 8.1, the system response in terms of displacement, velocity and acceleration is calculated.

As can be seen in Figure 8.2 - Figure 8.3, the system response for an undamped system that is loaded by a harmonic force, is increasing when $\beta \rightarrow 1$. When β=1 resonance effects appear in the system and the highest responses are achieved. If the value of β >1 and increases, i.e. $\beta \rightarrow \infty$, the system response have the opposite effect

than described previously. The response starts to decrease with increased value of β. However, as stated in the beginning of this chapter these solutions for $\beta > 1$ will not be treated any further in this thesis. The maximum and minimum values of displacement and acceleration for $\beta < 1$, are listed in Table 8.1

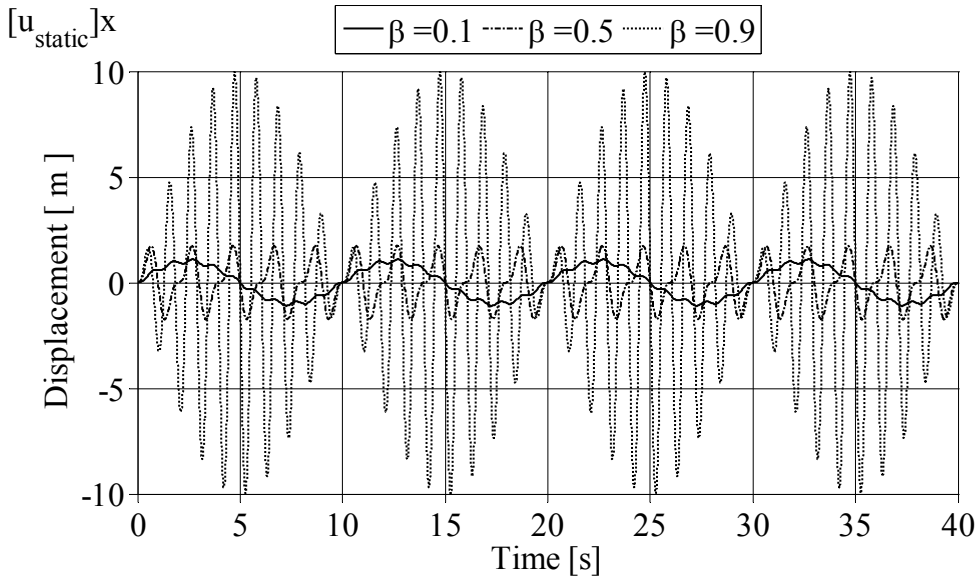

Figure 8.2: Displacements for load case 1 with β=0.1, β=0.5 and β=0.9.

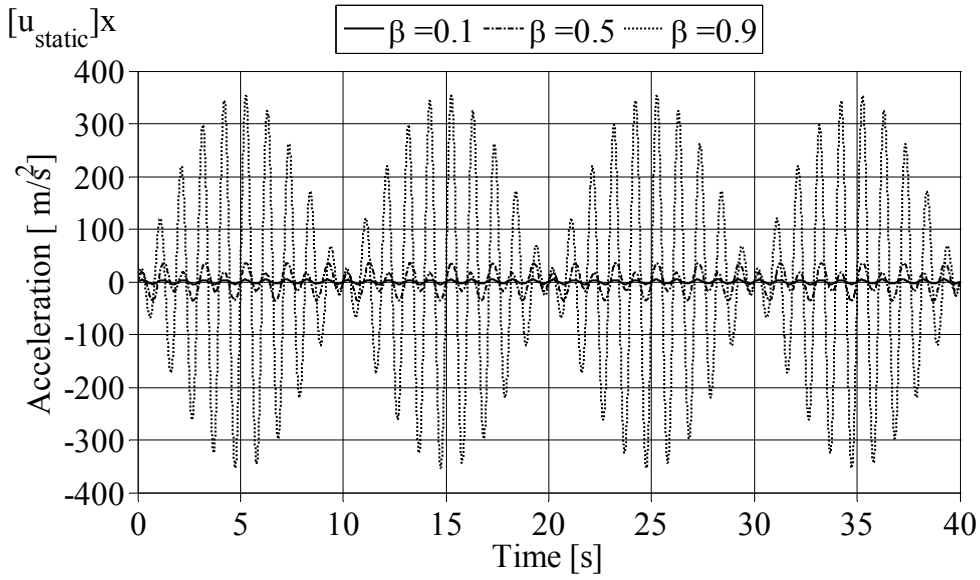

Figure 8.3: Accelerations for load case 1 with β=0.1, β=0.5 and β=0.9.

Table 8.1: Maximum and minimum values of displacement and acceleration for the undamped case, load case 1.

β	0.1	0.2	0.3	0.4	0.5	0.6	0.7	0.8	0.9
U_{max}	1.0998	1.0825	1.4182	1.6249	1.7320	2.5000	3.3191	4.9237	9.9652
$\lvert U_{min}\rvert$	1.0998	1.0825	1.4182	1.6249	1.7320	2.5000	3.3191	4.9237	9.9652
A_{max}	4.3816	9.5574	16.871	25.970	36.001	59.218	91.767	155.63	354.09
$\lvert A_{min}\rvert$	4.3816	9.5574	16.871	25.970	36.001	59.218	91.767	155.63	354.09

As can be seen in Table 8.1 the maximum and minimum values are the same, this because of that the load oscillates around its equilibrium at 0.

In Figure 8.4 - Figure 8.5 the results in form of displacements and accelerations from an undamped system loaded by load case 2 are displayed. The difference in loading between load case 1 and 2 is that load case 2 has no negative values and contains an angular shift, see Figure 8.1. As mentioned earlier, the system response for an undamped system that is loaded by a harmonic force, increases when $\beta \rightarrow 1$, and resonance effects appear when $\beta=1$. This is therefore also obtained in this case. The maximum and minimum values of displacement and acceleration for $\beta < 1$, are listed in Table 8.2.

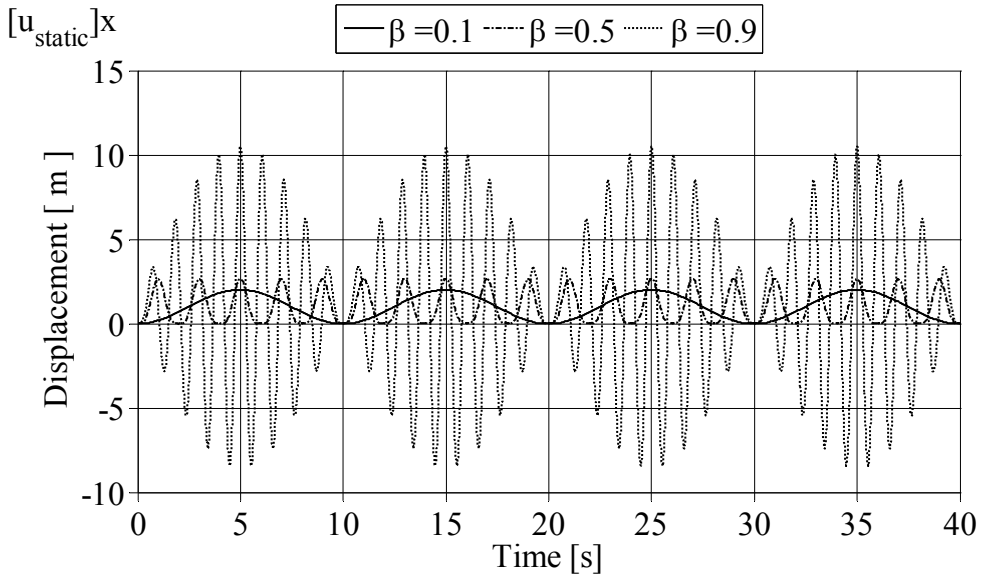

Figure 8.4: Displacements for load case 2 with β=0.1, β=0.5 and β=0.9.

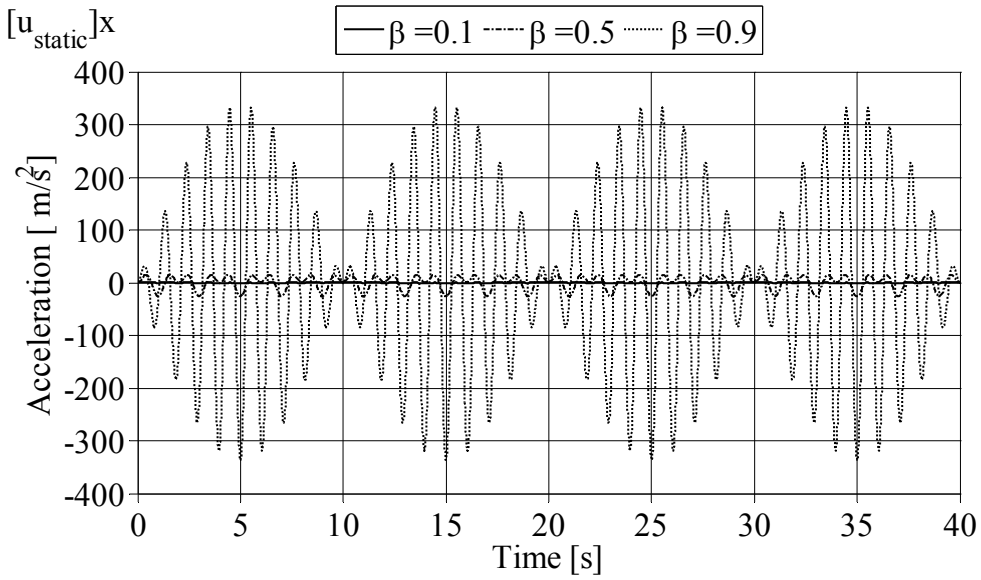

Figure 8.5: Acceleration for load case 2 with β=0.1, β=0.5 and β=0.9.

Table 8.2: Maximum and minimum values of displacement and acceleration for the undamped case, load case 2.

β	0.1	0.2	0.3	0.4	0.5	0.6	0.7	0.8	0.9
U_{max}	2.0202	2.0000	2.1978	2.2671	2.6667	2.9732	3.9216	5.2840	10.526
$\lvert U_{min}\rvert$	0	0	0.1710	0.3809	0	0.9732	1.8733	3.5556	8.3959
A_{max}	0.7782	2.9866	7.6331	15.039	14.804	41.236	74.605	140.37	332.03
$\lvert A_{min}\rvert$	0.7975	2.9866	7.8089	13.787	26.319	41.236	75.860	132.00	336.61

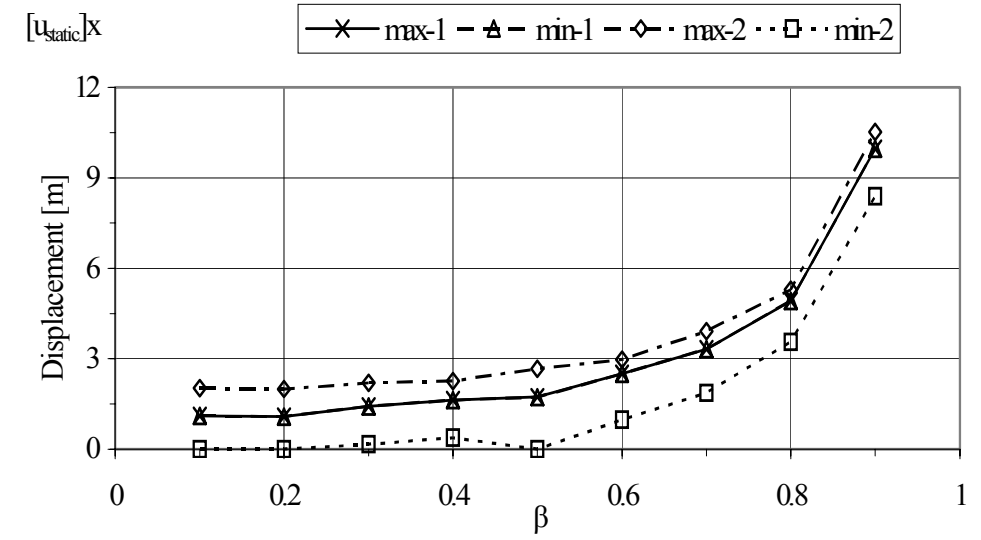

Figure 8.6: Variation in maximum and minimum displacements with changing β for the undamped load cases 1 and 2.

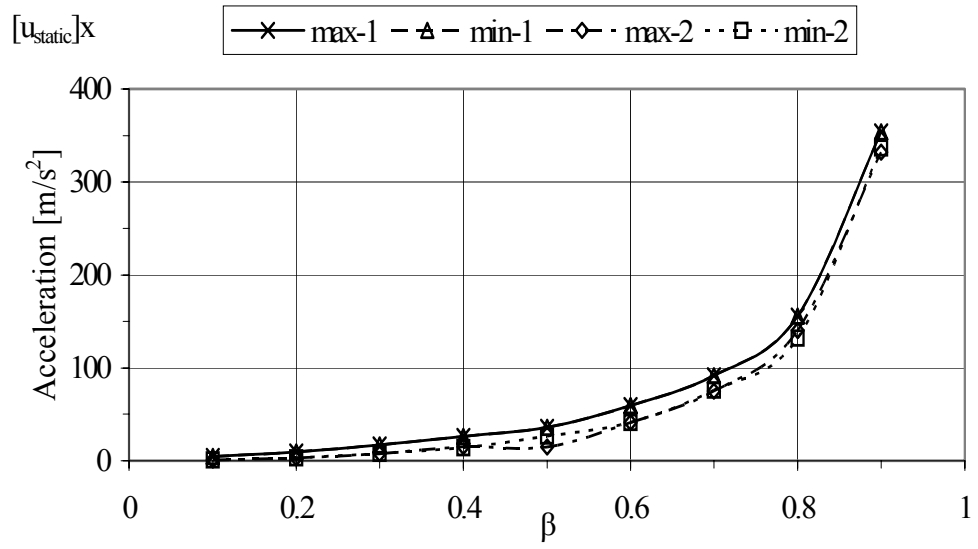

Figure 8.7: Variation in maximum and minimum accelerations with changing β for the undamped load cases 1 and 2.

In the results, when comparing Table 8.1 - Table 8.2, it can be seen that generally by assuming that the load do not contain any negative values and that the loading is applied with a phase shift, the maximum and minimum values decrease, except for the maximum displacements where it has the opposite effect, see Figure 8.6 - Figure 8.7. However, the load in load case 2 is only applied in one direction so this is an expected effect.

8.1.2 Damped system

By introducing a damper into the system, see Figure 7.2, and letting the same load act as in the undamped system, the system response can be calculated. The difference in the solutions for the damped versus the undamped system is described in Section 3.2.6. Besides the homogeneous solution u_h, an additional particular solution u_p appears. In all real systems there will be some kind of damping introduced into the system, and therefore the homogeneous solution will be damped out. This leads to that, in time, the particular solution alone will dominate the solution of the system response, see Figure 8.8

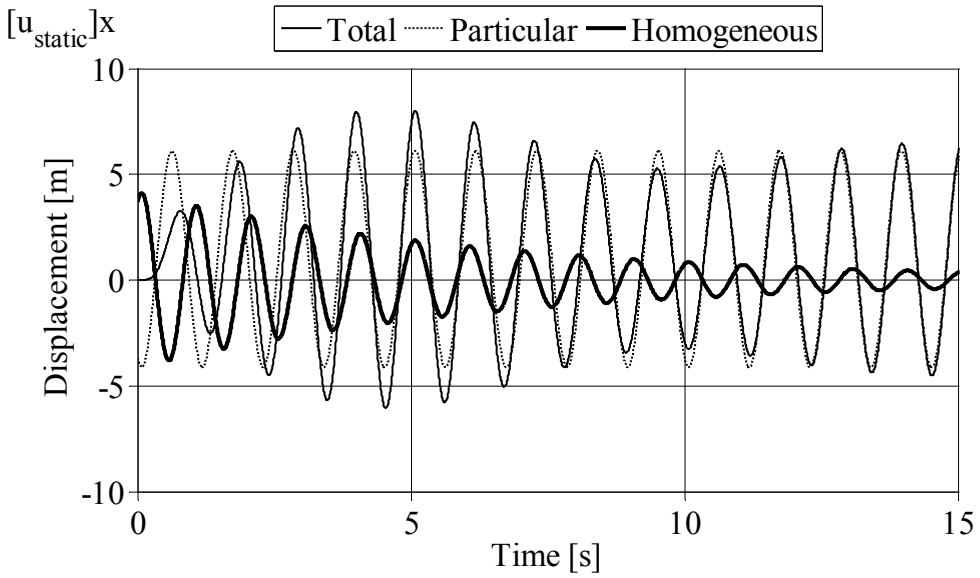

Figure 8.8: Particular solution dominating in load case 2, β=0.9.

In practice this means that the oscillation frequency and amplitude of the system will go towards and finally coincide with the frequency of the applied load. The system response for the damped system follows the same pattern as for the undamped system, i.e. that the response increases when $\beta \rightarrow 1$, and that resonance effects, with large system responses, appear when $\beta=1$. As can be seen in Figure 3.10 it is when $\beta \approx 1$ that the influence of the damping has largest effect. The main difference between the damped and undamped systems can be seen by comparing Figure 8.9 with the undamped system in Figure 8.2. For the first 5 seconds the response looks very similar and it is first after this time the influence of the damping starts to get noticeable. During the time while the homogeneous solution damps out, the system response goes toward a stabile oscillation with the same frequency as the applied load. The system response in terms of displacements and accelerations for a damped system applied with load case 1 is displayed in Figure 8.9 - Figure 8.10.

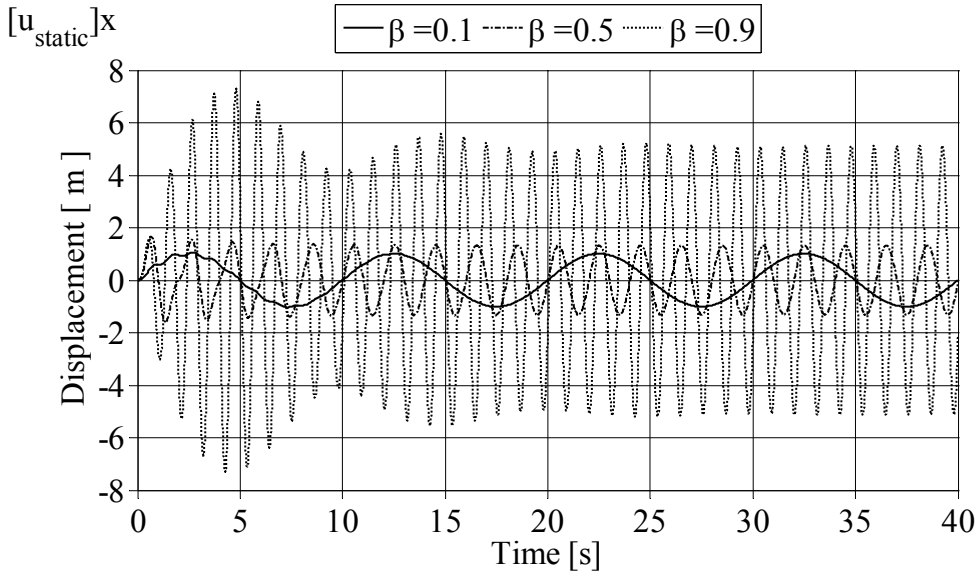

Figure 8.9: Displacement for load case 1 with β=0.1, β=0.5 and β=0.9.

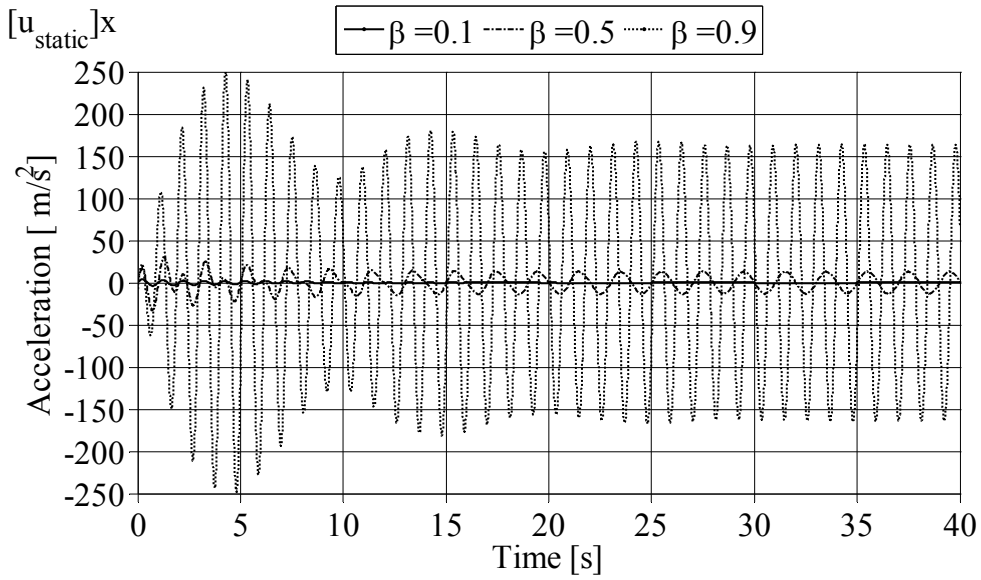

Figure 8.10: Acceleration for load case 1 with β=0.1, β=0.5 and β=0.9.

The maximum and minimum values of displacement and acceleration for β<1, are listed in Table 8.3.

Table 8.3: Maximum and minimum values of displacement, and acceleration for the damped case, load case 1.

β	0.1	0.2	0.3	0.4	0.5	0.6	0.7	0.8	0.9
U_{max}	1.0651	1.0606	1.3805	1.5750	1.6741	2.0799	2.9804	4.1261	7.2849
$\|U_{min}\|$	1.0328	1.0411	1.2436	1.4000	1.6242	2.3296	2.7720	4.2535	7.2891
A_{max}	3.7666	7.4085	12.5670	17.943	30.965	52.373	74.839	128.92	249.25
$\|A_{min}\|$	3.7152	8.6098	15.3740	23.880	33.300	42.614	78.037	123.08	247.84

Applying the same procedure as for the undamped system, the load is changed and the damped system is loaded by load case 2. As for the undamped system when the applied load was changed from load case 1 to load case 2, the basic appearance of the system response for the damped system is very similar to the previous case, see Figure 8.11 - Figure 8.12.

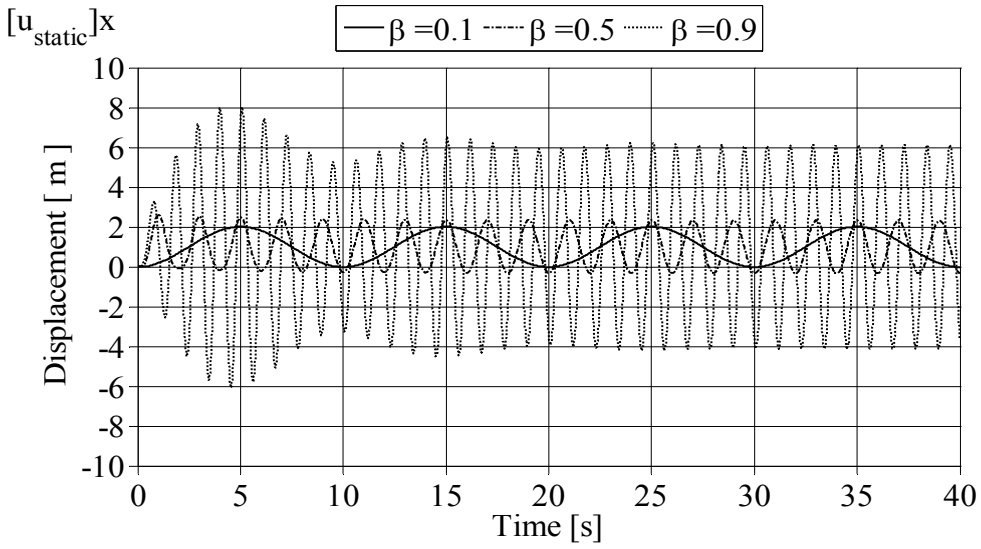

Figure 8.11: Displacement for load case 2 with β=0.1, β=0.5 and β=0.9.

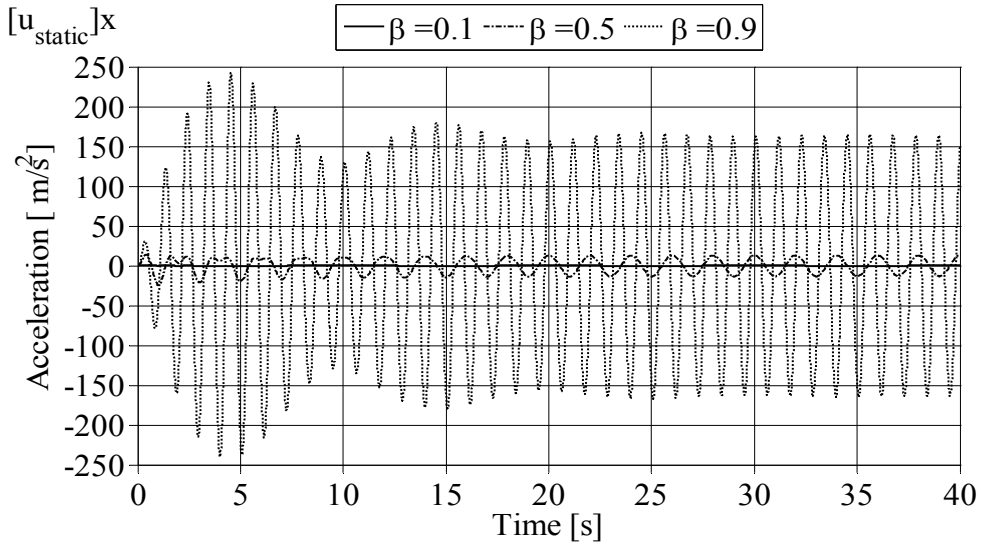

Figure 8.12: Acceleration for load case 2 with β =0.1, β=0.5 and β =0.9.

The maximum and minimum values of displacement, and acceleration for β <1, are listed in Table 8.4.

Table 8.4: Maximum and minimum values of displacement and acceleration for the damped case, load case 2.

β	0.1	0.2	0.3	0.4	0.5	0.6	0.7	0.8	0.9
U_{max}	2.0147	2.0415	2.1438	2.2497	2.6168	2.8994	3.4965	4.8165	8.0004
$\lvert U_{min}\rvert$	0.0101	0.0415	0.1360	0.3185	0.3317	0.8721	1.6684	2.9496	6.0658
A_{max}	0.7487	2.8720	6.0643	12.590	14.225	36.464	66.778	116.72	241.71
$\lvert A_{min}\rvert$	0.5805	2.5382	6.1131	12.643	24.384	38.352	60.581	114.12	239.42

When comparing the results from Table 8.3 - Table 8.4, the same effects can be seen on the maximum and minimum values of the system response, see Figure 8.13 - Figure 8.14. The values of maximum displacements increase when the load is shifted, but it has the opposite effect on the accelerations for both maximum and minimum values. It can also be seen that the response for the system has generally lower values of displacement and acceleration than in the undamped case.

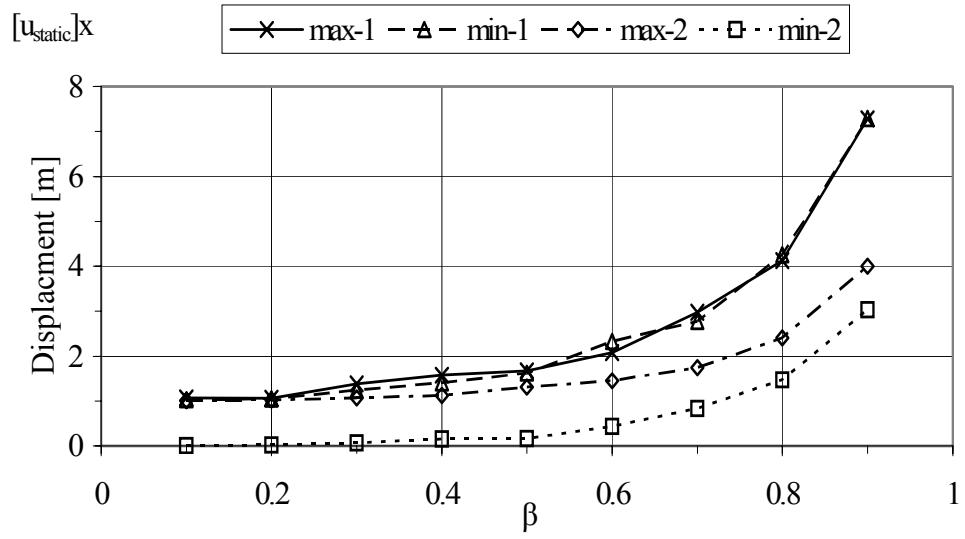

Figure 8.13: Variation in maximum and minimum displacements with changing β for the damped load cases 1 and 2.

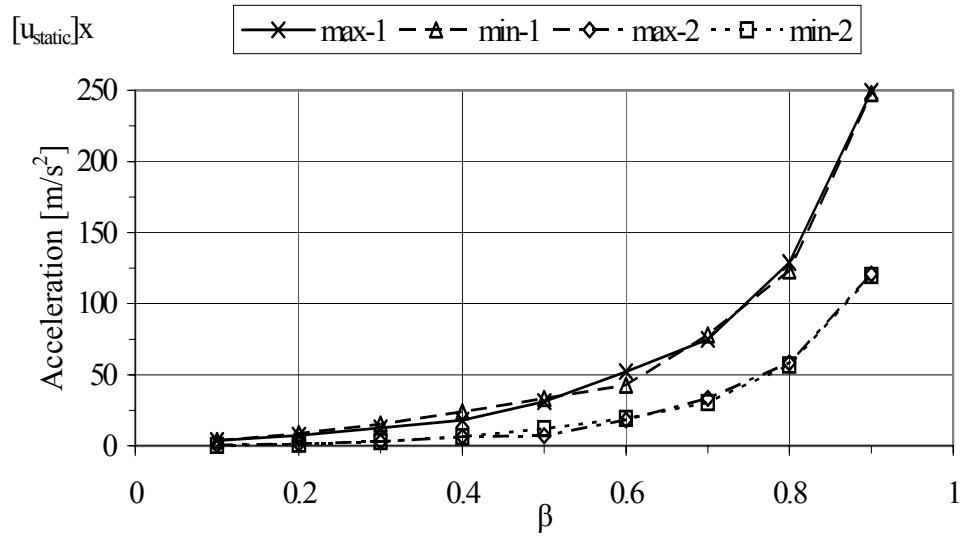

Figure 8.14: Variation in maximum and minimum displacements with changing β for the damped load cases 1 and 2.

The response of the system has also been studied for different values for the natural frequency of the system. When the eigenfrequency increases from f_n=1 Hz to f_n=5 Hz and f_n=10 Hz, respectively, the displacement is not affected in any case and that is because the relation between the eigenfrequency and load frequency remains the same. This relationship between the eigenfrequency and displacement is what makes the simplifications regarding mass, stiffness and applied loads justified. The results

for the velocity and the acceleration are on the other hand not unaffected. If the frequency is increased with a factor n, the value of the velocity also increases with a factor n, and the acceleration increases with the same factor as the frequency in square, i.e. n^2. This is why the results from velocity and acceleration calculations only can be used as a mutual comparison, as stated earlier in this chapter, and not as actual values. This phenomenon occurs independently of whether the system is damped or not.

8.1.3 Dynamic amplification factor for damped system

When the *DAF* is plotted as Figure 3.10 in Section 3.3, the damping factors used are very large, compared to what would exist in real structures, and are pedagogically useful to understand the influence of damping in a system. Therefore the same plot, as in Figure 3.10, is created but with a damping factor ξ <0.10, see Figure 8.15.

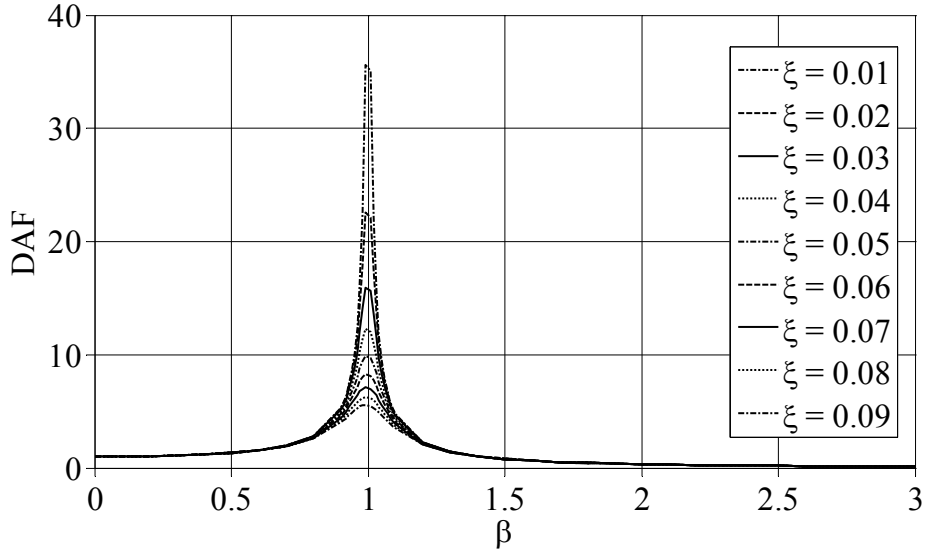

Figure 8.15: Dynamic Amplification Factor for damping factor ξ <0.10.

By applying that the focus of interest are on results for β <1 and that there seems to be no drastic change of *DAF* until β >0.5, the axis in Figure 8.15 can be scaled down, see Figure 8.16.

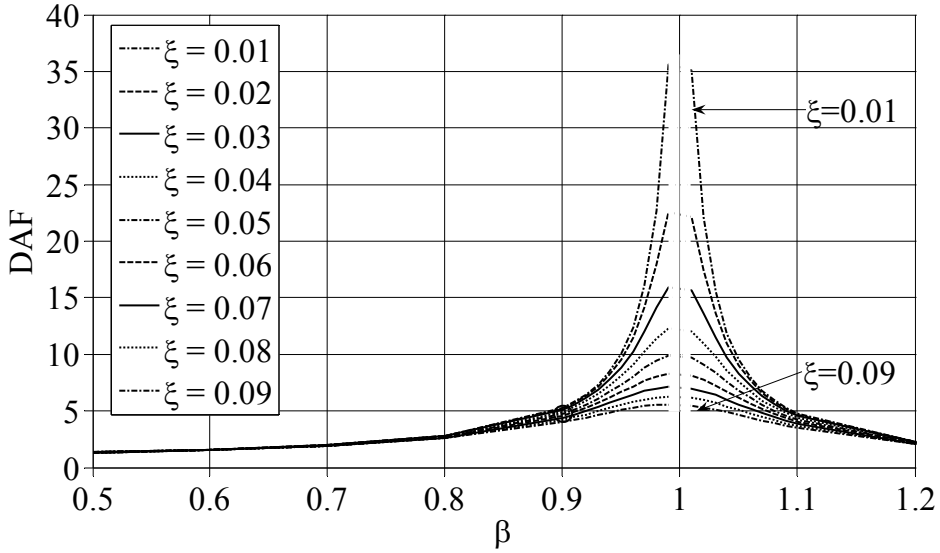

Figure 8.16: Theoretical DAF for the analytical solution, scaled from Figure 8.15.

Both Figure 8.15 and Figure 8.16 are plotted based on the equation stated in Section 3.3.2, i.e. Equation (3.43). According to Figure 8.15, considering a value of β=0.9 and ξ=2.5 %, the total displacement would be ~5 times the static displacement of the system. According to the results stated in Table 8.3, the largest value of displacement is for $|U_{min}|=7.2891u_{static}$. The difference between these two results can be explained by the fact that according to the derivation of the *DAF*, the homogeneous solution is assumed to die out and is therefore not included in the expression. So the expression for *DAF* is in other words only valid when the damping has totally excluded the influence of the homogeneous solution, see Figure 8.17

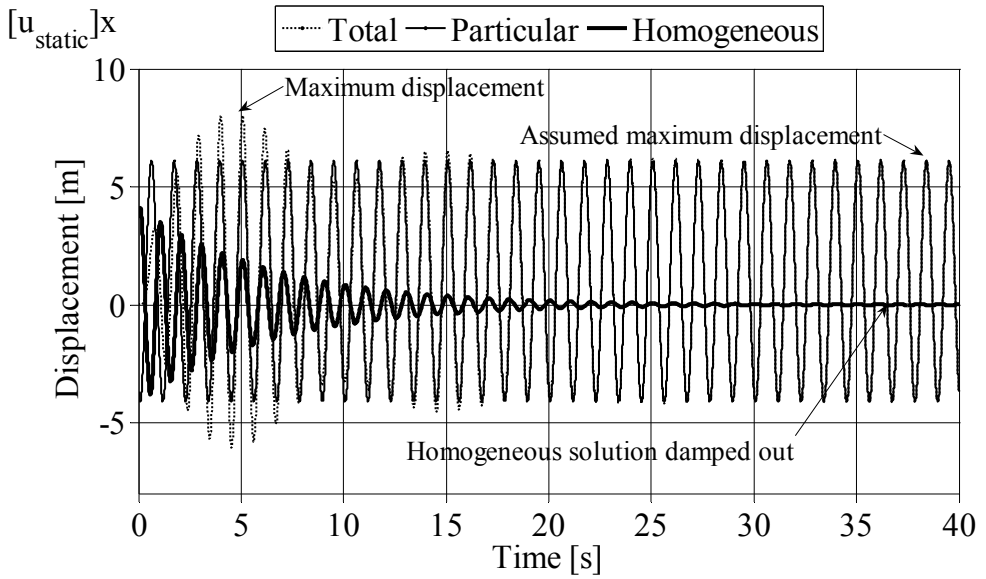

Figure 8.17: Only u_p is considered in calculation of DAF.

When calculating *DAF* as stated above, the real maximum displacement is not considered, which leads to an underestimation of the displacement. If the displacement is plotted in the same way as *DAF* it can be displayed as in Figure 8.18.

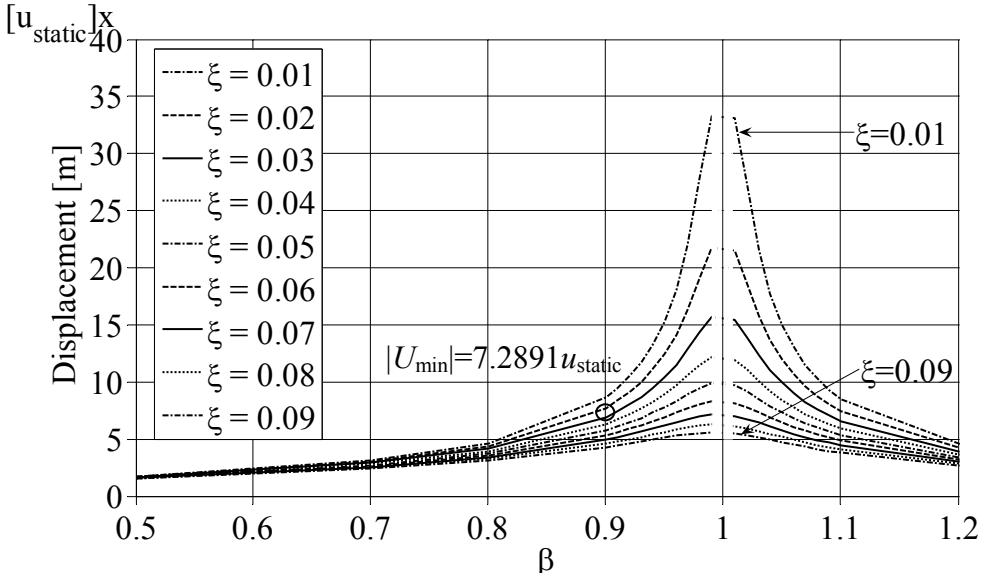

Figure 8.18: Amplification factor calculated with the total displacement.

Remembering the $|U_{min}|$ value stated above and comparing it in the same way as earlier it can be seen in Figure 8.18 that now the result seems more reasonable, and therefore this is the value that should be set as a reference value and not the theoretical *DAF*.

8.2 Numerical solution

In this section the results from the numerical analysis are presented. In the numerical analysis, more complicated load types are introduced and applied to the system. The result is presented in the same way as in the previous section, only displaying displacements and accelerations for selected values of $\beta<1$. Remaining calculated results are presented in Appendix E.

To be able to make the comparison between the two solutions some modifications of the analytical solution are made. In the analytical solution, the static displacement u_{static}, can be neglected or set to 1. In the numerical solution this is not possible, and variables such as stiffness k, mass m and applied load p_0 are needed in the expression, see Equation (7.11). To make the expression as simple as possible, this is solved by giving both the mass and applied load a value equal to 1, this is also described earlier in Section 7.3.2. With these variables set to 1, the stiffness is adjusted so that the system has an eigenfrequency of 1 Hz. To modify the results from the analytical solution it is then needed to divide the results with the applied stiffness.

8.2.1 Verification

To verify the numerical solution, load case 1 and 2 have been solved both analytically and numerically. The results from the numerical solution can then be verified by comparing the results of maximum and minimum values of displacement and acceleration from the two solution methods. The comparison shows that the numerical solution has a good accuracy, with a maximum error less than 0.7 %, see Appendix E. With the numerical solution method verified, only load case 2 will be used in the analysis and will be referred to as the sinusoidal load. Also only the damped case, with damping ξ =2,5 %, will be considered in this section.

8.2.2 Continuous triangular load

After verifying the numerical solution, more complicated load histories are implemented. First there is a continuous triangular load, i.e. load case 3, which is to be compared with the sinusoidal load, see Figure 8.19.

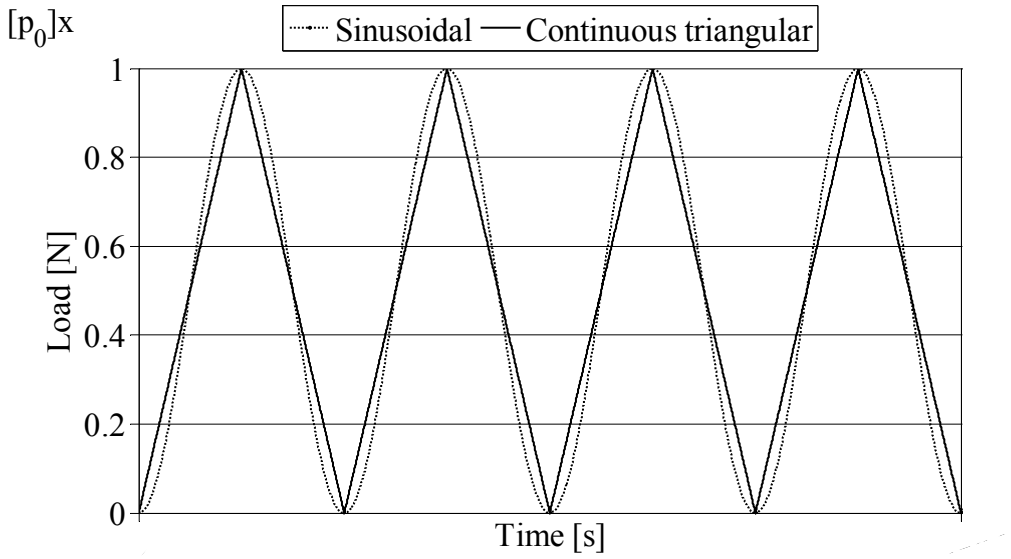

Figure 8.19: Continuous triangular load compared with the sinusoidal load.

As can be seen in Figure 8.19 the sinusoidal and continuous triangular load reminds a lot of each other, and the total impulse of each load pulse is the same for both cases. When the system response for the two loads is compared it appears that the value of β determines how well the result of the sinusoidal load and the continuous triangular load coincides with each other.

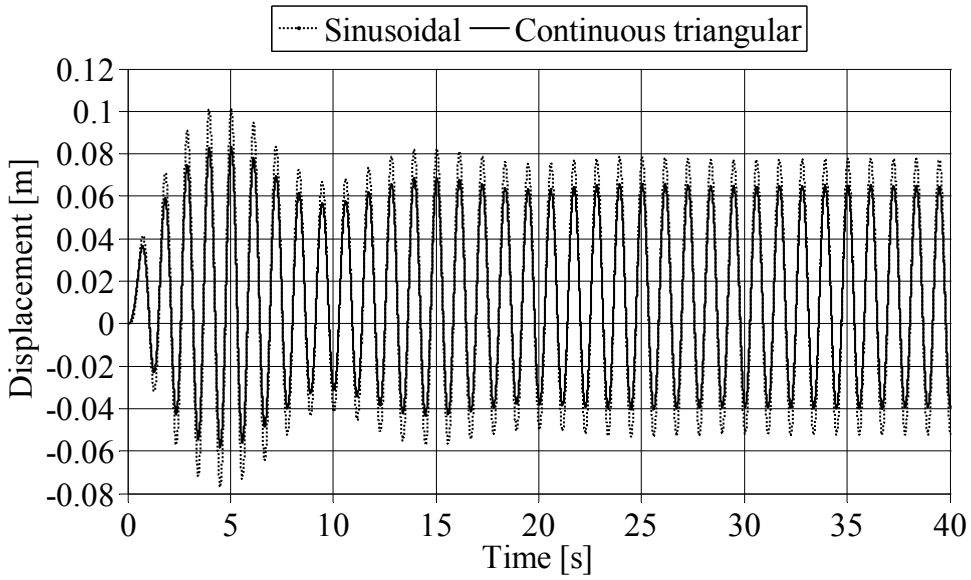

Figure 8.20: Displacement for the continuous triangular load compared with the sinusoidal load with β=0.9.

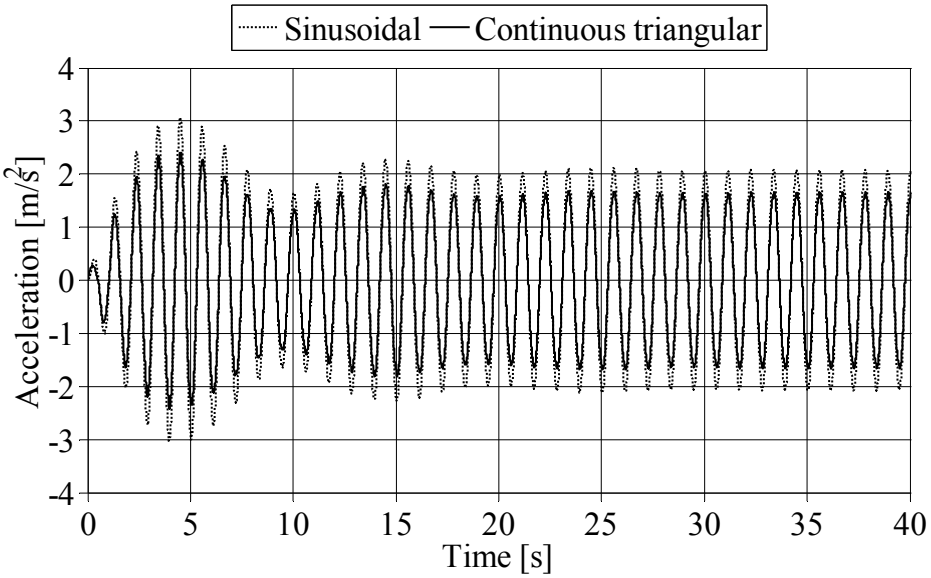

Figure 8.21: Acceleration for the continuous triangular load compared with the sinusoidal load with β=0.9.

In Figure 8.20 - Figure 8.21, β=0.9 is displayed and it can be seen that the shape of the principle response for the system excited by the continuous triangular load is identical to the response with the sinusoidal load, apart from the magnitude of the amplitude which is smaller for the continuous triangular load, for both displacements and accelerations. The difference in amplitude can probably be explained by that the sinusoidal load has higher impulse area at the peak. By examining every 1/10 of β, this behaviour can be seen down to $\beta\approx$0.4. At this ratio the acceleration starts to become larger for the continuous triangular load than for the sinusoidal load, and finally if the β value decreases even more, the total system response is larger for the continuous triangular load.

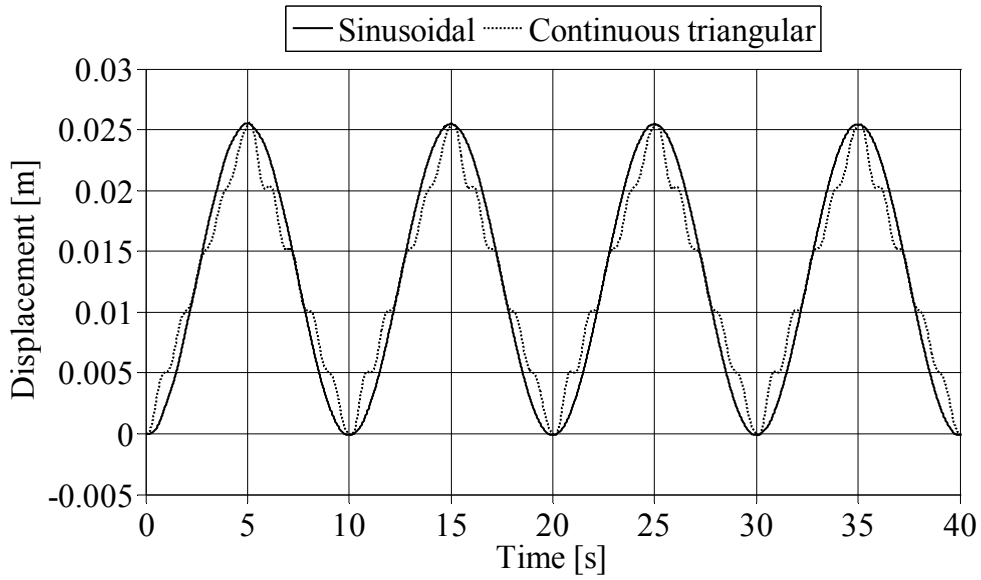

Figure 8.22: Displacement for the continuous triangular load compared with the sinusoidal load with β=0.1.

As can be seen in Figure 8.22 the difference in displacements are very small even for β=0.1, but when comparing the accelerations there can be seen a large difference, see Figure 8.23.

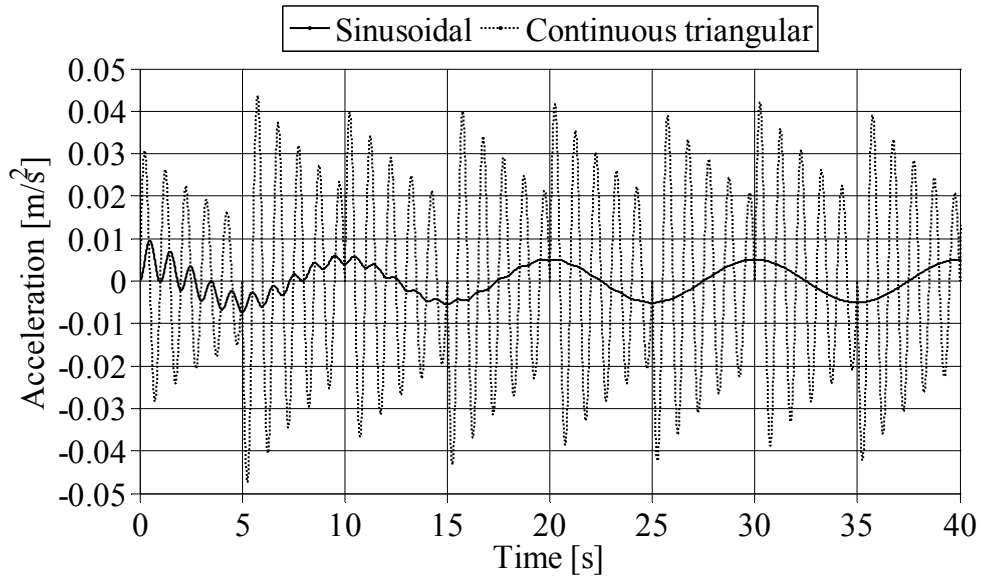

Figure 8.23: Acceleration for the continuous triangular load compared with the sinusoidal load with β=0.1.

The analysis were performed for every 1/10 in the interval $0.1 \leq \beta \leq 0.9$, and, if considering only the continuous triangular load, the expected behaviour was that the magnitude of the system response would have a constant decrease when $\beta \rightarrow 0$, but a noticeable increase in magnitude started to appear at β=0.4, see Table 8.5 and Figure 8.24 - Figure 8.25.

Table 8.5: Maximum and minimum values of displacement and acceleration for the damped case, load case 3.

β	0.1	0.2	0.3	0.4	0.5	0.6	0.7	0.8	0.9
U_{max}	0.0256	0.0325	0.0313	0.0265	0.0255	0.0297	0.0364	0.0499	0.0832
$\|U_{min}\|$	0.0001	0.0071	0.0055	0.0000	0.0001	0.0043	0.0123	0.0258	0.0585
A_{max}	0.0437	0.3758	0.2887	0.2523	0.1651	0.2986	0.5882	1.0804	2.4258
$\|A_{min}\|$	0.0473	0.3762	0.2757	0.2621	0.1754	0.3230	0.5437	1.1079	2.4182

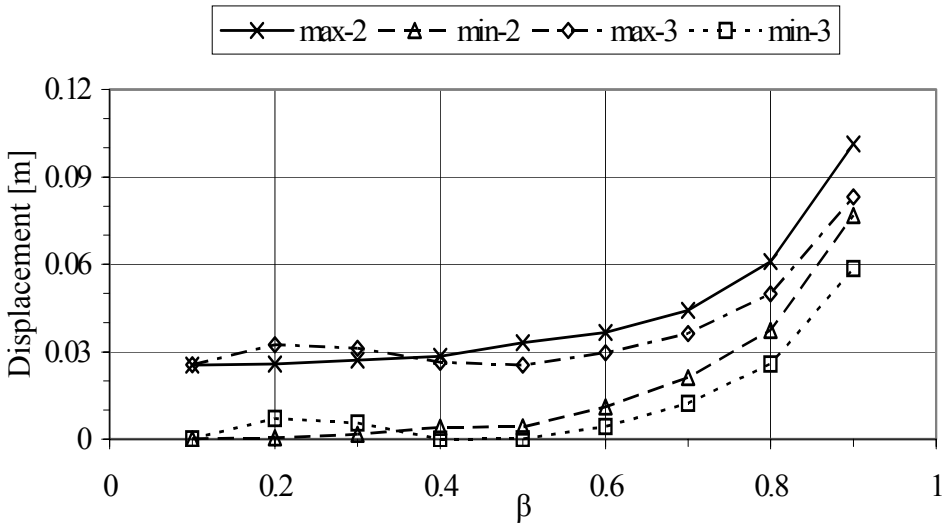

Figure 8.24: Variation in maximum and minimum displacements with changing β for the damped load cases 2 and 3.

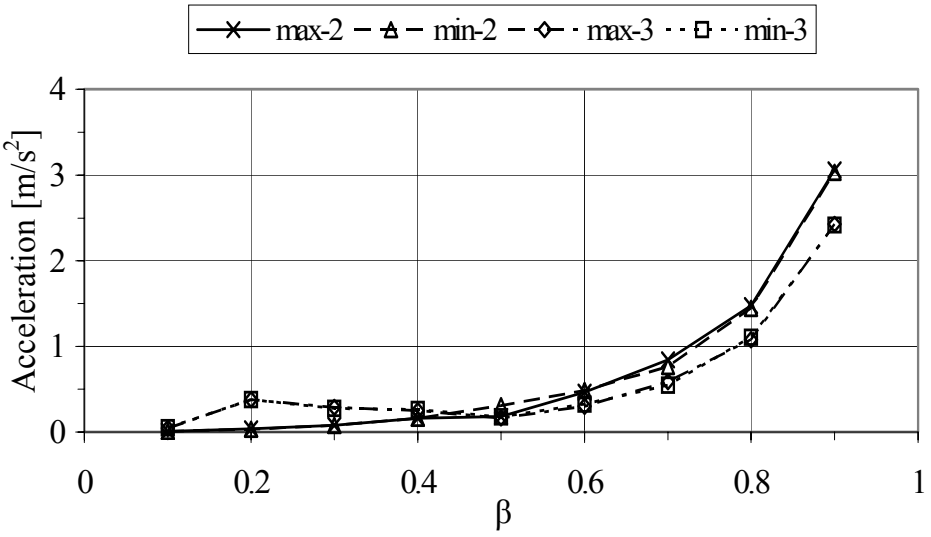

Figure 8.25: Variation in maximum and minimum accelerations with changing β for the damped load cases 2 and 3.

After further analysis for $\beta \leq 0.4$ it appears that a system excited for a continuous triangular load is sensitive to a ratio of $\beta = 1/(2n+1)$, where n=1, 2, 3, etc, see Figure 8.26 - Figure 8.27.

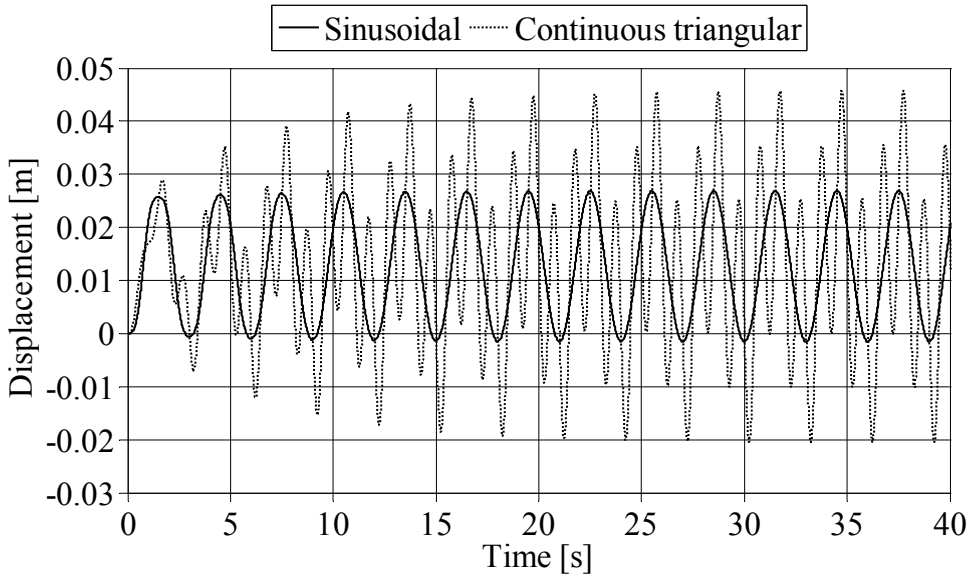

Figure 8.26: Displacement response for the continuous triangular and the sinusoidal load with β=1/3.

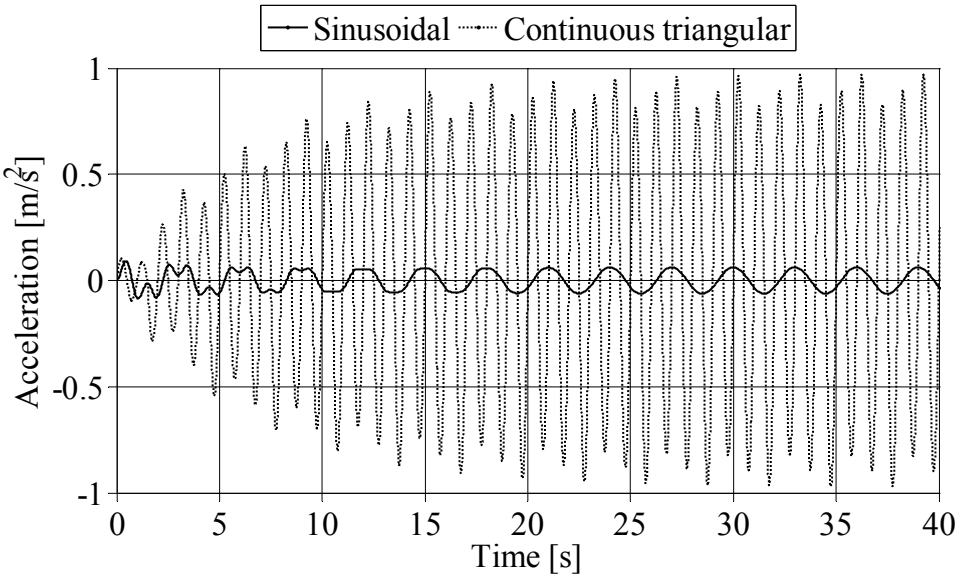

Figure 8.27: Acceleration response for the continuous triangular and the sinusoidal load with β=1/3.

The two figures above indicates that the response grows dramatically for $\beta = 1/3$. If the result from the response with $\beta = 1/3$ is compared with, e.g. $\beta = 0.4$, the difference is almost a factor 2 for the displacement and at least a factor 3 for the acceleration, see Figure 8.28 - Figure 8.29.

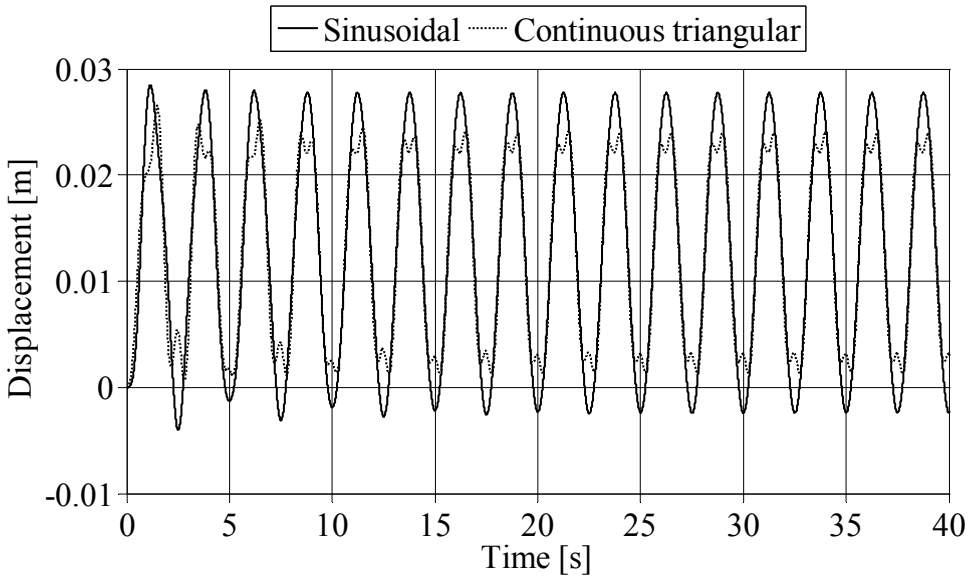

Figure 8.28: Displacement for the continuous triangular load compared with the sinusoidal load with β=0.4.

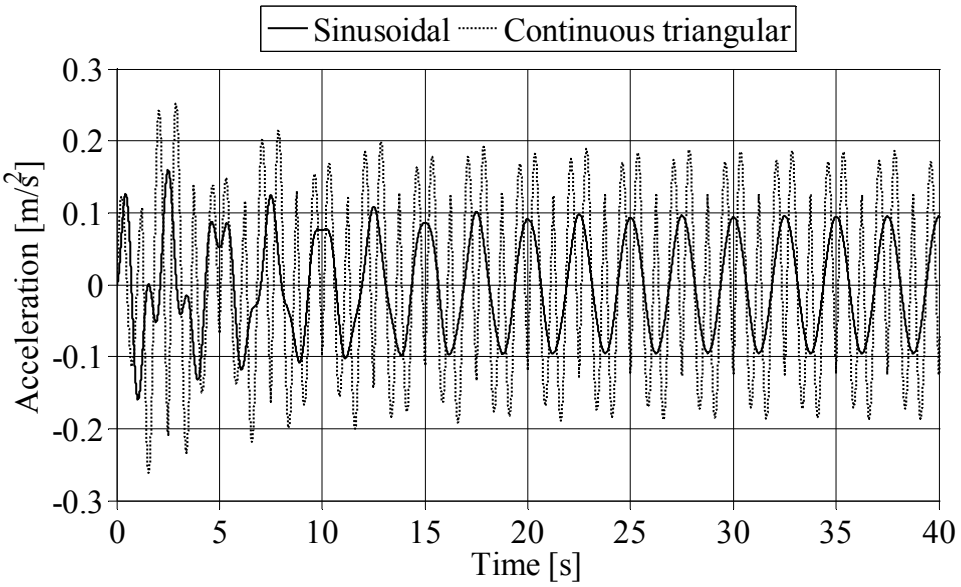

Figure 8.29: Acceleration for the continuous triangular load compared with the sinusoidal load with β=0.4.

To make the phenomenon even clearer the damping is set to zero, see Figure 8.30.

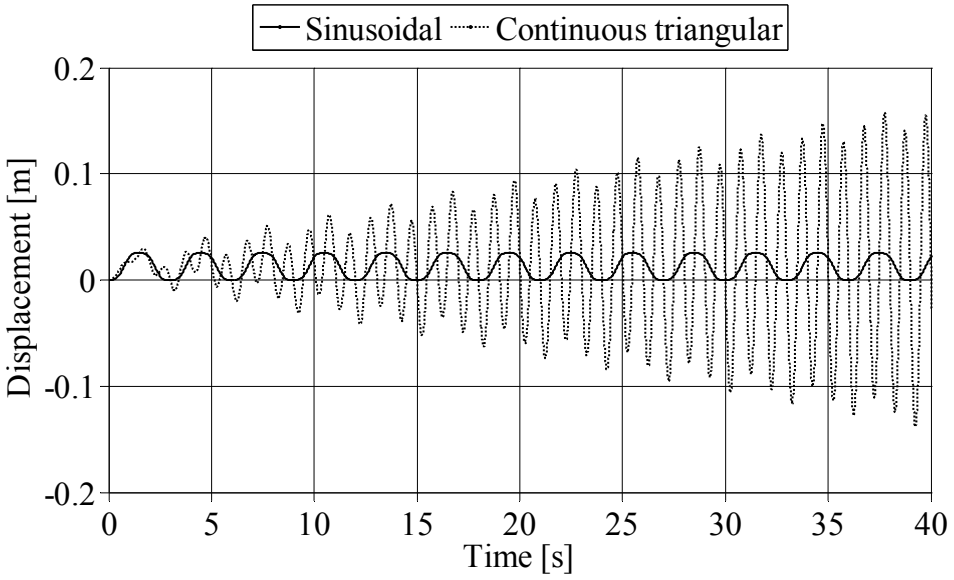

Figure 8.30: Resonance behaviour for the continuous triangular load with β=1/3 and ξ=0.

The result is that when β=1/(2n+1), the response has a typical resonance behaviour, i.e. the system response grows towards infinity, see Figure 8.30. This behaviour can not be seen for any other β<1 except for β=1/(2n+1).

8.2.3 Rectangular load

After the continuous triangular load, a rectangular load, i.e. load case 4, is applied. The rectangular load is adjusted so that the total area of each impulse is equal to the area for an impulse created by the continuous triangular load, see Figure 8.31.

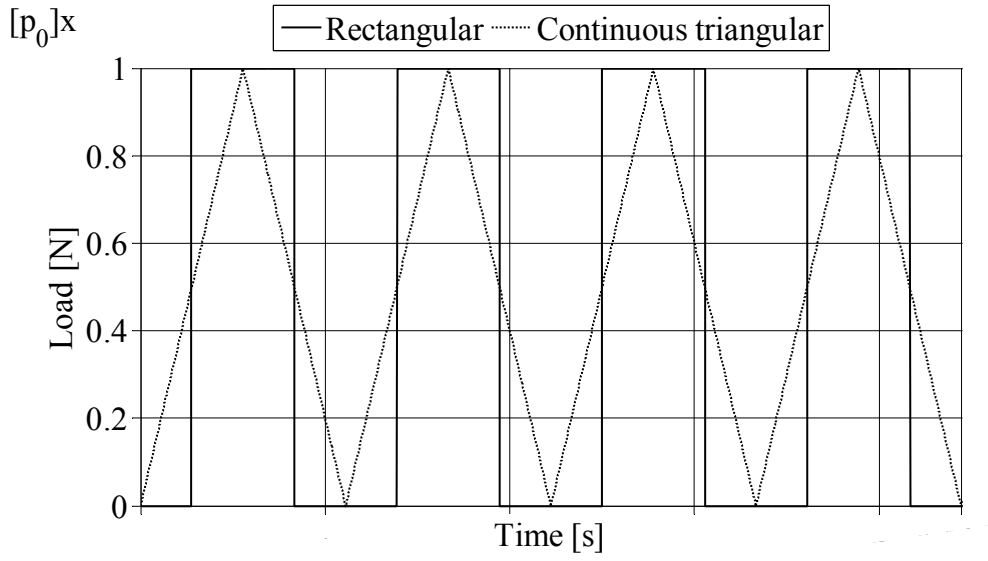

Figure 8.31: Rectangular load compared with the continuous triangular load.

From Figure 8.31 it is clear that the two types of loads have very different characteristics, even if the total impulse is the same. The continuous triangular load is never really unloaded, which is the case for the rectangular load. During this period when the system is unloaded, the system is allowed to oscillate with free oscillation and this may also be allowed during a real train load. The analysis of the rectangular load shows it has similar behaviour as the continuous triangular load, with the difference that the magnitude for the system response for the rectangular load is larger in all cases, see Figure 8.32 - Figure 8.35. This is explained in the same way as for the case in the previous section, i.e. that the impulse area is larger at the peak for the rectangular load.

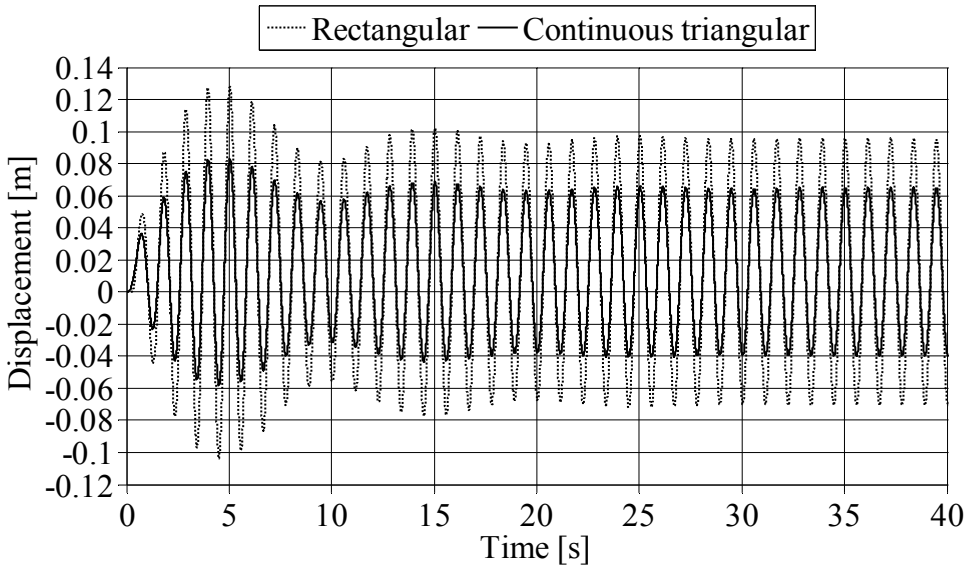

Figure 8.32: Displacement for the rectangular load compared with the continuous triangular load with β=0.9.

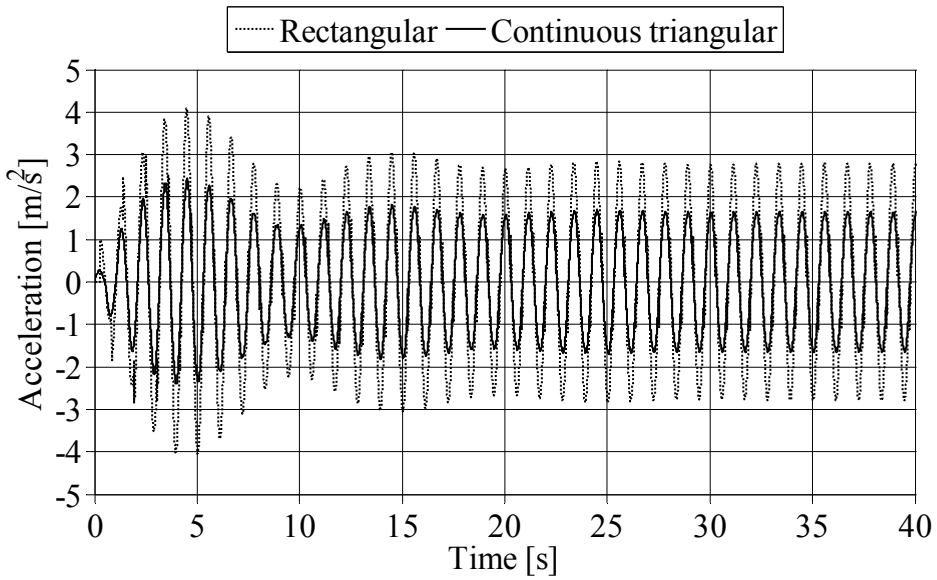

Figure 8.33: Acceleration for the rectangular load compared with the continuous triangular load with β=0.9.

Once again it can be seen that when a load with a β close to 1 is applied on the system the system response coincide and remembering the results from Figure 8.20 - Figure 8.21, the sinusoidal load gave a response with a magnitude somewhere between the continuous triangular and rectangular load for β=0.9.

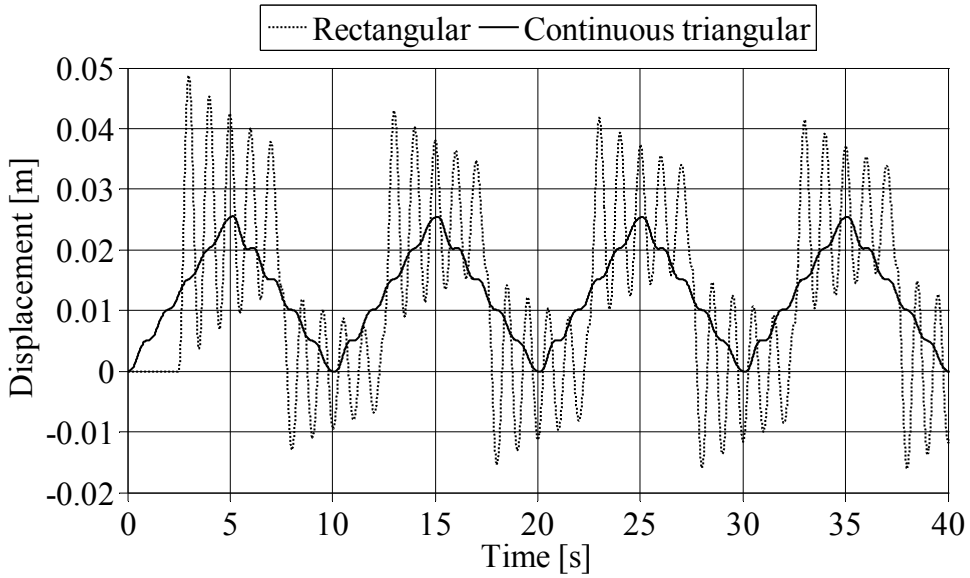

Figure 8.34: Displacement for the rectangular load compared with the continuous triangular load with β=0.1.

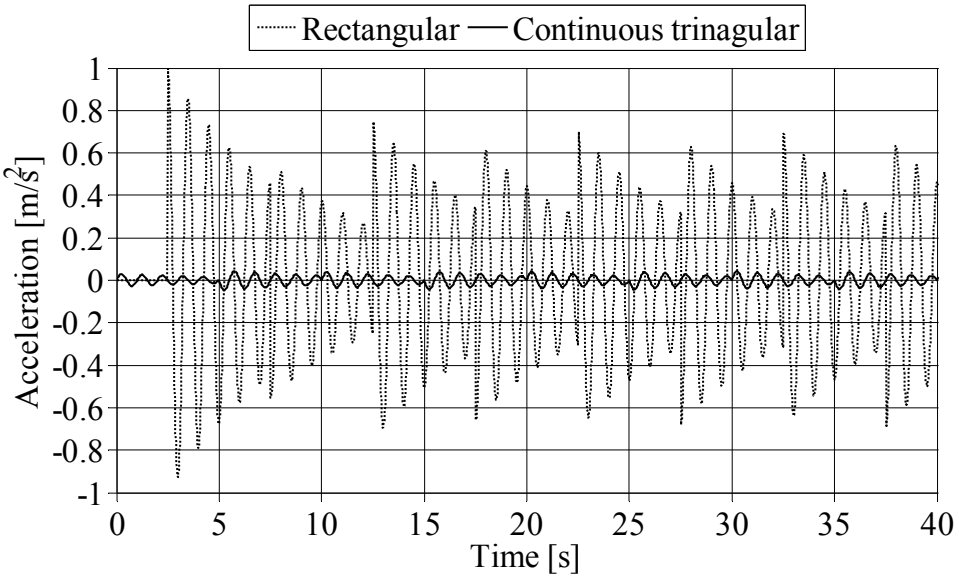

Figure 8.35: Acceleration for the rectangular load compared with the continuous triangular load with β=0.1.

For β=0.1 the rectangular load generates even more drastic oscillation than the continuous triangular load. An explanation for this may be that the change in loading, that becomes more dramatic when going from the sinusoidal load to the continuous triangular and finally the rectangular, has bigger influence for lower velocities. Also for the rectangular load the phenomena with β=1/(2n+1) occurs. The maximum and minimum values of displacement and acceleration for β<1, are listed in Table 8.6.

Table 8.6: Maximum and minimum values of displacement and acceleration for the damped case, load case 4.

β	0.1	0.2	0.3	0.4	0.5	0.6	0.7	0.8	0.9
U_{max}	0.0487	0.0972	0.0632	0.0487	0.0296	0.0487	0.0566	0.0776	0.1271
$\|U_{min}\|$	0.0160	0.0719	0.0359	0.0299	0.0043	0.0224	0.0350	0.0547	0.1036
A_{max}	0.1531	0.4700	0.2478	0.1812	0.07509	0.1531	0.2117	0.3422	0.6701
$\|A_{min}\|$	0.1415	0.4704	0.2353	0.1960	0.0797	0.1469	0.2290	0.3581	0.6775

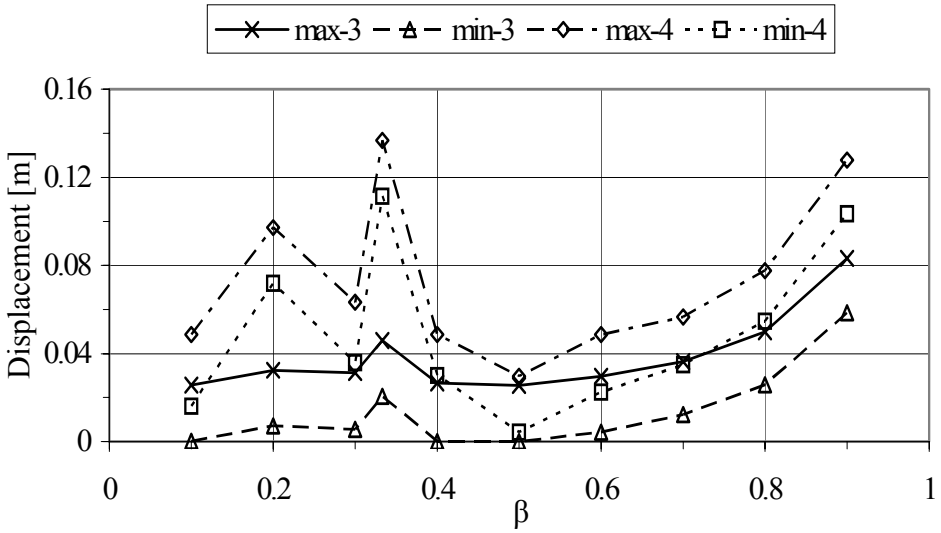

Figure 8.36: Variation in maximum and minimum displacements with changing β for the damped load cases 3 and 4.

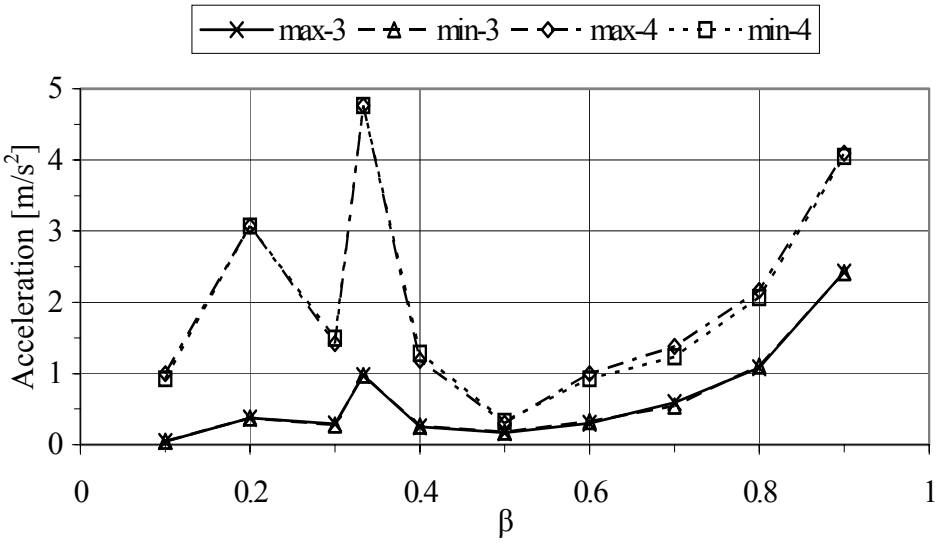

Figure 8.37: Variation in maximum and minimum accelerations with changing β for the damped load cases 3 and 4.

8.2.4 Double triangular load

This case is a modification of the previous load and also here the same total area of the impulse is kept equal between the two loads. The difference here is that the triangular load is divided so that two impulses have the same total area as the rectangular load. The spacing between the impulses is then increased so that the load starts to resemble the real bogie axle loads from the train.

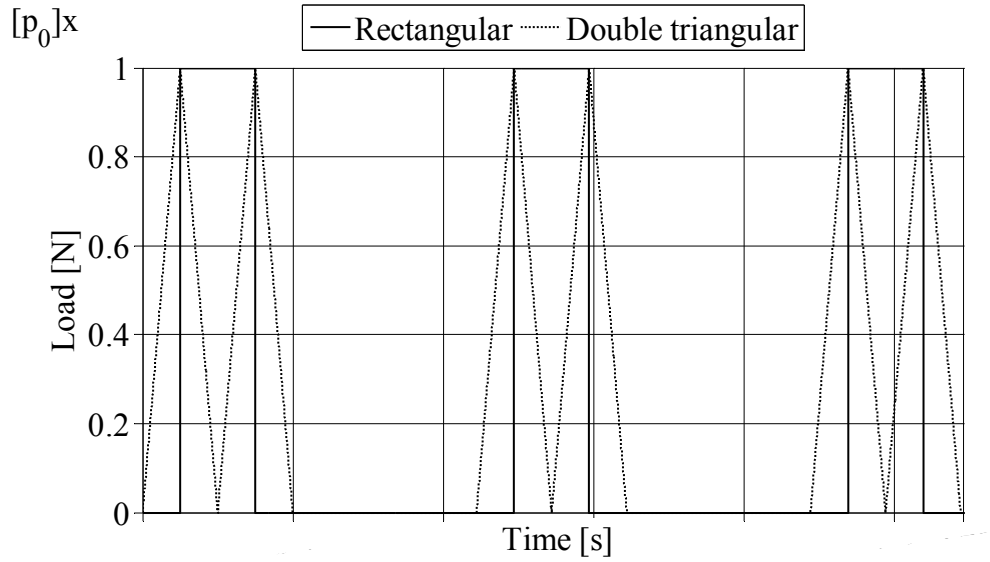

Figure 8.38: Comparison between rectangular and double triangular load.

In this part of the analysis it is of interest to find out what influence the frequency f_{p2}, i.e. the local frequency in the double triangular load, has on the total system response. This load case represents the intermediate coaches in the train and to be able to make any conclusions, the worst possible case is investigated, which is when $\beta_2 = f_{p2}/f_n = 1$. The number of intermediate coaches used in the HSLM-A varies between 11-18. By analysing different relationships between f_{p1} and f_{p2} it could be seen during how many impulses the system response is still growing. The analysis shows that already at the ratio $f_{p1}/f_{p2} \sim 6$ the system response has stopped to grow within the minimum number of intermediate coaches, i.e. 11 coaches. It should be remembered though that this result is obtained with no concern taken to the power car or end coach.

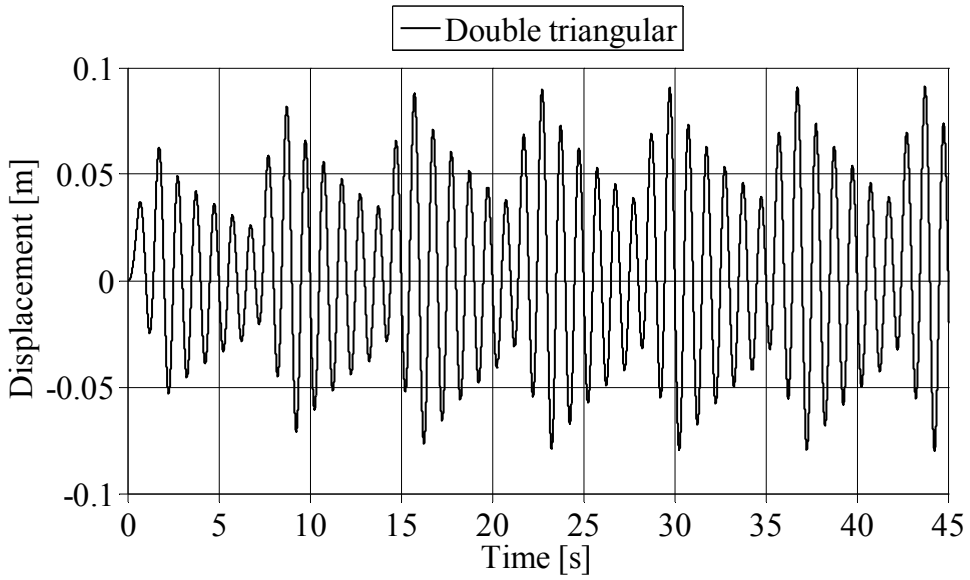

Figure 8.39: Maximum displacement is reached within minimum number of intermediate coaches already when $f_p1 \sim 6f_{p2}$, $\beta_2=1.0$.

As can be seen in Figure 8.39, the system response stabilizes and reaches maximum value of the system response after only a few loading cycles when the ratio between f_{p1} and f_{p2} is close to 6. Compare this to when the ratio between $f_{p1}/f_{p2} = 3$, when the maximum displacement is not reached until the number of 22 intermediate coaches has passed, see Figure 8.40.

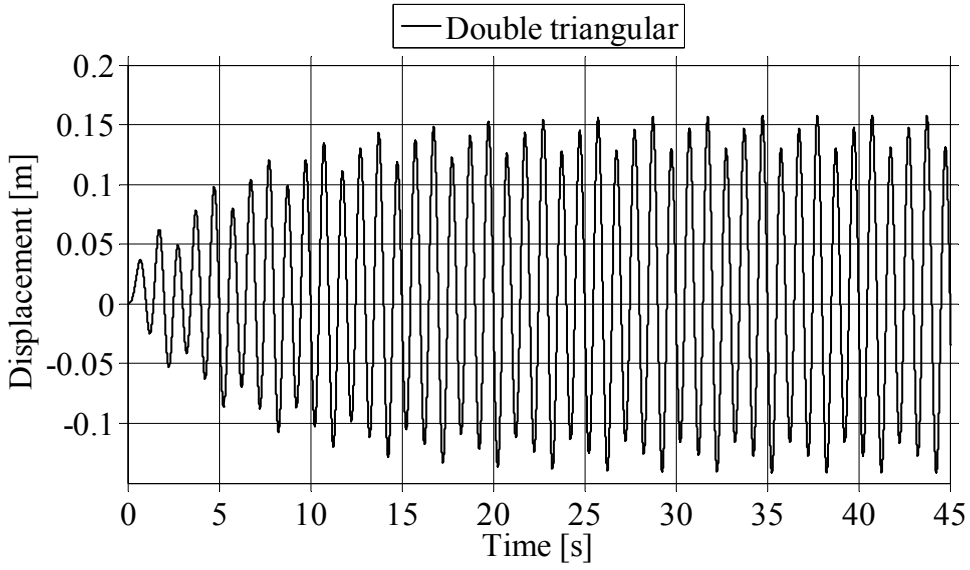

Figure 8.40: When $f_{p1}=3f_{p2}$, the number of intermediate coaches reaches 22 until the maximum displacement is obtained, $\beta_2=1.0$.

8.2.5 Train load, HSLM-A1

The last load case applied on the system is the complete train load based upon the train load HSLM-A, see Section 6.1.2. Only results from one train load are presented in this section, HSLM-A1, for β=0.2 and β=0.9. Other results are presented in Appendix E.4. The values of β are based on that the frequency f_{p1}, i.e. the distance between the bogie axle loads, is the main frequency for the applied load. However, the total train load can be divided into 5 different β -values, see Figure 8.41. All the different spacing between the axle loads generates different β -values. The spacing for the axle loads on the power car, and the spacing between the power car and the end coach is a fixed distance and will be the same during the analysis. The spacing D and d, which represent the distance for which the frequency f_{p1} and f_{p2} respectively are based on, varies between the different train loads. The aim with the analysis in this section is to show that it is possible to describe the system response in a beam loaded in midspan, with a SDOF-system. The results from the train loads are compared with results calculated with ADINA, and are presented in Chapter 10.

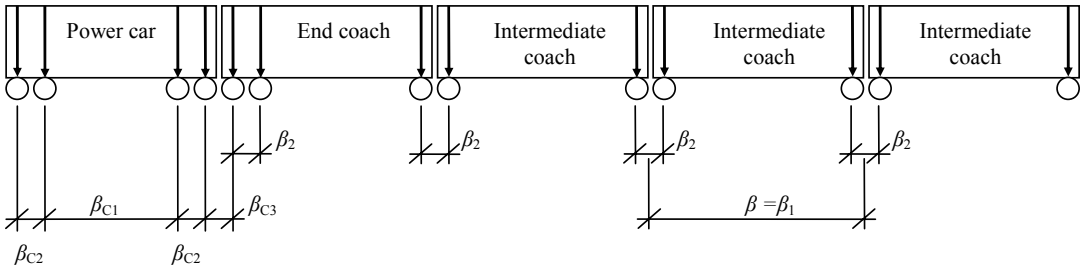

Figure 8.41: Different β-values related to different axle loads.

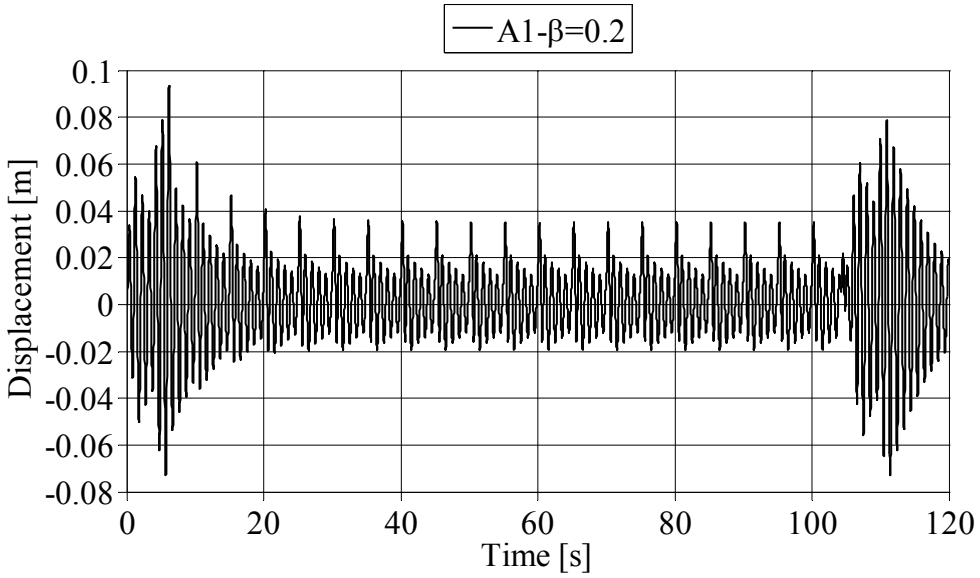

Figure 8.42: Displacement for train load HSLM-A1, β=0.2.

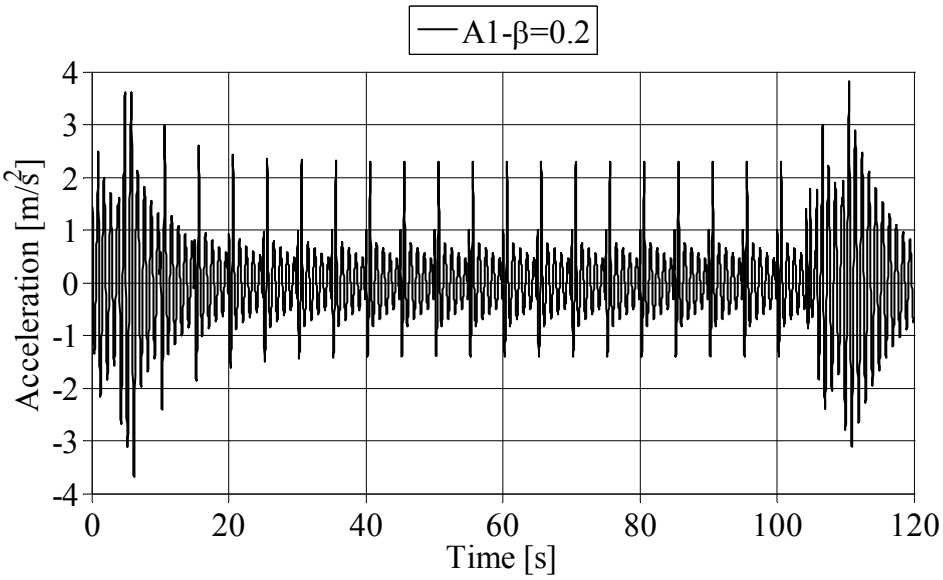

Figure 8.43: Acceleration for train load HSLM-A1, β=0.2.

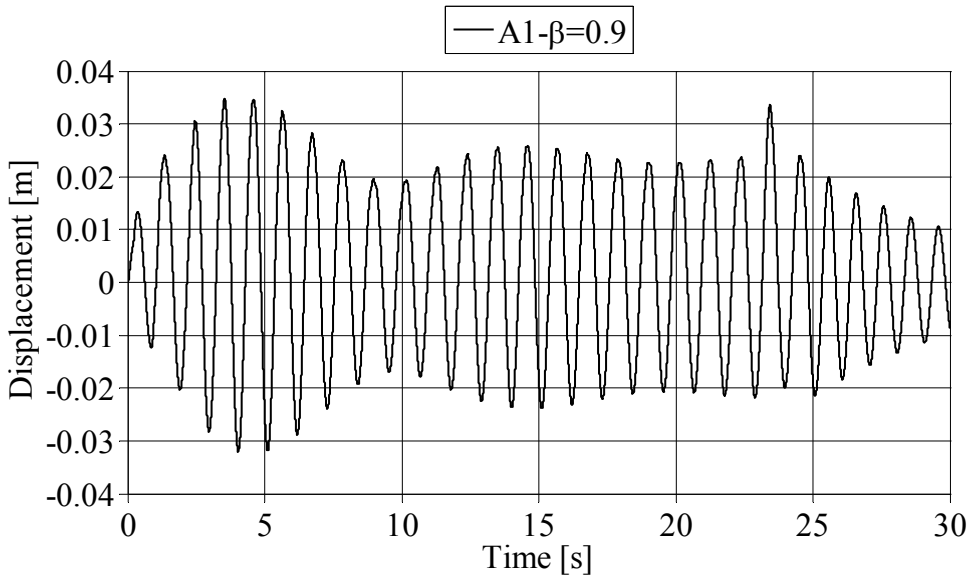

Figure 8.44: Displacement for train load HSLM-A1, β=0.9.

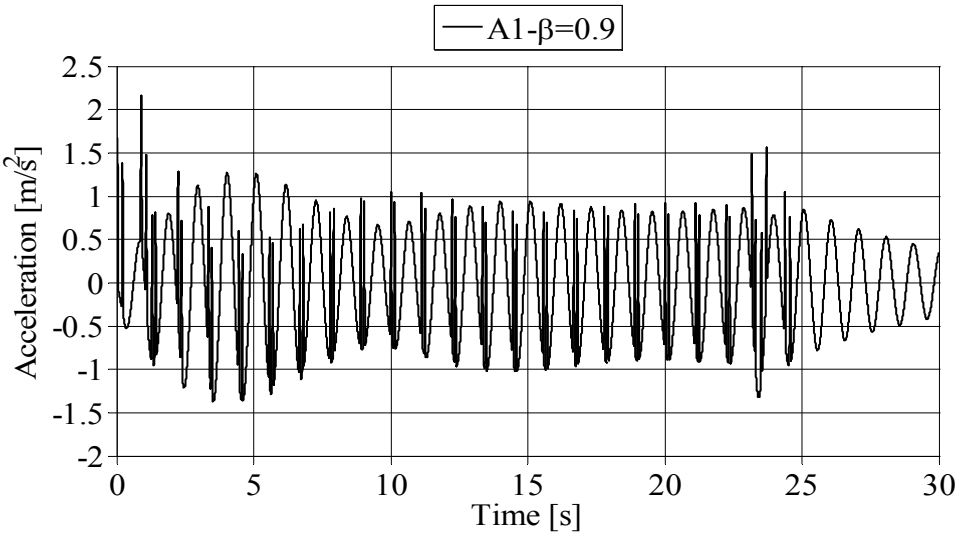

Figure 8.45: Acceleration for train load HSLM-A1, β=0.9.

The figures above clearly indicate that different parts of the train load are dangerous for different values of β. As can be seen in Table 8.7 the frequency ratio varies a lot depending on the velocity of the train and location of current β.

Table 8.7: Different β-values generated by HSLM-A1. Here $\beta = \beta_1$.

A1	D=18m d=2m				N=18	P=1.7N				
β_1=	0.1	0.2	0.3	0.33	0.4	0.5	0.6	0.7	0.8	0.9
β_2=	0.9	1.8	2.7	2.97	3.6	4.5	5.4	6.3	7.2	8.1
β_{c1}=	0.13	0.26	0.39	0.43	0.51	0.64	0.77	0.90	1.03	1.16
β_{c2}=	0.6	1.2	1.8	2	2.4	3	3.6	4.2	4.8	5.4
β_{c3}=	0.51	1.02	1.53	1.70	2.04	2.55	3.06	3.57	4.09	4.60

In Appendix E.3 all the values of the five different β for the different train loads are presented.

These variations in β makes it difficult to predict the structural responses. For instance, it would be easy to consider that the most severe response would appear for $\beta \approx 1$, but instead it appears already at β=0.2 for HSLM-A1. In Figure 8.42 it can be seen that the maximum response takes place very early in the response history, and according to Table 8.7 both β_{c2} and β_{c3} are close to 1. Even though no results are presented, analysis in SDOF is made for all the train loads HSLM-A1-10, and the analysis clearly shows that this variation of β has great influence. Generally, except for HSLM-A1-2, the most dangerous ratio for each load case is β=0.5 and is generated by the intermediate coaches. For HSLM-A1-2 the maximum response occurred for β=0.2, where the response for HSLM-A2 was the total maximum of all cases and generated by the power car and end coach. It can also be seen that displacements and accelerations have the same decisive β-values, i.e. the maximum occurs for the same value of β. It should still be remembered that in this case the resonance velocity is based upon $\beta = \beta_1$.

9 Finite element analysis

9.1 The finite element model

The finite element model abbreviated as FE-model is created in the finite element program ADINA, see ADINA (2004). The FE-model is produced with regard to the investigated SDOF system, where the SDOF system is transformed to FE-model by the transformation factors in Section 4.3. The FE-model is modelled as a simply supported beam.

9.1.1 Geometry

The beam is chosen to have the length L=10 m and a cross-section with a width b=1 m and a height h=1 m, see Figure 9.1.

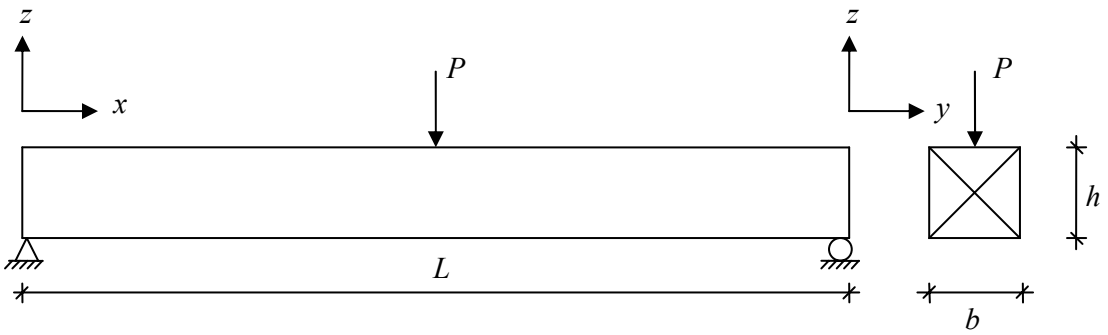

Figure 9.1: Shows the geometry for the chosen beam.

9.1.2 Material

The material is modelled as isotropic and linear elastic, where the strains and displacements are assumed to be small. The mass and modulus of elasticity is calculated so that the first natural frequency f_1 of the beam is equal to one. First the mass is calculated from Equation (4.6) to m=2.06 kg. Then inserting Equation (4.6) into Equation (4.3), the modulus of elasticity can be calculated to E=10013 N/m^2, see Appendix F.1. Poisson's ratio is set to υ=0.2, according to Swedish concrete codes.

9.1.3 Boundary conditions

The FE-model is modelled as a simply supported beam, where translation of the left boundary is fixed in the x-, y- and z-direction and translation of the right boundary is fixed in y- and z-direction. The FE-model is also fixed in x-, y-rotational degrees of freedom, see Figure 9.1.

9.1.4 Elements

The FE-model consists of 2D beam elements, which are a 2-node Hermitian beam, see Figure 9.2, with constant cross-section and six degrees of freedom at each node. The beam is divided into a mesh of twenty equally sized elements, which with a total length of 10 m gives an element size of 0.5 m. The elements are formulated based on the Bernoulli-Euler beam theory.

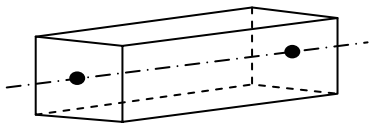

Figure 9.2: Beam element with constant cross-section.

9.1.5 Analysis methods

9.1.5.1 Static analysis

The linear static equilibrium for the finite element model in ADINA is:

$$KU = P \tag{9.1}$$

The static analysis is solved in ADINA by using a direct solution method, where the stiffness matrix is assumed to be symmetric and positive definite. The equation solver used in ADINA is a sparse matrix solver, which according to ADINA (2004) are one or two orders of magnitude faster than other available solution methods based on Gauss elimination. The solver is also very reliable and robust.

9.1.5.2 Frequency analysis

The natural frequencies and the mode shapes of vibration of the FE-model are calculated in ADINA by solving the eigenvalue problem:

$$K\phi_i = \omega_i^2 M\phi_i \tag{9.2}$$

where K is the stiffness matrix corresponding to the time the solution start, M is the mass matrix corresponding to the time of solution start, ω_i and ϕ_i are the circular frequency and mode shape, respectively, for mode i. Note that the frequencies are extracted in the eigenvalue solution in numerically ascending sequence. The eigenvectors are M-orthonormal, i.e. orthogonal and with a length equal to one:

$$\phi_i^T M\phi_i = 1 \tag{9.3}$$

There are several solution methods to choose between when deciding how ADINA should calculate the frequencies and mode shapes. The used method is the subspace iteration method, where the starting subspace is generated by the Lanczos method, see Bathe (1996). The subspace iteration method is default in ADINA.

9.1.5.3 Linear dynamic analysis

The following procedures are available in ADINA for solution of the finite element equations in a linear dynamic analysis, and they are described in Chapter 5. The procedures are the central difference method, Newmark method and mode superposition. The Newmark and mode superposition method are solved by the trapezoidal rule.

9.1.6 Damping

The damping is chosen to be 2.5 %, i.e. the same as in the SDOF model. When using the central difference method and Newmark method, the damping must be modelled as Rayleigh damping, see Section 5.1.3. Using the mode superposition the modal damping can be set to the value 2.5 % for each mode, see Section 5.2.

9.2 Load cases

The FE-model is loaded by different load cases, which becomes more and more similar to the train model HSLM-A described in Section 6.1.3. This is done in order to compare results from SDOF and ADINA and to find out if there is a possibility to use SDOF instead or in conjunction with ADINA or similar finite element programs.

9.2.1 Static analysis

The FE-model in the static analysis consist of a point load P placed in the middle of the beam, the load has a magnitude of 1 N and the self-weight of the beam is not included, see Figure 9.3. This analysis is used to verify the model by comparing hand calculations and results from ADINA. Compared results are reaction forces, moments and displacements.

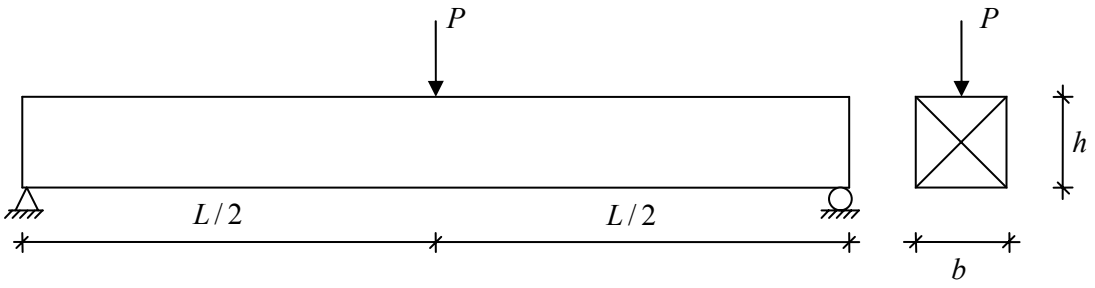

Figure 9.3: Beam loaded by a point load.

9.2.2 Eigenvalue analysis

The eigenvalue analysis is done to calculate the natural frequency $f_{n,i}$, the eigenmode shapes ϕ_i and the participation factors, i.e. the amount of structural mass that is active in each eigenmode, for the FE-model. These calculations are done to verify the FE-model by comparing the results from hand calculations with the results from ADINA.

9.2.3 Varying point load

To be able to compare results from SDOF with ADINA, the loading in the FE-model must be the same as in the SDOF system. Therefore the sinusoidal load shown in Figure 7.5 is used in the FE-model to be compared with SDOF. The load is applied and oscillated in the middle of the beam and the results are checked for both undamped and damped FE-models, see Figure 9.4. The compared results in this and the following load cases are the displacements, velocities and accelerations. The responses are also compared for different solution methods to dynamic problems, where the investigated methods are the explicit time integration, implicit time integration and mode superposition. The comparison between the different solution methods is made in order to verify for which method that the results are most similar to the SDOF results. This is done in order to limit the number of analysis methods down to just one. Also a convergence analysis has been made to find how the time step affect the solution obtained.

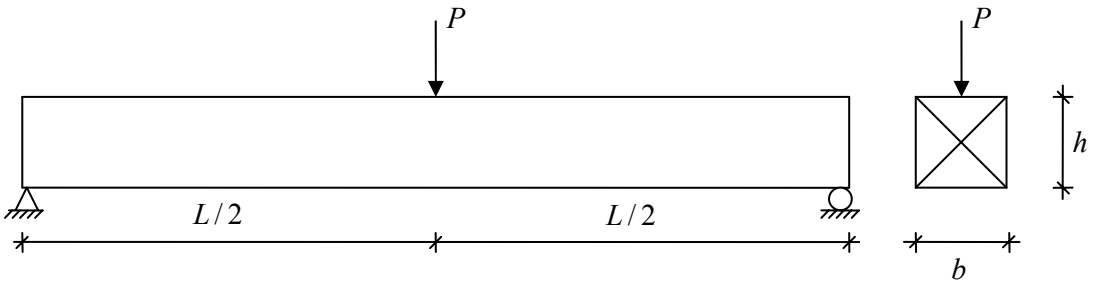

Figure 9.4: Beam loaded by a varying point load applied in the middle of the beam.

The FE-model is also loaded by the same train load that is modelled in SDOF, see Section 7.3.4. The train load is applied in the same way as above, see Figure 9.4, but here only the damped FE-models and SDOF systems are compared.

9.2.4 Single travelling point load

To have a loading that resembles a real train load, the load needs to travel along the beam. Therefore the load in the FE-model is modelled as a point load travelling along the beam with the velocity v. The first travelling load consists of a one point load, which has a magnitude of P=1.7 N, see Figure 9.5. The single travelling load is compared to the response of a SDOF system.

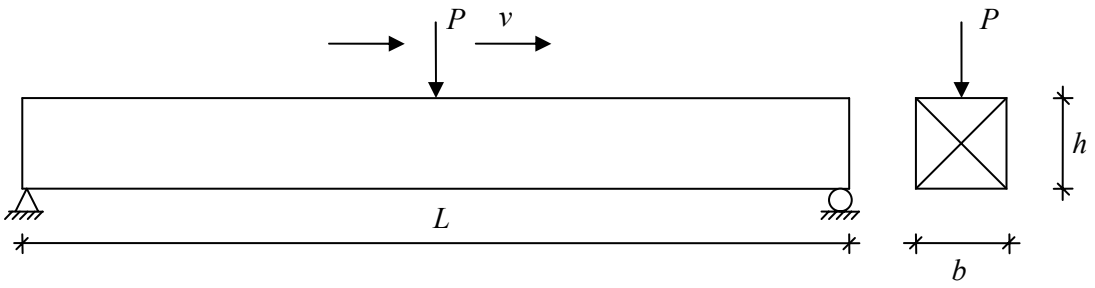

Figure 9.5: Single travelling point load.

9.2.5 Double travelling point load

The loading in the FE-model is modified from one travelling point load to two point loads travelling along the beam with velocity *v,* see Figure 9.6. The point loads have both the magnitude of P=1.7 N. The spacing between the loads are set to 2 m, which is the same spacing as between the bogie axels in the train model HSLM-A1, see Section 6.1.3. The double travelling load is also compared to the results from a SDOF system.

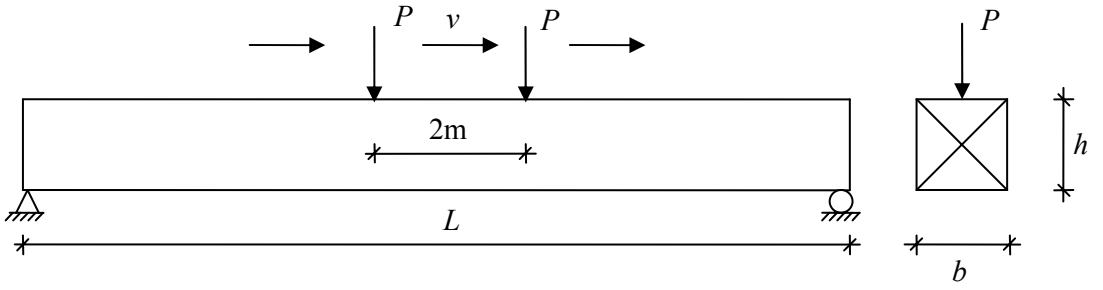

Figure 9.6: Double travelling point load.

9.2.6 Travelling power car load, HSLM-A1

The loading in the FE-model is further modified and now consists of four travelling point loads that are travelling along the beam with the velocity v, see Figure 9.7. The point loads all have the magnitude of P=1.7 N. The loading in this case is describing the power car in the train model HSLM-A1, which is shown in Figure 6.1. The travelling power car load is also compared to the results from SDOF system.

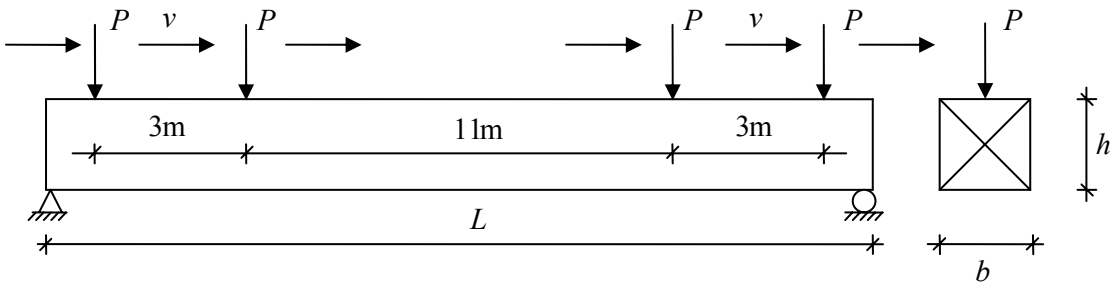

Figure 9.7: Travelling power car load.

9.2.7 Travelling train load, HSLM-A1

The last examined loading in the FE-model is the whole train load model HSLM-A1, where the loads are described by travelling point loads as in the previous load cases. The point loads have all the magnitude of P=1.7 N. The train load model HSLM-A1 is also examined for different velocities and compared with the response of the train load used in the SDOF system, see Section 7.3.4.

10 Results of finite element analysis

10.1 Verification of the model

The verification of the FE-model is done by comparing results of hand calculations, see Appendix F.1, where displacement, moment, reaction forces and the natural frequencies are compared. The model is also verified by comparing the participation factors for different masses and element sizes.

10.1.1 Static analysis

The results from the static analysis show that the FE-model has similar results as the hand calculations. There is no difference between the results of the moment and reaction forces, while a negligible small difference appears for the displacements. The difference appears since the FE-model approximates the values of the displacement by solving Equation (9.1). But also when the number of elements decreases the modelled beam becomes stiffer and will therefore obtain a somewhat smaller displacement, see Table 10.1.

Table 10.1: Comparison of displacement, moment and reaction forces.

Model	Displacement [mm]	Error [‰]	Moment [Nm]	Reaction force [N]
Beam Theory	24.97	-	2.50	0.50
20 Beam Elements	24.97	0.001	2.50	0.50
800 Beam Elements	24.97	0.003	2.50	0.50

10.1.2 Frequency analysis

The frequency analysis for the finite element model is analysed with both a consistent and lumped mass. The results of the analysis show that the case with a lumped mass coincides with the values that are calculated according to the beam theory, described in Chapter 4. The result also shows that 20 elements give a good approximation of the natural frequency, while 800 elements give the same values on the natural frequency as in the beam theory.

Table 10.2: Comparison of natural frequencies for a FE-model with 20 and 800 beam elements.

Mode Number	Beam Theory [Hz]	20 or 800 Elements. Consistent mass [Hz]	Error [%]	20 Elements. Lumped mass [Hz]	Error [%]	800 Elements. Lumped mass [Hz]	Error [%]
1	1.00	1.00	0.41	1.00	0.00	1.00	0.00
2	4.00	3.94	1.61	4.00	0.00	4.00	0.00
3	9.00	8.68	3.50	9.00	0.00	9.00	0.00
4	16.00	15.04	5.98	16.00	0.01	16.00	0.00
5	25.00	22.77	8.90	24.99	0.03	25.00	0.00
6	36.00	31.64	12.12	35.98	0.07	36.00	0.00
7	49.00	41.41	15.49	48.93	0.13	49.00	0.00
8	64.00	51.89	18.93	63.84	0.25	64.00	0.00
9	81.00	62.91	22.33	80.65	0.43	81.00	0.00
10	100.00	74.36	25.64	99.27	0.73	100.00	0.00

The first 19 vertical natural frequencies for a FE-model with a lumped mass and modelled with 20 or 800 elements are shown in Appendix F.2. The results show that the frequencies are similar except for the last 9, but those frequencies are less important to the responses of the FE-model since the amount of structural mass that is active in each eigenmode is higher in the first eigenmodes, see Appendix F.3.

10.2 Comparison of different calculation methods

The results from the static- and the frequency analysis of the FE-model show that it is possible to model the beam with 20 elements. This is also used in the following analyses. The mass is chosen to be modelled with lumped mass and this because it gives better response on the natural frequencies and will therefore give a better response of the examined displacements, velocities and accelerations.

10.2.1 Undamped beam loaded by a harmonic load

In Figure 10.1 and Figure 10.2 the displacements and accelerations from an undamped beam loaded by sinusoidal load shows that the explicit time integration for the FE-model gives results that do not coincide with the results from the SDOF system. While the results obtained using the implicit time integration and mode superposition in the FE-model have perfect accuracy compared to the results obtained in the SDOF system. The velocities are also compared and correspond well to each other, see Appendix F.4. The results from the implicit integration method and the mode superposition method are similar, since both methods use the Newmark trapezoidal rule.

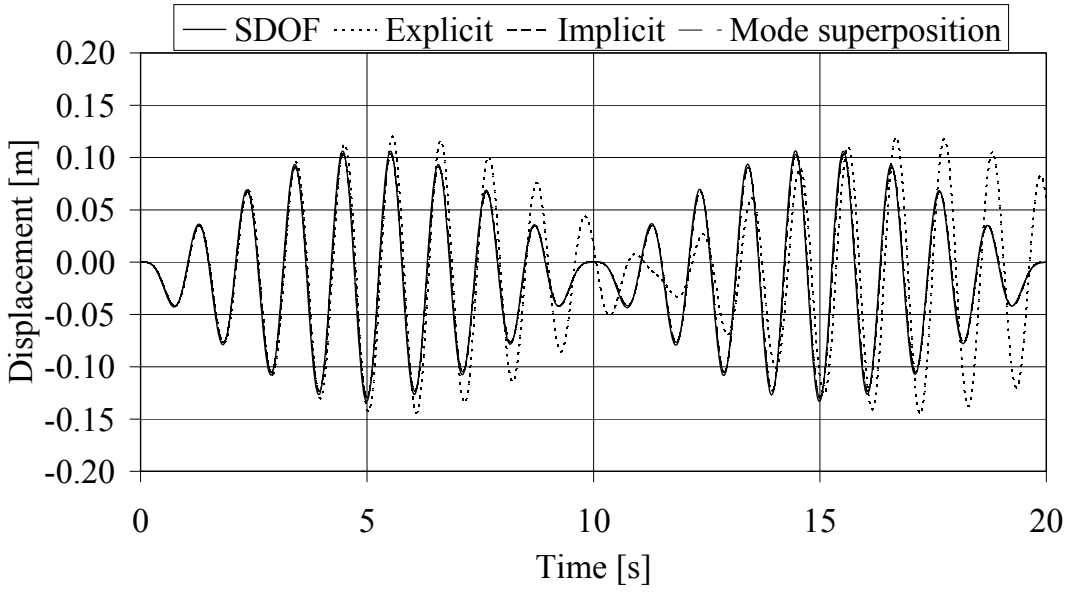

Figure 10.1: Displacement for an undamped beam loaded by a sinusoidal load with β=0.9.

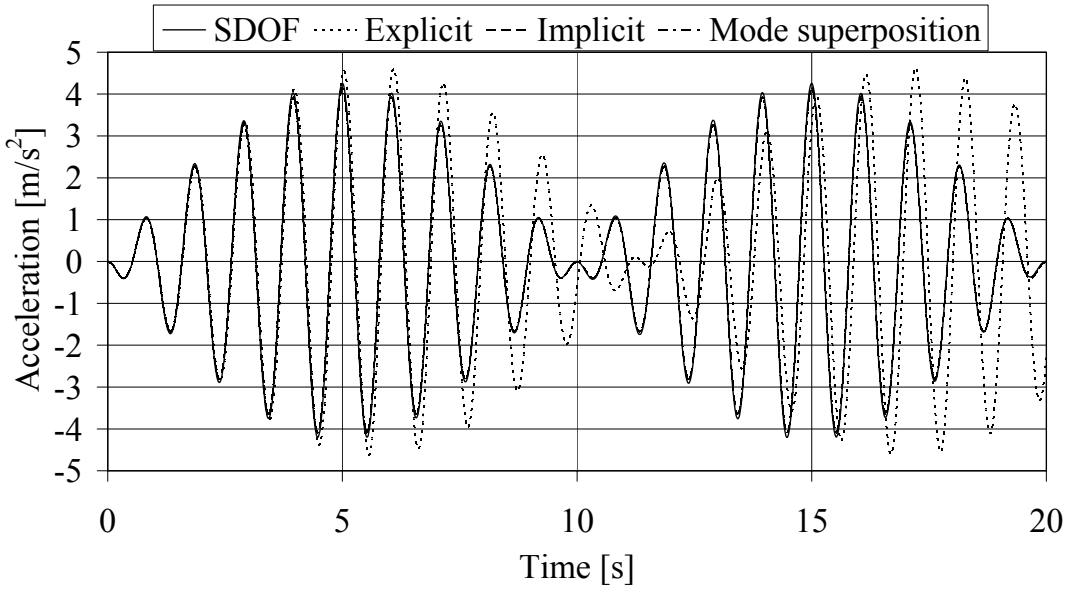

Figure 10.2: Acceleration for an undamped beam loaded by a sinusoidal load with β=0.9.

10.2.2 Damped beam loaded by a harmonic load

In Figure 10.3 and Figure 10.4 the displacements and accelerations from a damped beam loaded by sinusoidal load shows that the implicit time integration and the mode superposition method for the FE-model gives results that coincides with the results from the SDOF system. The velocities are also compared and they correspond to each other, see Appendix F.5. The results in this section also verifies that the statement about the equivalent damping c_e made in Section 4.3.3 is correct.

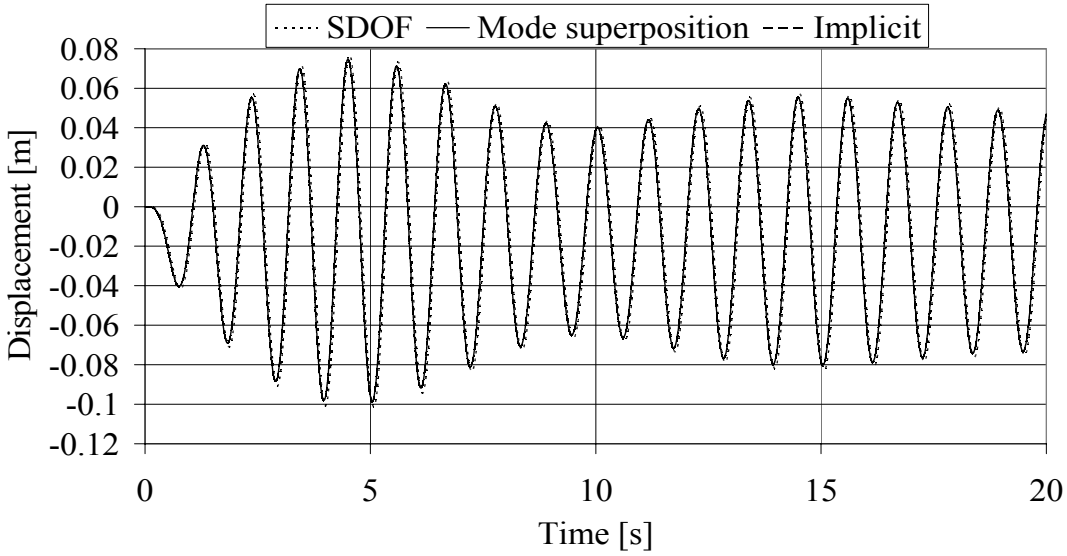

Figure 10.3: Displacement for a damped beam loaded by a sinusoidal load with β=0.9.

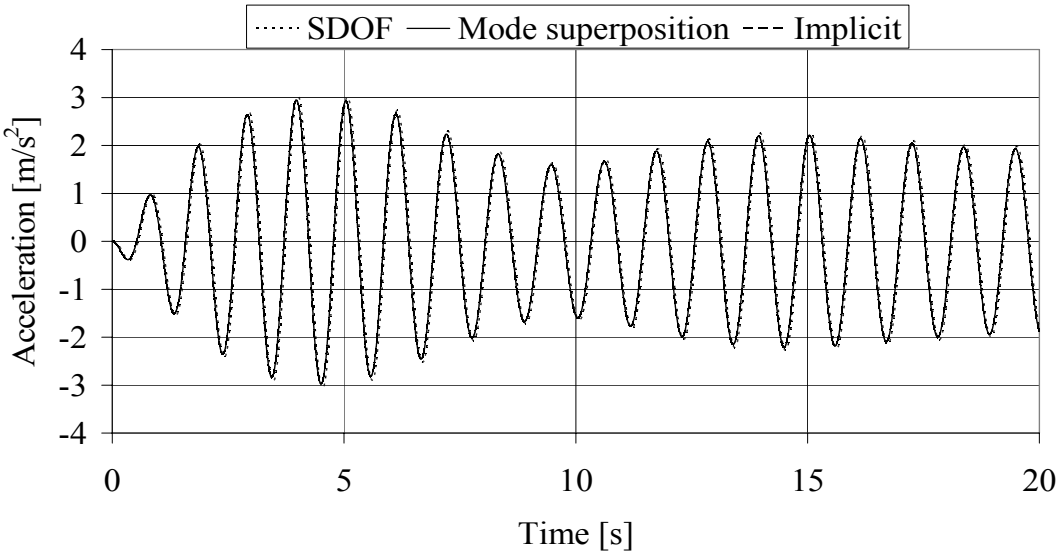

Figure 10.4: Acceleration for a damped beam loaded by a sinusoidal load with β=0.9.

The results from the implicit integration method and the mode superposition method are similar, since both methods use the Newmark trapezoidal rule. Further analyses are only made with the mode superposition method, because it is easier to model the damping with this method, than for the implicit time integration method. As mentioned earlier, in the implicit method the damping must be modelled as Rayleigh damping, while in the mode superposition method the damping can be introduced directly to the eigenfrequency modes. In the problem modelled here, the results from using Rayleigh damping are similar to those when using modal damping, but if the analysed FE-model was more complex the results would start to differ. The reason is that in the Rayleigh damping the damping ratio varies for different eigenmodes, but in this case the amount of structural mass that is active in the first eigenmodes are high and therefore the higher modes has less importance to the response, see Appendix F.3.

10.2.3 Convergence analysis

A convergence analysis for the damped FE-model shows that the time step of 0.01 s gives similar results as for the time step 0.001 s. Therefore it is concluded that for the problem studied here the mode superposition method needs only to have a time step of 0.01 s to have acceptable results. The displacement and the acceleration for the convergence analysis are shown in Figure 10.5 - Figure 10.6. The result for the velocity is the same as for the displacement and acceleration see Appendix F.7.

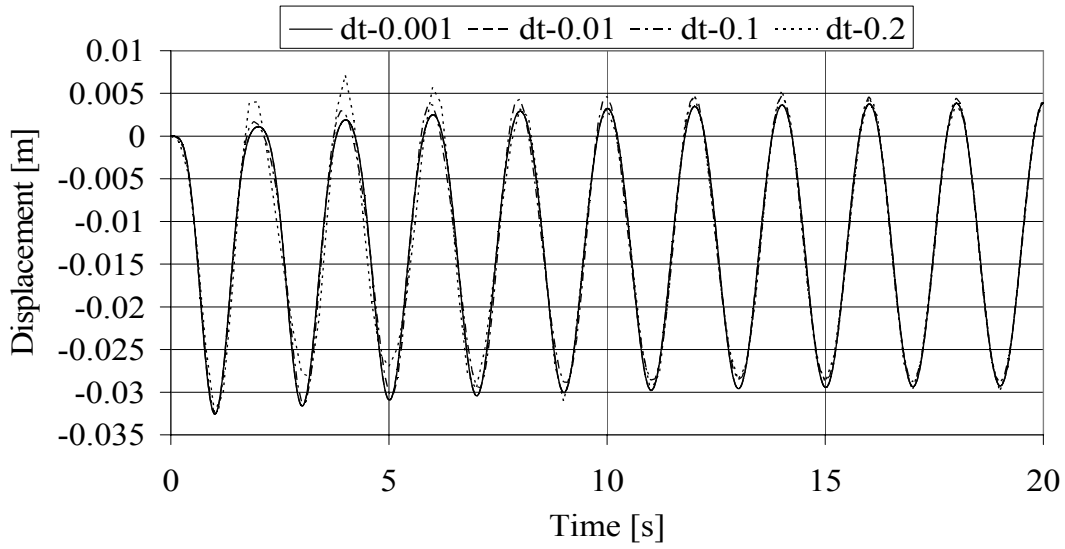

Figure 10.5: Convergence analysis of the displacement for a damped beam loaded by a sinusoidal load with β=0.5.

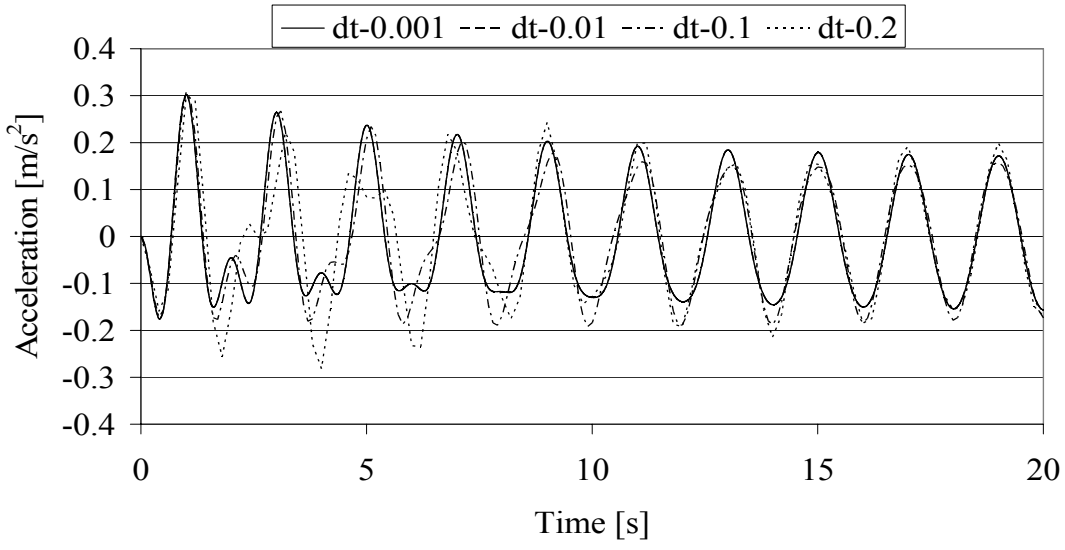

Figure 10.6: Convergence analysis of the acceleration for a damped beam loaded by a sinusoidal load with β=0.5.

For the undamped FE-model, the convergence analysis shows similar results regarding the time step as for the damped FE-model, see Appendix F.6.

10.2.4 Comparison of a varying point load

In this section the two systems are excited by HSLM-A1, see Figure 7.9, and the results from the SDOF and ADINA analysis shows that the compared displacements are very similar, see Figure 10.7, while the accelerations first starts to coincide for low β-values. Figure 10.8 shows that the acceleration for β=0.2. Both figures show only the first 20 seconds of the analysis time and the results from all comparison of displacements, velocities and accelerations are presented in Appendix F.7. The velocities are similar for $\beta \leq 0.7$ but after that the difference starts to grow. The differences that appear are due to that ADINA includes more mode shapes in analysis, compared with SDOF that only has 1 mode shape, see Section 4.1.

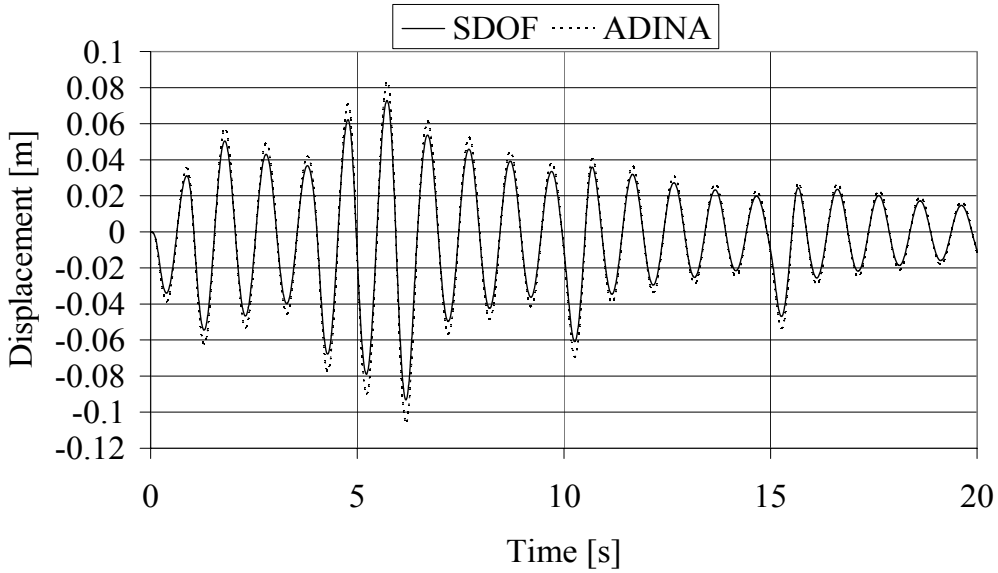

Figure 10.7: Displacement from dynamic analysis of a damped beam loaded by varying point load HSLM-A1 with β=0.2.

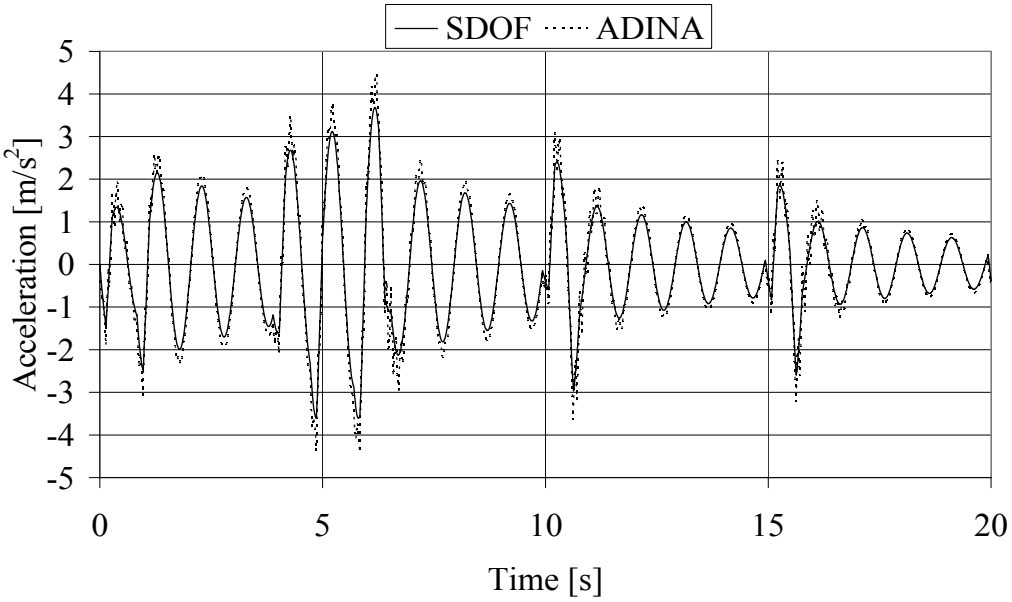

Figure 10.8: Acceleration from dynamic analysis of a damped beam loaded by varying point load HSLM-A1 with β=0.2.

10.3 Comparison of travelling point loads

The travelling point load describes in a more realistic way the loading from a train. When comparing the results from the travelling point load with the SDOF system, large differences in the response appeared. Therefore the loading in SDOF is modified and the results are again compared with a travelling point load. The result from the first SDOF analysis is called SDOF 1 and the result from the modified analysis is called SDOF 2. The travelling point load starts first with a single load and becomes thereafter more complex. However, due to the limited time for the master's thesis, the whole train model HSLM-A is not modified in this report. Also only velocities of the travelling point loads generating values of β=0.2, 0.5 and 0.9 are analysed.

10.3.1 Single travelling point load

The single travelling point load is compared with two different load cases in the SDOF system. The first load, SDOF 1, has the same loading time as the travelling load has in the FE-model. Here the time t_1 is the required time for the single travelling load to move between two adjacent nodes. The second modified load SDOF 2 has the loading time t_2, which is the time for the single travelling load to move the distance of 10 m along the beam, see Figure 10.9.

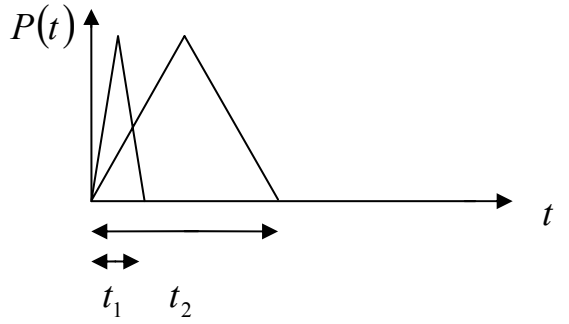

Figure 10.9: The change of loading time for the SDOF system.

The change of the loading time from t_1 to t_2 in the SDOF system, results in a response for the displacement and acceleration more similar to the response from the analysis of the FE-model, see Figure 10.10 - Figure 10.11.

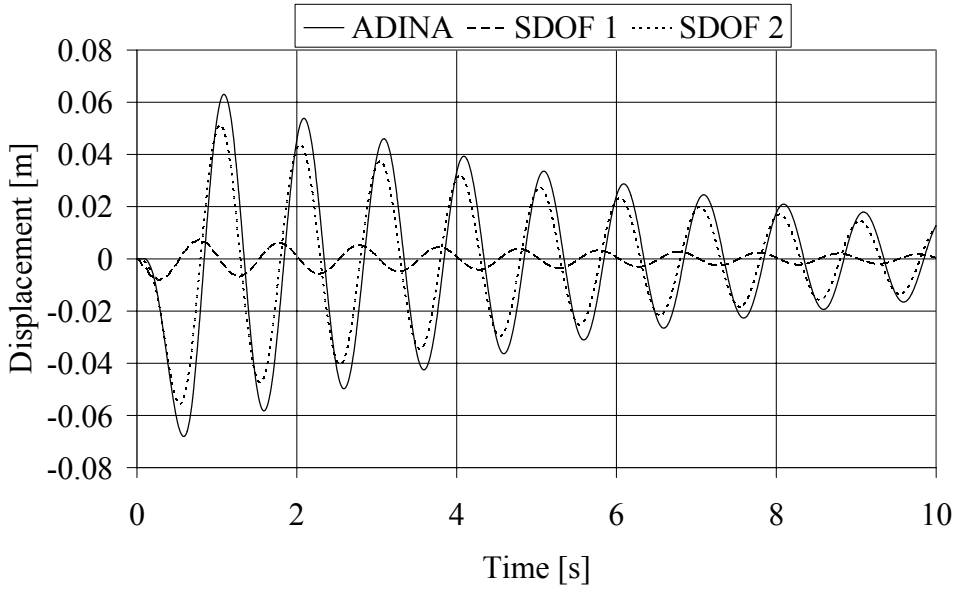

Figure 10.10: Comparison of displacements between different load cases of a single point load with β=0.9.

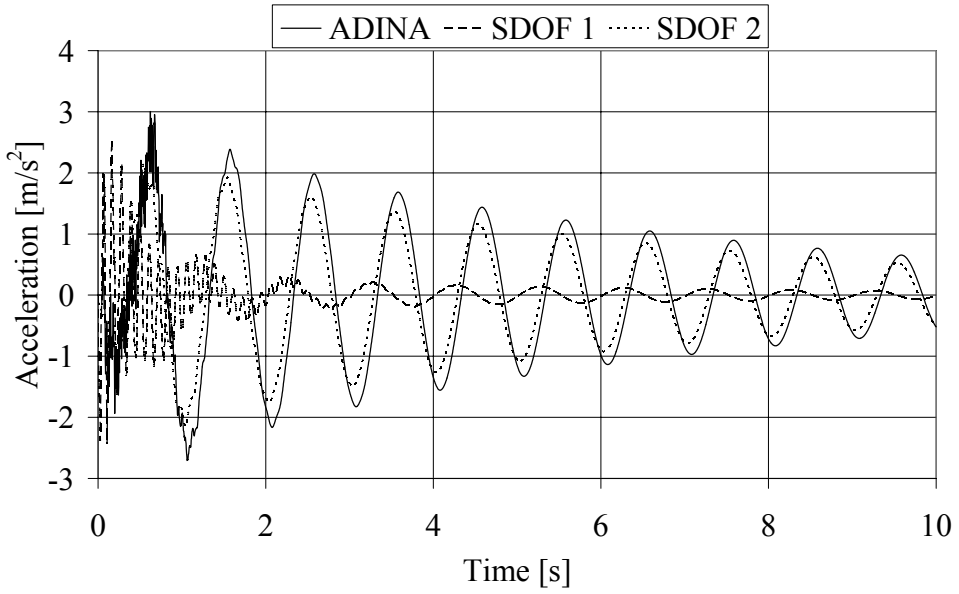

Figure 10.11: Comparison of accelerations between different load cases of a single point load with β=0.9.

The responses for β=0.9, shown in the figures above, are not only similar in amplitude but also almost in phase, but in the lower β-values the load SDOF 2 has a small phase angular difference compared to the results of the FE-model. The responses of load SDOF 1 are out of phase by an angle of about 90˚-180˚ and, with the exception of β=0.2, it generally has lower amplitudes on the response, see Appendix F.8.

10.3.2 Double travelling point load

The double travelling point load is compared with two different load cases for the SDOF system. The first load SDOF 1 has the same loading time as the travelling load has in the FE-model. The duration of each triangular load pulse is set to t_1, i.e. the required time for the single travelling load to move between two adjacent nodes. As described earlier in Section 9.1.4, the sizes of the beam elements are 0.5 m. The time between the two loads corresponds to the spacing within the bogie axle loads in HSLM-A1, where the spacing is 2 m, see Figure 10.12.

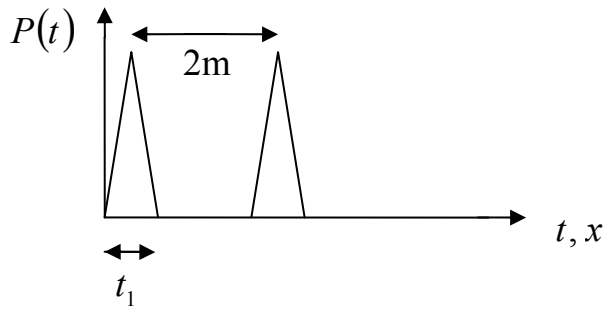

Figure 10.12: The modelled load SDOF 1.

The second modified load SDOF 2 has a loading history of a superposition of two triangular loads. The loading time for the triangular loads is t_2, which is the time for the single travelling load to move the distance of 10 m along the beam. The second triangular is delayed with the time t_3 that corresponds to the spacing within the bogie axles in the train model HSLM-A1, where the spacing is 2 m, see Figure 10.13.

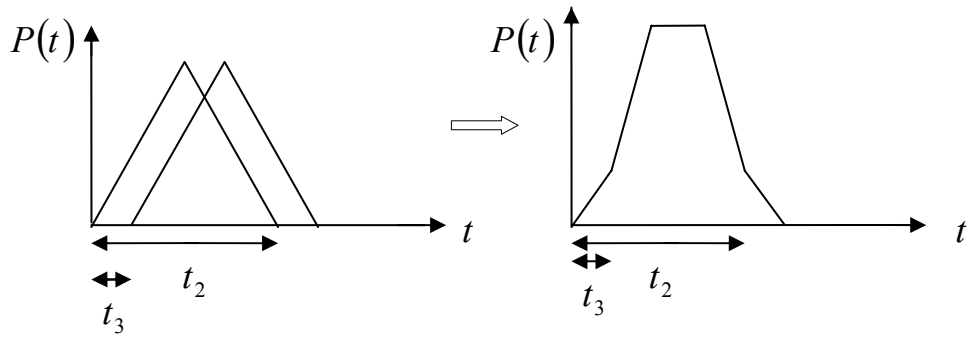

Figure 10.13: The modelled load SDOF 2.

The change in loading from SDOF 1 to SDOF 2 for the system shows the same phenomena as for the comparison of the single travelling load, see Section 10.3.1. The results show that the response of the displacement and acceleration becomes more similar to the response from the analysis of the FE-model, see Figure 10.14 - Figure 10.15.

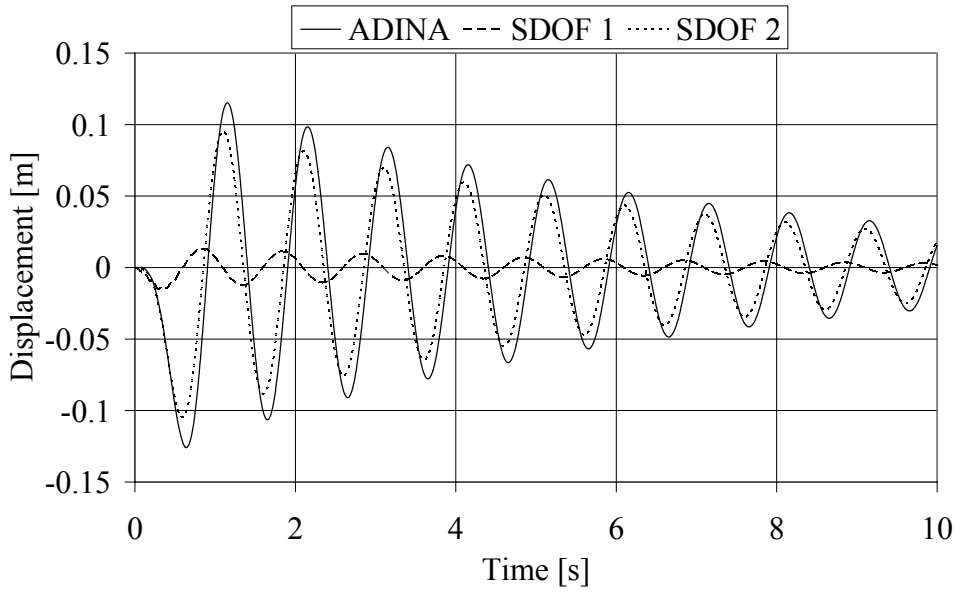

Figure 10.14: Comparison of displacements between different load cases with β=0.9.

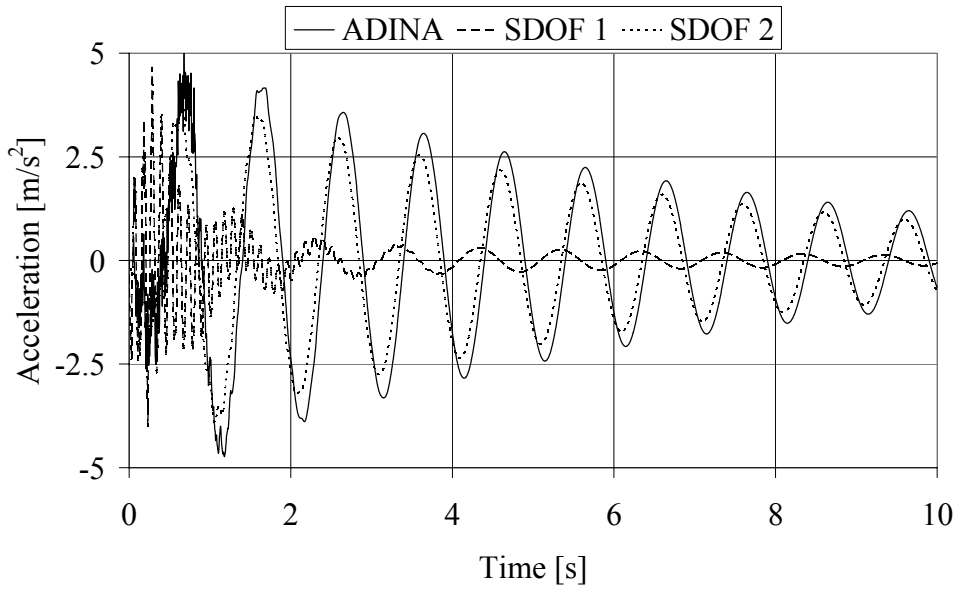

Figure 10.15: Comparison of accelerations between different load cases with β=0.9.

The responses for β=0.9, shown in the figures above, are not only similar in amplitude but also almost in phase, but in the lower β-values the load SDOF 2 has a small phase angular difference compared to the results of the FE-model. The responses of load SDOF 1 are out of phase by an angle of about 90˚-180˚. Further, it generally has lower amplitudes on the response, except for the velocity and the acceleration, when β=0.2, and for the acceleration when β=0.5, see Appendix F.9.

10.3.3 Travelling power car load, HSLM-A1

The travelling power car load is compared to two different load cases in the SDOF system. The first load SDOF 1 has the same loading time as the travelling load has in the FE-model. Here the time t_1 is the required time for the single travelling load to move between two adjacent nodes. The time delay between the four loads corresponds to the spacing within the bogie axle and between the two following bogie axles in the power car load HSLM-A1. The spacing between the axle loads is 3 m and 11 m respectively, see Section 9.2.6 and Figure 10.16.

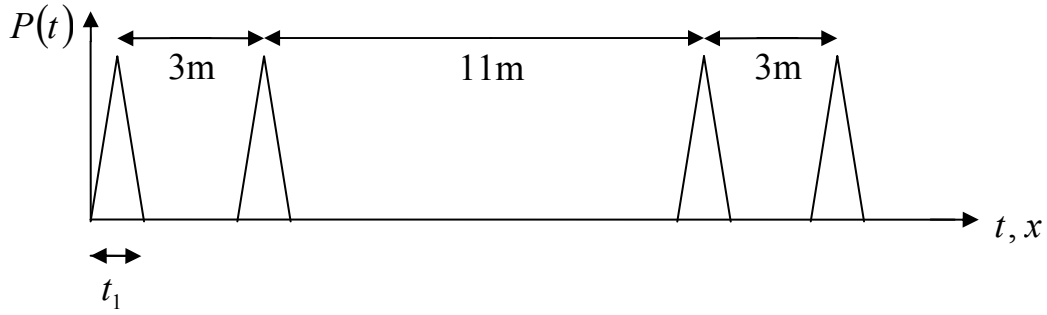

Figure 10.16: The modelled load SDOF 1.

The second modified load, SDOF 2, has a load history of a superposition of four triangular loads, where the triangular loads are combined in the same way as in Figure 10.13. The loading time for the triangular loads is t_2, which is the time for the single travelling load to move the distance of 10 m along the beam. The second triangular is delayed with the time t_3 that corresponds to the spacing within the bogie axle loads in HSLM-A1. The appearance time for the following combination of two triangular loads is delayed by the time that corresponds to a spacing of 1 m, i.e. since the length of the beam is 10 m, see Figure 10.17.

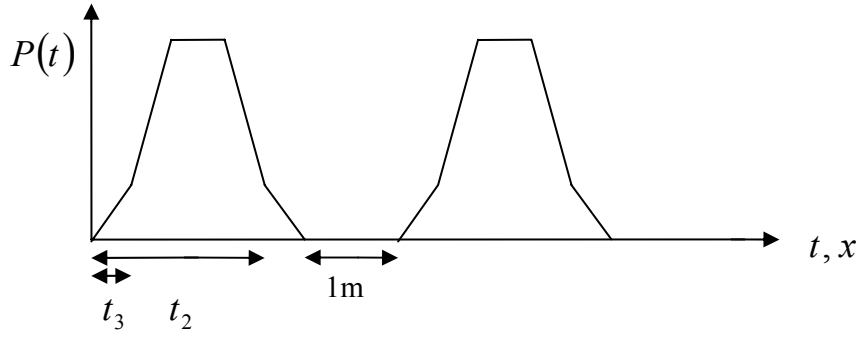

Figure 10.17: The modelled load SDOF 2.

The change in loading from SDOF 1 to SDOF 2 for the system, has the same phenomena as for the comparison of the single travelling load and the double travelling load, see Section 10.3.1 - Section 10.3.2. The results show that the response of the displacement and acceleration becomes more similar to the responses from the analysis of the FE-model by using SDOF 2, see Figure 10.18 - Figure 10.19.

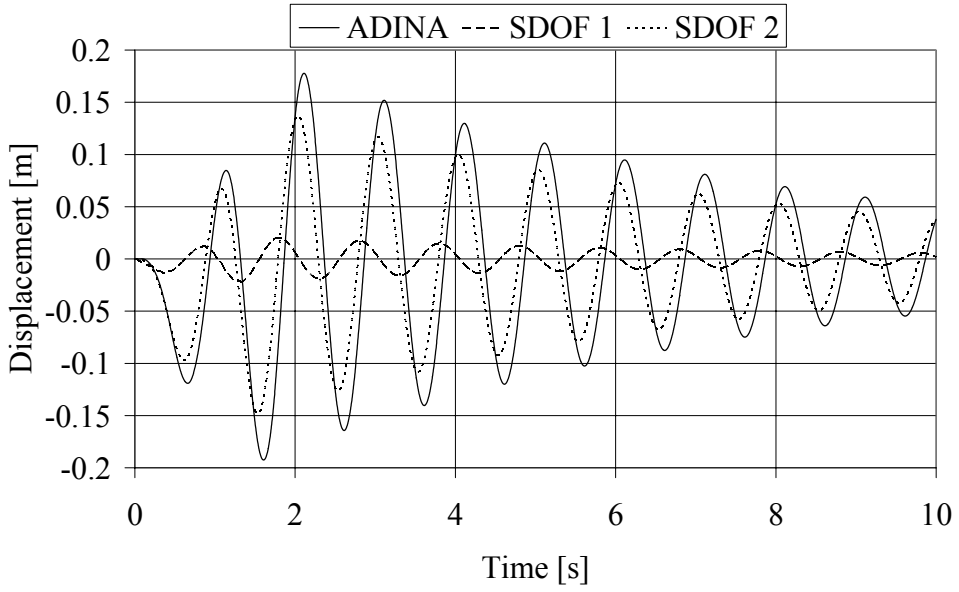

Figure 10.18: Comparison of displacements between different load cases with β=0.9.

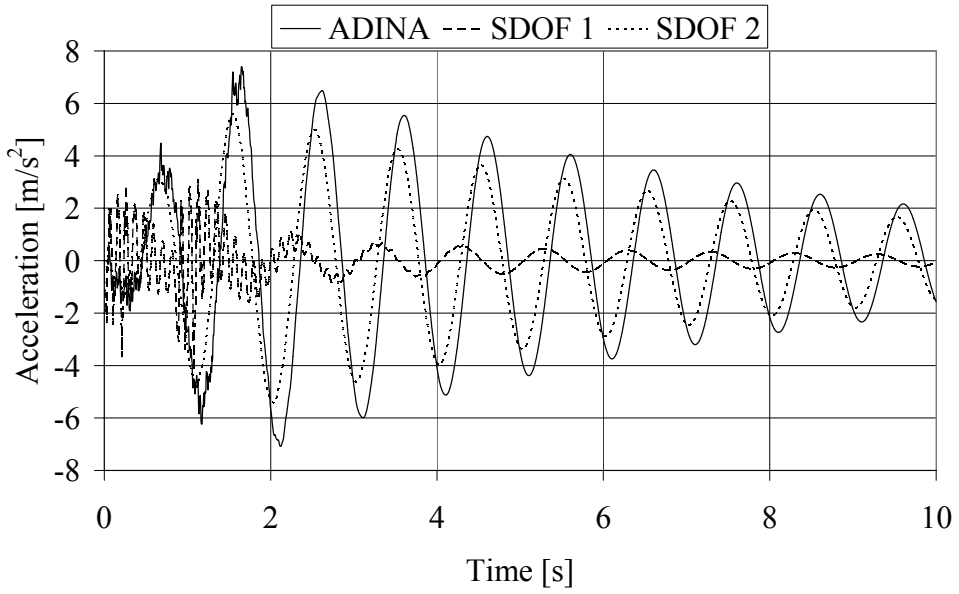

Figure 10.19: Comparison of accelerations between different load cases with β=0.9.

The responses for β=0.9, shown in the figures above, are not only similar in amplitude but also almost in phase, but in the lower β-values the load SDOF 2 has a small phase angular difference compared to the results of the FE-model. The responses of load SDOF 1 are out of phase by an angle of about 90˚-180˚. Further, it generally has lower amplitudes on the response, except for the velocity and the acceleration, when β=0.2, and for the acceleration when β=0.5, see Appendix F.10.

10.3.4 Travelling train load, HSLM-A1

The travelling load HSLM-A1 in ADINA is only compared with the train load that is not modified as in the previous load cases. The results from the analysis between SDOF and ADINA shows that the FE-model gives a larger response for all cases, except for β=0.2. Here the SDOF-model gives larger response in positive displacements and accelerations in general, see Figure 10.20 - Figure 10.21. The response of the SDOF system are out of phase compared to ADINA, see Appendix F.11.

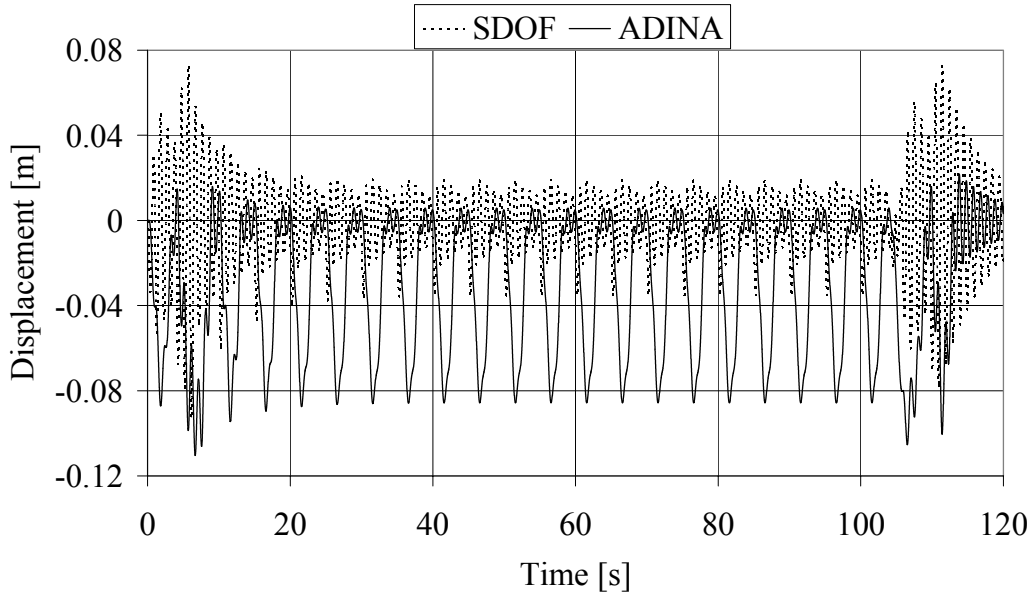

Figure 10.20: Displacement from dynamic analysis of a damped beam loaded by travelling train load HSLM-A1 with β=0.2.

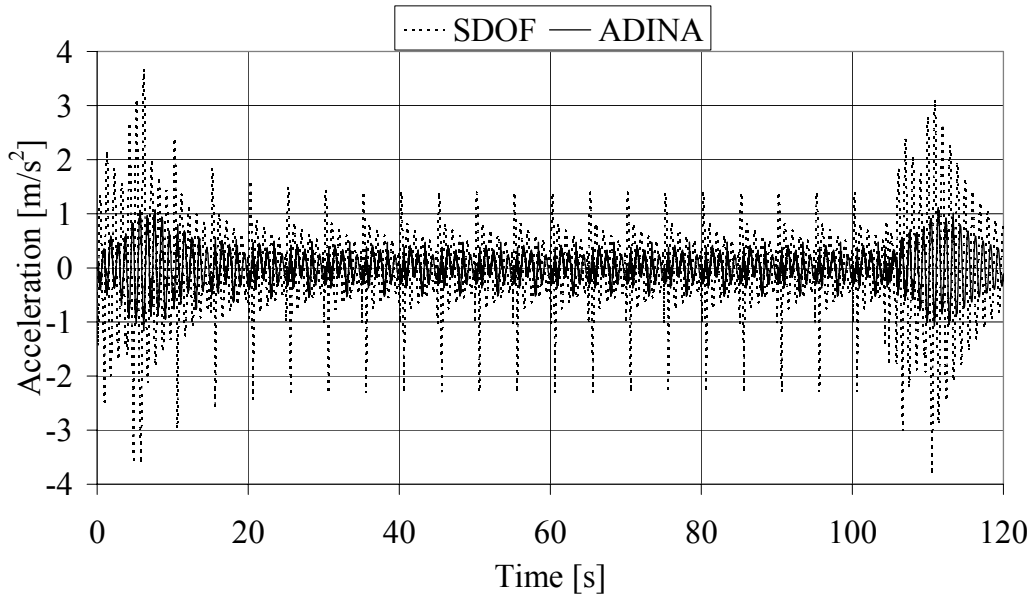

Figure 10.21: Acceleration from dynamic analysis of a damped beam loaded by travelling train load HSLM-A1 with β=0.2.

If ignoring the amplitude and only looking at the response shape, it can be seen that the response from the train load generally is well described by the SDOF system. When comparing the response, e.g. for β=0.5, the result from SDOF are normalized by factor *s*, it can be seen that the response shapes becomes very similar. The difference in phase angular is still unaffected. For this example with β=0.5 the factor *s* is ~3 for all responses, see Figure 10.22 -Figure 10.23.

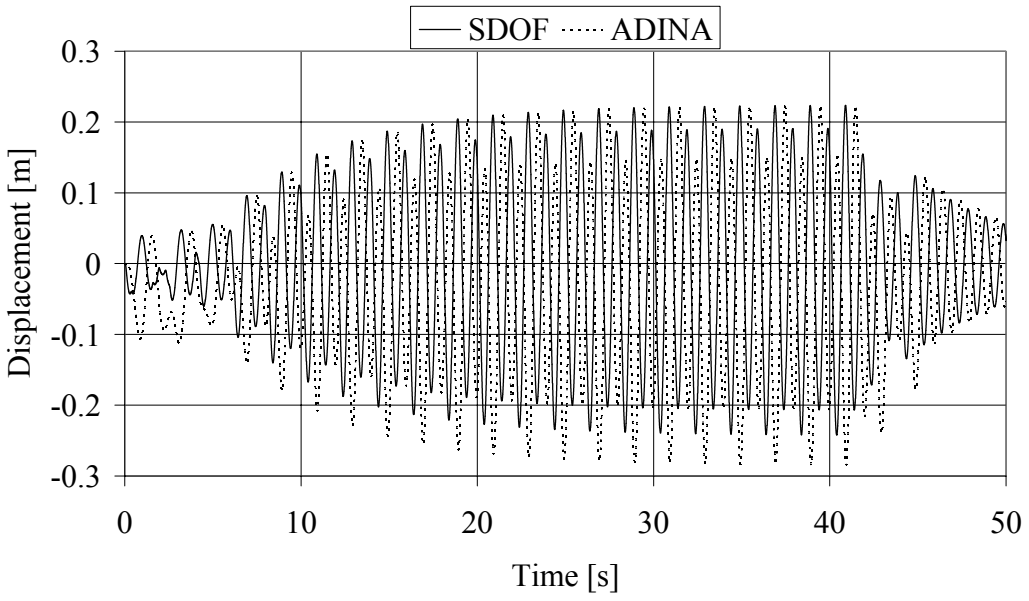

Figure 10.22: Comparison of normalized displacements between SDOF and ADINA response for β=0.5.

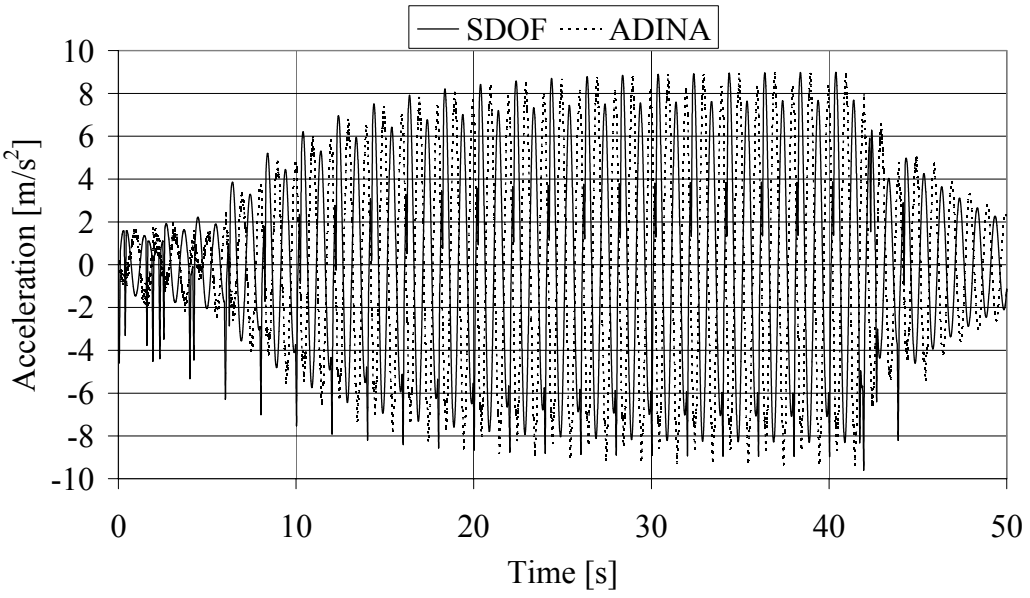

Figure 10.23: Comparison of normalized accelerations between SDOF and ADINA response for β=0.5.

11 Conclusions

11.1 General

In this thesis an attempt to make simplifications concerning calculations during dynamic analysis of railway bridges is made. A major part of the time was spent on literature studies and it soon got very clear that the analytical basic theory's behind dynamic behaviour excited by harmonic loading is very well documented. As soon as the load starts to get more complicated and not so easily predefined the area is not as well documented.

In this thesis large focus is put on what influence the frequency ratio $\beta=\omega_p/\omega_n$ has on a SDOF system for different types of loading The calculations in this thesis are not intended as real values, but are only intended to act as mutual comparison with each other. The inputs have been chosen in order to simplify the comparison between different load cases.

Different types of excitations have been studied in order to determine if some types are more critical or dangerous than others. Three different types of load shapes were used: sinusoidal, triangular and rectangular loads. By using different combinations a total of 5 load cases are examined. When determining which type of load that is more critical or dangerous the total impulse of the load pulse and loading frequency is kept constant. The analysis showed that the rectangular load had the most critical response. Why this is the most critical load is believed to depend on two reasons. First of all, this load has the maximum magnitude during the entire impulse, compared with the other examined loads that have maximum magnitude during only one Δt. The second reason is how the load is applied and unloaded. The rectangular load is applied very suddenly and reaches maximum magnitude instantly and is also removed in the same way, while the continuous triangular and sinusoidal load grows until maximum magnitude during half the impulse time. The difference between the different load types was velocity dependent, i.e. dependent of the ratio between the frequencies β. During faster applied loads the response shapes were very similar, with only difference in magnitude, while the slowly applied loads have large differences both in shape and magnitude. This means that for fast applied loads, all load cases can be reasonably well described by a harmonic excitation, considering the response shape.

As stated above the type of load has great influence on the response of the system, as well as the ratio between circular frequencies. It can also be seen that a combination by the two also seems to have great influence. For both the continuous triangular and rectangular load it could be seen that when the frequency ratio $\beta=1/(2n+1)$ the response started to grow dramatically and when undamped even show resonance behaviour. Exact reason for this phenomenon is not clearly investigated. This phenomenon could not be seen during harmonic excitation so the type of loading clearly has an influence, and especially how the load is applied and unloaded.

Double triangular loads were used to resemble the bogie axle loads generated by the intermediate coaches. The sensitivity of the relation between the two frequencies f_{p1} and f_{p2}, where f_{p1} and f_{p2} are the frequencies based upon the distances D and d in the train load model HSLM-A, was investigated. It is shown that already when $f_{p1}\sim 6f_{p2}$ the maximum displacements are obtained for less number of intermediate coaches

than the minimum number in the HSLM-A. It is also shown that for most of the train load cases the maximum response was generated by the intermediate coaches. By the fact, that for most load cases $f_{p1}>6\,f_{p2}$ it is reasonable to think that it is possible the limit he number of intermediate coaches that are included in the analysis, and thereby limit the analysis time consumed.

The analyses made in the SDOF system are compared with result from FE-model. The FE-model consists of a deformable body, and in this case a simply supported beam, that is transformed into a single degree of freedom system by using transformation factors. These transformation factors are applied on the mass m, stiffness k, and applied load p. The results between the two systems coincide very well. For the damping c it is assumed that the transformation into an equivalent c_e will be generated by the transformed values of the mass and stiffness. This assumption is verified by comparison between results calculated with the unmodified c with calculations with the equivalent value c_e and proved to be very reasonable.

By the different spacing between the bogie axle loads in the train model HSLM-A, it will be generated different frequency ratios β depending on the location of the spacing and the train velocity. When the analysis was made by use of SDOF for all the train loads HSLM-A1-10, the analysis clearly shows that this variation of β has great influence. It is shown that the maximum response occurs for HSLM-A2 with a train that has a velocity generating β=0.2. The responses are generated by the power car and end coach and it can also be seen that the displacements and accelerations have the same decisive β-values, i.e. the maximum occurs for the same value of β. Based on this it is clearly important to consider all different β-values and not only those generated by the spacing D and d in HSLM-A

HSLM-A1 was considered as a varying point load, and applied and compared between the SDOF system and FE-model. The response for displacements the results coincide very well, while for the accelerations the response coincides in terms of response shape but there is a large difference in magnitude. No clear explanation can be given for why the large difference appears for the acceleration, but one reason may be that the transformation factors not entirely capture the behaviour of the beam, which causes this difference. When applying the travelling load to the FE-model and comparing the results with the same point load as above, they can at first seem to have no similarities at all. However, after normalizing the values from the SDOF system it seems like the transformation from a deformable body into a SDOF system is a good approximation when interested in the system response shape.

In an attempt to make the SDOF system able to resemble the travelling point loads in a better way, the time that the load is applied were modified. It shows that by experimenting with load time and shape, it is possible to describe the response from at least up to four travelling point loads that is intended to resemble the power car in HSLM-A.

Based on analysis of the analytical solution it has been shown that the, commonly used Dynamic Amplification Factor *DAF* not are satisfying when looking at short term dynamic loading, since it neglects the time dependence of the damping and therefore will underestimate the maximum response.

11.2 Further investigations

To be able to increase the understanding about the dynamic behaviour, the reason why the system response have a growing tendency when the ratio between the circular frequencies β=1/(2n+1) needs to be investigated further.

Previously it could be seen that the results from modifying the SDOF system by superposition of triangular loads gave a satisfactory result in terms to resemble the moving power car. Therefore the entire HSLM-A needs to be modified to determine if this captures the behaviour in a better way.

To verify this method real material properties and load magnitudes should be introduced into the expressions and determine if the conclusion stated above still withhold. The method should also be investigated for the behaviour if the geometrical properties or boundary conditions change. In order to make the analysis method even more complex the response of moments and section forces should be included.

12 References

WRITTEN SOURCES:

ADINA (2004): *Theory and Modelling Guide Version 8.2.2*. ADINA R&D, Inc., Volume 1, Watertown, USA.

Banverket, (2006): BV BRO – *Banverkets ändringar och tillägg till Vägverkets Bro 2004,* (Revision and additions by the Swedish Railway Administration to the Swedish Bridge code, Bro 2004. In Swedish), inklusive supplement nr 1, Utgåva 8, BVS 583.10.

Bathe K.-J. (1996): *Finite Element Procedures*. Prentice Hall, Englewood Cliffs, New Jersey, USA.

Bergan, P.G., Larsen, P.K., Mollestad E. (1986): *Svingning av konstruksjoner*, (Structural oscillations. In Norwegian), No 2. Tapir, Norway.

Björklund, L. (2005): *Dynamic Analysis of a Railway Bridge*. Master of Science Thesis. Department of Civil and Architectural Structural Engineering, Royal Institute of Technology, Publication no. 05:218, Stockholm, Sweden, 2005.

Geradin, M., Rixen, D. (1992): *Mechanical vibrations*. John Wiley & sons, Inc., No 2, New York, USA.

Grahn, R., Jansson, P-Å. (2002): *Mekanik – Statik och dynamik,* (Mechanics – Static and dynamic. In Swedish), Studentlitteratur, No 2, Lund, Sweden.

Nyström, U. (2006): *Design with regard to explosions*. Master of Science Thesis. Department of Structural Engineering, Chalmers University of Technology, Publication no 06:14, Göteborg, Sweden.

Samuelsson, A., Wiberg, N-E. (1993): *Byggnadsmekanik – Hållfasthetslära*, (Solid mechanics. In Swedish), Studentlitteratur, No 2., Lund, Sweden.

WEB SOURCES:

KTH (2006) Notes for lesson in Structural Dynamics at the Royal institute of Technology, Stockholm. http://www2.mech.kth.se/~jean/dynamics/dc8.ppt#6.

Appendix A Continuous systems

In this appendix an attempt to, in a simplified way, present some background to the calculations of continuous systems, or systems with multi degree of freedom. How these calculations, which are expressed in terms of energy expression, e.g. Hamilton's principle, can be transferred into one-dimensional continuous systems. By using the expressions for the one-dimensional system calculating the eigenvalue problem the eigenfrequency expression seen in Section 4.1 can be stated. The chapter is entirely based on Géradin and Rixen (1992).

The theory presented in Chapter 3 and systems represented by discrete models are usually an idealized view. To be able to formulate the governing equations for a continuous system, the theory of continuum mechanics have to be applied. Here the equation of motion is expressed in terms of a displacement field:

$$u(x,y,z,t) \qquad v(x,y,z,t) \qquad \mathrm{w}(x,y,z,t)$$

The space variables x, y, z are continuous and therefore the system contains an infinity of degree of freedom. Continuous systems may be considered as limiting cases of discrete systems and therefore, the specific geometry of the continuous bodies allows simplified formulations of the equation of motion, only expressed by one or two displacement components, and themselves as functions of one or two space variables and time.

A.1 One-dimensional continuous systems

Beams in bending are a physical system that is included in a category called one-dimensional systems. The reason for this is that the displacement field is supposed to occur in one plane and is denoted:

$$u(x,t) \qquad v=0 \qquad w(x,t)$$

for either longitudinal or transverse motion. The equation of motion for such type of system can be obtained by Hamilton's principle, or it is also possible to generalize the formulation of the Lagrange equations to continuous one-dimensional systems.

The Lagrange equations are deduced from Hamilton's principle

$$\delta \int_{t_1}^{t_2} \mathbf{L} dt = 0 \tag{A.1}$$

Where $\mathbf{L} = \mathbf{W}_k - \mathbf{W}_p$ is the Lagrangian of the system. By integration over the one-dimensional system of length l the kinetic and potential energies can be stated as:

$$\mathbf{W}_k = \int_0^l W_k(x,t)dx \qquad \mathbf{W}_p = \int_0^l W_p(x,t)dx \tag{A.2}$$

If we suppose that the displacement field is one-dimensional and calling the displacement component v, it can generally be said that:

- The potential energy W_p is a function of the displacement v and its first and second derivatives with respect to the space variable.

$$W_p = W_p\left(v, v', v''\right) \tag{A.3}$$

- The kinetic energy W_k is always a function of the velocity field $\dot{v}$, but may also depend on the instantaneous configuration v, it is first derivative in space and the associated velocity $\dot{v}'$.

$$W_k = W_k\left(v, \dot{v}, v', \dot{v}'\right) \tag{A.4}$$

The general dynamic behaviour in terms of Lagrangian density can be stated as:

$$L = W_k - W_k = L\left(v, v', v'', \dot{v}, \dot{v}'\right) \tag{A.5}$$

Expressing the variation δL of Lagrangian density, the expression becomes:

$$\int_{t_1}^{t_2}\int_{0}^{l}\left(\frac{\partial L}{\partial v}\delta v + \frac{\partial L}{\partial v'}\delta v' + \frac{\partial L}{\partial v''}\delta v'' + \frac{\partial L}{\partial \dot{v}}\delta \dot{v} + \frac{\partial L}{\partial \dot{v}'}\delta \dot{v}'\right)dxdt = 0 \tag{A.6}$$

Using integration by parts, to express all variations in terms of virtual displacements, and that the application condition of Hamilton's principle implies that $\delta v(t_1) = \delta v(t_2) = 0$, it can be stated that:

Equation of motion:

$$\frac{\partial L}{\partial v} - \frac{\partial}{\partial x}\left(\frac{\partial L}{\partial v'}\right) + \frac{\partial^2}{\partial x^2}\left(\frac{\partial L}{\partial v''}\right) - \frac{\partial}{\partial t}\left(\frac{\partial L}{\partial \dot{v}}\right) + \frac{\partial}{\partial t}\left(\frac{\partial}{\partial x}\left(\frac{\partial L}{\partial \dot{v}'}\right)\right) = 0 \tag{A.7}$$

Boundary conditions:

$$\left[\frac{\partial L}{\partial v'} - \frac{\partial}{\partial x}\left(\frac{\partial L}{\partial v''}\right) - \frac{\partial}{\partial t}\left(\frac{\partial L}{\partial \dot{v}'}\right)\right]\delta v = 0 \text{ at } \begin{cases} x = 0 \\ x = l \end{cases} \tag{A.8}$$

and

$$\frac{\partial L}{\partial v''}\delta v' = 0 \text{ at } \begin{cases} x = 0 \\ x = l \end{cases} \tag{A.9}$$

A.2 Beam vibrations

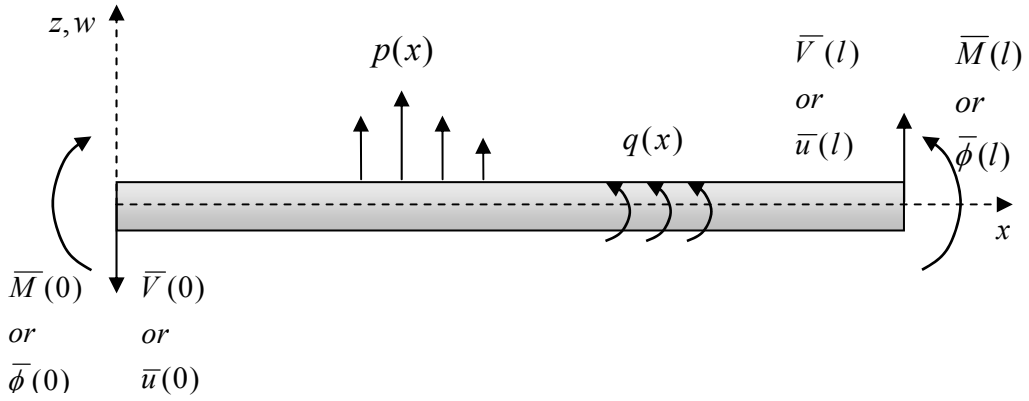

Figure A.1: Transverse vibrations of beams.

Transverse vibrations of beams, see Figure A.1, are simplest described by using a model with the kinematic assumptions that:

1. The beam cross section is not deformable.

2. The transverse displacement on it is uniform and is limited to the displacement in the *x*-*z* plane.

$$w = w(x), \qquad v = 0 \tag{A.10}$$

3. The axial displacement components results from the rotation of the cross section. The rotation is such that the cross section remains orthogonal to the neutral axis.

$$u(x,z) = -z\frac{\partial w}{\partial x} \tag{A.11}$$

With the assumption of geometric linearity, the strain expressions can be written as:

$$\varepsilon_x = \frac{\partial u}{\partial x} = -z\frac{\partial^2 w}{\partial x^2}$$

$$\varepsilon_z = \frac{\partial w}{\partial z} = 0 \tag{A.12}$$

$$\varepsilon_{xz} = \frac{1}{2}\left(\frac{\partial u}{\partial x} + \frac{\partial u}{\partial z}\right) = 0$$

Equation (A.12) shows that the assumption in Equation (A.11) is equivalent to neglecting the shear deformation of the material. This assumption, called Bernoulli assumption is described in Figure A.2.

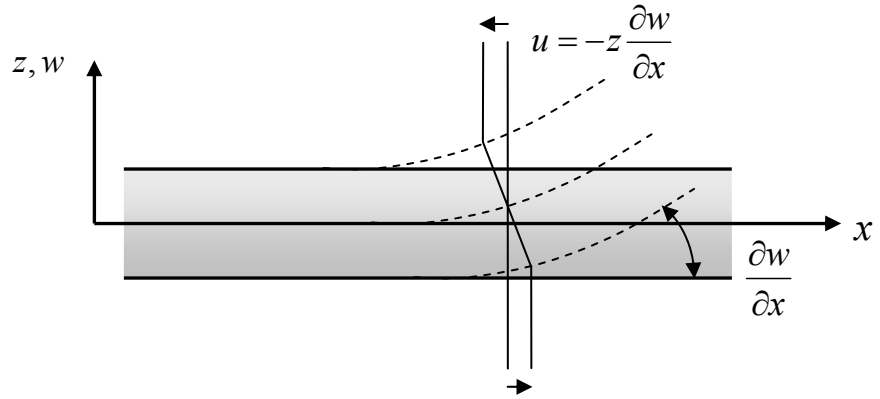

Figure A.2: Bernoulli's kinematic assumption.

The strain energy of the system can be written as:

$$W_{p,\text{int}} = \frac{1}{2}\int_0^l Ez^2\left(\frac{\partial^2 w}{\partial x^2}\right)^2 dxdA = \frac{1}{2}\int_0^l EI(x)\left(\frac{\partial^2 w}{\partial x^2}\right)^2 dx$$

where $I(x) = \int_A z^2 dA$ (A.13)

EI is the bending stiffness of the cross section.

$\frac{\partial^2 w}{\partial x^2}$ is the beam curvature.

The kinetic energy is given by:

$$W_k = \frac{1}{2}\int_0^l \int_{A(x)} \rho\left(\dot{u}^2 + \dot{w}^2\right)dAdx = \frac{1}{2}\int_0^l \int_{A(x)} \rho\left[z^2\left(\frac{\delta\dot{w}}{\delta x}\right)^2 + \dot{w}^2\right]dAdx =$$
$$= \frac{1}{2}\int_0^l \rho I\left(\frac{\partial\dot{w}}{\partial x}\right)^2 dx + \frac{1}{2}\int_0^l \rho A w^2 dx \quad \text{(A.14)}$$

By introducing

$m=A\rho$ the mass per unit of the beam length

$r^2=I/A$ where r is the gyration radius of the cross section

We obtain the expression:

$$W_k = \frac{1}{2}\int_0^l m\dot{w}^2 dx + \frac{1}{2}\int_0^l mr^2\left(\frac{\partial \dot{w}}{\partial x}\right)^2 dx \tag{A.15}$$

Here the first term describes the kinetic energy for vertical translation, while the second term describes the rotational kinetic energy of the cross section.

To be able to compute the potential energy of the external forces, imagine, as can be seen in Figure A.1, that the beam is subjected to a distributed vertical load $p(x,t)$ and distributed moments $q(x,t)$ per unit length. At the beam ends, either the shear loads $\overline{V}$ or the bending moments $\overline{M}$ are applied or the displacements $\overline{w}$ or rotations $\overline{\Phi}$ are imposed.

The potential associated with a bending moment M, shown in Figure A.3, can be computed as:

$$W_{p,ext,M} = -\int_A u\sigma_x dA = -\int_A\left(-z\frac{\partial w}{\partial x}\right)\sigma_x dA = -\overline{M}\frac{\partial w}{\partial x} \tag{A.16}$$

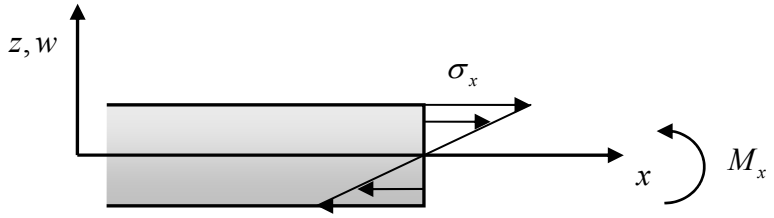

Figure A.3: Potential of a bending moment.

and the potential of external load is written as:

$$W_{p,ext} = -\int_0^l q\frac{\partial w}{\partial x}dx + \overline{V}(0)w(0) - \overline{V}(l)w(l) + \overline{M}(0)\left(\frac{\partial w}{\partial x}\right)_0 - \overline{M}(l)\left(\frac{\partial w}{\partial x}\right)_l \tag{A.17}$$

Now applying either Hamilton's principle or Lagrange equation with w as the only independent function, the equation of motion can be stated as:

$$m\ddot{w} - \frac{\partial}{\partial x}\left(mr^2\frac{\partial \ddot{w}}{\partial x}\right) + \frac{\partial^2}{\partial x^2}\left(EI\frac{\partial^2 w}{\partial x^2}\right) = p - \frac{\partial q}{\partial x} \tag{A.18}$$

with the boundary conditions at $x=0$ and at $x=l$

- on the transverse displacement

$$w = \overline{w} \qquad \text{or} \qquad V = mr^2\frac{\partial w}{\partial x}\left(EI\frac{\partial^2 w}{\partial x^2}\right) - q = \overline{V} \tag{A.19}$$

- on the rotation

$$\frac{\partial w}{\partial x} = \overline{\Phi} \qquad \text{or} \qquad M = EI\frac{\partial^2 w}{\partial x^2} = \overline{M} \tag{A.20}$$

Where M and T are, respectively, the bending moments and shear loads.

The equation for free vibration of the beam is obtained from Equation (A.18) by the assumption of a harmonic motion $w(x,t) = w(x)\sin\omega t$

$$\frac{d^2}{dx^2}\left(EI\frac{d^2 w}{dx^2}\right) - \omega^2 mw + \omega^2\frac{d}{dx}\left(mr^2\frac{dw}{dx}\right) = 0 \tag{A.21}$$

The kinetic assumption of no shear deformation remains valid provided that the ratio $I/A=r^2$ remains small. It is thus consistent in this case to neglect the rotary inertia of the cross sections, so that the free vibration equation of the beam becomes:

$$\frac{d^2}{dx^2}\left(EI\frac{d^2 w}{dx^2}\right) - \omega^2 mw = 0 \tag{A.22}$$

With the associated boundary conditions at $x=0$ and $x=l$

- on the displacement

$$w = 0 \qquad \text{or} \qquad V = \frac{d}{dx}\left(EI\frac{d^2 w}{dx^2}\right) \tag{A.23}$$

- on the rotation

$$\frac{dw}{dx} = 0 \qquad \text{or} \qquad M = EI\frac{d^2 w}{dx^2} = 0 \tag{A.24}$$

When the bending stiffness EI and the mass per unit length m remain constant over the beam length, the eigenvalue problem can be stated as:

$$\frac{d^4 w}{dx^4} - \omega^2\frac{m}{EI}w = 0 \tag{A.25}$$

A.3 Eigenmodes and frequencies for a uniform beam

For a structure, in this case a beam, the eigenfrequencies are the frequencies for which the structure will vibrate of its own accord when exposed to a perturbation. The different shapes of the structure for the different eigenfrequencies are called eigenmodes, and each eigenmode is related to one specific eigenfrequency.

To determine the beam response versus time the eigenmodes for a simply supported beam can be computed, by verifying the eigenvalue equation with the homogeneous boundary conditions.

$$EI\frac{d^4u}{dx^4} - \omega^2 mu = 0 \text{ for } 0 < x < l$$
$$u = \frac{d^2u}{dx^2} = 0 \text{ at } x = 0, l \tag{A.26}$$

After normalization they can be expressed as:

$$u_{(n)}(x) = \sqrt{\frac{2}{ml}}\sin\frac{n\pi x}{l} \text{ where } n = 1, 2, 3,\ldots.. \tag{A.27}$$

with the associated eigenvalues:

$$\omega_{(n)}^{\ 2} = (n\pi)^4 \frac{EI}{ml^4} \tag{A.28}$$

In Figure 4.1, the three first eigenmodes for a simply supported beam are shown. The first eigenmode corresponds to the lowest eigenfrequency.

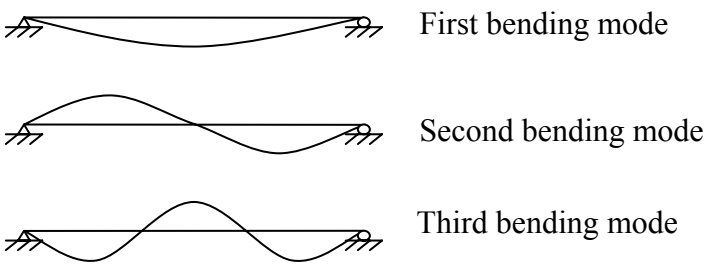

Figure A.4: The three first eigenmodes for a simply supported beam.

Normally, when a beam is subjected to a dynamic load, the load frequency will not coincide with the eigenfrequencies and therefore the resulting shape of deformation will not be the same as any of the eigenmodes. However, the dominating shape of deformation is usually the first eigenmode but it is influenced by higher modes. SDOF systems have only one eigenmode and hence there are no influences from higher modes.

Appendix B Solution algorithms

B.1 Newmark method

Table B.1: Algorithm for Newmark method when having linear elastic behaviour, according to Bathe (1996).

A: *Initial calculations*:

1: Form stiffness matrix K, mass matrix M and damping matrix C.

2: Initialize ${}^0U$, ${}^0\dot{U}$ and ${}^0\ddot{U}$.

3: Select time step Δt and parameters α and δ to calculate integration constants:

$$\delta \geq 0.50 \qquad \alpha \geq 0.25(0.5+\delta)^2$$

$$a_0 = \frac{1}{\alpha \Delta t^2} \qquad a_1 = \frac{\delta}{\alpha \Delta t} \qquad a_2 = \frac{1}{\alpha \Delta t} \qquad a_3 = \frac{1}{2\alpha} - 1$$

$$a_4 = \frac{\delta}{\alpha} - 1 \qquad a_5 = \frac{\Delta t}{2}\left(\frac{\delta}{\alpha} - 2\right) \qquad a_6 = \Delta t(1-\delta) \qquad a_7 = \delta \Delta t$$

4: Form lumped stiffness matrix $\hat{K}$.

$$\hat{K} = K + a_0 M + a_1 C$$

B: *For each time step*:

1: Calculate lumped loads at time t.

$${}^{t+\Delta t}\hat{P} = {}^{t+\Delta t}P + M\left(a_0\,{}^tU + a_2\,{}^t\dot{U} + a_3\,{}^t\ddot{U}\right) + C\left(a_1\,{}^tU + a_4\,{}^t\dot{U} + a_5\,{}^t\ddot{U}\right)$$

2: Solve for displacements at time $t + \Delta t$.

$$\hat{K}\,{}^{t+\Delta t}U = {}^{t+\Delta t}\hat{P}$$

3: Calculate accelerations and velocities at time $t + \Delta t$.

$${}^{t+\Delta t}\ddot{U} = a_0\left({}^{t+\Delta t}U - {}^tU\right) - a_2\,{}^t\dot{U} - a_3\,{}^t\ddot{U}$$

$${}^{t+\Delta t}\dot{U} = {}^t\dot{U} + a_6\,{}^t\ddot{U} + a_7\,{}^{t+\Delta t}\ddot{U}$$

B.2 Central difference method

Table B.2: Step-by-step solution with central difference method, according to Bathe (1996).

A: *Initial calculations*:

1: Form stiffness matrix K, mass matrix M and damping matrix C.

2: Initialize ${}^{0}U$, ${}^{0}\dot{U}$ and ${}^{0}\ddot{U}$.

3: Select time step Δt ($\Delta t \le \Delta t_{cr}$).

Calculate ${}^{-\Delta t}U = {}^{0}U - \Delta t\,{}^{0}\dot{U} + \frac{\Delta t^2}{2}\,{}^{0}\ddot{U}$

4: Form effective mass matrix $\hat{M}$.

$$\hat{M} = \frac{1}{\Delta t^2} M + \frac{1}{2\Delta t} C$$

B: *For each time step*:

1: Calculate effective loads at time t.

$${}^{t}\hat{P} = {}^{t}P - \left(K - \frac{2}{\Delta t^2} M \right) {}^{t}U - \left(\frac{1}{\Delta t^2} M - \frac{1}{2\Delta t^2} C \right) {}^{t-\Delta t}U$$

2: Solve for displacements at time $t + \Delta t$.

$$\hat{M}\,{}^{t+\Delta t}U = {}^{t}\hat{P}$$

If required evaluate accelerations and velocities at time t.

$${}^{t}\ddot{U} = \frac{1}{\Delta t^2}\left({}^{t-\Delta t}U - 2\,{}^{t}U + {}^{t+\Delta t}U \right)$$

$${}^{t}\dot{U} = \frac{1}{2\Delta t}\left(-{}^{t-\Delta t}U + {}^{t+\Delta t}U \right)$$

Appendix C Derivation analytical solution

C.1 Free vibration – damped system

Free vibrations - Damped system

$$m\ddot{u} + c\dot{u} + ku = 0 \qquad 1)$$

Assume:

$$u = Ce^{\lambda t}$$
$$\dot{u} = \lambda Ce^{\lambda t}$$
$$\ddot{u} = \lambda^2 Ce^{\lambda t} \qquad \Rightarrow$$

Insert into 1)

$$m\lambda^2 Ce^{\lambda t} + c\lambda Ce^{\lambda t} + kCe^{\lambda t} = 0 \qquad \Rightarrow$$

$$\lambda^2 + \frac{c}{m}\lambda + \frac{k}{m} = 0, \qquad \omega = \sqrt{\frac{k}{m}}$$

$$\lambda^2 + \frac{c}{m}\lambda + \omega^2 = 0$$

$$\lambda = \frac{-c}{2m} \pm \sqrt{\left(\frac{c}{2m}\right)^2 - \omega^2} \qquad \Rightarrow$$

$$\lambda = \omega\left(\frac{-c}{2m\omega} \pm \sqrt{\left(\frac{c}{2m\omega}\right)^2 - 1}\right), \qquad \xi = \frac{c}{2m\omega}$$

Insert weak damping ξ<1

$$\lambda = \omega\left(-\xi \pm \sqrt{\xi^2 - 1}\right) = -\xi\omega \pm i\omega\sqrt{1-\xi^2}$$

Introduce damped angular frequency ω_d

$$\omega_d = \omega\sqrt{1-\xi^2}$$

Insert λ into $u = Ce^{\lambda t}$ $\Rightarrow$

$$u(t) = e^{-\xi\omega t}\left(C_1 e^{i\omega_d t} + C_2 e^{-i\omega_d t}\right) = e^{-\xi\omega t}\left(A\sin\omega_d t + B\cos\omega_d t\right) = u_h$$

C.2 Forced harmonic vibration – Load case 1

$$m\ddot{u} + c\dot{u} + ku = p_0 \sin \omega_p t \qquad 1)$$

Assume harmonic response:

$$u_p = C_1 \sin \omega_p t + C_2 \cos \omega_p t$$
$$\dot{u}_p = \omega_p C_1 \cos \omega_p t - \omega_p C_2 \sin \omega_p t$$
$$\ddot{u}_p = -\omega_p{}^2 C_1 \sin \omega_p t - \omega_p{}^2 C_2 \cos \omega_p t$$

Insert into 1)

$$-m\omega_p{}^2 C_1 \sin \omega_p t - m\omega_p{}^2 C_2 \cos \omega_p t +$$
$$+ c\omega_p C_1 \cos \omega_p t - c\omega_p C_2 \sin \omega_p t +$$
$$+ kC_1 \sin \omega_p t + kC_2 \cos \omega_p t = -p_0 \sin \omega_p t$$

$$\left.\begin{aligned} -m\omega_p^2 C_1 - c\omega_p C_2 + kC_1 &= p_0 \quad \text{(sinus part)} \\ -m\omega_p^2 C_2 - c\omega_p C_1 + kC_2 &= 0 \quad \text{(cosinus part)} \end{aligned}\right\} \Rightarrow$$

$$\left.\begin{aligned} \mathrm{C}_1 &= \frac{p_0}{k} \frac{1-\beta^2}{\left(1-\beta^2\right)^2 + \left(2\xi\beta\right)^2} \\ C_2 &= -\frac{p_0}{k} \frac{2\xi\beta}{\left(1-\beta^2\right)^2 + \left(2\xi\beta\right)^2} \end{aligned}\right\} \Rightarrow$$

$$u_p = \frac{p_0}{k} \frac{1}{\left(1-\beta^2\right)^2 + \left(2\xi\beta\right)^2} \left[\left(1-\beta^2\right)\sin \omega_p t - 2\xi\beta \cos \omega_p t\right]$$

Using that $a \sin x + b \cos x = r \sin\left(x + \varphi\right)$ gives:

$$u_p = R \sin\left(\omega_p t - \theta\right)$$

where

$$R = \sqrt{\left(C_1^2 + C_2^2\right)} = \frac{p_0}{k} \frac{1}{\sqrt{\left(1-\beta^2\right)^2 + \left(2\xi\beta\right)^2}}$$

$$\theta = \arctan\left(-\frac{C_2}{C_1}\right) = \arctan\left(\frac{2\xi\beta}{1-\beta^2}\right) \qquad \text{for } \beta < 1$$

$$\theta = \pi + \arctan\left(-\frac{C_2}{C_1}\right) = \pi + \arctan\left(\frac{2\xi\beta}{1-\beta^2}\right) \quad \text{for } \beta > 1$$

Set $u(t) = u_h + u_p \quad \Rightarrow$

$$u(t) = e^{-\xi\omega t}\left(A\sin\omega_d t + B\cos\omega_d t\right) + R\sin\left(\omega_p t - \theta\right)$$

$$\dot{u}(t) = e^{-\xi\omega t}\omega_d\left(A\cos\omega_d t + B\sin\omega_d t\right) - \xi\omega e^{-\xi\omega t}\left(A\sin\omega_d t + B\cos\omega_d t\right) + \omega_p R\sin\left(\omega_p t - \theta\right)$$

Set the initial conditions to:

$$u(0) = u_0, \qquad \dot{u}(0) = \dot{u}_0 \qquad \Rightarrow$$

$$u_0 = B + R\sin(-\theta) \quad \Rightarrow$$
$$B = u_0 + R\sin(-\theta)$$

$$\dot{u}_0 = \omega_d A - \xi\omega B + R\omega_p\cos(-\theta) \qquad \Rightarrow$$
$$A = \frac{\dot{u}_0}{\omega_d} + \frac{\xi\omega}{\omega_d}\left(u_0 + R\sin(-\theta)\right) - R\frac{\omega_p}{\omega_d}\cos(-\theta)$$

Set $u_0 = \dot{u}_0 = 0$

$$A = \frac{\xi\omega}{\omega_d}R\sin(\theta) - R\frac{\omega_p}{\omega_d}\cos(\theta), \qquad B = R\sin(\theta) \quad \Rightarrow$$

$$u(t) = R\left[e^{-\xi\omega t}\left(\sin\theta\cos\omega_d t + \frac{\xi\omega}{\omega_d}\sin\theta\sin\omega_d t - \frac{\omega_p}{\omega_d}\cos\theta\sin\omega_d t\right) + \sin\left(\omega_p t - \theta\right)\right]$$

$$\dot{u}(t) = R\left[e^{-\xi\omega t}\left[\xi\omega\left(\frac{\omega_p}{\omega_d}\cos\theta\sin\omega_d t - \frac{\xi\omega}{\omega_d}\sin\theta\sin\omega_d t - \sin\theta\cos\omega_d t\right) - \right.\right.$$
$$\left.\left. -\left(\omega_d\sin\theta\sin\omega_d t - \xi\omega\sin\theta\cos\omega_d t + \omega_p\cos\theta\cos\omega_d t\right)\right] + \omega_p\cos\left(\omega_p t - \theta\right)\right]$$

$$\ddot{u}(t) = R\left[e^{-\xi\omega t}\left[\xi^2\omega^2\left(\sin\theta\cos\omega_d t + \frac{\xi\omega}{\omega_d}\sin\theta\sin\omega_d t - \frac{\omega_p}{\omega_d}\cos\theta\sin\omega_d t\right) + \right.\right.$$
$$+ 2\xi\omega\left(\omega_d\sin\theta\sin\omega_d t - \xi\omega\sin\theta\cos\omega_d t + \omega_p\cos\theta\cos\omega_d t\right) -$$
$$\left.\left. -\left({\omega_d}^2\sin\theta\cos\omega_d t - \xi\omega\omega_d\sin\theta\sin\omega_d t - \omega_p\omega_d\cos\theta\sin\omega_d t\right)\right] - {\omega_p}^2\sin\left(\omega_p t - \theta\right)\right]$$

C.3 Forced harmonic vibration – Load case 2

$$m\ddot{u} + c\dot{u} + ku = -p_0 \cos\omega_p t + p_0 \qquad 1)$$

First solve the system

$$m\ddot{u} + c\dot{u} + ku = -p_0 \cos\omega_p t \qquad 2)$$

Assume harmonic response:

$$u_p = C_1 \sin\omega_p t + C_2 \cos\omega_p t$$

$$\dot{u}_p = \omega_p C_1 \cos\omega_p t - \omega_p C_2 \sin\omega_p t$$

$$\ddot{u}_p = -\omega_p{}^2 C_1 \sin\omega_p t - \omega_p{}^2 C_2 \cos\omega_p t$$

Insert into 2)

$$\begin{aligned} &- m\omega_p{}^2 C_1 \sin\omega_p t - m\omega_p{}^2 C_2 \cos\omega_p t + \\ &+ c\omega_p C_1 \cos\omega_p t - c\omega_p C_2 \sin\omega_p t + \\ &+ kC_1 \sin\omega_p t + kC_2 \cos\omega_p t = -p_0 \cos\omega_p t \end{aligned}$$

$$\left.\begin{aligned} &- m\omega_p^2 C_1 - c\omega_p C_2 + kC_1 = p_0 \quad \text{(sinus part)} \\ &- m\omega_p^2 C_2 - c\omega_p C_1 + kC_2 = 0 \quad \text{(cosinus part)} \end{aligned}\right\} \Rightarrow$$

$$\left.\begin{aligned} \mathrm{C}_1 &= -\frac{p_0}{k}\frac{2\xi\beta}{\left(1-\beta^2\right)^2 + \left(2\xi\beta\right)^2} \\ C_2 &= -\frac{p_0}{k}\frac{1-\beta^2}{\left(1-\beta^2\right)^2 + \left(2\xi\beta\right)^2} \end{aligned}\right\} \Rightarrow$$

$$u_p = -\frac{p_0}{k}\frac{1}{\left(1-\beta^2\right)^2 + \left(2\xi\beta\right)^2}\left[2\xi\beta \sin\omega_p t + \left(1-\beta^2\right)\cos\omega_p t\right]$$

Using that $a\sin x + b\cos x = r\sin\left(x+\varphi\right)$ gives:

$$u_p = R\cos\left(\omega_p t - \theta\right)$$

where

$$R = \sqrt{\left(C_1^2 + C_2^2\right)} = \frac{p_0}{k} \underbrace{\frac{1}{\sqrt{\left(1-\beta^2\right)^2 + \left(2\xi\beta\right)^2}}}_{G} = \frac{p_0}{k} G$$

$$\theta = \arctan\left(\frac{C_1}{C_2}\right) = \arctan\left(\frac{2\xi\beta}{1-\beta^2}\right) \qquad \text{for } \beta > 1$$

$$\theta = \pi + \arctan\left(\frac{C_1}{C_2}\right) = \pi + \arctan\left(\frac{2\xi\beta}{1-\beta^2}\right) \qquad \text{for } \beta < 1$$

Set $u(t) = u_h + u_p \quad \Rightarrow$

$$u(t) = e^{-\xi\omega t}\left(A\sin\omega_d t + B\cos\omega_d t\right) + R\cos\left(\omega_p t - \theta\right)$$

Now we need the solution to the system

$$m\ddot{u} + c\dot{u} + ku = p_0$$

$$\ddot{u} + \frac{c}{m}\dot{u} + \frac{k}{m}u = p_0 \quad \Rightarrow$$

$$u_p = \frac{p_0}{k}$$

This gives the solution

$$u(t) = e^{-\xi\omega t}\left(A\sin\omega_d t + B\cos\omega_d t\right) + \frac{p_0}{k} G\cos\left(\omega_p t - \theta\right) + \frac{p_0}{k}$$

$$\dot{u}(t) = e^{-\xi\omega t}\left(\omega_d A\cos\omega_d t - \omega_d B\sin\omega_d t\right) - \xi\omega e^{-\xi\omega t}\left(A\sin\omega_d t + B\cos\omega_d t\right) -$$
$$- \frac{p_0}{k} G\omega_p \sin\left(\omega_p t - \theta\right)$$

Set the initial conditions to:

$$u(0) = u_0, \qquad \dot{u}(0) = \dot{u}_0 \quad \Rightarrow$$

$$u_0 = B + \frac{p_0}{k} G\cos\left(-\theta\right) + \frac{p_0}{k} \quad \Rightarrow$$

$$B = u_0 - \frac{p_0}{k} G\cos\theta - \frac{p_0}{k}$$

$$\dot{u}_0 = \omega_d A - \xi\omega B - \frac{p_0}{k} G\omega_p \sin(-\theta) \quad \Rightarrow$$

$$A = \frac{\dot{u}_0}{\omega_d} + \frac{\xi\omega}{\omega_d}\left(u_0 - \frac{p_0}{k} G\cos\theta - \frac{p_0}{k}\right) - \frac{p_0}{k} G\frac{\omega_p}{\omega_d}\sin\theta$$

Set $u_0 = \dot{u}_0 = 0$

$$A = -\frac{p_0}{k}\left[\frac{\xi\omega}{\omega_p}(G\cos\theta + 1) + G\frac{\omega_p}{\omega_d}\sin\theta\right], \qquad B = -\frac{p_0}{k}(G\cos\theta + 1)$$

Then set

$$A_{\cos} = \left[\frac{\xi\omega}{\omega_p}(G\cos\theta + 1) + G\frac{\omega_p}{\omega_d}\sin\theta\right], \qquad B_{\cos} = (G\cos\theta + 1) \quad \Rightarrow$$

$$u(t) = \frac{p_0}{k}\left[e^{-\xi\omega t}(-A_{\cos}\sin\omega_d t - B_{\cos}\cos\omega_d t) + G\cos(\omega_p t - \theta) + 1\right]$$

$$\dot{u}(t) = \frac{p_0}{k}\left[e^{-\xi\omega t}(-\omega_d A_{\cos}\cos\omega_d t + \omega_d B_{\cos}\sin\omega_d t + \xi\omega A_{\cos}\sin\omega_d t + \xi\omega B_{\cos}\cos\omega_d t) - \right.$$
$$\left. - G\omega_p sin(\omega_p t - \theta)\right]$$

$$\ddot{u}(t) = \frac{p_0}{k}\left[e^{\xi\omega t}\left[(\omega_d{}^2 A_{\cos} - 2\xi\omega\omega_d B_{\cos} - \xi^2\omega^2 A_{\cos})\sin\omega_d t + \right.\right.$$
$$\left.\left. + (\omega_d{}^2 B_{\cos} + 2\xi\omega\omega_d A_{\cos} - \xi^2\omega^2{}_{\cos})\cos\omega_d t\right] - G\omega_p\cos(\omega_p t - \theta)\right]$$

Appendix D Examined load cases

Table D.1: Shows the examined load cases.

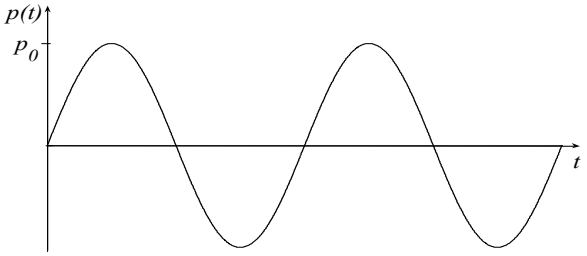

Load Case 1

Harmonic load

$$p(t) = p_0 \sin \omega_P t$$

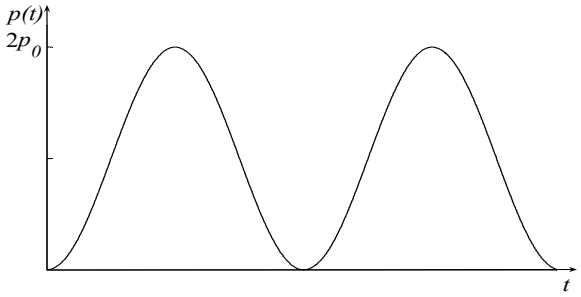

Load Case 2

Harmonic load

$$p(t) = p_0 - p_0 \cos \omega_P t$$

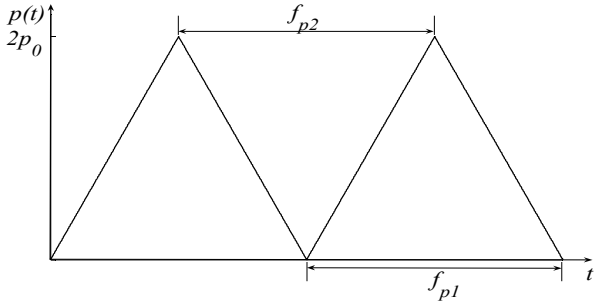

Load Case 3

Continuous triangular

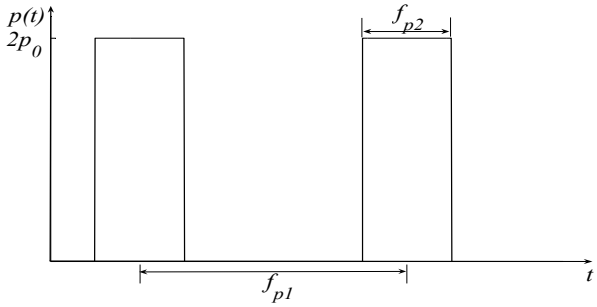

Load Case 4

Rectangular

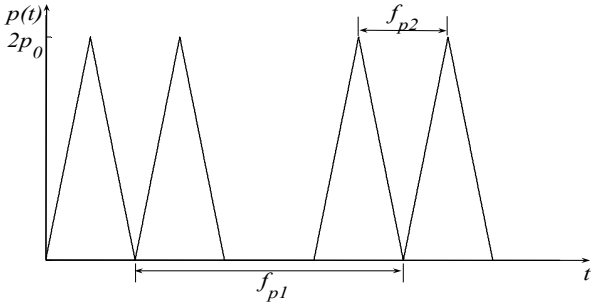

Load Case 5

Double triangular

Appendix E Results of SDOF analysis

E.1 Verification numerical solution, Load case 1

β=0.1	u_{max}	u_{min}	v_{max}	v_{min}	a_{max}	a_{min}
Central D.M.	0.0270	-0.0262	0.0302	-0.0234	0.0957	-0.0944
Analytical	0.0270	-0.0262	0.0302	-0.0234	0.0954	-0.0941
error %	0.00 %	0.00 %	0.00 %	0.00 %	0.29 %	0.27 %

β=0.2	u_{max}	u_{min}	v_{max}	v_{min}	a_{max}	a_{min}
Central D.M.	0.0269	-0.0264	0.0579	-0.0512	0.1883	-0.2187
Analytical	0.0269	-0.0264	0.0579	-0.0512	0.1877	-0.2181
error %	0.00 %	0.04 %	0.00 %	0.00 %	0.35 %	0.28 %

β=0.4	u_{max}	u_{min}	v_{max}	v_{min}	a_{max}	a_{min}
Central D.M.	0.0399	-0.0355	0.1269	-0.1274	0.4559	-0.6066
Analytical	0.0399	-0.0355	0.1269	-0.1274	0.4545	-0.6049
error %	0.01 %	0.01 %	0.01 %	0.02 %	0.30 %	0.28 %

β=0.6	u_{max}	u_{min}	v_{max}	v_{min}	a_{max}	a_{min}
Central D.M.	0.0527	-0.0590	0.2450	-0.2577	1.3308	-1.0840
Analytical	0.0527	-0.0590	0.2451	-0.2578	1.3266	-1.0794
error %	0.02 %	0.02 %	0.04 %	0.04 %	0.31 %	0.42 %

β=0.8	u_{max}	u_{min}	v_{max}	v_{min}	a_{max}	a_{min}
Central D.M.	0.1044	-0.1077	0.5881	-0.5751	3.2812	-3.1306
Analytical	0.1045	-0.1077	0.5887	-0.5756	3.2656	-3.1177
error %	0.07 %	0.09 %	0.10 %	0.10 %	0.48 %	0.42 %

β=1.2	u_{max}	u_{min}	v_{max}	v_{min}	a_{max}	a_{min}
Central D.M.	0.1041	-0.1008	0.7121	-0.7215	4.9828	-5.0757
Analytical	0.1039	-0.1006	0.7109	-0.7203	4.9939	-5.0899
error %	0.19 %	0.20 %	0.17 %	0.16 %	0.22 %	0.28 %

β=1.4	u_{max}	u_{min}	v_{max}	v_{min}	a_{max}	a_{min}
Central D.M.	0.0567	-0.0509	0.4130	-0.4043	2.8929	-3.2331
Analytical	0.0566	-0.0508	0.4125	-0.4038	2.8963	-3.2365
error %	0.16 %	0.16 %	0.12 %	0.12 %	0.12 %	0.10 %

β=1.6	u_{max}	u_{min}	v_{max}	v_{min}	a_{max}	a_{min}
Central D.M.	0.0321	-0.0390	0.2964	-0.2767	2.5246	-2.2302
Analytical	0.0321	-0.0389	0.2961	-0.2764	2.5265	-2.2316
error %	0.12 %	0.13 %	0.09 %	0.09 %	0.08 %	0.06 %

β=1.8	u_{max}	u_{min}	v_{max}	v_{min}	a_{max}	a_{min}
Central D.M.	0.0239	-0.0288	0.2178	-0.2389	2.1370	-1.9113
Analytical	0.0239	-0.0287	0.2176	-0.2387	2.1380	-1.9115
error %	0.13 %	0.13 %	0.08 %	0.07 %	0.05 %	0.01 %

β=2	u_{max}	u_{min}	v_{max}	v_{min}	a_{max}	a_{min}
Central D.M.	0.0212	-0.0205	0.1185	-0.2041	1.7935	-1.7744
Analytical	0.0212	-0.0205	0.1185	-0.2040	1.7936	-1.7748
error %	0.12 %	0.12 %	0.01 %	0.06 %	0.00 %	0.02 %

β=4	u_{max}	u_{min}	v_{max}	v_{min}	a_{max}	a_{min}
Central D.M.	0.0078	-0.0073	0.0716	-0.0816	1.2787	-1.3087
Analytical	0.0078	-0.0073	0.0718	-0.0816	1.2787	-1.3104
error %	0.04 %	0.08 %	0.18 %	0.01 %	0.00 %	0.13 %

β=6	u_{max}	u_{min}	v_{max}	v_{min}	a_{max}	a_{min}
Central D.M.	0.0047	-0.0045	0.0502	-0.0524	1.1759	-1.1831
Analytical	0.0047	-0.0045	0.0503	-0.0524	1.1758	-1.1844
error %	0.06 %	0.09 %	0.24 %	0.11 %	0.01 %	0.11 %

β=8	u_{max}	u_{min}	v_{max}	v_{min}	a_{max}	a_{min}
Central D.M.	0.0034	-0.0032	0.0383	-0.0387	1.1230	-1.1344
Analytical	0.0035	-0.0032	0.0385	-0.0388	1.1248	-1.1301
error %	0.31 %	0.32 %	0.57 %	0.36 %	0.16 %	0.38 %

β=10	u_{max}	u_{min}	v_{max}	v_{min}	a_{max}	a_{min}
Central D.M.	0.0027	-0.0025	0.0309	-0.0307	1.0991	-1.1041
Analytical	0.0027	-0.0025	0.0310	-0.0309	1.0981	-1.1030
error %	0.60 %	0.56 %	0.58 %	0.66 %	0.09 %	0.10 %

Mean Error						
β <1	0.02 %	0.03 %	0.03 %	0.03 %	0.35 %	0.33 %
1< $\beta \leq$2	0.14 %	0.15 %	0.09 %	0.10 %	0.09 %	0.10 %
β >2	0.25 %	0.26 %	0.39 %	0.29 %	0.05 %	0.21 %
0< $\beta \leq$*10*	0.13 %	0.14 %	0.16 %	0.13 %	0.18 %	0.21 %

E.2 Verification numerical solution, Load case 2

β=0.1	u_{max}	u_{min}	v_{max}	v_{min}	a_{max}	a_{min}
Central D.M.	0.05103	-0.00025	0.01695	-0.01644	0.01896	-0.01471
Analytical	0.05103	-0.00025	0.01695	-0.01644	0.01896	-0.01470
error %	0.00 %	0.12 %	0.00 %	0.00 %	0.00 %	0.00 %

β=0.2	u_{max}	u_{min}	v_{max}	v_{min}	a_{max}	a_{min}
Central D.M.	0.0517	-0.0011	0.0338	-0.0331	0.0728	-0.0643
Analytical	0.0517	-0.0010	0.0338	-0.0331	0.0727	-0.0643
error %	0.00 %	0.16 %	0.00 %	0.00 %	0.00 %	0.00 %

β=0.4	u_{max}	u_{min}	v_{max}	v_{min}	a_{max}	a_{min}
Central D.M.	0.0570	-0.0081	0.1003	-0.0891	0.3189	-0.3202
Analytical	0.0570	-0.0081	0.1003	-0.0891	0.3189	-0.3203
error %	0.00 %	0.00 %	0.00 %	0.00 %	0.01 %	0.00 %

β=0.6	u_{max}	u_{min}	v_{max}	v_{min}	a_{max}	a_{min}
Central D.M.	0.0734	-0.0221	0.1986	-0.2224	0.9237	-0.9715
Analytical	0.0734	-0.0221	0.1986	-0.2224	0.9236	-0.9715
error %	0.00 %	0.00 %	0.00 %	0.01 %	0.00 %	0.00 %

β=0.8	u_{max}	u_{min}	v_{max}	v_{min}	a_{max}	a_{min}
Central D.M.	0.1220	-0.0747	0.5250	-0.5412	2.9566	-2.8909
Analytical	0.1220	-0.0747	0.5250	-0.5412	2.9566	-2.8907
error %	0.01 %	0.00 %	0.01 %	0.00 %	0.00 %	0.01 %

β=1.2	u_{max}	u_{min}	v_{max}	v_{min}	a_{max}	a_{min}
Central D.M.	0.1380	-0.0872	0.7846	-0.7599	5.3685	-5.4395
Analytical	0.1380	-0.0872	0.7846	-0.7598	5.3685	-5.4392
error %	0.00 %	0.00 %	0.00 %	0.01 %	0.00 %	0.01 %

β=1.4	u_{max}	u_{min}	v_{max}	v_{min}	a_{max}	a_{min}
Central D.M.	0.0901	-0.0428	0.4982	-0.4475	3.6329	-3.5566
Analytical	0.0901	-0.0428	0.4982	-0.4474	3.6324	-3.5559
error %	0.00 %	0.00 %	0.00 %	0.01 %	0.01 %	0.02 %

β=1.6	u_{max}	u_{min}	v_{max}	v_{min}	a_{max}	a_{min}
Central D.M.	0.0740	-0.0249	0.3232	-0.3916	2.9800	-2.7819
Analytical	0.0740	-0.0249	0.3232	-0.3916	2.9796	-2.7815
error %	0.00 %	0.02 %	0.00 %	0.00 %	0.01 %	0.01 %

β=1.8	u_{max}	u_{min}	v_{max}	v_{min}	a_{max}	a_{min}
Central D.M.	0.0694	-0.0118	0.2702	-0.3252	2.4631	-2.7021
Analytical	0.0694	-0.0118	0.2702	-0.3252	2.4628	-2.7017
error %	0.00 %	0.03 %	0.01 %	0.01 %	0.01 %	0.01 %

β=2	u_{max}	u_{min}	v_{max}	v_{min}	a_{max}	a_{min}
Central D.M.	0.0650	0.0000	0.2663	-0.2574	1.4898	-2.5654
Analytical	0.0650	0.0000	0.2663	-0.2574	1.4894	-2.5652
error %	0.01 %	0.00 %	0.00 %	0.00 %	0.03 %	0.01 %

β=4	u_{max}	u_{min}	v_{max}	v_{min}	a_{max}	a_{min}
Central D.M.	0.0520	0.0000	0.1969	-0.1829	1.8047	-2.0528
Analytical	0.0520	0.0000	0.1968	-0.1828	1.8048	-2.0514
error %	0.01 %	0.00 %	0.01 %	0.03 %	0.00 %	0.07 %

β=6	u_{max}	u_{min}	v_{max}	v_{min}	a_{max}	a_{min}
Central D.M.	0.0501	0.0000	0.1793	-0.1693	1.8991	-1.9793
Analytical	0.0501	0.0000	0.1792	-0.1692	1.8989	-1.9771
error %	0.01 %	0.00 %	0.02 %	0.04 %	0.01 %	0.11 %

β=8	u_{max}	u_{min}	v_{max}	v_{min}	a_{max}	a_{min}
Central D.M.	0.0495	0.0000	0.1737	-0.1609	1.9369	-1.9550
Analytical	0.0495	0.0000	0.1737	-0.1608	1.9369	-1.9530
error %	0.01 %	0.00 %	0.00 %	0.04 %	0.00 %	0.10 %

β=10	u_{max}	u_{min}	v_{max}	v_{min}	a_{max}	a_{min}
Central D.M.	0.0492	0.0000	0.1684	-0.1579	1.9559	-1.9439
Analytical	0.0492	0.0000	0.1683	-0.1579	1.9520	-1.9421
error %	0.00 %	0.00 %	0.05 %	0.01 %	0.20 %	0.09 %

Mean Error						
β <1	0.00 %	0.06 %	0.00 %	0.00 %	0.00 %	0.00 %
1< $\beta \leq$2	0.00 %	0.01 %	0.00 %	0.01 %	0.01 %	0.01 %
β >2	0.01 %	0.00 %	0.02 %	0.03 %	0.01 %	0.09 %
0< $\beta \leq$*10*	0.00 %	0.02 %	0.01 %	0.01 %	0.01 %	0.03 %

E.3 Frequency relationships

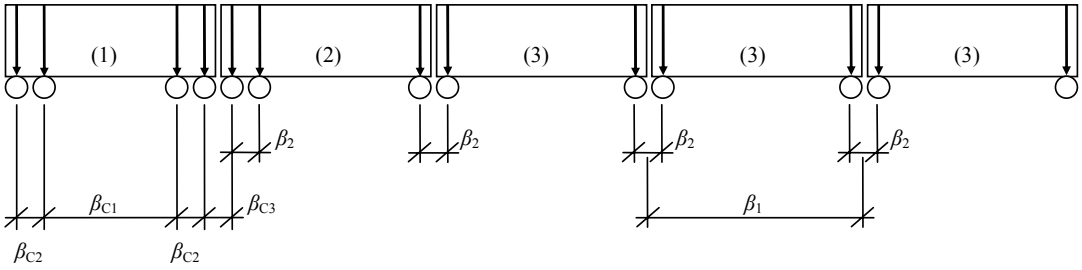

A1	D=18m	d=2m			N=18	P=1.7N				
β_1=	0.1	0.2	0.3	0.33	0.4	0.5	0.6	0.7	0.8	0.9
β_2=	0.9	1.8	2.7	2.97	3.6	4.5	5.4	6.3	7.2	8.1
β_{c1}=	0.13	0.26	0.39	0.43	0.51	0.64	0.77	0.90	1.03	1.16
β_{c2}=	0.6	1.2	1.8	2	2.4	3	3.6	4.2	4.8	5.4
β_{c3}=	0.51	1.02	1.53	1.70	2.04	2.55	3.06	3.57	4.09	4.60

A2	D=19m	d=3,5m			N=17	P=2.0N				
β_1=	0.1	0.2	0.3	0.33	0.4	0.5	0.6	0.7	0.8	0.9
β_2=	0.54	1.09	1.63	1.81	2.17	2.71	3.26	3.80	4.34	4.89
β_{c1}=	0.14	0.27	0.41	0.45	0.54	0.68	0.81	0.95	1.09	1.22
β_{c2}=	0.63	1.27	1.90	2.11	2.53	3.17	3.80	4.43	5.07	5.70
β_{c3}=	0.54	1.08	1.62	1.80	2.16	2.70	3.23	3.77	4.31	4.85

A3	D=20m	d=2m			N=16	P=1.8N				
β_1=	0.1	0.2	0.3	0.33	0.4	0.5	0.6	0.7	0.8	0.9
β_2=	1.00	2.00	3.00	3.33	4.00	5.00	6.00	7.00	8.00	9.00
β_{c1}=	0.14	0.29	0.43	0.48	0.57	0.71	0.86	1.00	1.14	1.29
β_{c2}=	0.67	1.33	2.00	2.22	2.67	3.33	4.00	4.67	5.33	6.00
β_{c3}=	0.57	1.13	1.70	1.89	2.27	2.84	3.40	3.97	4.54	5.11

A4	D=21m	d=3m			N=15	P=1.9N				
β_1=	0.1	0.2	0.3	0.33	0.4	0.5	0.6	0.7	0.8	0.9
β_2=	0.70	1.40	2.10	2.33	2.80	3.50	4.20	4.90	5.60	6.30
β_{c1}=	0.15	0.30	0.45	0.50	0.60	0.75	0.90	1.05	1.20	1.35
β_{c2}=	0.70	1.40	2.10	2.33	2.80	3.50	4.20	4.90	5.60	6.30
β_{c3}=	0.60	1.19	1.79	1.99	2.38	2.98	3.57	4.17	4.77	5.36

A5	D=22m	d=2m			N=14	P=1.7N				
β_1=	0.1	0.2	0.3	0.33	0.4	0.5	0.6	0.7	0.8	0.9
β_2=	1.10	2.20	3.30	3.67	4.40	5.50	6.60	7.70	8.80	9.90
β_{c1}=	0.16	0.31	0.47	0.52	0.63	0.79	0.94	1.10	1.26	1.41
β_{c2}=	0.73	1.47	2.20	2.44	2.93	3.67	4.40	5.13	5.87	6.60
β_{c3}=	0.62	1.25	1.87	2.08	2.50	3.12	3.74	4.37	4.99	5.62

A6	D=23m	d=2m			N=13	P=1.8N				
β_1=	0.1	0.2	0.3	0.33	0.4	0.5	0.6	0.7	0.8	0.9
β_2=	1.15	2.30	3.45	3.83	4.60	5.75	6.90	8.05	9.20	10.35
β_{c1}=	0.16	0.33	0.49	0.55	0.66	0.82	0.99	1.15	1.31	1.48
β_{c2}=	0.77	1.53	2.30	2.56	3.07	3.83	4.60	5.37	6.13	6.90
β_{c3}=	0.65	1.30	1.96	2.17	2.61	3.26	3.91	4.57	5.22	5.87

A7	D=24m	d=2m			N=13	P=1.9N				
β_1=	0.1	0.2	0.3	0.33	0.4	0.5	0.6	0.7	0.8	0.9
β_2=	1.20	2.40	3.60	4.00	4.80	6.00	7.20	8.40	9.60	10.80
β_{c1}=	0.17	0.34	0.51	0.57	0.69	0.86	1.03	1.20	1.37	1.54
β_{c2}=	0.80	1.60	2.40	2.67	3.20	4.00	4.80	5.60	6.40	7.20
β_{c3}=	0.68	1.36	2.04	2.27	2.72	3.40	4.09	4.77	5.45	6.13

A8	D=25m	d=2,5m			N=12	P=1.9N				
β_1=	0.1	0.2	0.3	0.33	0.4	0.5	0.6	0.7	0.8	0.9
β_2=	1.00	2.00	3.00	3.33	4.00	5.00	6.00	7.00	8.00	9.00
β_{c1}=	0.18	0.36	0.54	0.60	0.71	0.89	1.07	1.25	1.43	1.61
β_{c2}=	0.83	1.67	2.50	2.78	3.33	4.17	5.00	5.83	6.67	7.50
β_{c3}=	0.71	1.42	2.13	2.36	2.84	3.55	4.26	4.96	5.67	6.38

A9	D=26m	d=2m			N=11	P=2.1N				
β_1=	0.1	0.2	0.3	0.33	0.4	0.5	0.6	0.7	0.8	0.9
β_2=	1.30	2.60	3.90	4.33	5.20	6.50	7.80	9.10	10.40	11.70
β_{c1}=	0.19	0.37	0.56	0.62	0.74	0.93	1.11	1.30	1.49	1.67
β_{c2}=	0.87	1.73	2.60	2.89	3.47	4.33	5.20	6.07	6.93	7.80
β_{c3}=	0.74	1.48	2.21	2.46	2.95	3.69	4.43	5.16	5.90	6.64

A10	D=27m	d=2m			N=11	P=2.1N				
β_1=	0.1	0.2	0.3	0.33	0.4	0.5	0.6	0.7	0.8	0.9
β_2=	1.35	2.70	4.05	4.50	5.40	6.75	8.10	9.45	10.80	12.15
β_{c1}=	0.19	0.39	0.58	0.64	0.77	0.96	1.16	1.35	1.54	1.74
β_{c2}=	0.90	1.80	2.70	3.00	3.60	4.50	5.40	6.30	7.20	8.10
β_{c3}=	0.77	1.53	2.30	2.55	3.06	3.83	4.60	5.36	6.13	6.89

E.4 Train load, HSLM-A1

Table E.1: Displacements for SDOF system loaded by the Train load HSLM-A1.

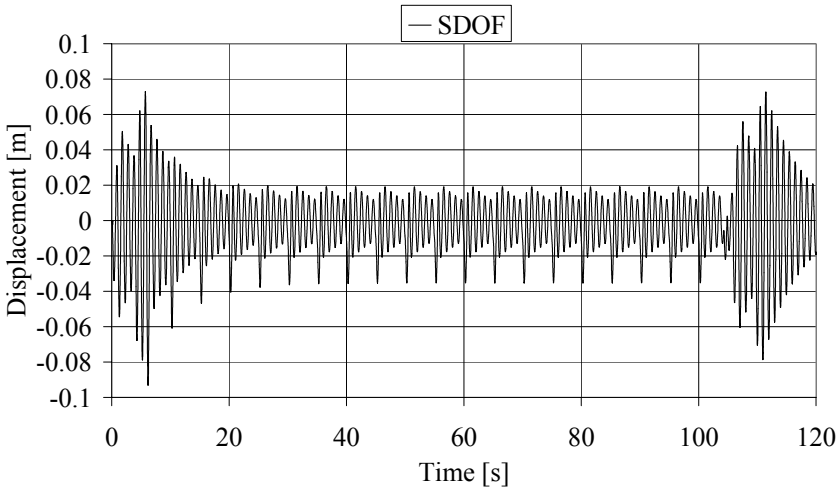

β=0.2

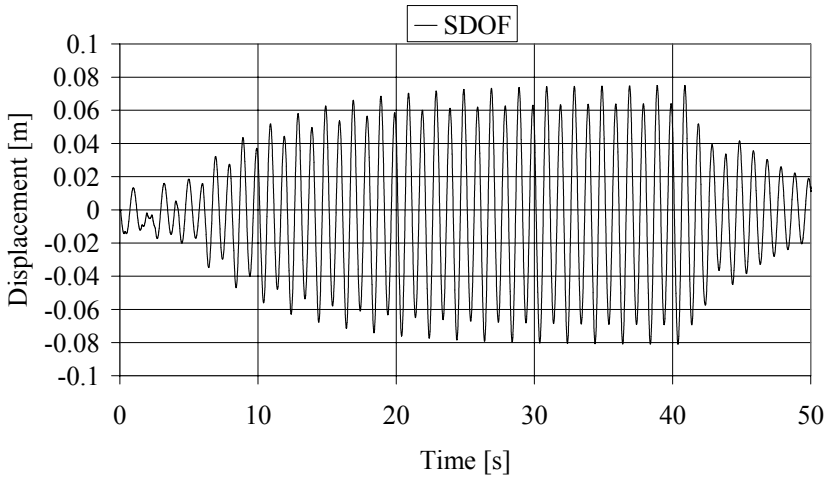

β=0.5

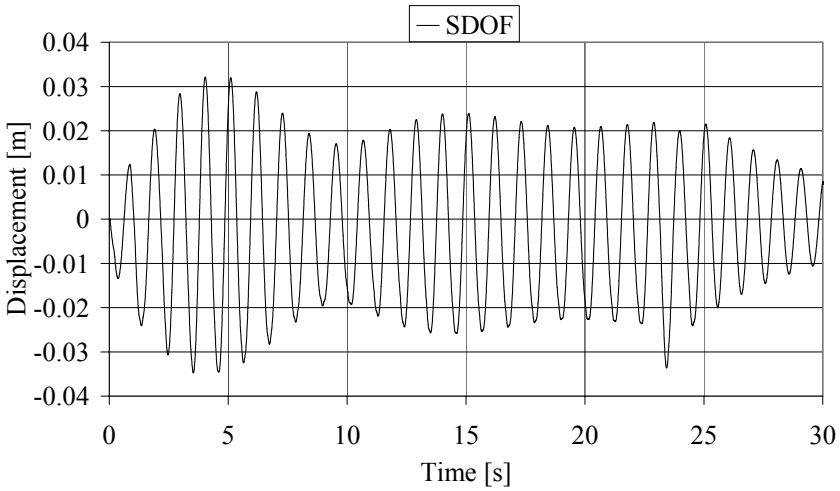

β=0.9

Table E.2: Velocities for SDOF system loaded by the Train load HSLM-A1.

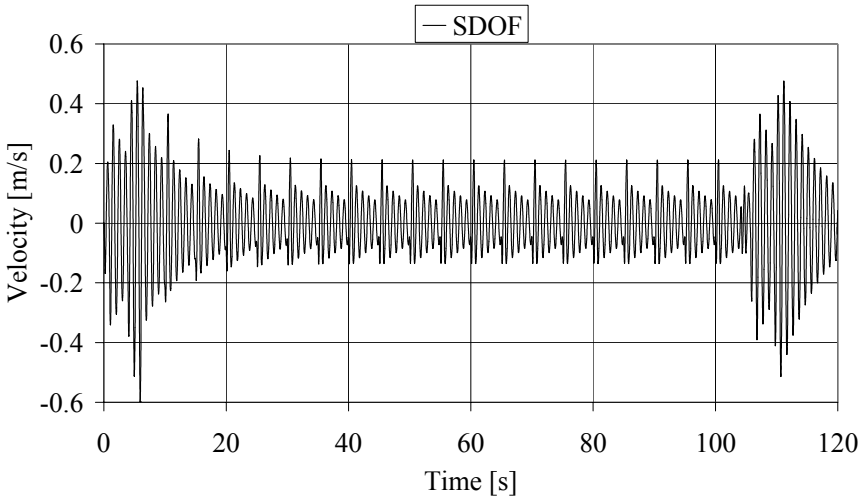

β=0.2

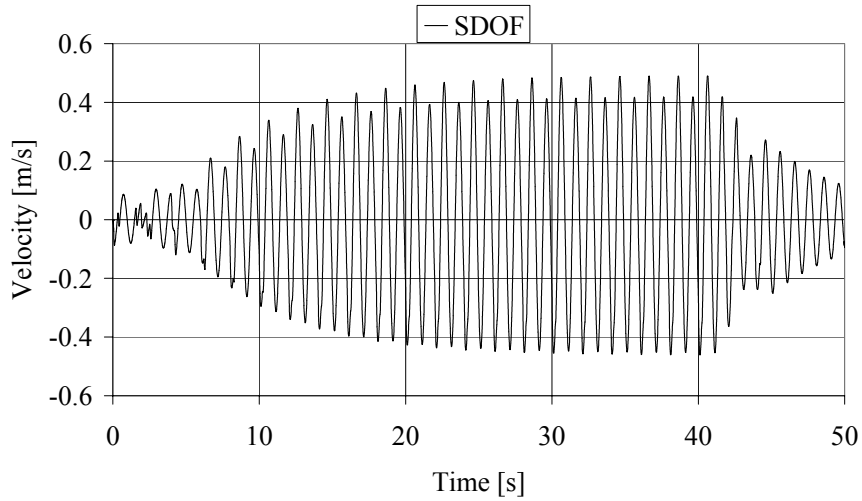

β=0.5

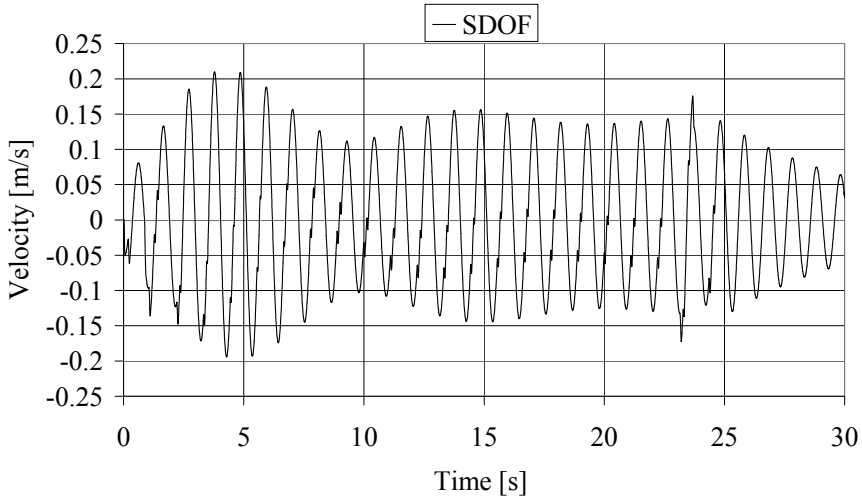

β=0.9

Table E.3: Accelerations for SDOF system loaded by the Train load HSLM-A1.

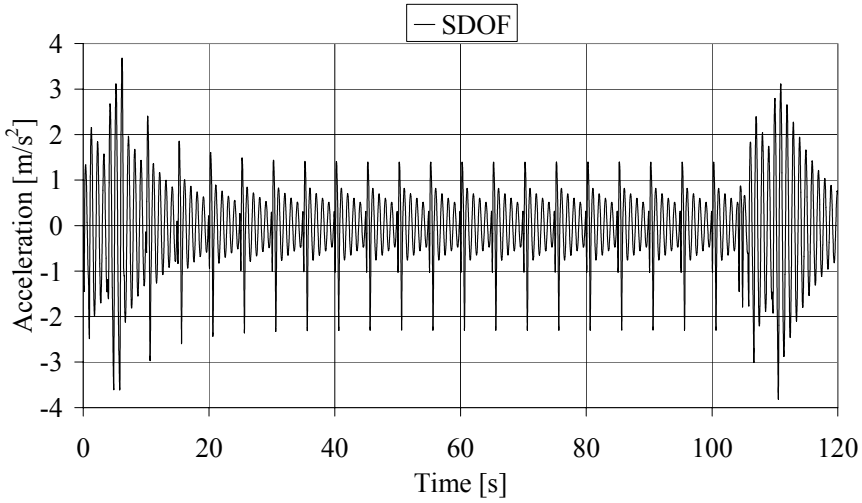

β=0.2

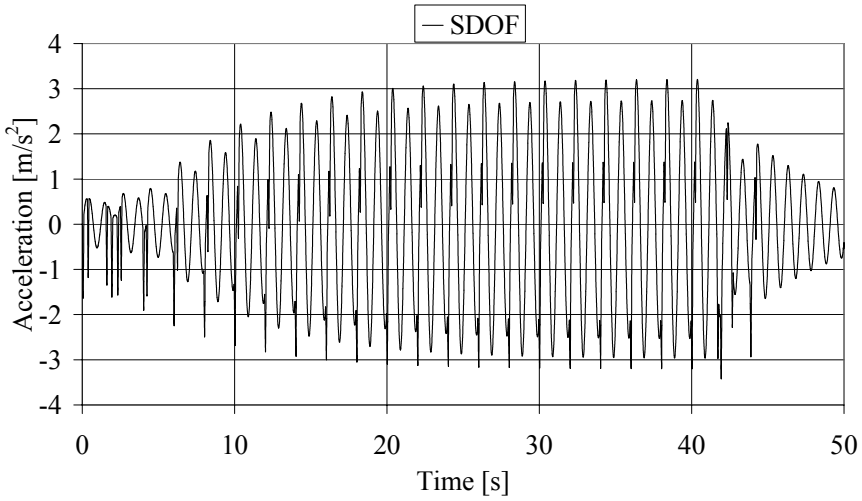

β=0.5

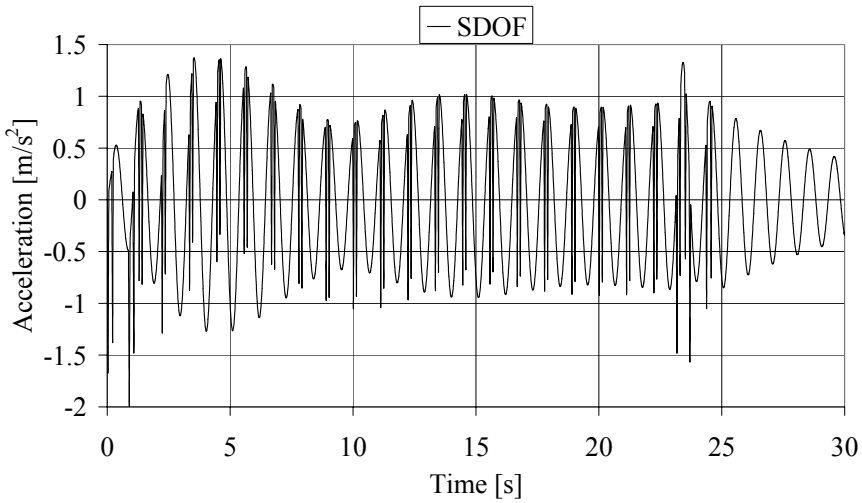

β=0.9

Appendix F Results of finite element analysis

F.1 Static – hand calculations

The FE-model is verified by comparing results of ADINA with hand calculations. The beam is simply supported and loaded by a point load P=1 N. The geometry of the beam has been chosen to a length L=10 m, width b=1 m and a height h=1 m, see Figure F.1.

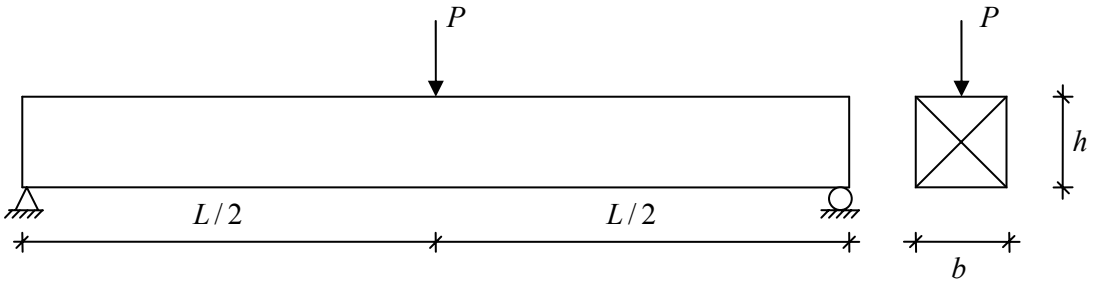

Figure F.1: Simply supported beam loaded by a point load.

The mass of the SDOF system is transformed into a mass of the beam by using Equation (4.31):

$$m = \frac{m_e}{\kappa_M} = \frac{1}{0.4857} = 2.06\,\text{kg} \tag{F.1}$$

The moment of inertia for the beam is calculated as:

$$I = \frac{bh^3}{12} = 0.083\,\text{m}^4 \tag{F.2}$$

The modulus of elasticity E is calculated from the relation between the circular eigenfrequencies ω_n and the chosen natural frequency f_n.

$$\omega_n = (n\pi)^2 \sqrt{\frac{EI}{mL^4}}$$

$$\omega_n = f_n 2\pi \text{ where } n\text{=1 and } f_1\text{=1 Hz gives;} \tag{F.3}$$

$$E = \frac{\omega_n^2 mL^4}{(n\pi)^4 I} = 10013.21\,\text{N/m}^2$$

The reaction forces at the supports are calculated as:

$$R_1 = R_2 = \frac{P}{2} = 0.50\,\text{N} \tag{F.4}$$

The moment in the middle of the beam is calculated as:

$$M_{L/2} = \frac{PL}{4} = 2.50\text{Nm} \tag{F.5}$$

The displacement in the middle of the beam is calculated as:

$$u = \frac{PL^3}{48EI} = 24.97\text{mm} \tag{F.6}$$

F.2 Eigenmodes for a simply supported beam

Table F.1: The first 19:th eigenmodes and natural frequencies for a simply supported beam with 20 or 800 elements.

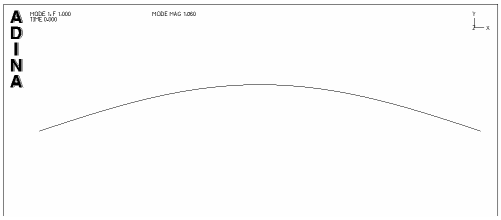

$f_{1,\,20}$ =1.00 Hz

$f_{1,800}$=1.00 Hz

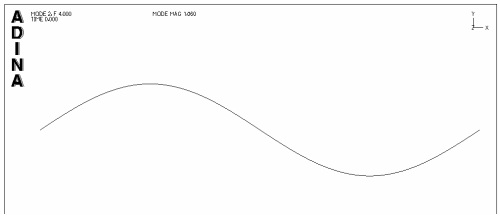

$f_{2,\,20}$ =4.00 Hz

$f_{2,800}$=4.00 Hz

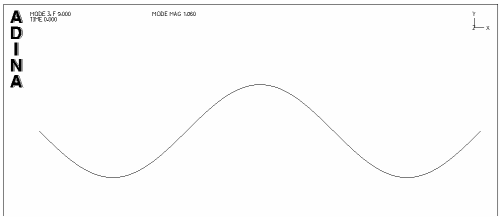

$f_{3,\,20}$ =9.00 Hz

$f_{3,800}$=9.00 Hz

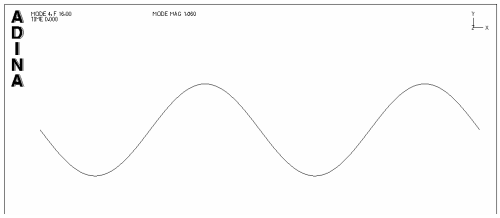

$f_{4,\,20}$ =16.00 Hz

$f_{4,800}$=16.00 Hz

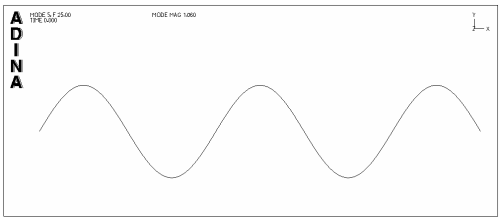

$f_{5,\,20}$ =24.99 Hz

$f_{5,800}$=25.00 Hz

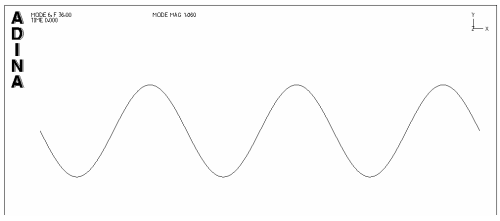

$f_{6,\,20}$ =35.98 Hz

$f_{6,800}$=36.00 Hz

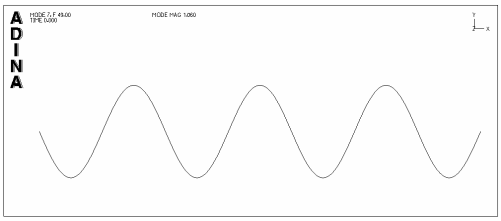

$f_{7,\,20}$ =48.93 Hz

$f_{7,800}$=49.00 Hz

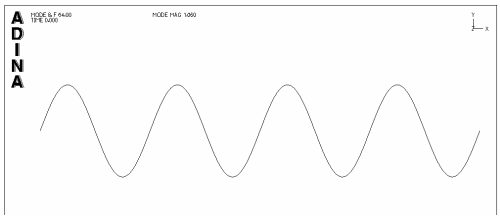

$f_{8,\,20}$ =63.84 Hz

$f_{8,800}$=64.00 Hz

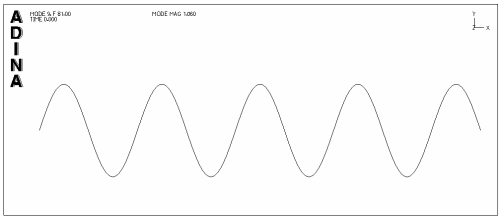

$f_{9,\ 20}$ =80.65 Hz

$f_{9,800}$=81.00 Hz

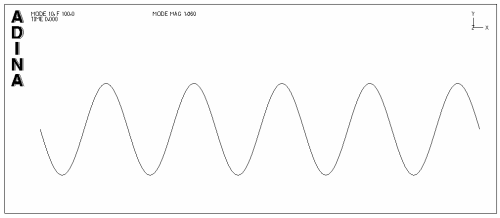

$f_{10,\ 20}$ =99.27 Hz

$f_{10,800}$=100.00 Hz

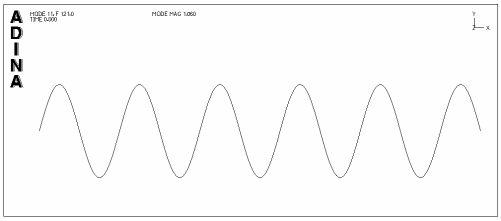

$f_{11,\ 20}$ =119.58 Hz

$f_{11,800}$=121.00 Hz

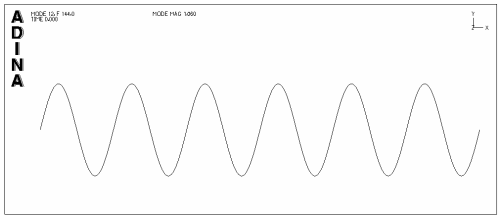

$f_{12,\ 20}$ =141.33 Hz

$f_{12,800}$=144.00 Hz

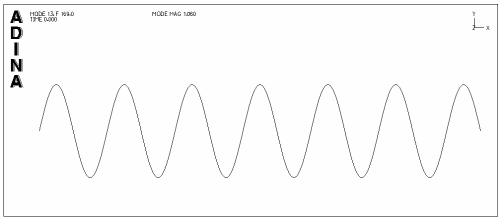

$f_{13,\ 20}$ =164.18 Hz

$f_{13,800}$=169.00 Hz

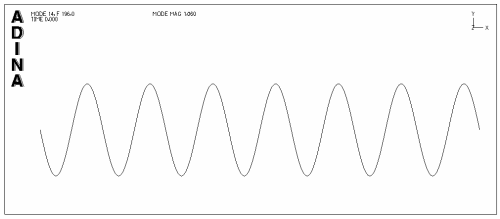

$f_{14,\ 20}$ =187.58 Hz

$f_{14,800}$=196.00 Hz

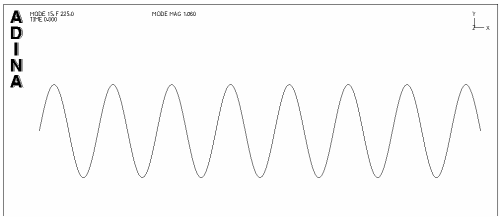

$f_{15,\ 20}$ =210.78 Hz

$f_{15,800}$=225.00 Hz

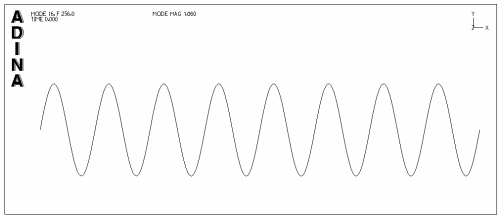

$f_{16,\ 20}$ =232.72 Hz

$f_{16,800}$=256.00 Hz

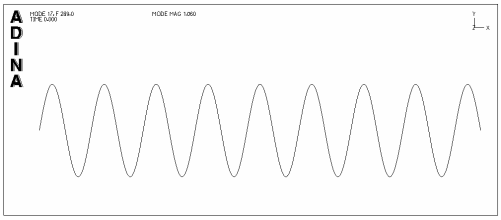

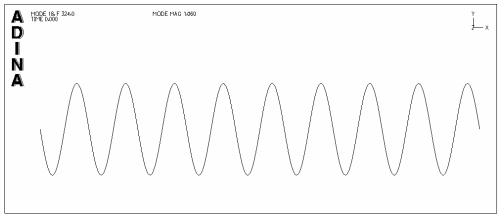

$f_{17,\ 20}$ =252.10 Hz

$f_{18,\ 20}$ =267.45 Hz

$f_{17,800}$=289.00 Hz

$f_{18,800}$=324.00 Hz

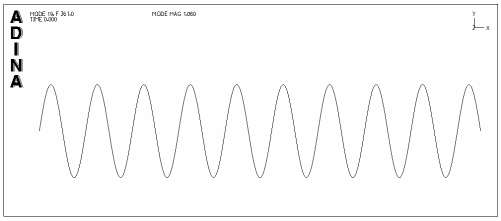

$f_{19,\ 20}$ =277.36 Hz

$f_{19,800}$=361.00 Hz

F.3 Modal participation factor

Table F.2: Comparison of the natural frequencies and modal participation factor for a FE-mode modelled with 20 or 800 elements.

20 Elements				**800Elements**		
Mode	Freq. f_n [Hz]	Mass [%]	Acc. mass [%]	Freq. f_n [Hz]	Mass [%]	Acc. mass [%]
1	1.00	80.72	80.72	1.00	81.06	81.06
2	4.00	0.00	80.72	4.00	0.00	81.06
3	9.00	8.68	89.40	9.00	9.00	90.06
4	16.00	0.00	89.40	16.00	0.00	90.06
5	24.99	2.91	92.31	25.00	3.24	93.30
6	35.98	0.00	92.31	36.00	0.00	93.30
7	48.93	1.33	93.64	49.00	1.65	94.96
8	63.84	0.00	93.64	64.00	0.00	94.96
9	80.65	0.69	94.33	81.00	1.00	95.96
10	99.27	0.00	94.33	100.00	0.00	95.96
11	119.58	0.36	94.69	121.00	0.67	96.63
12	141.33	0.00	94.69	144.00	0.00	96.63
13	164.18	0.19	94.88	169.00	0.48	97.11
14	187.58	0.00	94.88	196.00	0.00	97.11
15	210.78	0.09	94.97	225.00	0.36	97.47
16	232.72	0.00	94.97	256.00	0.00	97.47
17	252.10	0.03	95.00	289.00	0.28	97.75
18	267.45	0.00	95.00	324.00	0.00	97.75
19	277.36	0.00	95.00	361.00	0.22	97.97

F.4 Undamped beam loaded by a harmonic load

Table F.3: Displacements for an undamped beam, loaded by a harmonic load with β=0.1, 0.5 and 0.9.

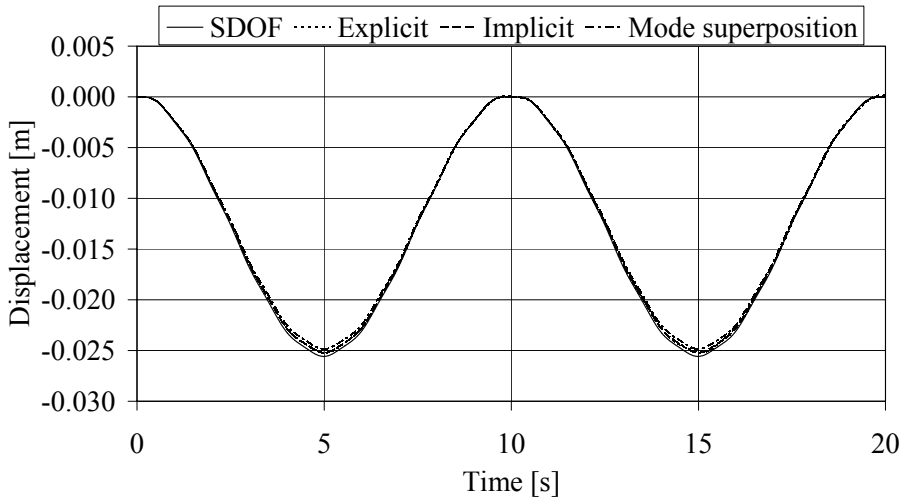

β=0.1

:

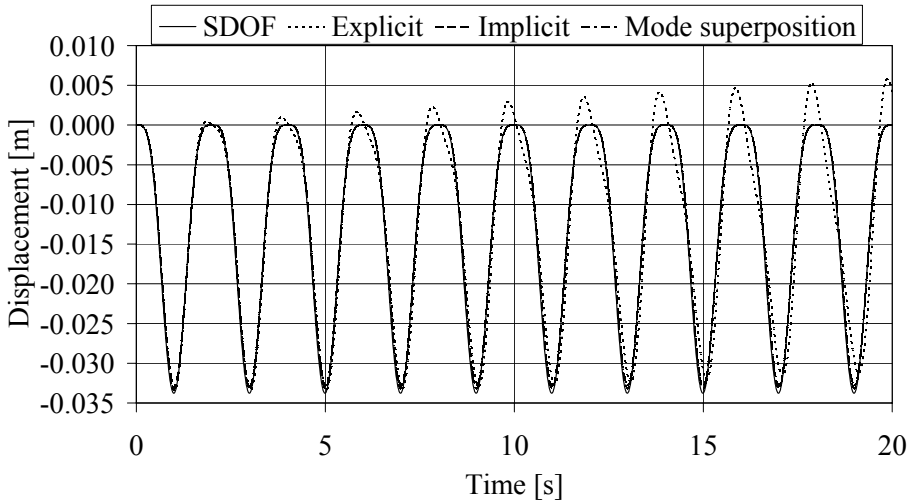

β=0.5

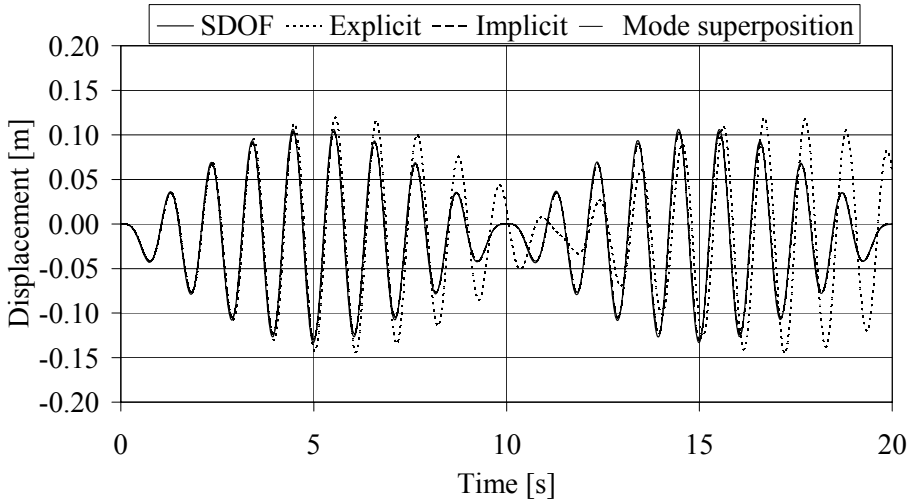

β=0.9

Table F.4: Velocities for an undamped beam, loaded by a harmonic load with β =0.1, 0.5 and 0.9.

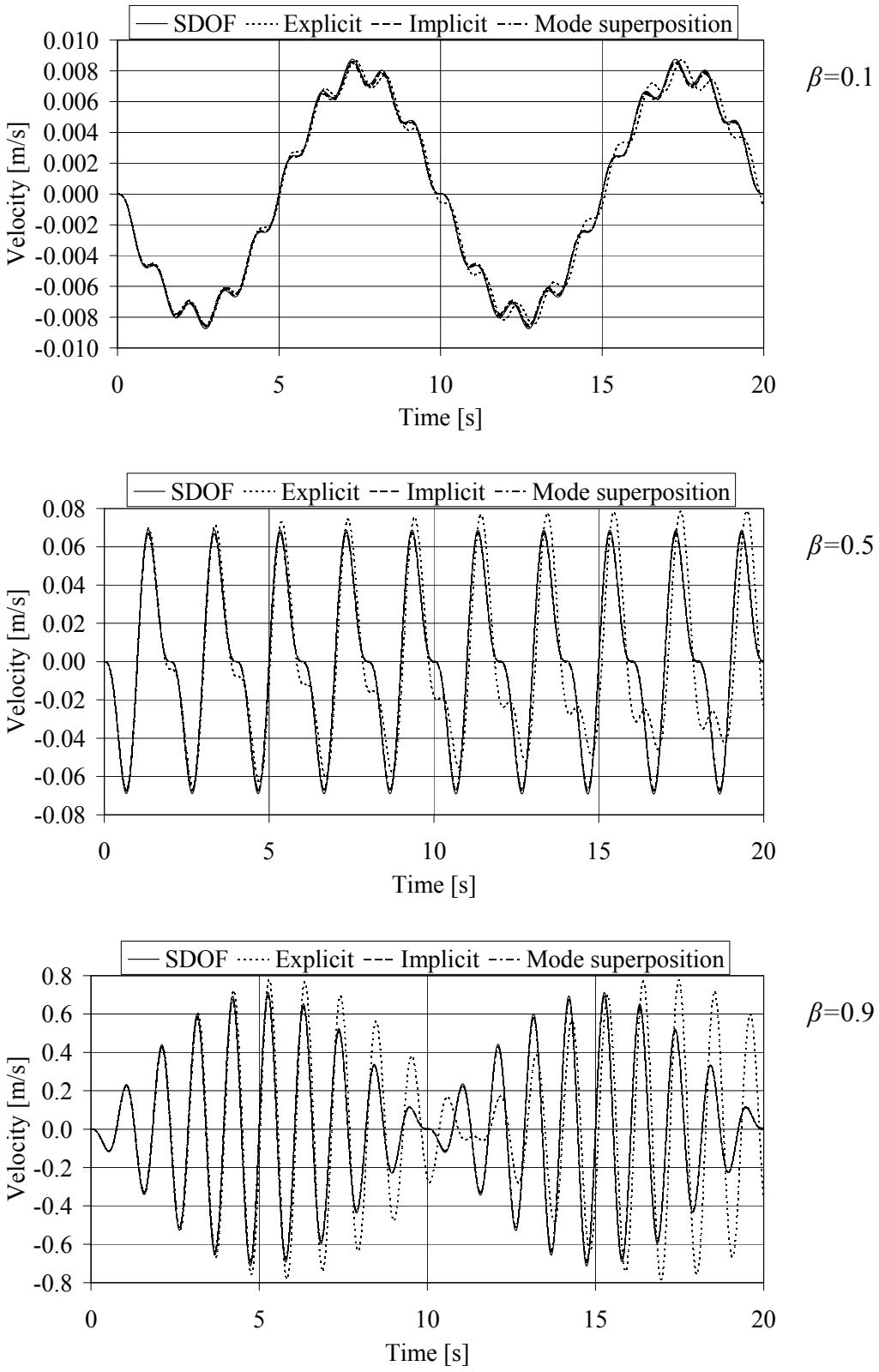

Table F.5: Accelerations for an undamped beam, loaded by a harmonic load with β=0.1, 0.5 and 0.9.

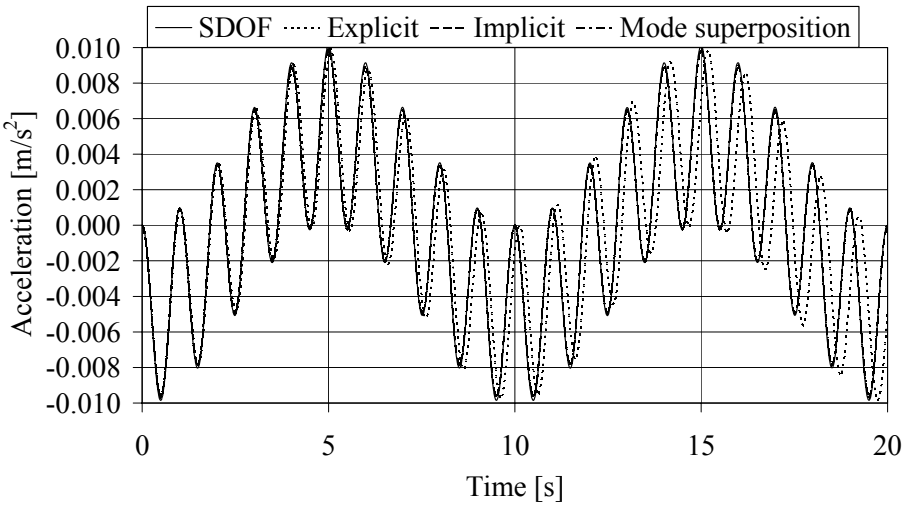

β=0.1

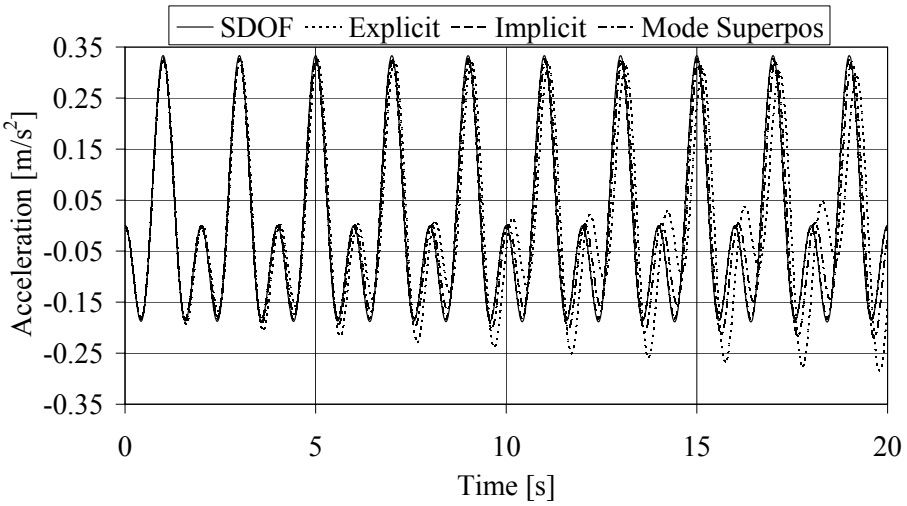

β=0.5

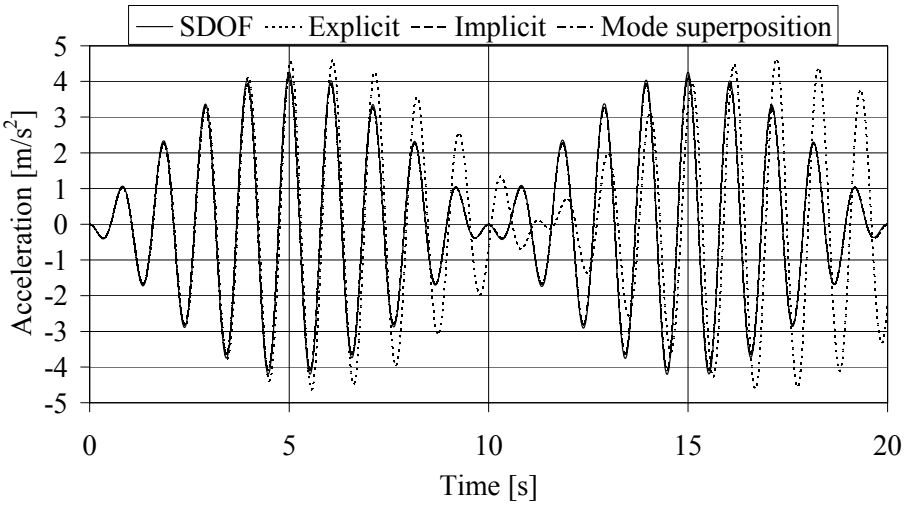

β=0.9

F.5 Damped beam loaded by a harmonic load

Table F.6: Displacements for a damped beam, loaded by a harmonic load with β=0.1, 0.5 and 0.9.

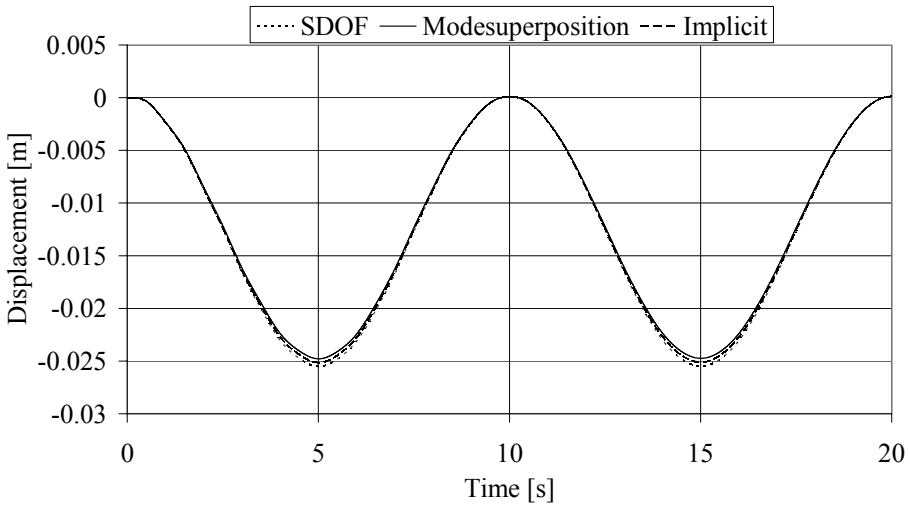

β=0.1

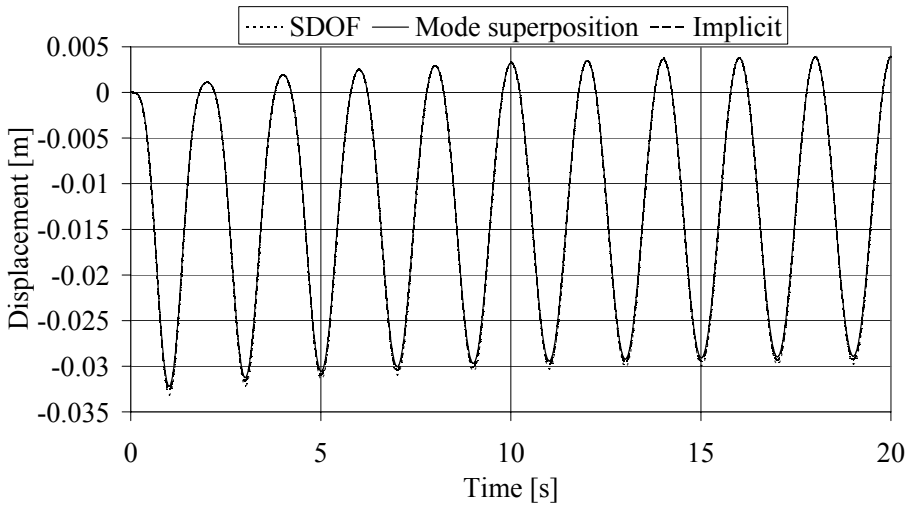

β=0.5

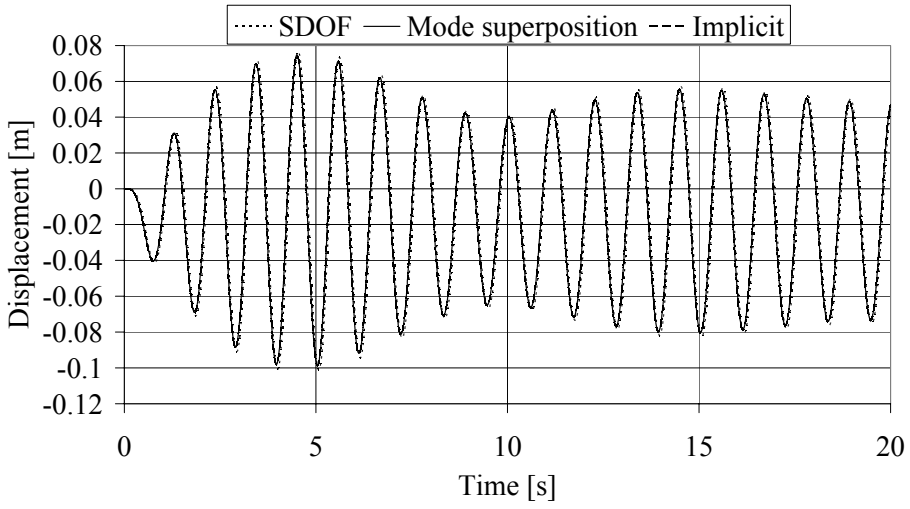

β=0.9

Table F.7: Velocities for a damped beam, loaded by a harmonic load with β=0.1, 0.5 and 0.9.

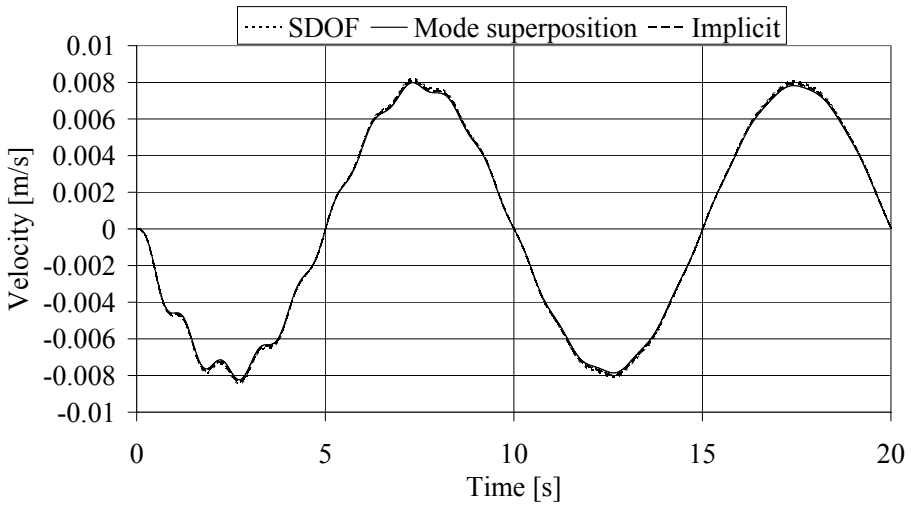

β=0.1

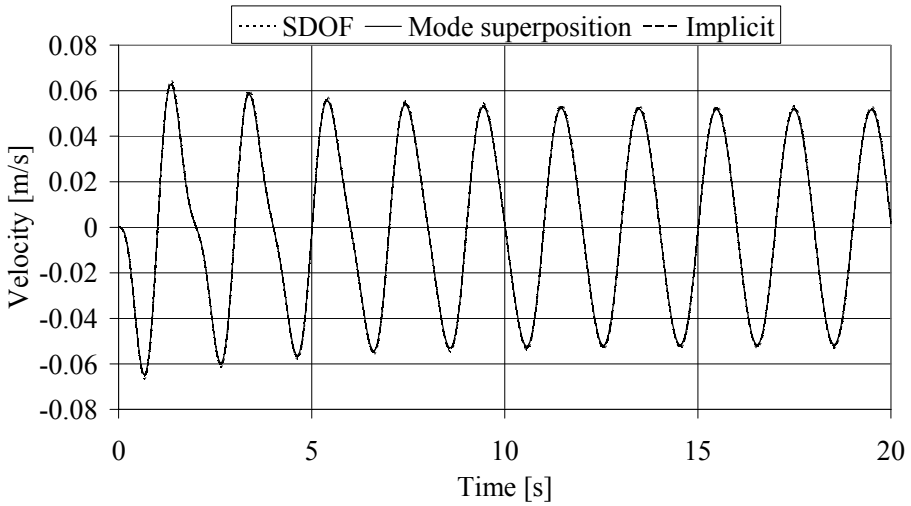

β=0.5

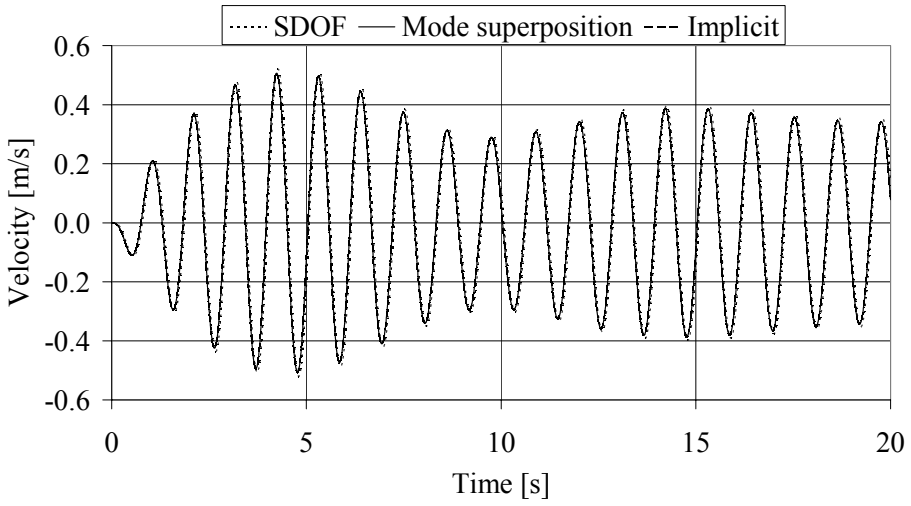

β=0.9

Table F.8: Accelerations for a damped beam, loaded by a harmonic load with β=0.1, 0.5 and 0.9.

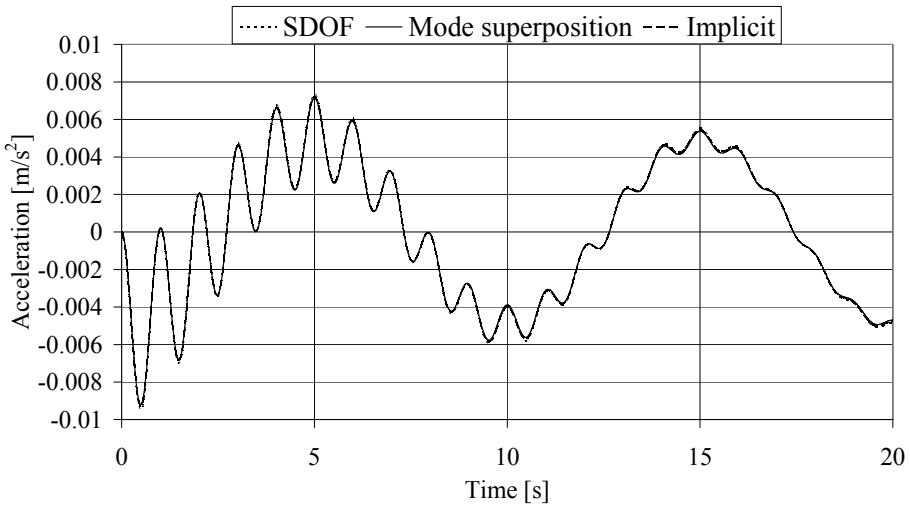

β=0.1

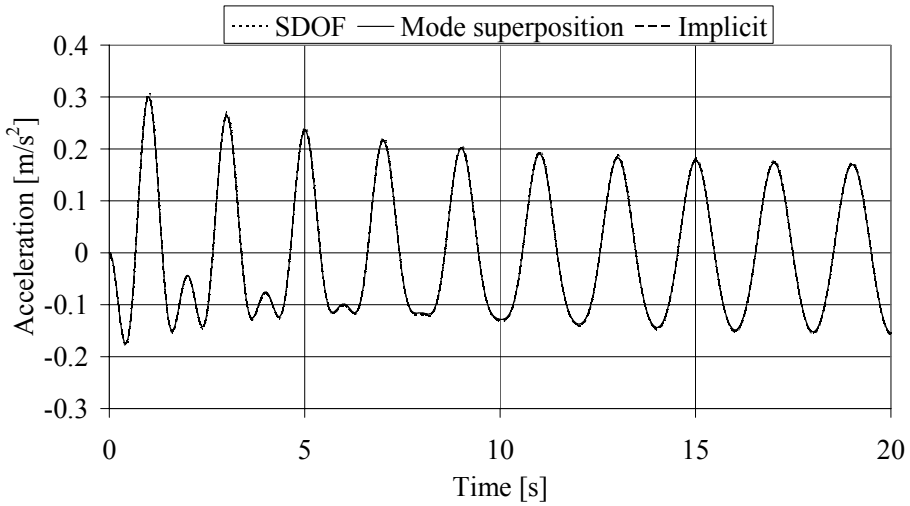

β=0.5

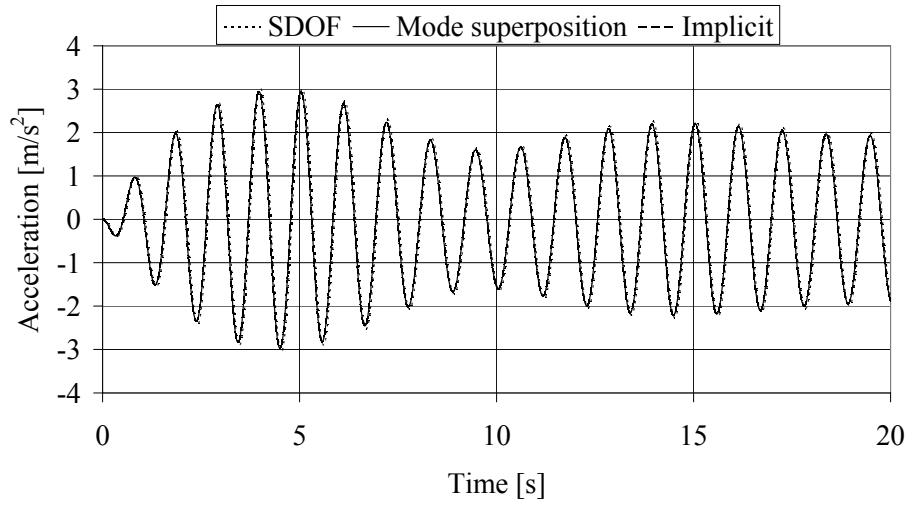

β=0.9

F.6 Convergence analysis – harmonic load

Table F.9: Convergence analysis for an undamped beam, loaded by a harmonic load with β=0.5.

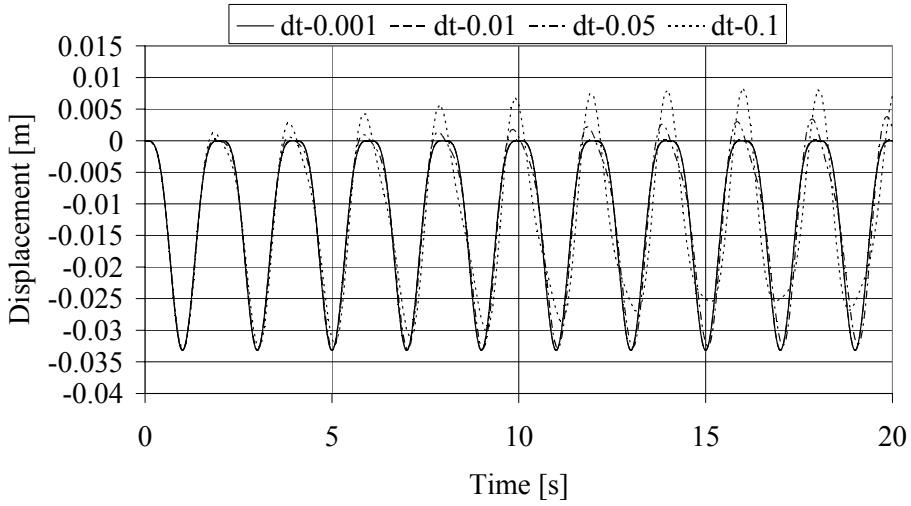

β=0.5

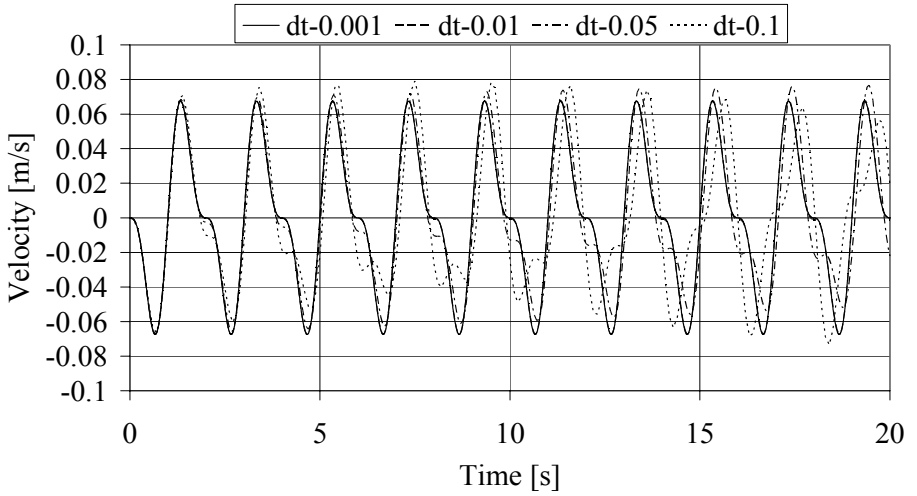

β=0.5

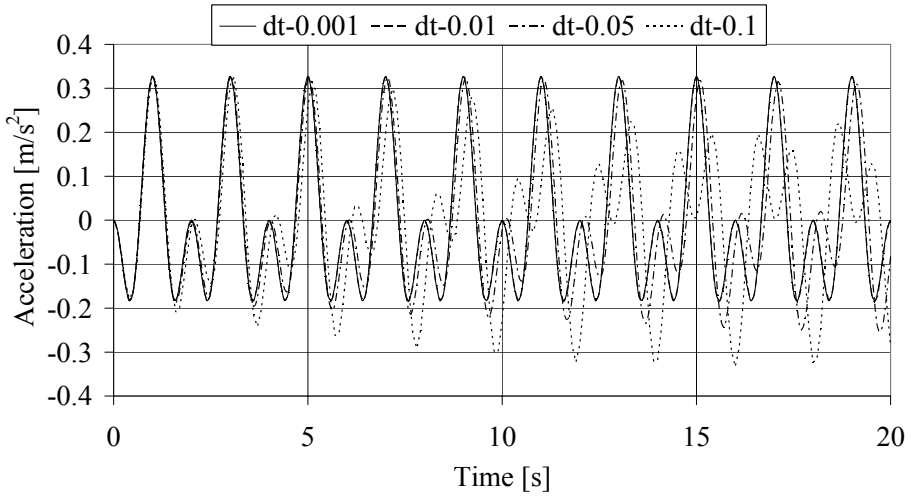

β=0.5

Table F.10: Convergence analysis for a damped beam, loaded by a harmonic load with β=0.5.

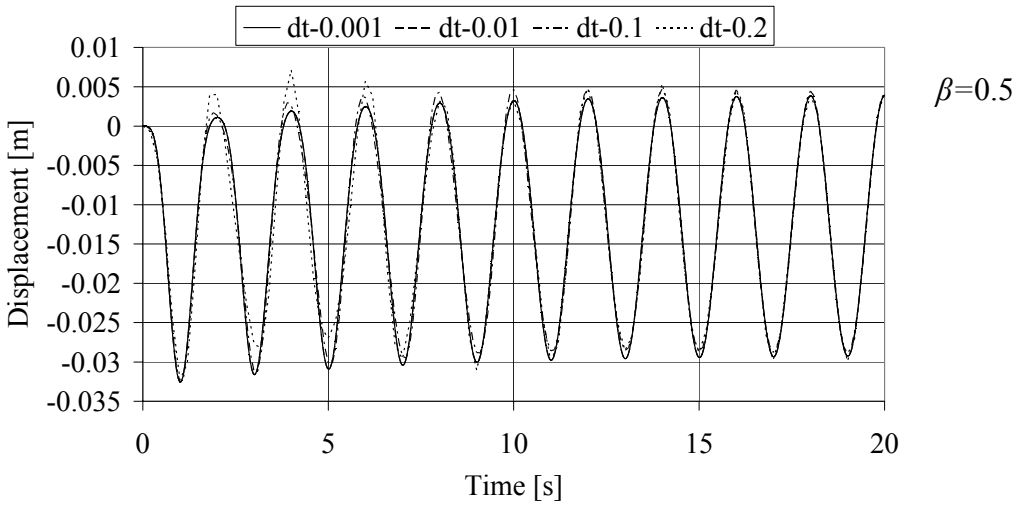

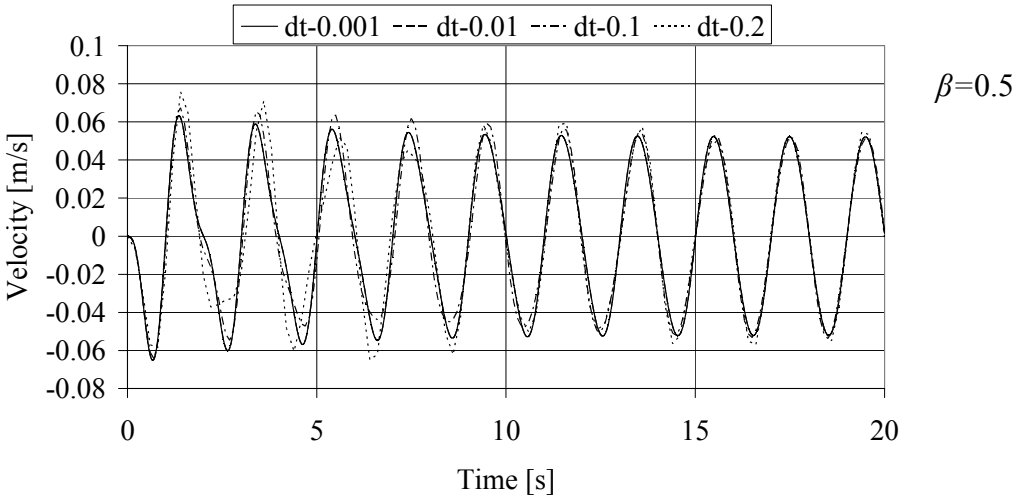

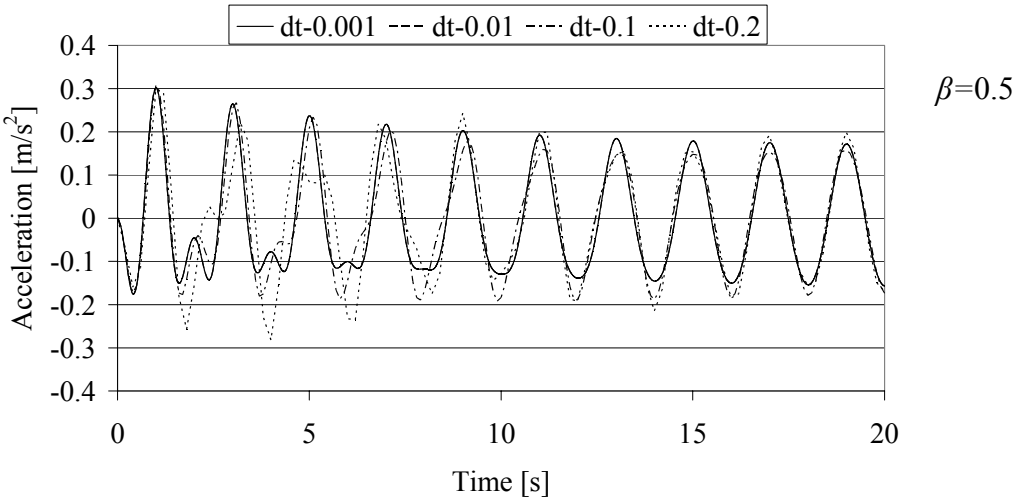

F.7 Train load, HSLM-A1 – Varying point load

Table F.11: Displacement, velocity and Acceleration for Train load HSLM-A1.

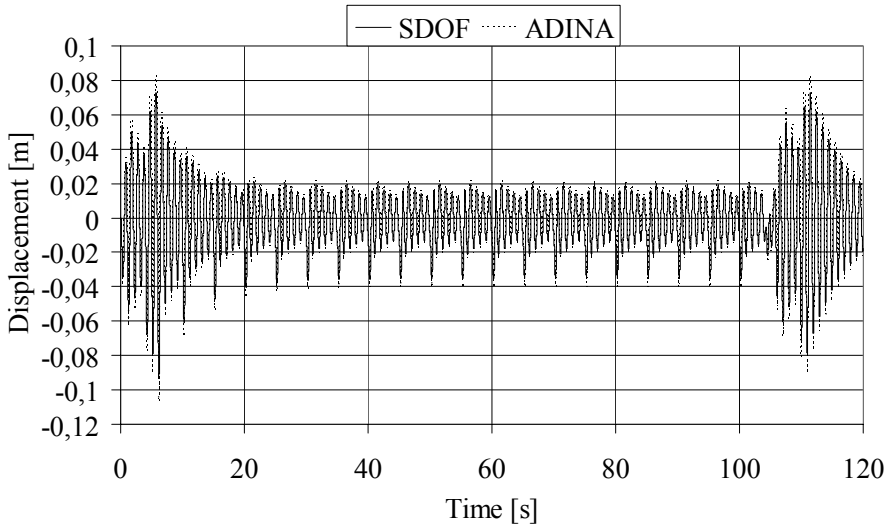

β=0.2

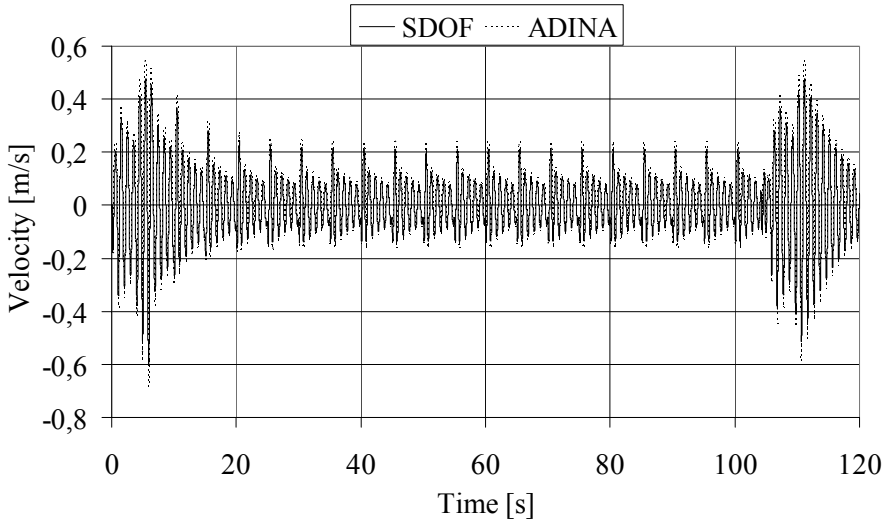

β=0.2

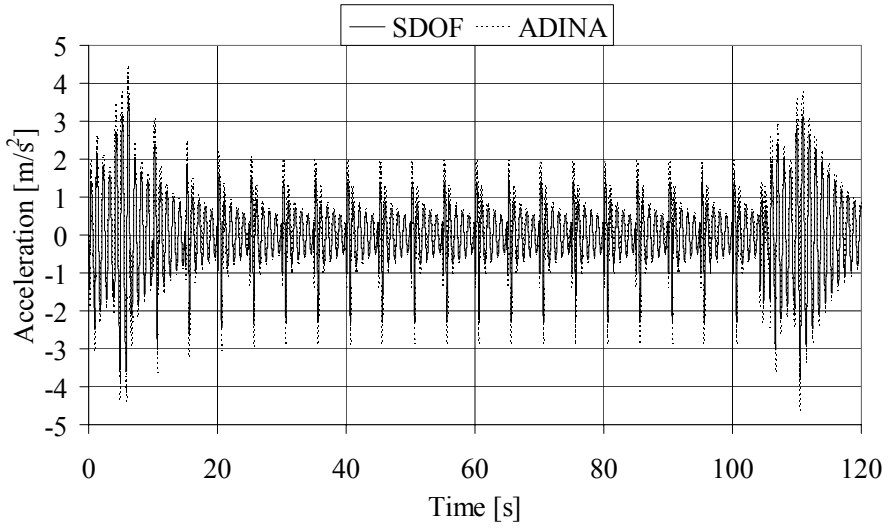

β=0.2

Table F.12: Displacement, velocity and Acceleration for Train load HSLM-A1.

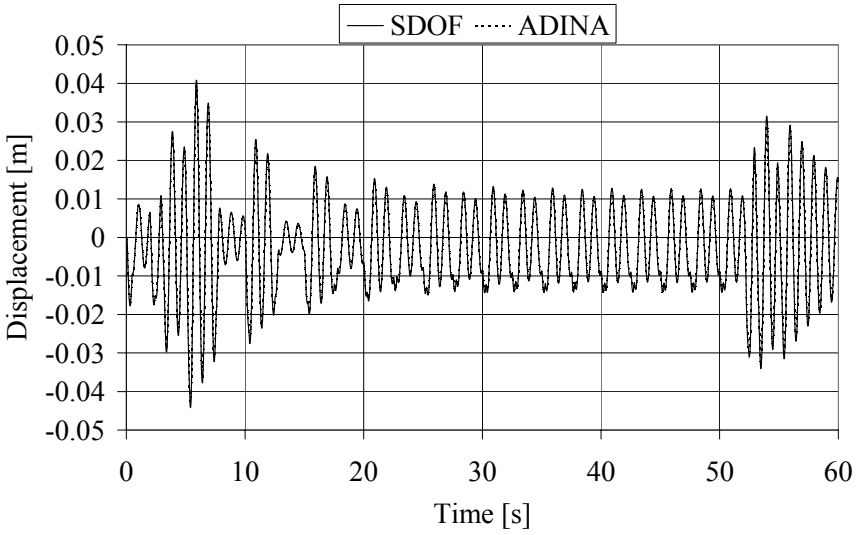

β=0.4

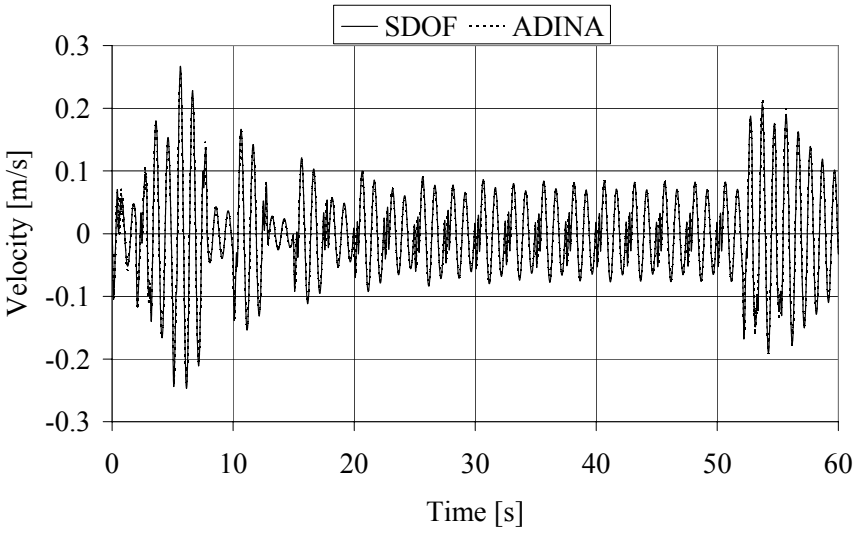

β=0.4

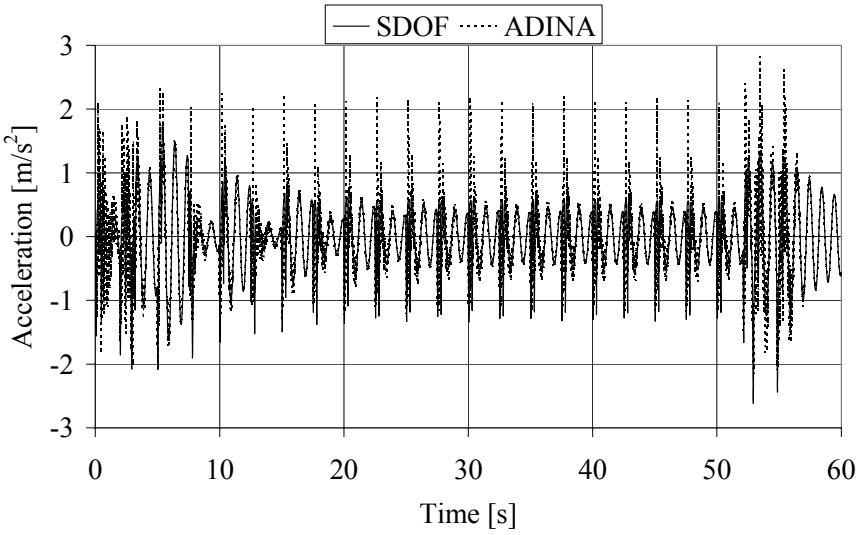

β=0.4

Table F.13: Displacement, velocity and Acceleration for Train load HSLM-A1.

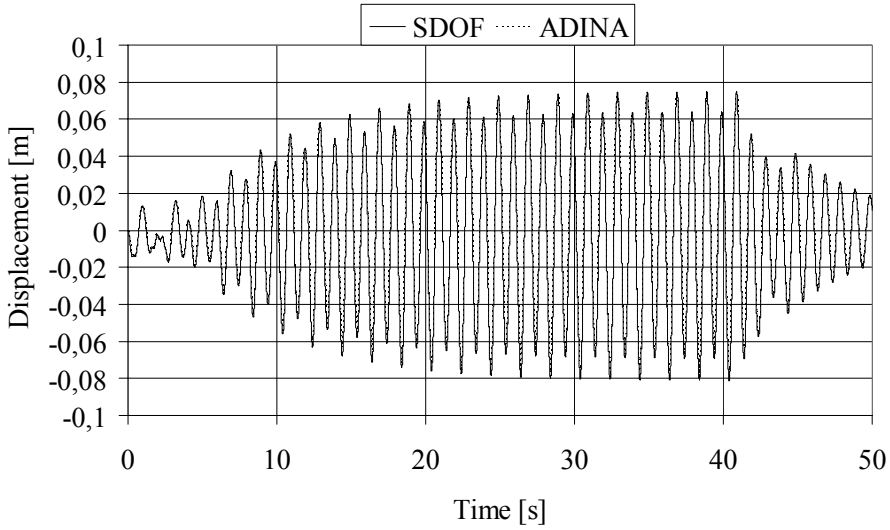

β=0.5

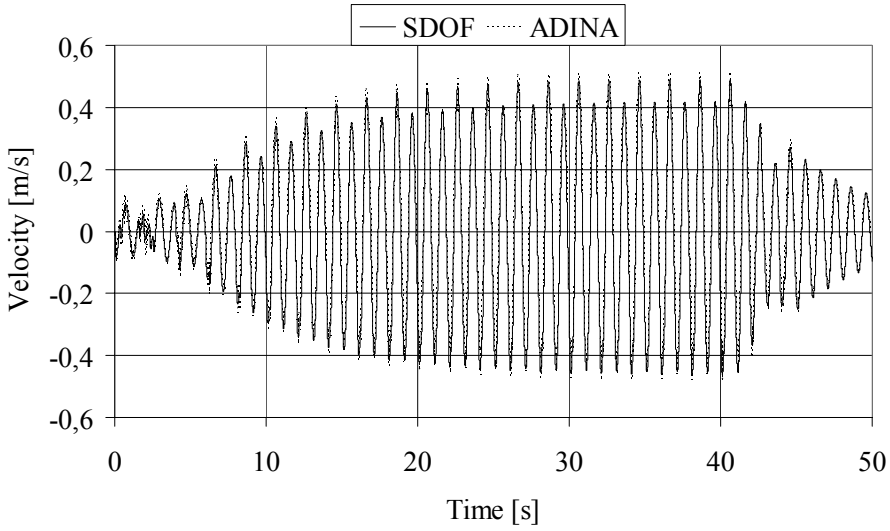

β=0.5

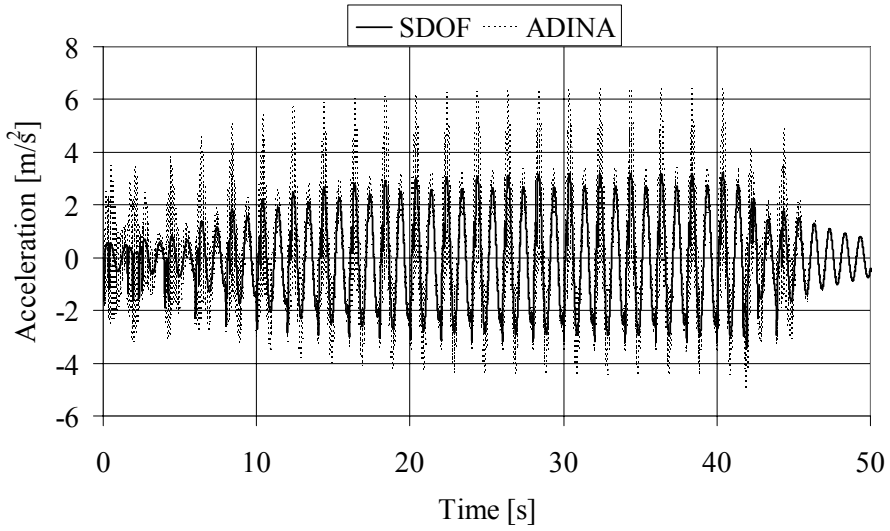

β=0.5

Table F.14: Displacement, velocity and Acceleration for Train load HSLM-A1.

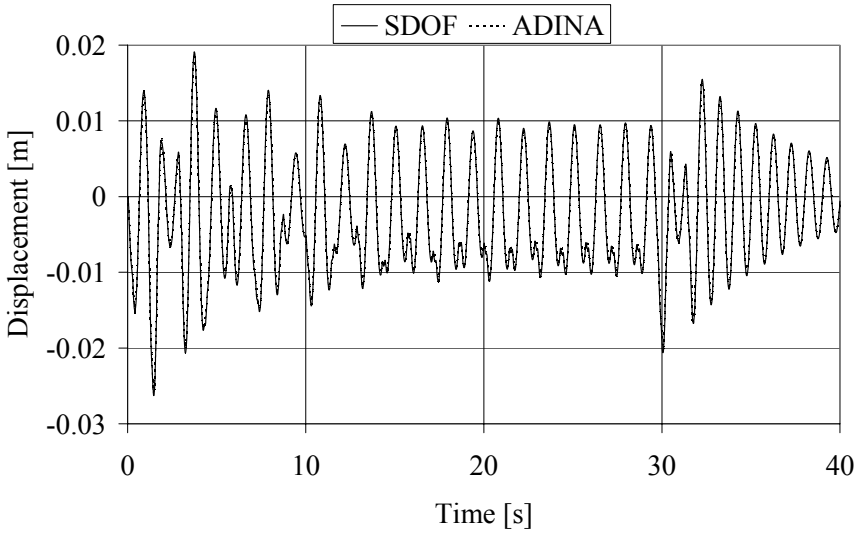

β=0.7

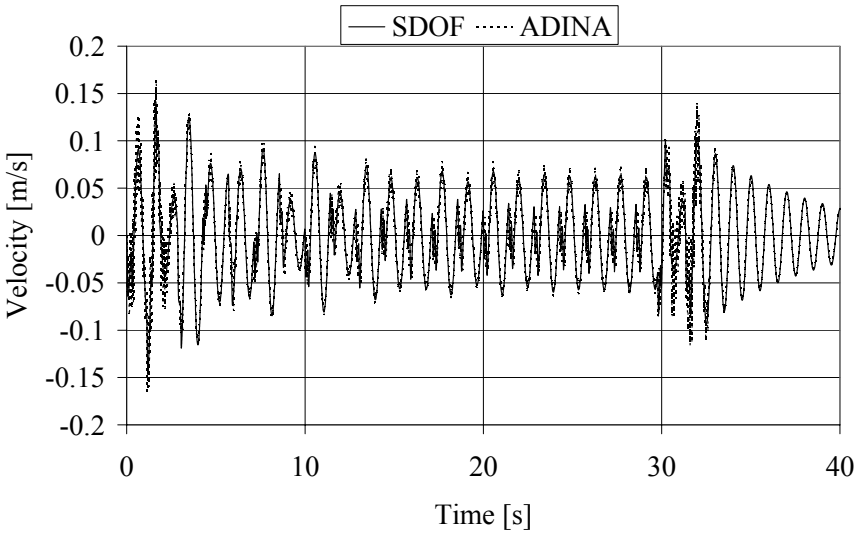

β=0.7

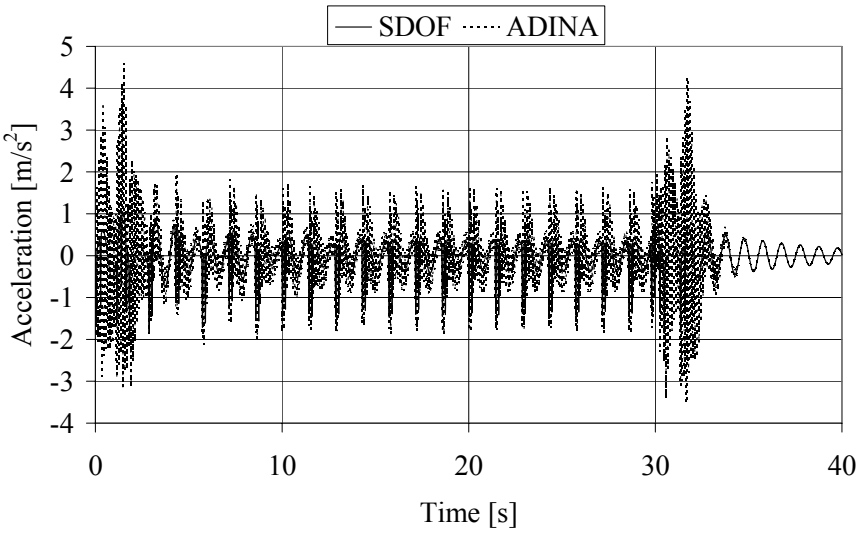

β=0.7

Table F.15: Displacement, velocity and Acceleration for Train load HSLM-A1.

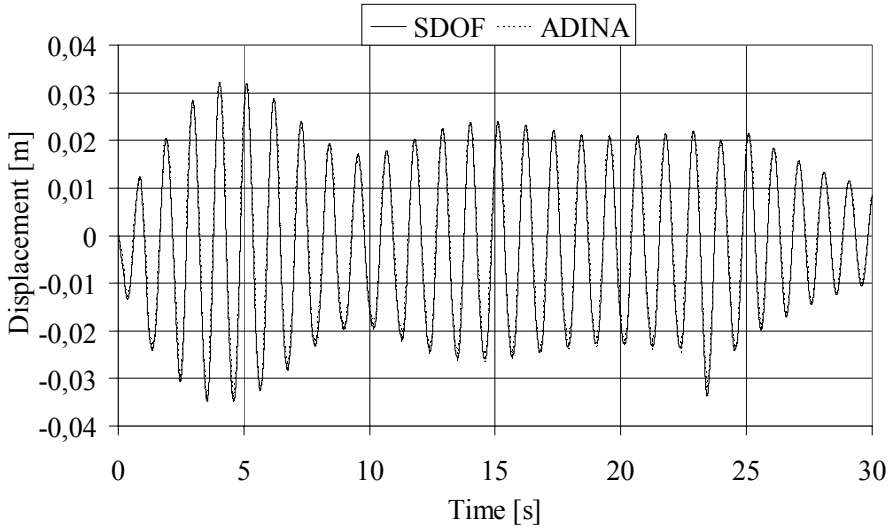

β=0.9

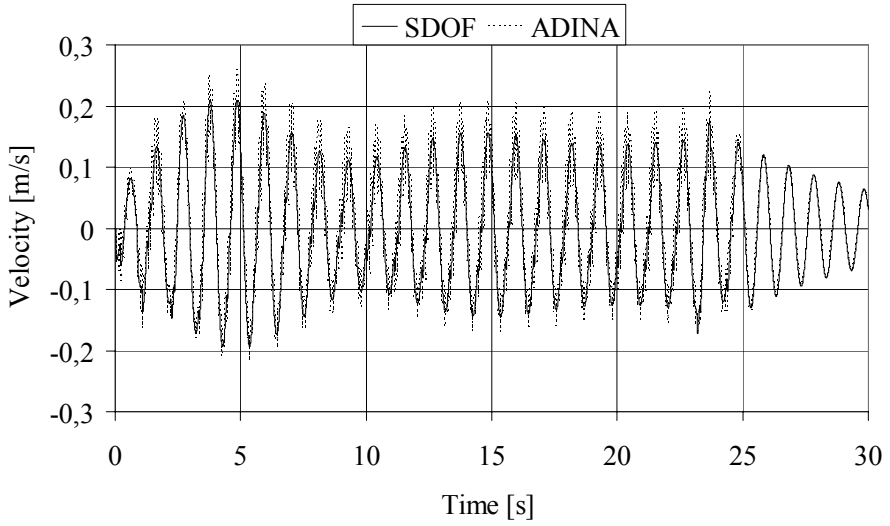

β=0.9

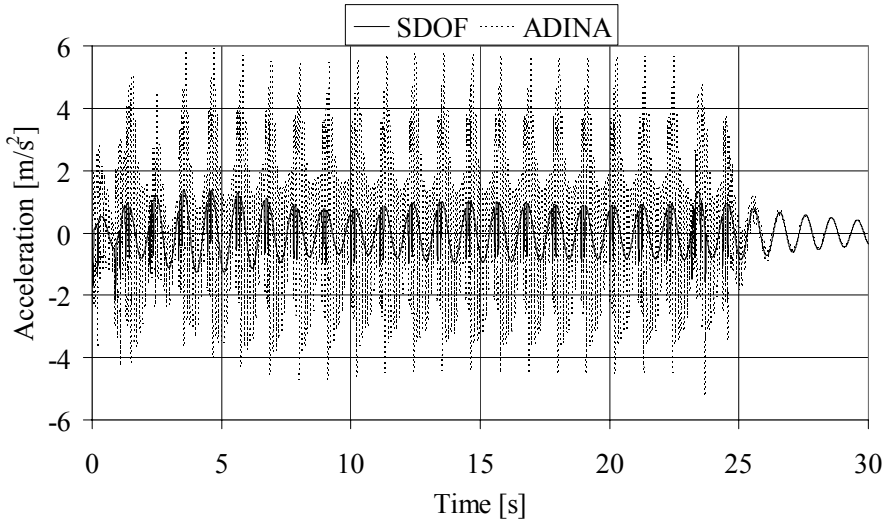

β=0.9

F.8 Single travelling point load

Table F.16: Displacement, velocity and acceleration for different load cases.

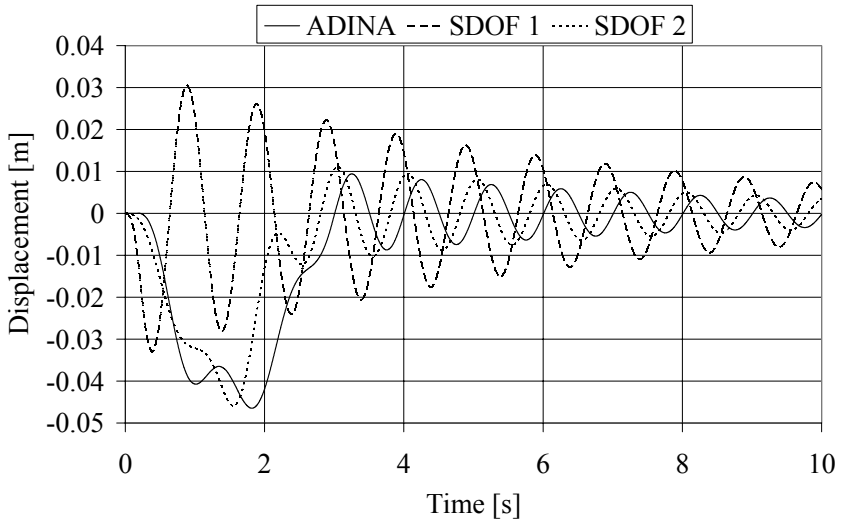

β=0.2

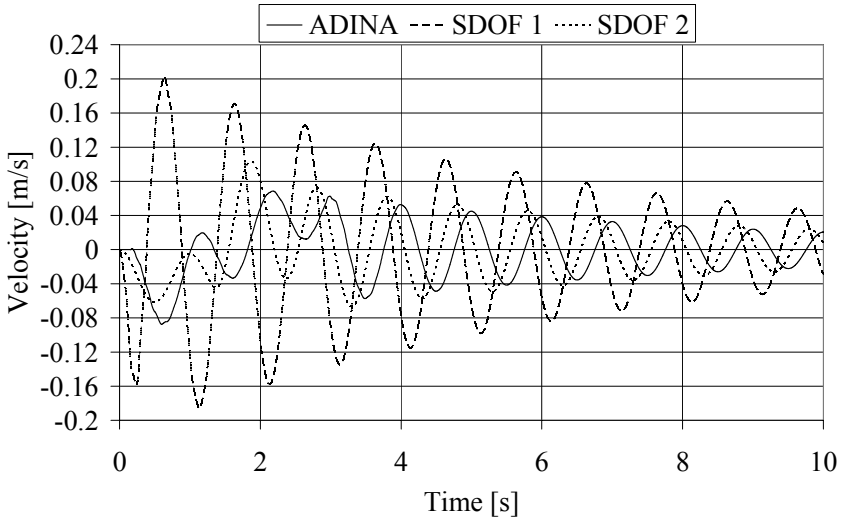

β=0.2

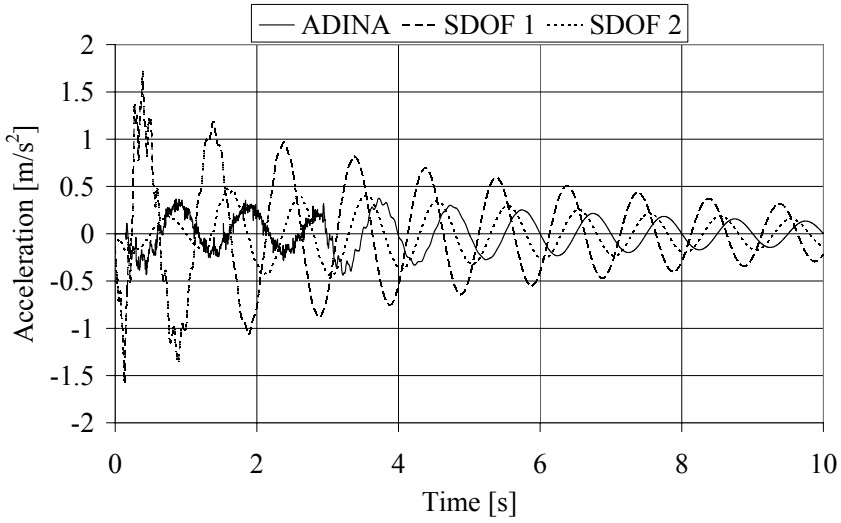

β=0.2

Table F.17: Displacement, velocity and acceleration for different load cases.

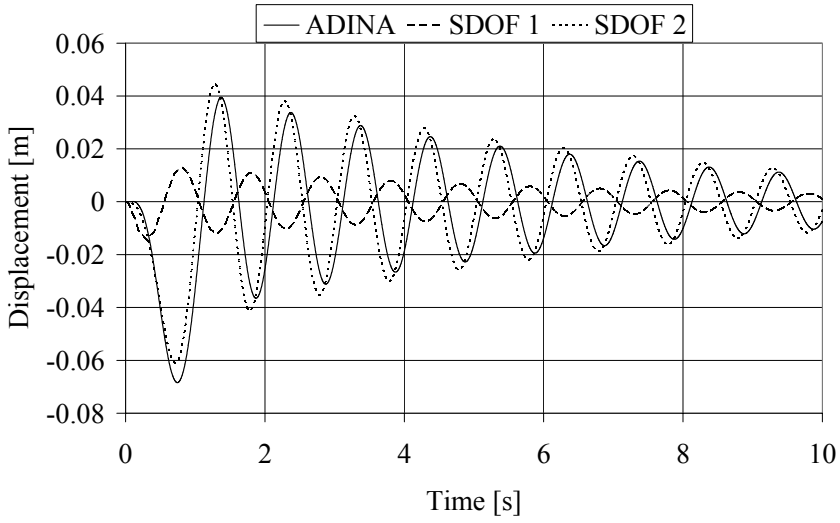

β=0.5

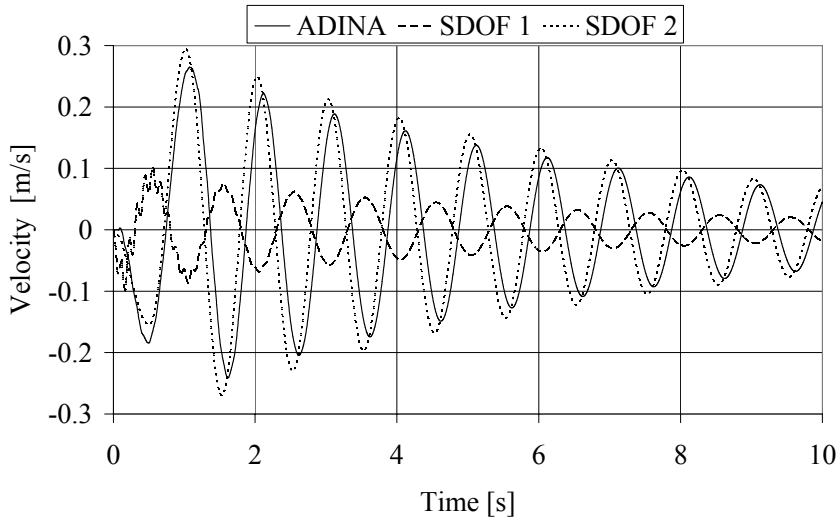

β=0.5

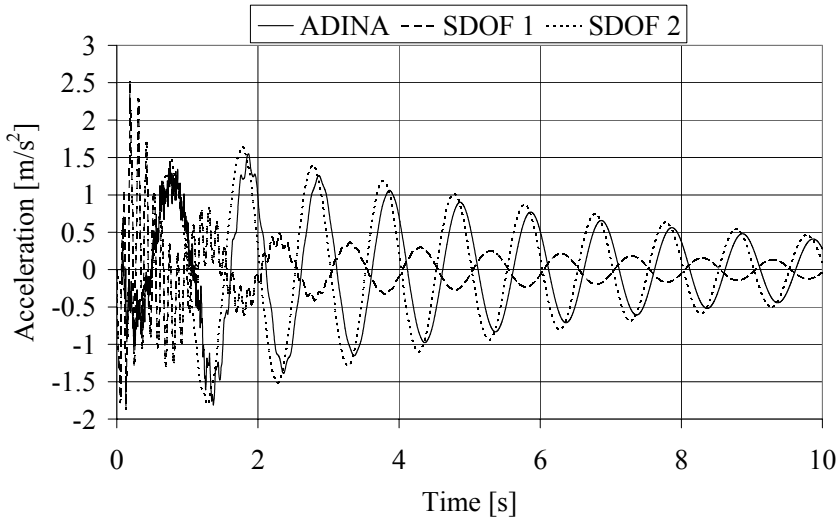

β=0.5

Table F.18: Displacement, velocity and acceleration for different load cases.

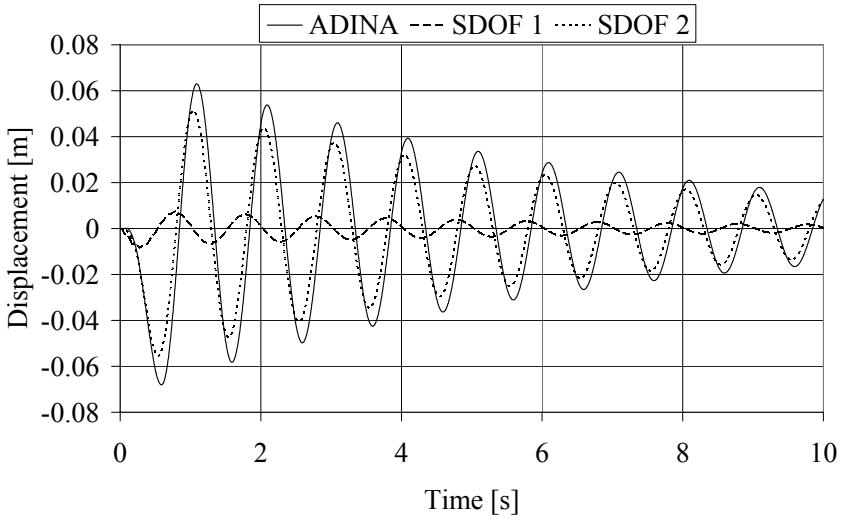

β=0.9

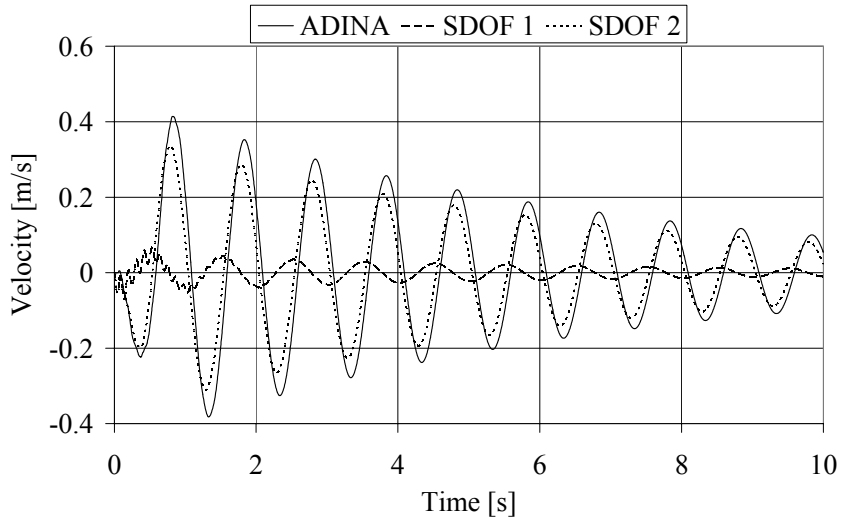

β=0.9

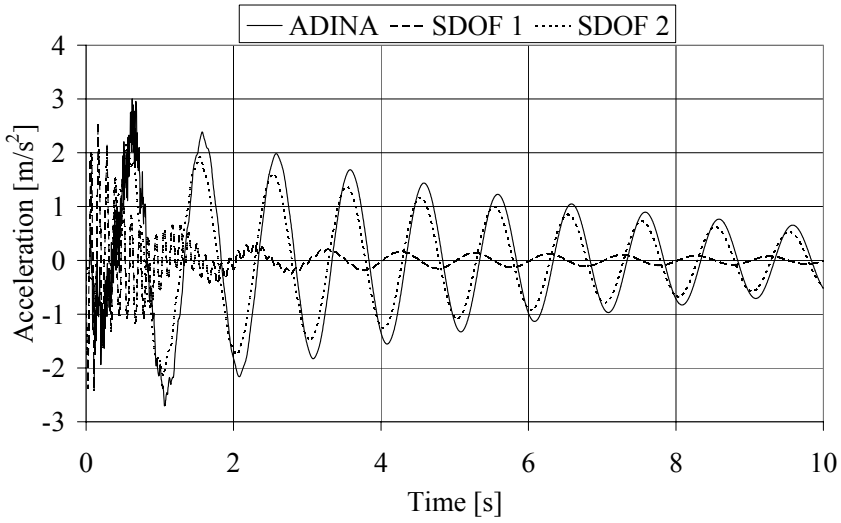

β=0.9

F.9 Double travelling point load

Table F.19: Displacement, velocity and acceleration for different load cases.

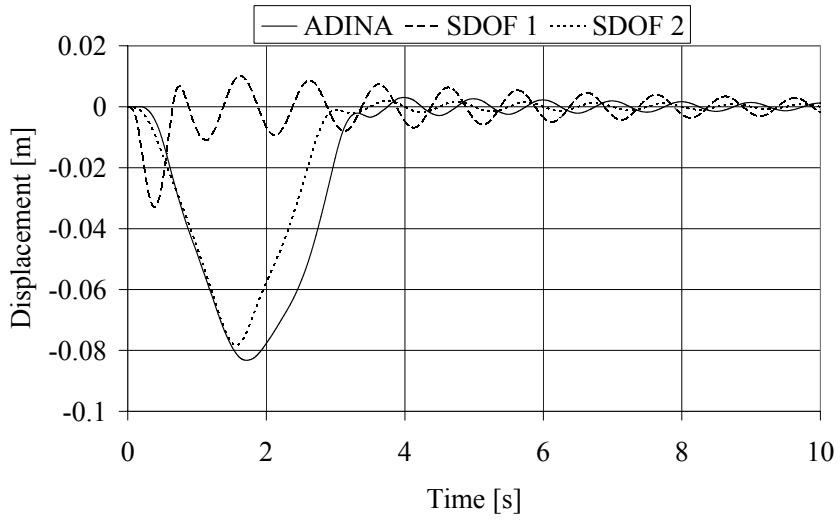

β=0.2

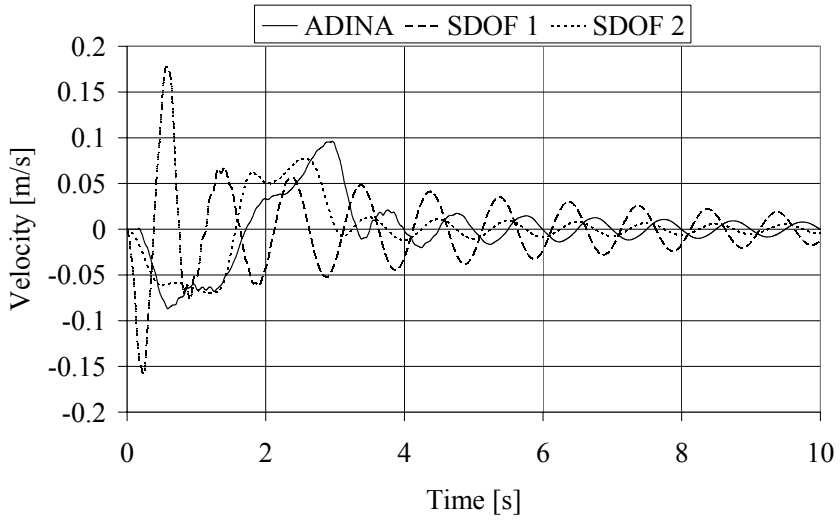

β=0.2

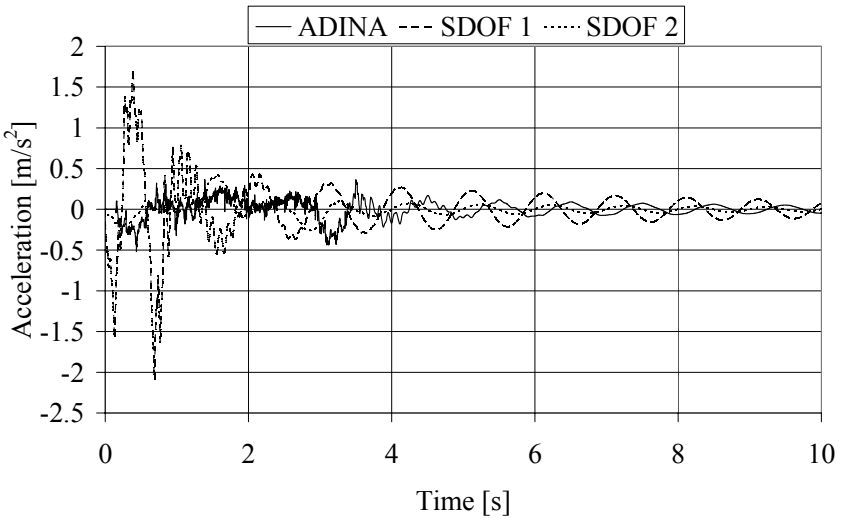

β=0.2

Table F.20: Displacement, velocity and acceleration for different load cases.

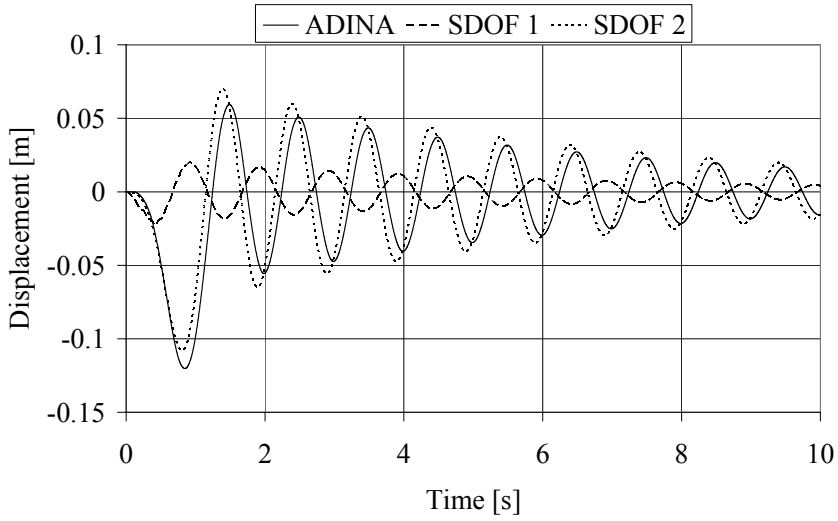

β=0.5

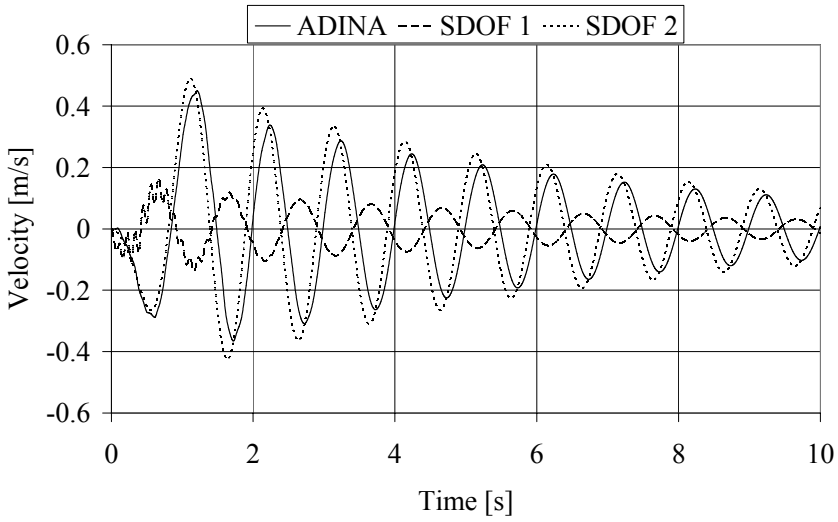

β=0.5

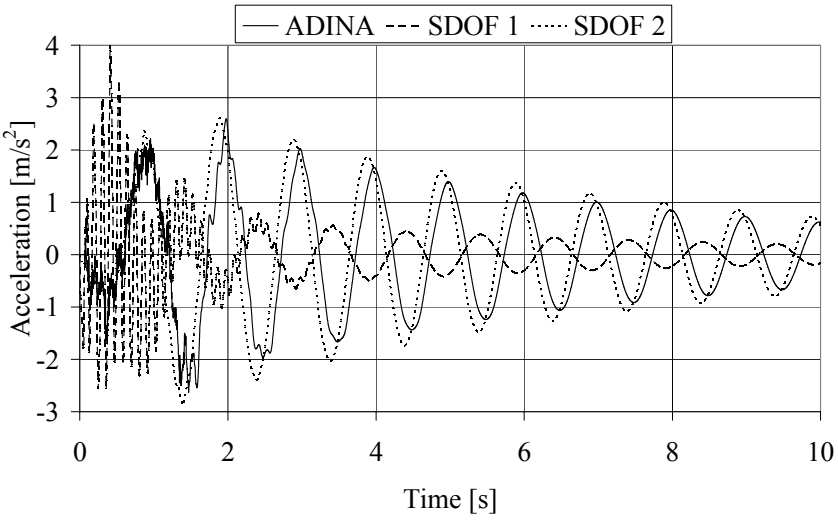

β=0.5

Table F.21: Displacement, velocity and acceleration for different load cases.

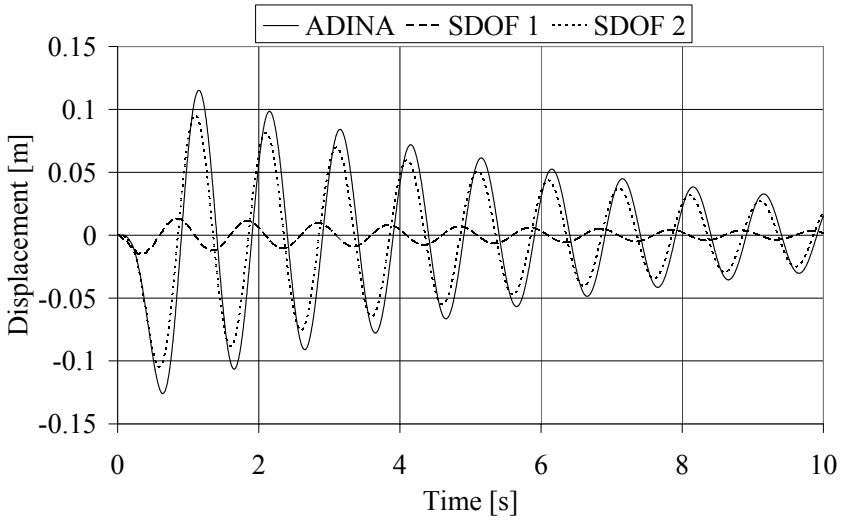

β=0.9

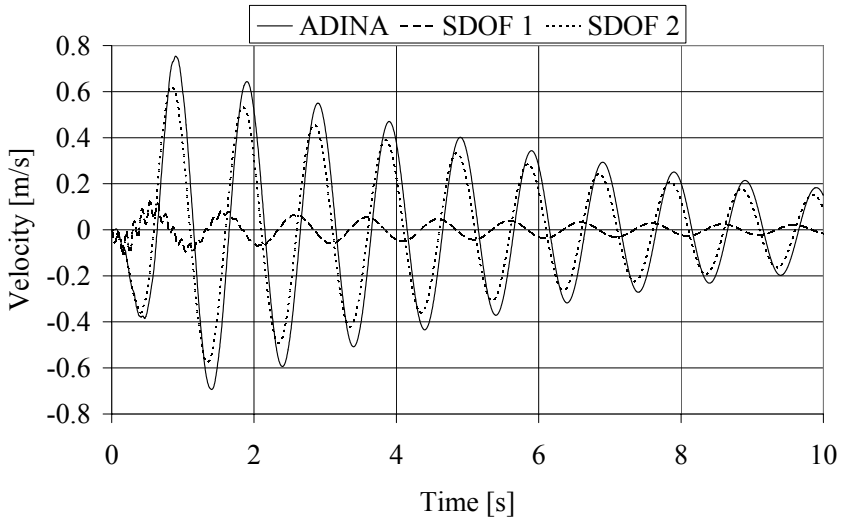

β=0.9

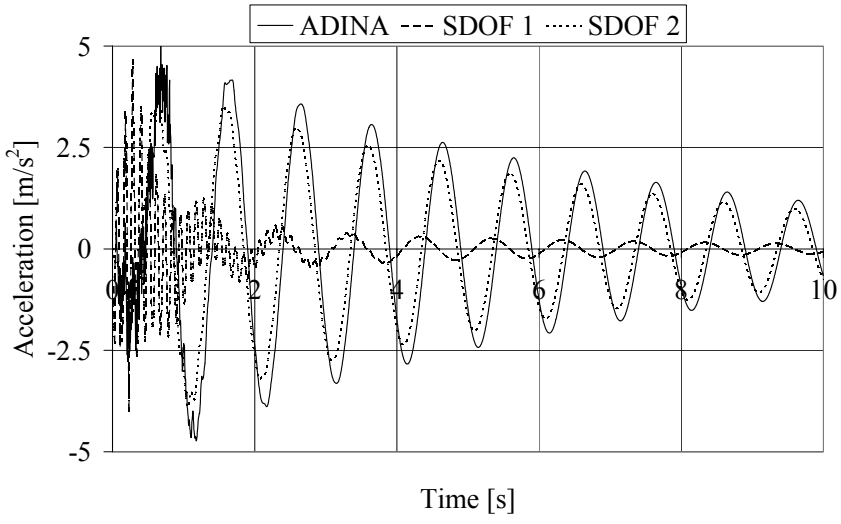

β=0.9

F.10 Travelling power car load, HSLM-A1

Table F.22: Displacement, velocity and acceleration for different load cases.

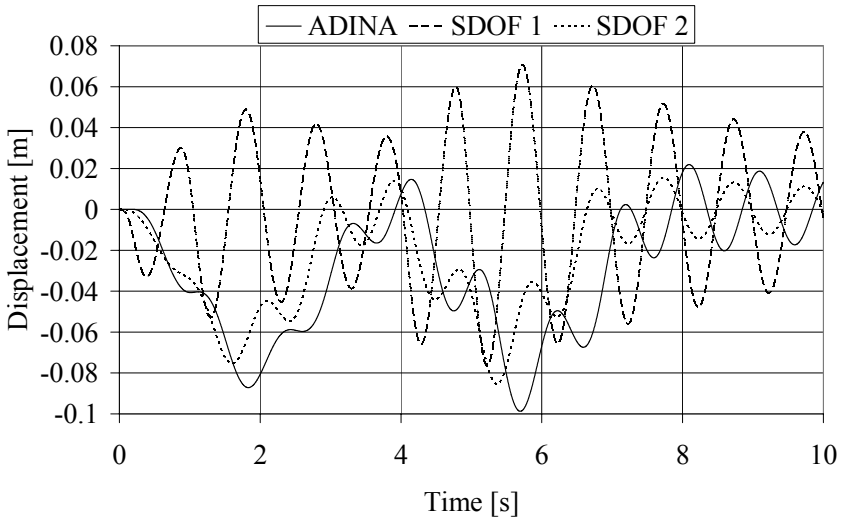

β=0.2

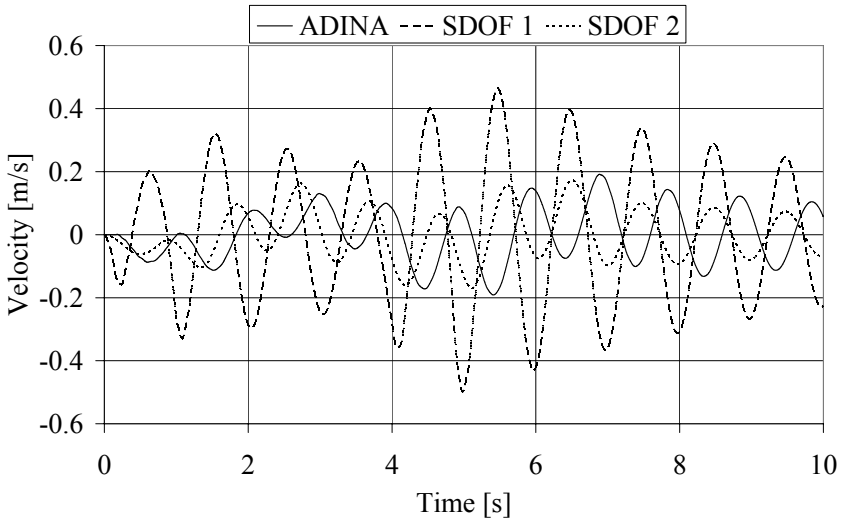

β=0.2

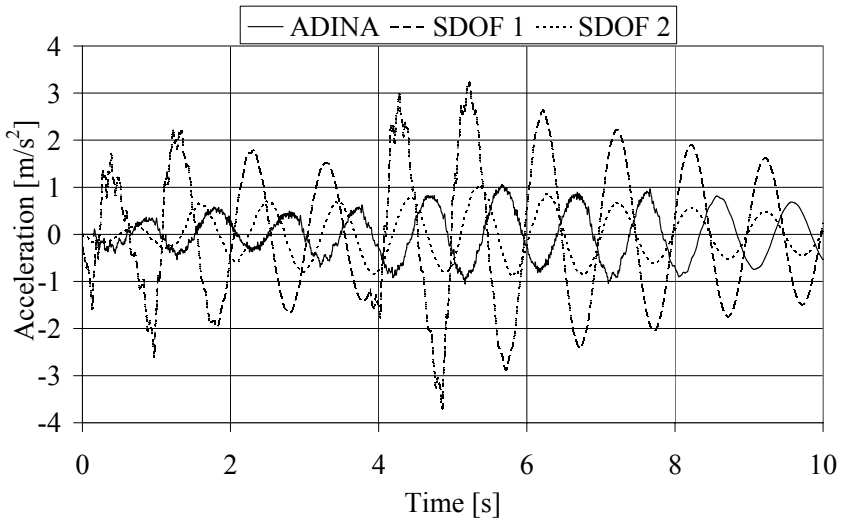

β=0.2

Table F.23: Displacement, velocity and acceleration for different load cases.

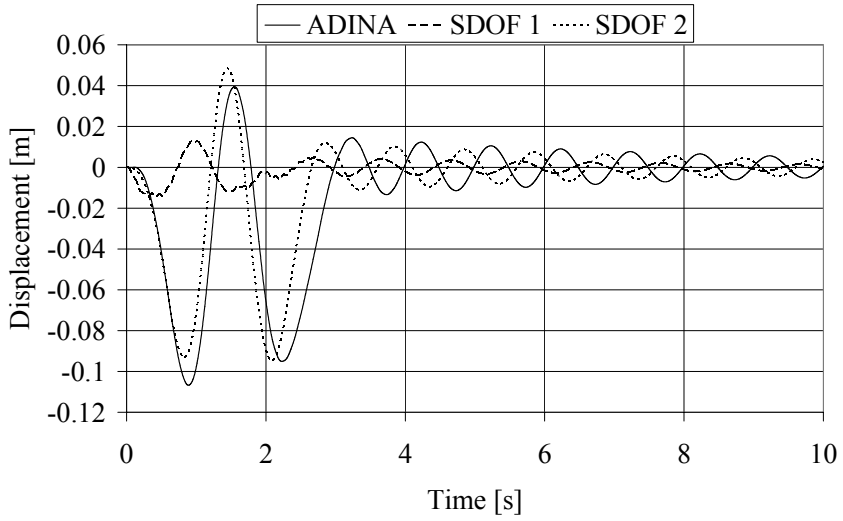

β=0.5

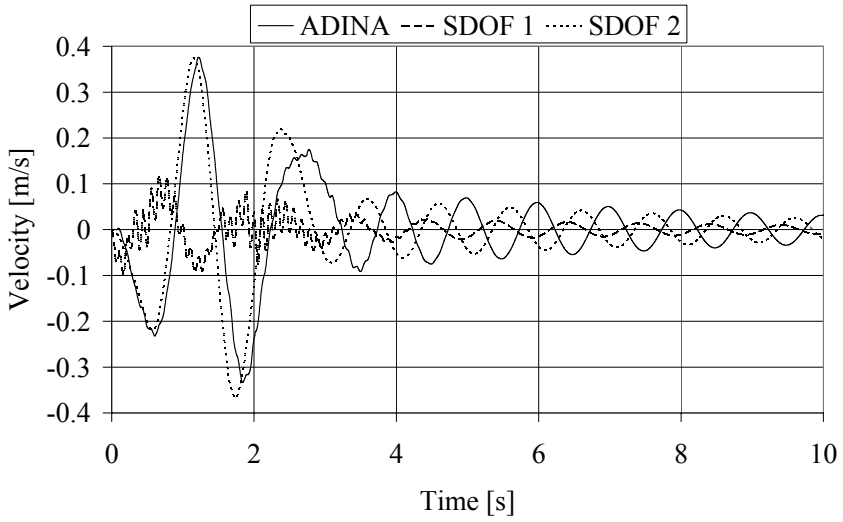

β=0.5

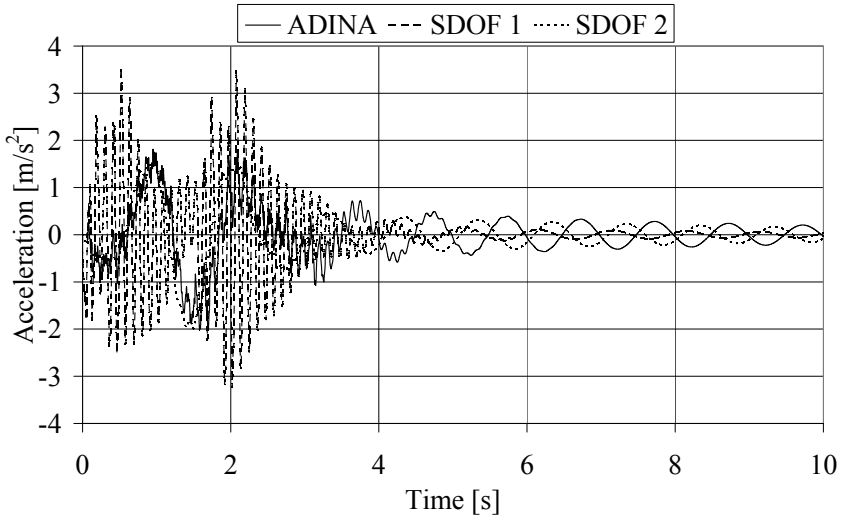

β=0.5

Table F.24: Displacement, velocity and acceleration for different load cases.

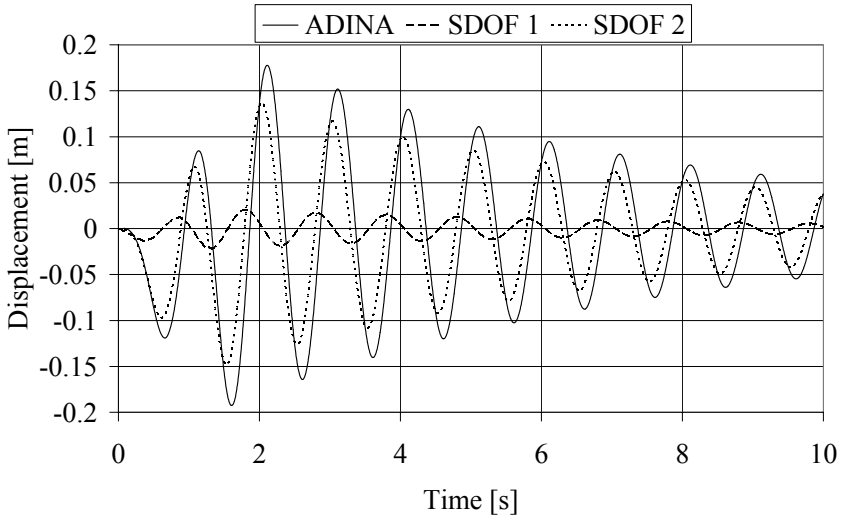

β=0.9

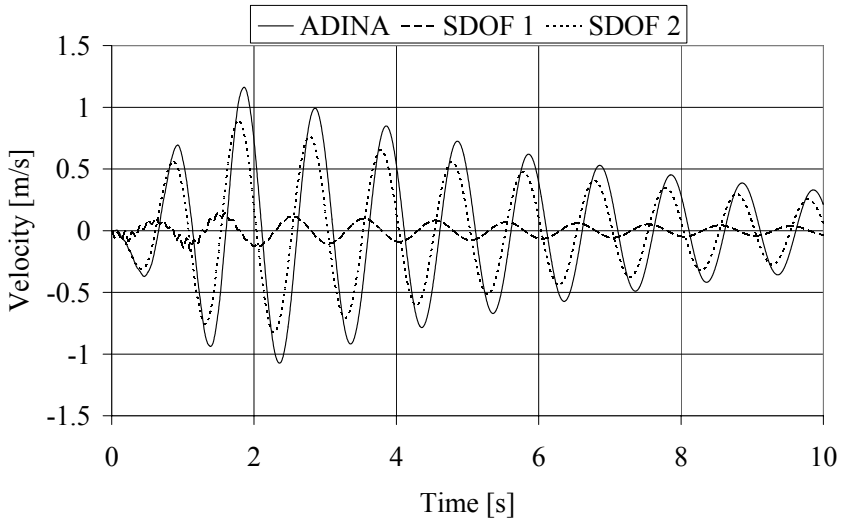

β=0.9

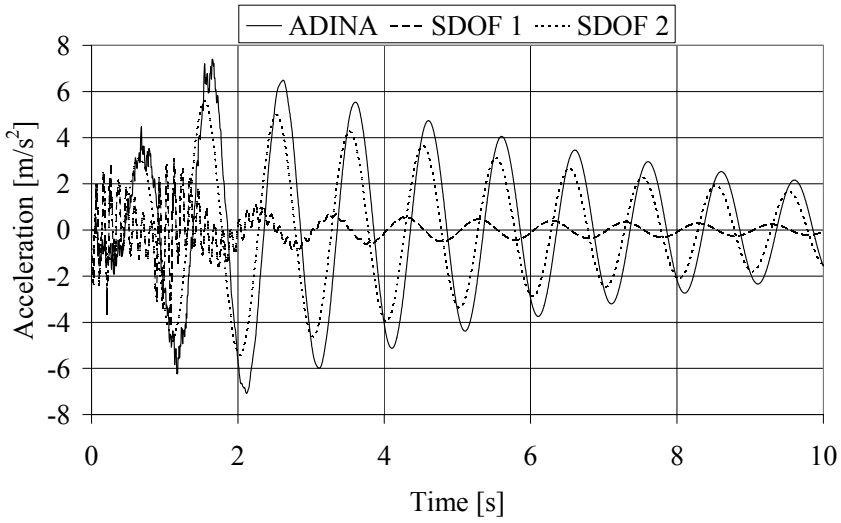

β=0.9

F.11 Train load, HSLM-A1 – Travelling load

Table F.25: Displacement, velocity and Acceleration for Train load HSLM-A1.

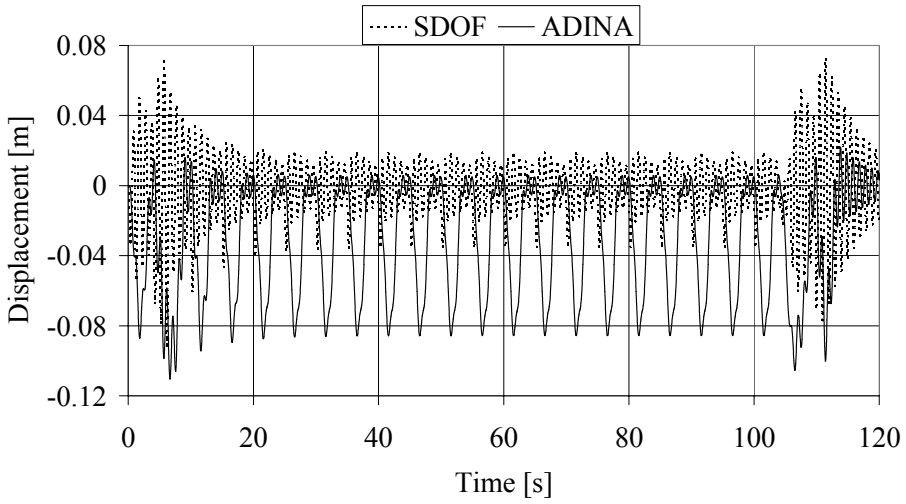

β=0.2

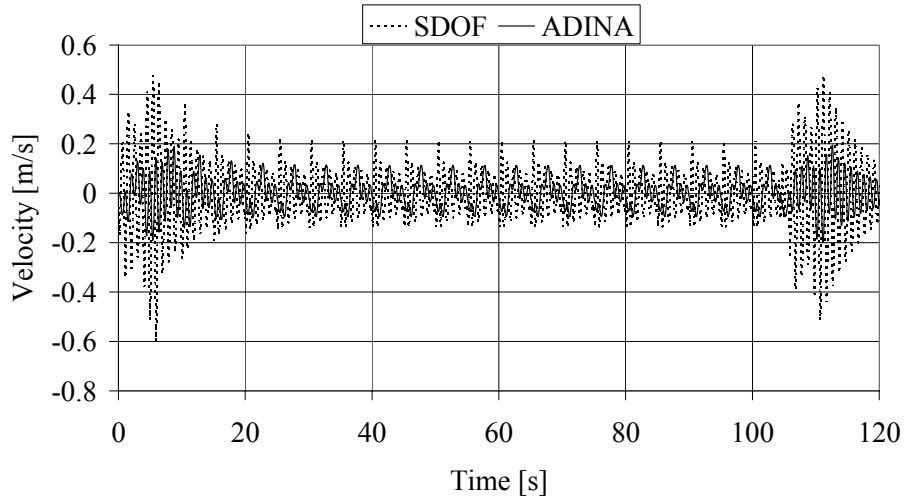

β=0.2

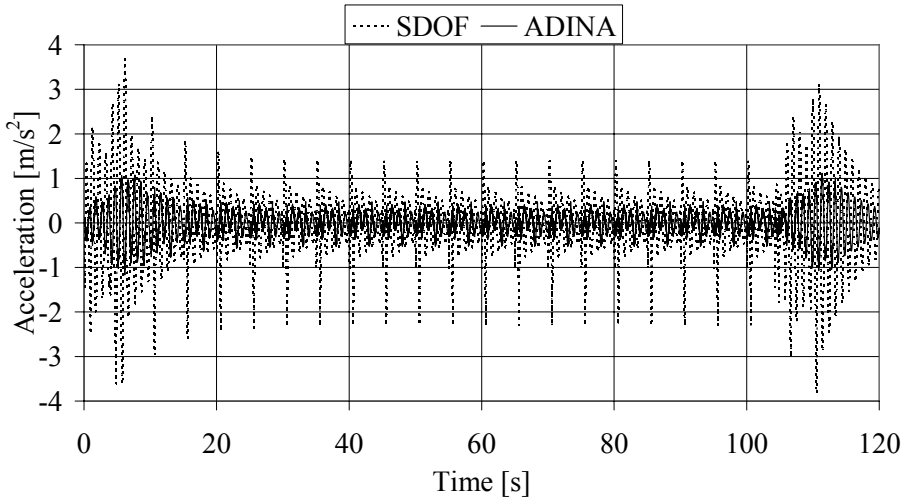

β=0.2

Table F.26: Displacement, velocity and Acceleration for Train load HSLM-A1.

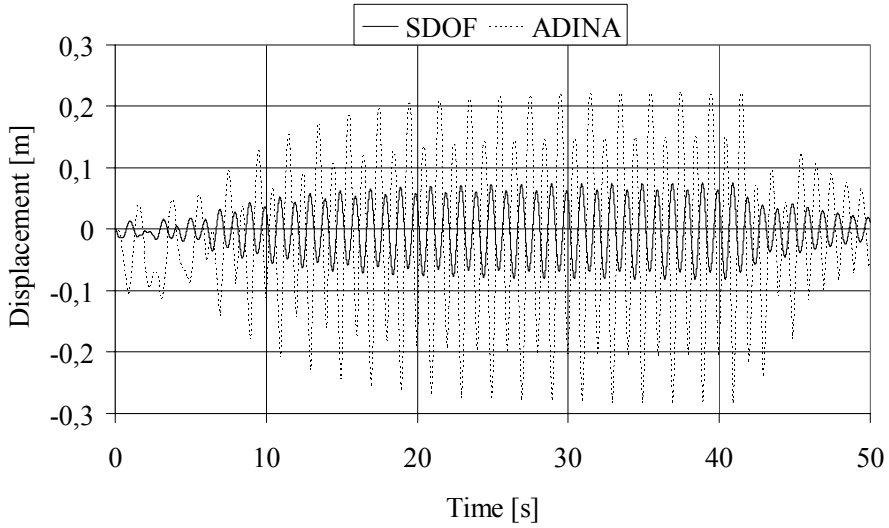

β=0.5

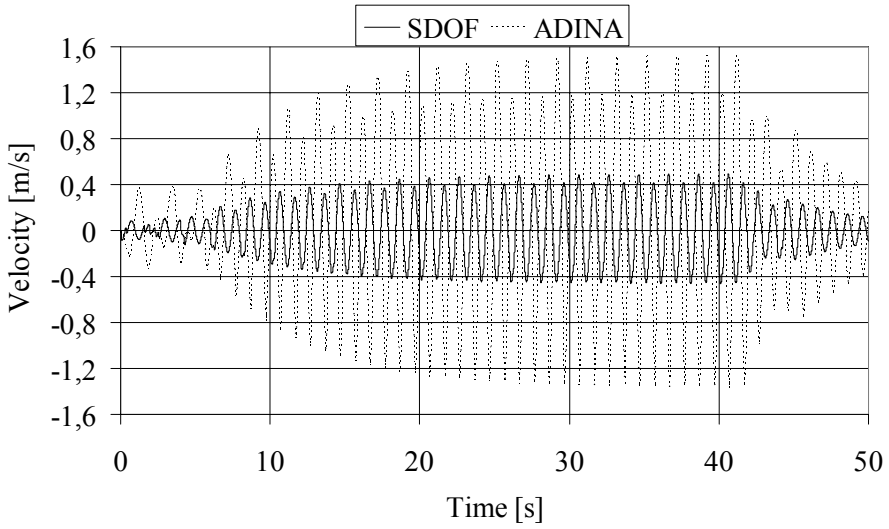

β=0.5

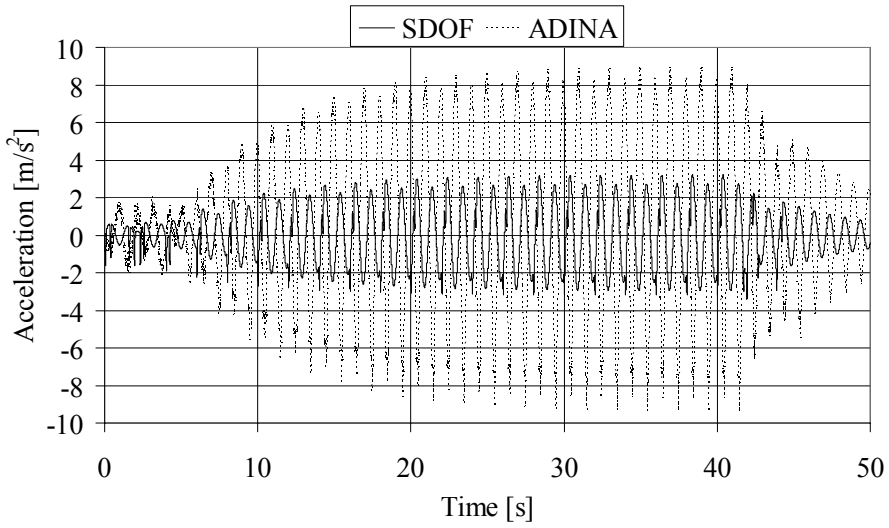

β=0.5

Table F.27: Displacement, velocity and acceleration for Train load HSLM-A1.

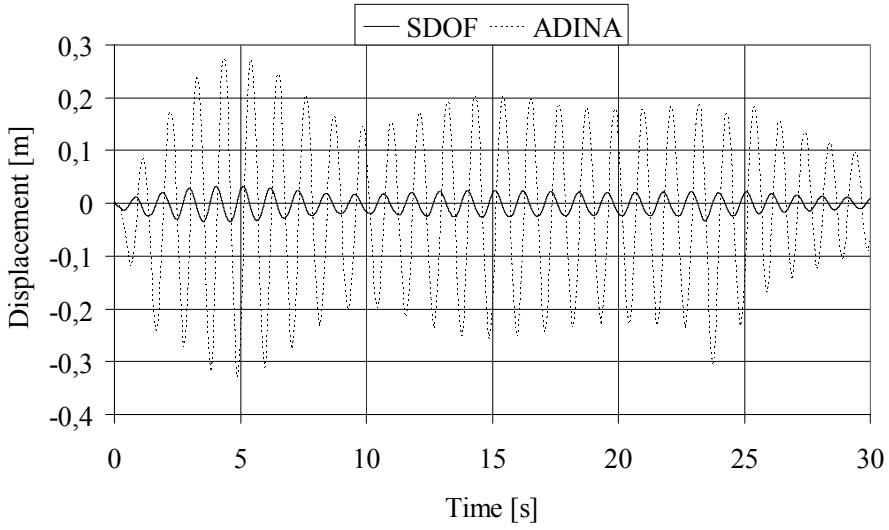

β=0.9

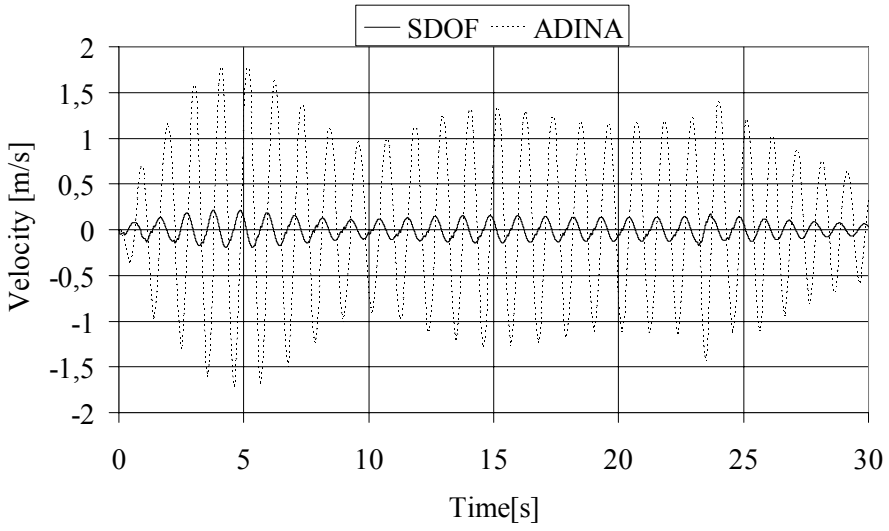

β=0.9

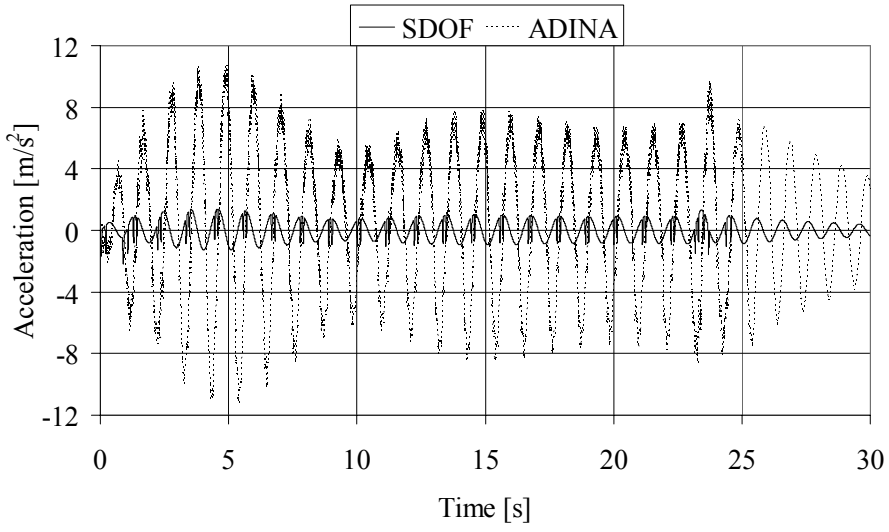

β=0.9